Development of Novel Impedimetric Micro-biosensor Devices for Bioanalysis

THESIS

Submitted in partial fulfillment
of the requirements for the degree of
DOCTOR OF PHILOSOPHY

By

GAUTAM G. BACHER

Under the Supervision of

Prof. Sunil Bhand

BITS Pilani
Pilani | Dubai | Goa | Hyderabad

BIRLA INSTITUTE OF TECHNOLOGY AND SCIENCE
PILANI (RAJASTHAN) INDIA
2015

BIRLA INSTITUTE OF TECHNOLOGY AND SCIENCE

PILANI (RAJASTHAN)

CERTIFICATE

This is to certify that the thesis entitled **"Development of Novel Impedimetric Micro-biosensor Devices for Bioanalysis"** and submitted by **GAUTAM G. BACHER,** ID No. **2008PHXF006G** for award of Ph.D. Degree of the Institute embodies original work done by him under my supervision.

Signature in full of the Supervisor: S Bhand

Name in capital block letters: **Dr. SUNIL BHAND**

Designation: Professor, Department of Chemistry

Date: 18.02.2015

ACKNOWLEDGEMENTS

With immense pleasure and a deep sense of gratitude, I take this opportunity to thank several outstanding individuals and scholars who guided me throughout the period of my Ph.D. thesis.

First and foremost I offer my sincerest gratitude to my supervisor, Prof. Sunil Bhand for his guidance, encouragement and support right from the beginning of my thesis. I could achieve my research goals through his valuable suggestions and directions. Prof. Bhand always had a new approach to solving every experimental challenge I faced over the years and I thank for his critical suggestions to bring out the best of me. I am sincerely thankful to him for giving me good exposure through international/ national conferences and workshops. I have been extremely fortunate to be a part of his lab.

I am extremely grateful to Prof. B. N. Jain (Vice Chancellor, BITS, Pilani), Prof. K. E. Raman (Director, BITS, Pilani - K. K. Birla Goa Campus), Prof. S. K. Verma (Dean, Academic Research, Ph. D. Programme, BITS, Pilani), and Dr. P. K. Das (Associate Dean, Academic Research, BITS, Pilani - K. K. Birla Goa Campus) for providing me with the facilities to conduct my research work at BITS, Pilani - K. K. Birla Goa Campus.

I express my gratitude to the members of the Doctoral Advisory Committee, Prof. K. R. Anupama, and Dr. A. Amalin Prince, Department of EEE & I, for their guidance and co-operation. I also express my sincere thanks to Prof. M. K. Deshmukh, Head, Department of EEE & I, and Dr. C. K. Ramesha, Convener, Departmental Research Committee, for their support. I am also very thankful to my departmental colleagues for their help and support.

I extend my sincere thanks to Prof. A. P. Koley (Associate Dean, Instruction Division), Dr. R. N. Behera, Head, Department of Chemistry, and Prof. Utpal Roy, Department of Biology for their valuable advice, motivation, and support at various phases of my work.

I express my sincere thanks to Prof. Sudhir Chandra, Centre for Applied Research in Electronics (CARE), IIT Delhi and Prof. G. S. Lodha**,** Professor and Head X-ray Optics, Raja Ramanna Centre for Advanced Technology (RRCAT), (Indore) DAE, Govt. Of India, for their active collaboration.

My gratitude also extends to Prof. Bengt Danielsson, Acromed Invest Lund, Sweden, Dr. S. F. D'Souza, Ex. Associate Director, Nuclear Agriculture and Biotechnology Division, BARC, Mumbai and Prof. M. Willander, Linkoping University, Sweden, for scientific interaction and fruitful discussions.

I am very thankful to my collaborators within Biosensor laboratory Dr. Lizy Kanungo, Mr. Souvik Pal and Mr. Geetesh Mishra for their active collaboration, constant support, and fruitful scientific discussions. I extend my thanks to my other lab mates, Dr. Kanchanmala Deshpande, Dr. Rupesh Mishra, Atul Sharma, Arun Prusty and Aruna Singh. I extend sincere thanks to my external collaborators Dr. Hardik Pandya, CARE, IIT Delhi, and Mr. Vishal Dhamgaye, RRCAT, Indore.

I also want to acknowledge Prof. Z. J. Khan, Prof. V. K. Deshpande and Prof. Iven Jose for their help over the years. I also thank my friends Anjum Gous, Jayprakash Singh and Pramod Lanjewar, who had been actually friends in need. Though they are far away, their contribution to make my life worth living is unmatchable.

No words can express my gratefulness towards my parents, Shri Gurupada Bacher and Smt. Uma Bacher, I would never forget those days when they sacrificed little joys of life to support my education, and this thesis is dedicated to them. I express my sincere thanks to father-in-law Shri Sushil Vaidya, my sister Manabi Katoch and brother-in-law Aditya Katoch for their constant support, motivation and love throughout the entire duration of my Ph.D. work.

My wife, Sunita has always acted as the most reliable pillar of my life. I could achieve all this success because of her single handed dedication towards my family in my absence. Just a thank you would not be enough to show my thankfulness towards her. My daughters, Bhoomika and Kritika, My niece Sidhiksha have been the inspirations who drove me towards this achievement. Their unconditional love even after spending almost negligible time with them has been my strength all the way. I thank Shree Shree Thakur for his grace and blessing.

Gautam G. Bacher

CONTENTS

ABSTRACT

Recent trends in biosensors highlight the importance of accurate and continuous monitoring of contaminants in food and environment such as chemical compounds, toxins and bacteria. It is also necessary to assess and avoid risks of toxic contaminants in both, human and environmental health. The main advantages of the use of biosensors as compared to other conventional methods are; sensitivity, short analysis time, low cost of sample analysis and the possibility to perform under field condition. Owing to their high sensitivity, selectivity and versatility, affinity-based biosensor devices are attractive for monitoring contaminants in food and the environment. Affinity biosensors can be classified as labelled and label-free biosensors. In a labelled biosensor, the target analyte is attached to the enzyme or fluorophores as a label. During the measurement, the electrochemical signal generated by label in response to the biosensing process is detected, assuming a direct relation between the concentration of label and target analyte present. Labels can be biological such as enzyme, chemical materials such as fluorophores and non-chemical materials such as magnetic beads. In a label-free biosensor, the changes caused by the interaction between target analyte and recognition element are measured. Label-free biosensors are preferred over labelled ones, because of reduction in analysis time and cost. It has also been reported that labeling the target analyte changes the binding property which may result in inaccurate measurements. Surface plasmon resonance (SPR) based optical biosensing is also much reported as sensitive label-free affinity biosensor, capable of high throughput multi-analyte analysis. However, it has limitations such as long analysis time, high operational cost and possibility of field deployment. Whereas, impedimetric biosensors have potential for simple yet rapid detection, label-free sensitive analysis, low-cost of detection as well as has potential for field deployment. Electrochemical impedance spectroscopy (EIS) has emerged as a powerful technique for the analysis of interfacial properties related to bio-affinity analysis. The antibody–antigen interaction is one such event, which can be directly measured through EIS without the use of labels. Moreover, in EIS technique, the impedance response obtained from the interaction of target analyte and receptor is validated using equivalent circuit analysis. An equivalent circuit is used to fit the impedance data obtained experimentally and to get the necessary information about the electrical parameters responsible for this impedance change due to antibody-antigen interaction.

Impedance biosensors can be divided into non-faradaic and faradaic impedance biosensors. In faradaic impedance biosensor, antibody-antigen interaction is quantified by charge transfer resistance which requires a redox indicator. Whereas, non-faradaic impedance measurements does not require a redox indicator and the antibody-antigen interaction can be quantified by a change in capacitance. This thesis is mainly focused on non-faradaic impedance measurements, due to its simple, inexpensive, and direct signal transduction features. The need for rapid, reliable, specific, and sensitive methods of detecting contaminants in food and environment at low cost is the prime focus of current research and technological developments in developing countries. The work presented in this thesis, described the development of micro biosensor platforms towards realizing these requirements (chapter1).

Chapter 2 of this thesis presents the basic concept about construction of a simple, sensitive and low cost impedimetric immunosensor, operating on the EIS principle. Impedance measurement requires either three electrodes or two electrodes. A two electrode system has only the working and reference electrode. If the current density is low enough (< μAcm^{-2}) then the reference electrode can carry the charge with no adverse effect, which is achievable in a miniaturized format of an electrochemical cell. The selection of electrode materials and modification of electrode is crucial for immunosensor operation and performance. Various electrode materials such as Gold (Au), Silver (Ag) and Copper (Cu) were screened for impedance measurement. The Ag wire electrode was found suitable as compared to Cu wire electrode. Most of the impedance biosensors utilize self-assembled monolayers (SAMs) to attach probes at the electrode-solution interface. Long chain SAMs provides good electrical insulation, which is desired for non-faradaic impedance biosensor. Therefore, 11-marcaptoundecanoic acid (11-MUA) was selected for surface modification. The modified electrodes were characterized by Scanning electron microscope (SEM), Fourier transform infrared (FT-IR) spectra, and fluorescence microscopy to confirm the changes in surface morphology of electrode after modification with SAMs. Following parameters were optimized to study antibody-antigen interaction, such as antibody dilution, applied potential, applied frequency, incubation time and sample volume. A simple two electrode setup using EIS for analysis of antibody- antigen interaction was developed as a proof of concept, choosing aflatoxin M1 (AFM1) as model analyte.

Chapter 3 of this thesis presents the implementation of two electrode based impedance measurement setup for the analysis of AFM1, aflatoxin B1 (AFB1) and *Escherichia coli*

(*E.Coli*). Aflatoxins are highly toxic, mutagenic, carcinogenic, and teratogenic compounds. The consumption of milk and milk products by human population is quite high, particularly in infants and children, thereby increasing the risk of exposure to AFM1. The AFM1 level in milk has been restrictively set to 50 pg mL^{-1} for adult and 25 pg mL^{-1} for infants. In order to ensure set level of AFM1 in milk, a highly sensitive and selective label-free impedimetric immunosensor based on silver (Ag) wire electrode, for the detection of AFM1 in milk was developed. The sensor was constructed by functionalizing Ag wire coupled with selective monoclonal antibodies of AFM1 through SAMs of 11-MUA. The antibody–antigen interaction was quantified by measuring impedance in the frequency range (1Hz to 100 Hz) at 10 mV applied ac potential. The immunosensor showed an excellent linear range for the AFM1 present in spiked milk in the range (6.25–100 pg mL^{-1}) with a good sensitivity. The developed immunosensor showed an astoundingly low limit of detection of 1 pg mL^{-1} with a short analysis time of 20 min. The sensor was also validated with simple equivalent circuit with double layer capacitance (C_{dl}). With the developed immunosensor setup, volume reduction has also been achieved through custom made glass cell with a total assay volume of 700 µL. The immunosensor developed is useful for sensitive analysis of AFM1 in milk. The developed sensor demonstrated excellent selectivity for AFM1 as against aflatoxin M2 (AFM2).

The developed sensor was further extended to study the matrix effect of various milk products such as certified reference material (CRM) (ERM-BD 282, zero level of AFM1 for milk powder), flavored milk and yogurt. It was observed that the sensor response was similar for ERM-BD 282 and flavored milk with ideal capacitor behavior at a frequency of 52 Hz. Whereas, for yogurt this behavior was observed at 159 Hz. The developed sensor can be used for analysis of different matrices.

Many foodstuffs, including corn, peanuts, beans and rice have been found to be contaminated with aflatoxins. Maximum residue levels (MRLs) of AFB1 in peanut products are regulated not greater than 2 ng/g. Using the similar concept of antibody-antigen interaction, a highly sensitive and selective label-free impedimetric immunosensor was also developed for the detection of AFB1 in peanut. Two electrode based impedance measurement setup was further miniaturized through measurements in 384 micro well plates with assay volume of 105 µL, accordingly the electrode size was varied. The size and the diameter of the Ag wire electrodes were optimized. The sensor was constructed by functionalizing Ag wire

coupled with polyclonal antibodies of AFB1 through self assembled monolayers. The antibody-antigen interaction was analyzed by measuring impedance in the frequency range (1 Hz to100 kHz) at 5 mV applied ac potential. A working range (0.01–100 pg mL^{-1}) for AFB1 was obtained with 20 min analysis time with limit of detection 0.01 pg mL^{-1}. The measurement data were validated with an equivalent circuit. The developed sensor meets the regulatory requirements of both national and international standards.

E.coli is a type of fecal coliform bacteria commonly found in the intestines of animals and humans. The presence of *E.coli* in water is a strong indication of animal waste contamination, thus, World Health Organization (WHO) has set the limit of zero bacteria in 100 mL water sample. Conventional methods of analysis of bacteria in water are laborious and time consuming. The developed two electrode based impedance immunosensor concept was deployed for the detection of *E.coli* in water. A linear trend of increasing impedance was achieved when the *E.coli* concentration increased from 10^2–10^8 CFU mL^{-1}. The sensor shows a good promise towards development of rapid method for detection of bacteria in water.

Miniaturized biosensors are necessary for many food testing applications that needs portability. Advances in microfabrication technologies have facilitated the use of micro electrodes towards development of miniaturized biosensor devices. Chapter 4 of the thesis presents the development of a novel micro biosensor device based on interdigitated electrodes (IDEs) and their application for label-free detection and analysis of AFM1 in milk using EIS technique. The IDEs devices were designed and fabricated in collaboration with Centre for Applied Research in Electronics (CARE), IIT Delhi and had resulted in joint intellectual property**.** These devices were successfully developed as ultrasensitive biosensors for mycotoxin analysis with novelty in fabrication process, multi-sensing capability and low sample volume**.** The developed biosensor meets the stringent regulatory standards of the European Union (EU) cutoff of 50 pg mL^{-1} and below for AFM1 analysis in milk. Moreover, the developed biosensor device was validated for unknown sample analysis and possibility of field detection.

Chapter 5 of the thesis presents the development of a monolithic coil microelectrode array (CMEA) biochip, fabricated using UV and X-ray lithography techniques. The developed CMEA biochip was demonstrated for conductivity measurement of KCl solution. The CMEA biochip was also demonstrated for application in glucose biosensing. A linear

range of detection for glucose (100 nM-10 mM) was achieved using glucose oxidase (GOD) immobilized CMEA biochip with a detection limit of 10 nM and analysis time of 2 min. The biosensor device requires less than 0.5 µL sample volume. An important feature of the developed biochip device is its reusability that makes it an attractive feature over existing disposable biochips.

In brief, impedimetric micro-biosensors for analysis of food toxin (AFM1, AFB1 and *E.coli*) and clinical analyte (Glucose) have been developed in this thesis work. The major highlight of this work includes the development of;

- Ag wire two electrode based impedimetric immunosensor for AFM1 and AFB1 analysis in milk and *E.Coli* in drinking water.
- a novel IDEs based impedimetric micro biosensor device for ultrasensitive AFM1 analysis in milk samples.
- a monolithic coil microelectrode array (CMEA) biochip platform with demonstrated application in glucose sensing.

Table of Content for Chapters

List of Figures

List of Tables

List of Symbols & Abbreviations

Symbol	Description
µA	microampere
µF	microfarad
µg	microgram
µL	microliter
µm	micrometer
µS	microsiemens
1º Ab	primary antibody
2º Ab	secondary antibody
A	area
Ab	antibody
ac	alternating current
Ag	silver
Al	aluminium
Au	gold
C	capacitance
C_{dl}	double layer capacitance
Cl	chloride
cm	centimeter
Cu	copper
eV	electron Volt
F	farad
g	gram
hr	hour

Hz	hertz
I	current
IU	international Unit
KCl	potassium Chloride
kHz	kilohertz
kV	kilovolt
kΩ	kiloohm
L	liter
m	meter
M	molar
mg	milligram
MHz	megahertz
min	minute
mL	milliliter
mm	millimeter
mM	millimolar
mV	millivolt
MΩ	megaohm
ng	nanogram
nL	nanoliter
pF	picofarad
pg	picogram
pH	acidity measurement unit
ppb	parts per billion
ppt	parts per trillion
Pt	platinum

R_s	solution Resistance
R_{ct}	charge transfer resistance
rpm	revolutions per minute
s	second (time)
H_2O_2	hydrogen peroxide
Si	silicon
Ti	titanium
V	volt
Z	impedance
Z`	real part of impedance
Z``	imaginary part of impedance
ε	permittivity
ε_0	permittivity of free space
Φ	phase shift
Ω	Ohm

Abbreviations	**Description**
µEDM	Micro electrical discharge machining
11-MUA	11-mercaptoundecanoic acid
AFB1	Aflatoxin B1
AFM1	Aflatoxin M1
AFM2	Aflatoxin M2
AFP	α-1-fetoprotein
AOAC	Association of analytical communities
ATR	Attenuated total reflectance
BSA	Bovine serum albumin

CB	Carbonate buffer
CFU	Colony forming unit
CMEA	Coil microelectrode array
CPE	Constant-phase element
CRM	Certified reference material
CV	Cyclic voltametry
DNA	Deoxyribonucleic acid
DPV	Differential pulse voltametry
DW	Distilled water
E. coli	*Escherichia coli*
EC	European commission
EDC	1-ethyl-3(3/-dimethylaminopropyl) carbodiimide
EIS	Electrochemical impedance spectroscopy
ELISA	Enzyme-linked immunosorbent assay
EMF	Electromotive force
EU	European Union
FITC	Fluorescein isothiocyanate
FSSAI	Food Safety and Standards Authority of India
FT-IR	Fourier Transform Infrared
GOD	Glucose oxidase
HPLC	High performance liquid chromatography
HRP	Horseradish peroxidase
IARC	International agency for research on cancer
IC_{50}	Half maximal inhibitory concentration
IDEs	Interdigitated electrodes
IUPAC	International union of pure and applied chemistry

LIGA	X-ray lithography electrodeposit on molding
LOD	Limit of detection
LOQ	Limit of quantification
mAb	Monoclonal antibody
MEMS	Micro electromechanical systems
MRL	Maximum residue limit
MTCC	Microbial type culture collection
NHS	N-hydroxysuccinimide
OTA	Ochratoxin A
pAb	Polyclonal antibody
PB	Phosphate buffer
PBS	Phosphate buffered saline
PBST	Phosphate buffered saline with Tween
PSA	Prostate-specific antigen
QCM	Quartz crystal microbalance
RSD	Relative standard deviation
SAMs	Self assembled monolayers
SD	Standard deviation
SEM	Scanning electron microscope
SPE	Screen Printed Electrodes
SPR	Surface plasmon resonance
TLC	Thin layer chromatography
USFDA	United States food and drug administration
UV	Ultra violet
WHO	World Health Organization

Chapter 1

Introduction

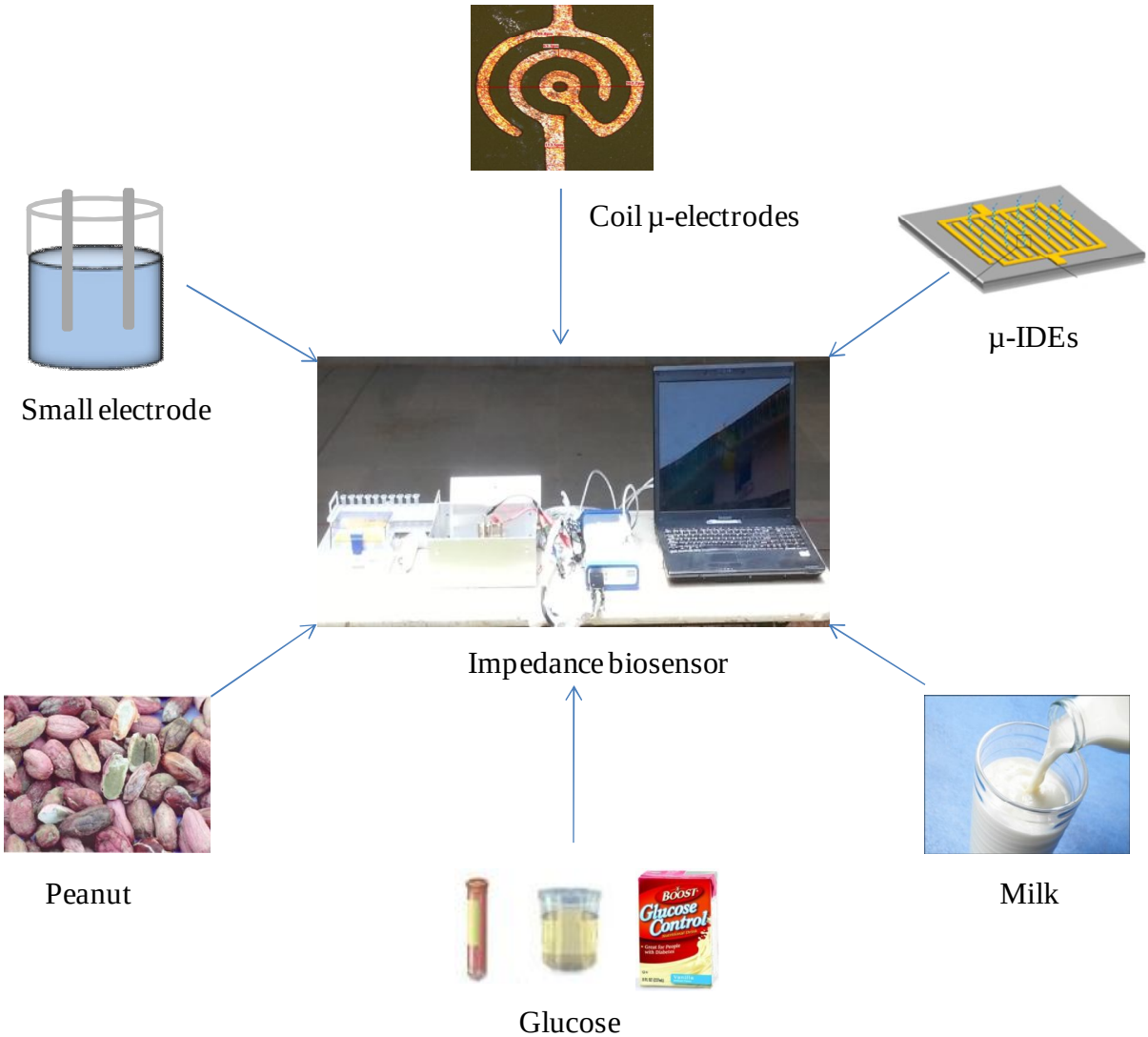

Graphical abstract of the thesis contents

1.1 Background

In a world where biological threats may take multiple forms associated with environmental and health issues, the need for versatile biosensing platforms is of vital concern. Identification and quantification of one or several biological species with harmful potential has been the design target for majority of existing biosensors (Nicu, 2014). Recent years have seen continued growth of the inter-disciplinary field of biosensors, due to an increased interest among basic and applied sciences researchers and engineers for the development of novel electronic devices that can be utilized for a variety of applications (Wanekaya *et al*., 2008). Miniaturization is a growing trend in recent years in the field of biosensor. In order to design and manufacture a small biosensor, the transducer needs to be small and portable (Ronkainen *et al*., 2010). Portability of biosensors has become very important since in many remote areas a full-scale biological lab implementation is difficult. The development of reusable sensor in conjunction with handheld device for detection of analyte has featured prominently. Microfabrication technology has played an important role in achieving such miniaturized biosensor. Microfabrication technology has provided cheap, mass producible, easy to use and disposable sensors. Electrochemical methods have played a pivotal role in detecting changes that occur during a biorecognition event. The merging of microfabrication with electrochemical detection has led to the development of various handheld biosensor devices. The need for miniaturization arises from the need to increase throughput and automation while reducing the cost of the diagnostic assays, that consume hundreds of microliters of expensive reagents. Miniaturized systems, on the contrary, reduce reagent consumption by a factor of 10^3 to 10^4, providing dramatic savings for the repetitive assays often performed in diagnostic laboratories (Figeys and Pinto, 2000).

Design and development of microsensor system such as, micro biosensor requires the interaction among several subjects like fluids mechanics, electromagnetic, material science, bio-chemistry, etc. Hence demands multidisciplinary teams and system approaches. Microsensors are built to sense the existence and measure the intensity of certain physical, chemical, or biological quantities such as temperature, pressure, force, sound, light, and magnetic flux compositions of chemical and biological substances (Muramatsu *et al*., 1987). Microsensors have the advantage of being sensitive and accurate with minimal amount of required sample substance. Microsystems are a major step toward the miniaturization of machines and devices. The need for miniaturization has become more prominent than ever in

recent decades, as engineering systems and devices have become increasingly complex and sophisticated. This thesis work focuses on the development of miniaturized biosensor devices to address the need for rapid, low cost, portable, miniaturized devices and label-free systems for environmental applications.

The work presented in this thesis contributes development of different biosensing platforms based on electrochemical impedance readout with the ultimate goal of performing label-free, real time measurement of various analytes. The use of functionalized electrodes was exploited to carry out impedance/capacitance measurements at low frequency. The small change in capacitance was quantified at the electrode/electrolyte interface upon binding of relevant biomolecules. In this thesis, initially the proof of principle approach is followed to verify the quantification of antibody-antigen interaction using EIS with two electrode setup. By analyzing immunosensors as an example, we showed that EIS based biosensing is a highly sensitive detection technique, which can be used for the detection of a wide variety of analytes with ample scope for miniaturization.

1.2 Introduction to biosensors

1.2.1 What is biosensor?

According to International Union of Pure and Applied Chemistry (IUPAC) nomenclature, biosensor is a device that uses specific biochemical reactions mediated by isolated enzymes, immune-systems, tissues, organelles or whole cells to detect chemical compounds usually by electrical, thermal or optical signals (McNaught and Wilkinson, 1997). Biosensors produce an electrical or an optical signal proportional to the specific interaction between the analyte and the recognition molecule present on the biosensor (Turner, 2000). Biosensors transform biological interactions into electrical signals that can be conveniently measured and recorded. Biosensors can detect a wide range of targets from small protein molecules to large pathogens. Compared to the conventional methods, biosensor can be used for the detection of pathogenic antigens and does not require highly trained personnel for using them. Biosensors are highly sensitive and selective, and it can provide results more rapidly than culture-based methods, making them ideal for practical and field applications. The elements of a biosensor are shown in Figure 1.1.

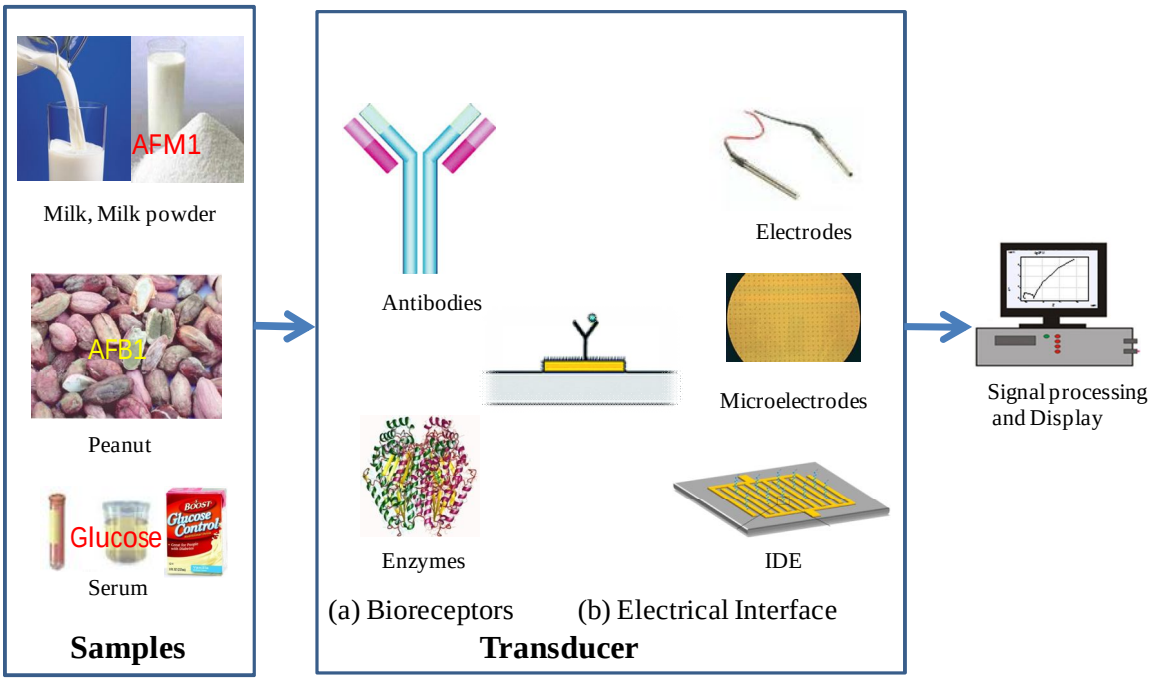

Figure 1.1 Elements of biosensor.

1.2.2 Generations of biosensors

There are three generations of biosensors; the first generation of biosensors where the normal product of the reaction diffuses to the transducer and causes the electrical response, second generation biosensors used specific mediators between the reaction and the transducer in order to generate an improved response and third generation biosensors where the reaction itself caused the response and no product or mediator diffusion is directly involved. The three generations of biosensors are shown in Figure 1.2.

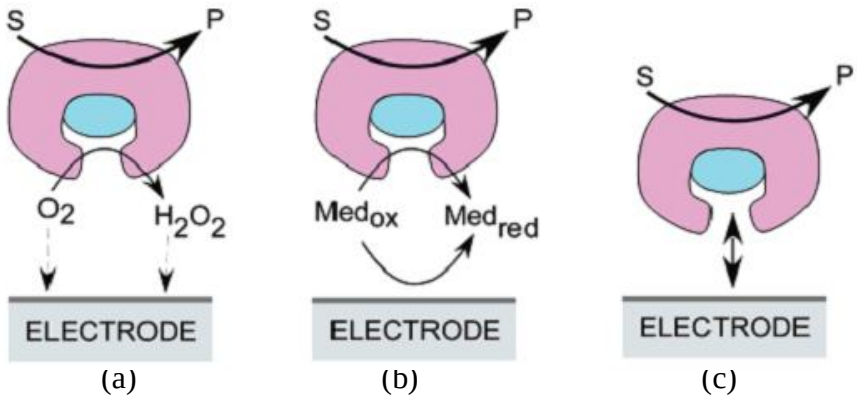

Figure 1.2 Three generations of glucose biosensor using enzyme electrodes based on (a) use of the natural oxygen cofactor (b) artificial redox mediators (c) direct electron transfer between glucose oxidase (GOD) and electrode (Wang, 2008).

1.2.3 Classification of biosensors

Biosensors can be classified either by the type of biological signalling mechanism they utilize or by the type of signal transduction they employ. The classification of biosensor is shown in Figure 1.3.

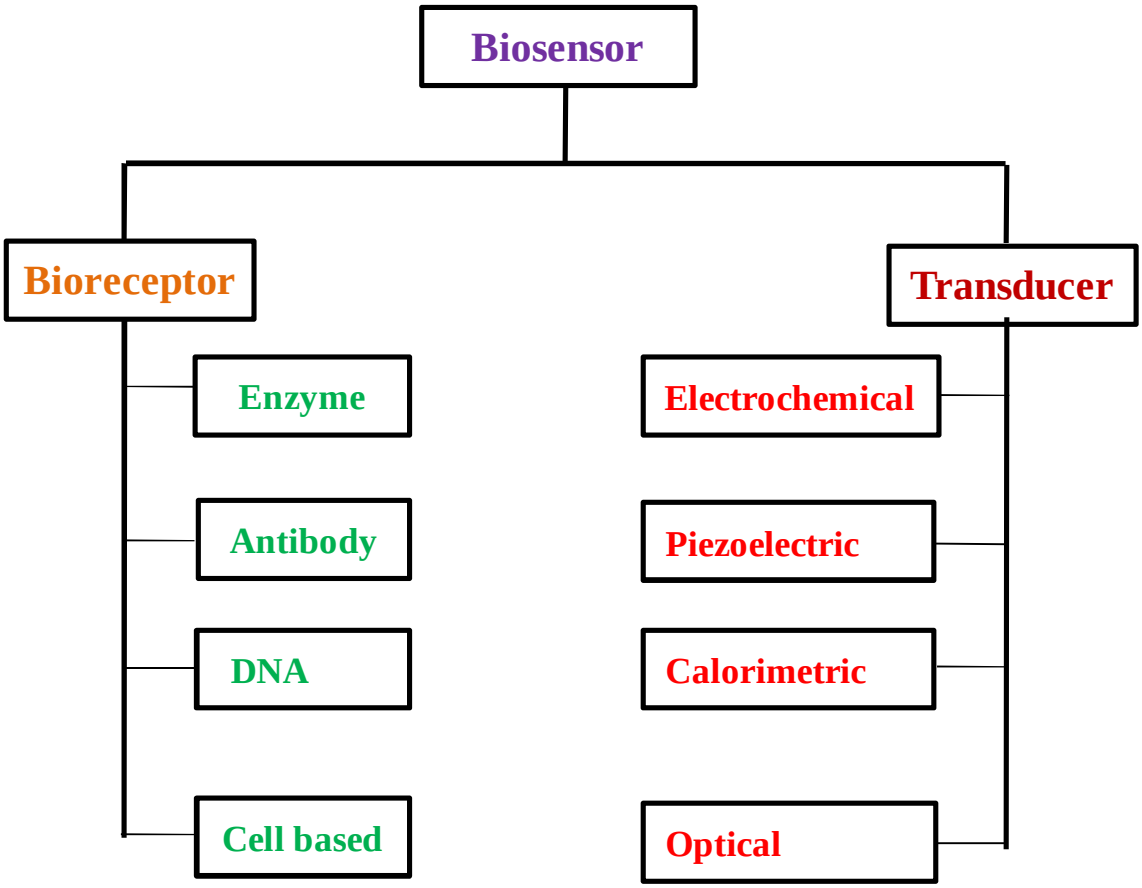

Figure 1.3 Classification of biosensors.

1.2.4 Biological recognition elements

The biological recognition element or bioreceptor is a crucial component of the biosensor device. Essentially, it is crucial for a bioreceptor to be selective and sensitive towards the specific target analyte to prevent interference by another substance from the sample matrix. Biosensors can be classified as catalytic, when the biological recognition element reacts with the analyte or as affinity, when the biological recognition element forms a complex with the analyte (Patel, 2002). The mechanism of affinity based biosensor is presented as Figure 1.4.

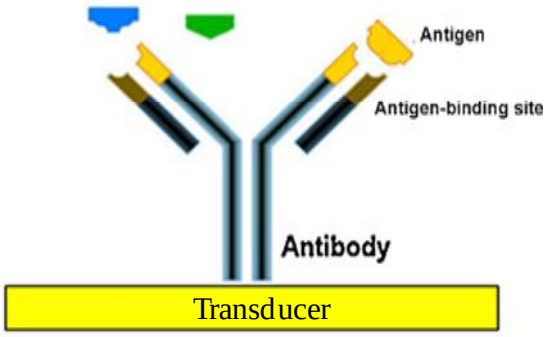

Figure 1.4 Method of biosensing with a biological signal mechanism for affinity biosensors.

1.2.4.1 Catalytic biosensors

Enzyme-based biosensors associate intimately a biocatalyst-containing a sensing layer with a transducer. The working principle of these biosensor is based on catalytic action and the binding capabilities for specific detection. The most widely used enzyme-based biosensors reported in literature are Glucose oxidase (GOD) and horseradish peroxidase (HRP). Recent studies have shown that enzyme based biosensors can be used for food safety detection and environmental monitoring (Amine *et al.*, 2006). However, the number of available enzyme-based biosensors is still lesser than the number of potential analytes. Another disadvantage of enzyme electrodes are that, the enzyme layer in the biosensor has to be replaced periodically since it gradually loses activity. Some authors have used the enzymatic inhibition produced by mycotoxins to obtain enzymatic biosensors for these analytes. Nevertheless, the main problem of this kind of biosensors is the lack of selectivity, as other toxins or molecules from the sample might also inhibit the enzyme response (Arduini *et al.*, 2007).

1.2.4.2 Affinity biosensors

Affinity sensors use the selective and strong binding of biomolecules such as antibodies, membrane receptors, or oligonucleotides, with a target analyte to produce a measurable electrical signal (Wang, 2006). The molecular recognition in affinity biosensors is mainly determined by the complementary size and shape of the binding site to the analyte of interest. The high affinity and the specificity of the biomolecules for its ligand make these sensors very sensitive and selective.

1.2.4.2.1 Immunosensors

When antibodies or antibody fragments are used as a molecular recognition element for specific analytes (antigens) to form a stable complex, the device is called immunosensor (Ricci *et al.*, 2007). Because of the inherent high affinity and specificity of antibodies, the target (analyte) doesn't need to be purified in order to be detected. The availability of highly selective antibodies for an increasingly wide variety of important analytes was also an important factor in the growth of this method over the following decades. The development of more sensitive labels and detection devices, improved the sensitivity of the assays even further. Immunosensors are well known among analytical methods for their extremely low detection limits (Ronkainen-Matsuno *et al.*, 2002). Immunosensors have been developed for both quantitative and qualitative detection. Immunosensors are most commonly used in majority of rapid detection systems. Immunosensors can be used to detect trace levels (ppt, ppb) of toxins, bacteria and viruses (Wang, 2006). The applications of immunosensor have increased over the years in the field of clinical diagnostics, environmental field and food industries. The advantages of immunosensor such as exceptionally high specificity of antibody for antigen, small sample volumes, low detection limits, little or no sample preparation, reduced use of chemicals, less waste and ease of automation have far outweigh their limitations, thus making the immunosensor an attractive alternative to the more conventional quantitative analytical methods like chromatography and mass spectrometry (Ronkainen-Matsuno *et al.*, 2002). The summary of electrochemical immunosensors for different analytes is presented in Table 1.1.

1.2.4.2.2 Nucleic acid biosensors

Nucleic acid sensors are based on affinity based detection of target sequences via the use of immobilized complementary DNA or RNA fragments. Detection is based on the hybridization event taking place when a complementary target sequence exists within a given sample. During the hybridization event no new molecules, electrons or photons are produced. In a similar manner to antibody based sensors, the formation of double stranded DNA must be recognized by the alterations in the electrical and chemical (or other) properties of the conductive surface (Davis *et al.*, 2005). Electrochemical DNA hybridization biosensors are useful in the diagnosis of infectious diseases, in environmental monitoring and to detect microorganism contaminants in food and beverages. However, DNA probe technology requires a long culture-enrichment step, and 1or 2 days are always needed to perform the

analysis. Nevertheless, most of this hybridization, DNA biosensors has a huge lack of selectivity and sensitivity for environmental or toxicological applications and very few reports are dedicated to these to date.

Table 1.1 Summary of electrochemical immunosensor for different analyte

Detection Technique	**Analyte**	**Range of Detection**	**Limit of Detection (LOD)**	**Reference**
Impedimetric	AFM1	15-1000 ng mL^{-1}	15 ng mL^{-1}	Vig *et al*., 2009
EIS	OTA	0.01–5 ng mL^{-1}	0.01 ng mL^{-1}	Zamfir *et al*., 2011
Differential pulse voltammetry	OTA	0.005−0.06 ng mL^{-1}	0.003 ng mL^{-1}	Kaushik *et al*., 2009
Potentiometry	PSA	3.5−30 ng mL^{-1}	2.6 ng mL^{-1}	Shen *et al*., 2011
EIS and cyclic voltammetry	AFP	1.0−55.0 ng mL^{-1}	0.6 ng mL^{-1}	Lin *et al*., 2009
Amperometric	AFM1	0.030–0.060 ng mL^{-1}	0.025 ng mL^{-1}	Micheli *et al*., 2005
Impedimetric	AFB1	0.5-10 ng mL^{-1}	0.1 ng mL^{-1}	Liu *et al*., 2006

Aflatoxin M1 (AFM1); Ochratoxins A (OTA); Prostate-specific antigen (PSA); Aflatoxin B1 (AFB1); α-1-fetoprotein (AFP)

1.3 Transducers used in biosensor

Sensors and mainly biosensors are an exciting alternative to the more traditional methods for the detection of pathogens and toxins in food (Alocilja and Radke, 2003; Arora *et al*., 2006). Biosensors allow the detection of a broad spectrum of analytes in complex sample matrices, and have shown great promise in areas such as clinical diagnostics, food analysis, bioprocess and environmental monitoring. The main advantages in the use of biosensors as compared to other conventional methods are the short analysis time, low cost of analysis, the suitability to be integrated in automated assays and the possibility to perform *in-situ* real-time analysis. Biosensors may be classified into different groups depending on the method of signal transduction such as optical, mass, magnetic and thermal sensors as presented in Table 1.2.

In recent years, optical and electrochemical detection methods have been frequently used in affinity biosensors. Optical transduction have been used in immunosensor (Olkhov and Shaw, 2008; Banada and Guo, 2007). However, optical method has suffered from poor sensitivity when coupled with radioimmunoassay, health hazards due to radioactive agents and disposal problems, whereas an electrochemical method is free from these issues. However, in the field of biosensors for food safety, clinical analysis and environmental analysis, there is still a lack of handheld integrated systems. Electrochemical detection allows simple integration with electronic system used for readout, making it a preferred choice among the other transduction method.

Table 1.2 Transducers used in biosensor

Transducer	**Analyte**	**LOD**	**Reference**
Impedimetric (Electrochemical)	*E. coli* O157:H7	10^2 CFU mL^{-1}	Chowdhury *et al*., 2012
SPR (Optical)	*Salmonella*	2.50×10^5 cells mL^{-1}	Barlen *et al*., 2007
QCM (Piezoelectric)	AFB1	0.3 ng mL^{-1}	Spinella *et al*., 2013
Cantilever sensors (Mass)	*E. coli* O157:H7	1 cell/mL	Campbell and Mutharasan, 2007
Micro cantilever resonators(Mass)	OTA	3 ng mL^{-1}	Ricciardi *et al*., 2013
Thermister (Calorimetric)	Urea	0.1mM	Mishra *et al*., 2010

Surface plasmon resonance (SPR), Quartz crystal microbalance (QCM)

1.4 Microfabrication in biosensor

Microfabrication refers to a wide range of device fabrication techniques at the centre of which lie lithographic processes to transfer a set of desired structures onto planar substrates (Madau, 2012). Microfabrication technologies are powerful tools for the construction of miniaturized structure and have been widely used for the development of biosensors (Pemberton *et al*., 2013). The application of microfabrication technologies to biosensors are becoming very common owing to its advantages such as reduction in size, small sample volume, highly uniform and geometrically well defined sensor elements (Lee *et al*., 2008, Qin *et al*., 2010). Microfabrication technologies also exhibit many other features such as

mass-production of sensors with good reproducibility, decrease in production costs, low power consumption and low cost devices. Electrochemical biosensors have been significantly benefited through micro technological intervention such as the reduction in size of electrode, size of the transducer, etc. The advances in microfabrication enabled replacement of macroelectrodes with easy-to-use sensing devices and have led to significant advances in the development of miniaturized electrochemical sensors and sensor arrays (Bourgeois *et al*., 2003). Innovative techniques such as thin film technology (Hakim *et al*., 2012), silicon-based techniques (Dávila *et al*., 2011) and photolithography (Baccar *et al*., 2014) were used in designing electrochemical sensors for biosensor applications. Basic techniques for pattern formation in manufacturing of micro devices originate from semiconductor related processes which includes photolithography, thin film deposition and chemical etching. Any noble metals used for conventional macroscopic electrodes can be patterned. In general, silicon micromachining and other such micro sized device fabrication technology has been standardized, which follows a set of known protocols. However, this has greatly facilitated interdisciplinary research connecting science and engineering discipline. A comprehensive information about microfabricaiton has been well documented (Madou, 2012). A brief survey of reported microfabrication techniques has been presented in Table 1.3.

Table 1.3 A brief survey of microfabrication method

Microfabrication method	**Features size**	**Reference**
Photolithography and micromachining	150 µm diameter spaced 750 µm	Hollenberg *et al*., 2006
Electrochemical microfabrication and micromachining	150 ×150 μm^2	Ferrara *et al*., 2003
Laser micromachining	5 µm	Reynaerts *et al*., 1997
UV-LIGA	120–600 µm	Young-Min *et al*., 2010
µEDM	10–25 µm	Benavides *et al*., 2002
Micromilling	100 to 500 µm	Cardoso and Davim, 2012

X-ray lithography electrodeposit on molding (LIGA), Micro electrical discharge machining (µEDM)

1.5 Self assembled monolayers (SAMs)

Self-assembled monolayer is a layer of molecular thickness formed by self-organization of molecules in an ordered manner by chemisorption on a solid surface. The stability, uniform surface structure and relative ease of varying thickness of a SAMs make it suitable for development of biosensors. The immobilization of biomolecules on a SAMs requires a very small amount and desired analytes can be easily detected via various transduction modes. A monolayer can be utilized to reduce non-specific binding and to minimize steric hindrance between molecule and its binding with counterpart (Fragoso *et al*., 2008). The advantages of SAMs lie in their integration with a biological recognition element for the development of biosensors (Mizutani, 2008). Most impedance biosensors utilize self-assembled monolayers (SAMs) to attach probes at the electrode-solution interface. The most common types of attachment chemistries are based on thiols (-SH) bound to metal surfaces (Love *et al*., 2005). The use of appropriate SAMs helps in oriented and controlled immobilization of biomolecules (Cheng *et al*., 2008). SAMs can be used to prevent protein denaturation at electrode surface and for enhancing stability of biomolecules (Kafi *et al*., 2007). For non-faradaic sensors a tightly-packed (high leakage resistance, R_{leak}) SAM is desirable, in contrast with faradaic sensors where the electrode surface needs to be accessible to the redox species but not to adsorption of other molecules (Lai *et al*., 2006). SAMs with longer carbon chains form more dense monolayers due to hydrophobic interactions of the chains. The general rule of thumb is that C_{11} or greater gives packed films (Poirier *et al*., 1994). Longer SAMs are more stable and that preservatives can ensure stability over one month with reproducible results (Lai *et al*., 2006). Boubour *et al*., reported 40 hrs of incubation to form a tightly-packed SAMs, having capacitive behaviour at low frequencies (Boubour and Lenox, 2000), whereas (Campuzano *et al*., 2006) reported 15–20 hrs depending on SAMs composition. SAMs for bio-sensing applications can be modified by adopting many other strategies.

1.5.1 SAM modification via physical adsorption

Physical adsorption for immobilization of desired biomolecules is based on interaction of charges present on the SAMs surface and biomolecules under desired conditions (de Groot *et al*., 2006). This method is particularly suitable for SAMs having ionic group on the surface.

1.5.2 SAM modification using chemical activators

Binding of biomolecules using chemical activators has shown great potential for development of commercial biosensors due to stability of resultant bond. Chemical modification of a SAMs using an activator can be achieved by various methods (Dannenberger *et al.*, 2000). N-Ethyl-N'-(3-dimethylaminopropyl) carbodiimide (EDC) /N-hydroxysuccinimide (NHS) coupling has been widely employed for chemical modification in biosensor fabrication (Jang and Keng, 2008).

1.6 Immobilization of receptor

For fabrication of a biosensor, immobilization of a biomolecules on a SAMs surface is an important concern (Arya *et al.*, 2009). The molecular recognition receptor of an affinity biosensor is prepared by immobilizing antibodies onto a substrate, which can be a conductor or semiconductor material. The schematic of SAMs modified electrode and antibody-antigen binding are shown in Figure 1.5. Noble metal substrates of platinum (Pt), Gold (Au) and silver (Ag) seem very suitable for this purpose, since they are easy to functionalize (Hou *et al.*, 2004). The immobilization method not only affects the stability of biomolecules, but also affects the immune-recognition event of antibodies towards antigens, making the immobilization process a crucial step for the immunosensor construction (Sassolas *et al.*, 2012). Various immobilization procedures have been used in biosensor construction. In general, the choice of procedure depends on the nature of the biological element, the type of transducer used, the physicochemical properties of the analyte and the operating conditions in which the biosensor is to function. There are in principle four methods of immobilization i.e. entrapment and encapsulation, covalent binding, cross-linking and adsorption. The advantages and disadvantages of these methods have been given in Table 1.3.

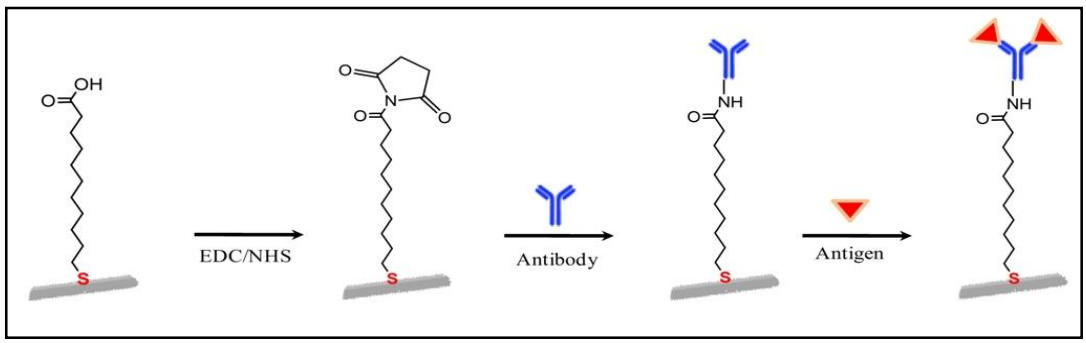

Figure 1.5 Schematic showing functionalization of electrode surface by SAMs and binding of antibody-antigen.

Table 1.4 Methods of biological component immobilization

Method	**Advantages**	**Disadvantages**
Adsorption	Gentle treatment of biocatalyst, No modification of biological component Matrix can be regenerated Maximal retention of activity.	Very weak bonds, Susceptible to changes in pH, temperature, ionic strength.
Cross-linking	Used in conjunction with entrapment to reduce loss of bio-component.	Harsh treatment of biocatalyst with toxic chemicals. Covalent links formed between protein molecules rather than matrix and protein.
Entrapment and encapsulation	Gentle treatment of biocatalyst. No direct chemical modification of biocatalyst. Specific of biocatalyst and analyte interaction retained.	Applicable only for small analyte detection. High diffusion barrier to both substrate and product transport. Continuous loss of biocatalyst.

1.7 Electrochemical biosensors

In electrochemical sensor, electrodes re used as the transduction element, represents an important subclass of sensors. According to a IUPAC recommendation in 1999, an electrochemical biosensor is a self-contained integrated device; that is capable of providing specific quantitative or semi-quantitative analytical information using a biological recognition element (biochemical receptor) which is kept in direct spatial contact with an electrochemical transduction element (Thevenot *et al.*, 2001). Most biosensors use electrochemical detection for the transducer because of the low cost, ease of use, portability and simplicity of construction (Wang, 2006). The reaction being monitored electrochemically typically generates a measurable current (amperometry), a measurable charge accumulation or potential (potentiometry) or alters the conductive properties of the medium between electrodes (conductometry). Use of EIS for monitoring both resistance and reactance in the

biosensor is also becoming more common (Grieshabe *et al*., 2008). Electrochemistry is a surface technique and offers certain advantages for detection in biosensors. It does not have a strong dependence on the reaction volume, and therefore only small sample volumes are required for measurement (Ronkainen-Matsuno *et al*., 2002). Electrochemical biosensors are classified into different categories: amperometric, potentiometric and impedimetric depending upon the nature of the electrochemical changes such as current, potential and impedance detected during a bio-recognition event.

1.7.1 Amperometric biosensor

Amperometric sensors are based on the measurement of current as a function of time. The current results from the oxidation and reduction of an electroactive species in a biochemical reaction that mainly depends on the concentration of an analyte with a fixed potential. There are three types of electrode that are usually employed in an amperometric sensor; the working electrode, a reference electrode and the counter electrode (Wang *et al*., 2008). As certain molecules are oxidized or reduced (redox reactions) at inert metal electrodes, electrons are transferred from the analyte to the working electrode or to the analyte from the electrode (Banica, 2012). The amperometric transduction can be integrated with enzymes, nucleic acids and an immunosensor biological recognition element for various applications such as cholestrol detection, dental disease and environmental monitoring (Fang *et al*., 2011; Ivnitski *et al*., 2003; Amine *et al*., 2006). However, there are limitations to the use of this biosensor where the presence of electroactive interference in the sample matrix can cause the transducer to generate a false current reading (Rogers and Mascini, 1999).

1.7.2 Potentiometric biosensor

Potentiometric biosensors rely on the use of ion-selective electrodes for obtaining the analytical information. In this sensor, the biological recognition element converts the recognition process into a potential signal to provide an analytical signal. It consists of two electrodes: an indicator electrode to develop a variable potential from the recognition process and a reference electrode (usually Ag/AgCl) which is required to provide a constant half-cell potential. The working principle of the potentiometric transduction depends on the potential difference between the indicator electrode and reference electrode which accumulate during the recognition process in an electrochemical cell, when a zero or negligible amount of current flows through the electrode. The electrical potential difference or electromotive force

(EMF) between two electrodes is measured using a high impedance voltmeter. The measurement of potential response of a potentiometric device is governed by Nernst equation in which the logarithm of the concentration of the substance being measured is proportional to the potential difference (Grieshaber *et al*., 2008; Wang *et al*., 2008). Due to the logarithmic relationship between a potential generated and analyte concentration, a wide detection range is possible. However, this method requires a very stable reference electrode, which may be a limitation of the transducers (Sharma and Rogers, 1994).

1.7.3 Impedimetric biosensor

EIS described by Lorenz and Schulze in 1975 (Lorenz and Schulze, 1975), measures the resistive and capacitive properties of materials upon perturbation of a system by a small amplitude sinusoidal ac excitation signal typically of 2-10 mV (Bartlett, 2008; Suni, 2008). The frequency is varied over a wide range to obtain the impedance spectrum. The in-phase and out-of-phase current responses are then determined to obtain the resistive and capacitive components of impedance, respectively. Impedance methods are powerful because they are capable of sampling electron transfer at high frequency and mass transfer at low frequency. Impedimetric detection is primarily used for affinity biosensors (Van Emon, 2007). It can be used to monitor immunological binding events such as antibody-antigen binding on an electrode surface, for example, where the small changes in impedance are proportional to the concentration of the measured species, the antigen. The surface of the electrode can be modified by a highly specific biological recognition element. During the detection step, a known voltage is applied to the electrode and the resulting current is measured. The electron transfer resistance at the interface between the electrode and the solution changes slightly when analyte binds. Direct monitoring of an antibody-antigen conjugated layer formation provides a label-free detection system with many potential advantages such as higher signal-to-noise ratio, ease of detection, lower assay cost, faster assays and shorter detector response times. Among the various types of immunosensors that enable the direct monitoring of such interactions, impedimetric immunosensors have recently received particular attention since they possess a number of attractive characteristics associated with the use of electrochemical transducers, namely, low cost of electrode mass production, cost effective instrumentation, the ability to miniaturize and to integrate into multi-array or microprocessor-controlled diagnostic tools and remote control of implanted sensors etc. Indeed, due to the above mentioned characteristics, EIS based sensors are considered as promising candidates for use

at on-site applications. The label-free nature of EIS is its major advantage over amperometric and potentiometric sensors. Hence, impedimetric biosensors have potential for simple, rapid, label-free and low cost detection of biomolecules.

1.8 Performance criteria of biosensor

The performance of a biosensor is evaluated on the basis of various parameters. Significant parameters in evaluating electrochemical biosensor performance are listed below in the Table 1.4 (Thevenot *et al.*, 1999).

Table 1.5 Performance criteria of electrochemical biosensor

Parameter	**Electrochemical biosensor**
Specificity	Ability of sensor to detect a particular analyte in presence of another anayte.
Selectivity	The extent to which other substances interfere with the determination of a substance according to a given procedure.
Sensitivity	A sensor's sensitivity indicates how much the sensor's output changes when the input quantity being measured changes.
Dynamic range	Concentration range over which signal varies in a monotonic manner with analyte concentration.
Limit of detection, LOD	Lowest concentration of the analyte which can be measured at a specific confidence level.
Limit of quantification, LOQ	The lowest concentration level at which a measurement is quantitatively meaningful, normally more than the LOD.
Response Time	It is the time necessary to reach 90% of the steady-state response.
Reproducibility	Reproducibility is the ability to obtain the same response with repeated measurements of a same analyte concentration.
Reusability	The ability of biosensors to use them most number of times with same efficiency.

1.9 Electrochemical impedance spectroscopy (EIS)

EIS is a very powerful tool for the analysis of interfacial properties related to bio-recognition events occurring at the modified surfaces. As compared to other electrochemical methods such as cyclic voltammetry (CV) or differential pulse voltammetry (DPV), EIS is less destructive to the measured biological interactions (Bogomolova *et al.*, 2009). EIS detects antibody-antigen interaction as electrical signals directly, and does not require a label or other pre-treatment process. The easy and rapid detection aspect of EIS promises the application of easy diagnosis (Daniels and Pourmand, 2007). EIS analyzes the resistance and capacitance that occurs at the electrode surface, which is very sensitive to biological binding events. This feature makes EIS suitable for measuring antibody-antigen interaction. To date, several immunosensors based on EIS have been developed (Lisdat and Schäfer, 2008; Qi *et al.*, 2010). Label-free detection for biological and chemical analysis has been reported to detect bio-toxins (Mohd Syaifudin *et al.*, 2009) and food products was also evaluated by electrical impedance (Li *et al.*, 2011).

1.9.1 Basics of impedance spectroscopy

The impedance (Z) of a system is generally determined by applying a voltage perturbation with small amplitude and detecting the current response. From above definition, Z is the quotient of the voltage–time function V (t) and the resulting current-time function I (t) given by Equation 1.1

$$Z = \frac{V(t)}{I(t)} = \frac{V_0 \sin(2\pi ft)}{I_0 \sin(2\pi ft+\varphi)} \qquad (1.1)$$

Where V_0 and I_0 are the maximum voltage and current signals, f is the frequency, t is the time, and φ is the phase shift between the voltage and current functions. The impedance (Z), accounts for the combined opposition of all the components within the electrochemical cell (resistors, capacitors, inductors) to the flow of electrons and ions. In an electrochemical cell, electrode kinetics, redox reactions, diffusion phenomena and molecular interactions at the electrode surface can be considered analogous to the above mentioned components that impede the flow of electrons in an ac circuit (Macdonald, 1987). However, specifically in impedimetric immunosensor, the contribution from inductance is of minor importance. Impedance is usually expressed as a complex number, where the ohmic resistance is the real component and the capacitive reactance is the imaginary one. The most popular formats for

evaluating electrochemical impedance data are the Nyquist and Bode plots. In the Nyquist plot, the imaginary impedance component Z'' (out-of-phase) is plotted against the real impedance component Z' (in-phase) at each excitation frequency as shown in Figure 1.6.

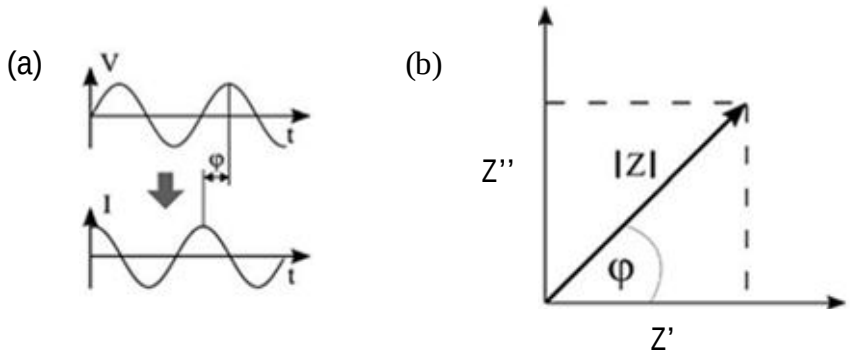

Figure 1.6 (a) Voltage and current waveforms and (b) Impedance expressed as the modulus |Z| and the phase angle φ.

Capacitive biosensors are usually referred to a subcategory of impedance biosensors in which the changes in capacitance value are measured indirectly. Capacitive immunosensor exploit the change in dielectric properties and/or thickness of the dielectric layer at the electrode-electrolyte interfaces. An electrolytic capacitor (working electrode/dielectric/electrolyte; the second plate is represented by the electrolyte) allows the detection of an analyte specific to the receptor that has been immobilized on the insulating dielectric layer, which has previously been deposited on the surface of the working electrode (Berggren *et al*., 2001; Katz and Willner, 2003; K'Owino and Sadik, 2005). Ideally, this configuration resembles a capacitor and its ability to store charge. The electric capacitance between the working electrode and the electrolyte is given by Equation 1.2.

$$C = \frac{\in_o \in A}{d} \qquad (1.2)$$

Where ε, is the dielectric constant of the medium between the plates, ε_o, is the permittivity of free space (8.85419 pF/m), A, is the surface area of the plates (m^2) and d, is the thickness of the insulating layer (m).

1.9.2 EIS measurement

Electrochemical sensors are part of an electrochemical cell that consists of either three electrode or two electrode. A typical three electrode electrochemical cell consists of a

working electrode of a chemically stable, solid, conductive materials such as Pt, Ag, or graphite; a reference electrode, usually consisting of silver metal coated with a layer of silver chloride (Ag/AgCl); and a platinum wire auxiliary electrode. The reference electrode is usually further removed from the site of the redox reaction in order to maintain a known and stable reference potential. One advantage of this system is the charge from electrolysis passes through the auxiliary electrode instead of the reference electrode, which protects the reference electrode from changing its half-cell potential. A two electrode system has only the working and reference electrode. If the current density is low enough, then the reference electrode can carry the charge with no adverse effects. Both three electrode systems as well as two electrode systems are used for sensors. However, two electrode systems are generally preferred for disposable sensor because long-term stability of the reference is not needed and the cost is lower. In impedance biosensors, the applied voltage V(t) should be quite small, usually 10 mV in amplitude or less for several reasons. First, the current-voltage relationship is often linear only for small perturbations (Barbero *et al.*, 2005), and only in this regime impedance is strictly defined. A second reason for using a small excitation signal is to avoid disturbing the probe layer. Covalent bond energies are on the order of 1-3 eV but probe-target and electrode-probe binding energies can be much less and applied voltages will apply a force on charged molecules. Correctly performed EIS does not damage or even disturb the biomolecular probe layer, which is an important advantage over voltametry or amperometry where extreme voltages are usually applied.

1.9.2.1 Interpretation of EIS data

The detection technique used in this thesis is based on the EIS. This technique involves the application of a sinusoidal voltage across the electrode and measuring the current. The impedance is calculated from voltage and current according to Ohm's law as given in Equation 1.3.

$$Z = V / I = Z' + j\,Z'' \qquad (1.3)$$

Where the impedance, Z is generally a frequency-dependent phasor composed of a real term Z' (related to the resistive behaviour of the system) and an imaginary term Z″ (in the absence of inductive terms, such as our case, it is only related to the capacitive behaviour of the system). In order to interpret the data, we make use of equivalent circuits. An equivalent circuit is the expression of the physical system parameters in terms of electrical components,

mainly resistors, capacitors, or constant phase elements, to name but the most relevant to the present case. These elements are arranged in series or in parallel depending on how and when different events occur in the system under study. The data interpretation via equivalent circuits is broadly accepted.

1.9.2.2 Labelled *vs* label-free detection

Most biosensors require a label attached to the target; during readout the amount of label is detected and assumed to correspond to the number of bound targets (Daniels and Pourmand, 2007). Labels can be fluorophores, magnetic beads and active enzymes with an easily detectable product. However, labelling a biomolecule can drastically change its binding properties and the yield of the target-label coupling reaction is highly variable (Haab, 2003). This requires two probes that bind to different regions of the target, yielding enhanced selectivity, but increasing development costs and limiting use in research settings. The first probe is immobilized on the solid support, the analyte is introduced and then a secondary probe is introduced after washing. This second probe is labelled or can be detected by introducing yet another labelled probe that binds to all the secondary probes. Labelling requires extra time, expense and sample handling. Whereas, in label-free system a target molecule interacts with a bio-probe functionalized surface resulting in changes in the electrical properties of the surface exclusively from the presence of the target molecule. Moreover, label-free operation enables detection of target-probe binding in real time (Skladal, 1997), that is generally not possible with label-based systems.

1.9.2.3 Faradaic *vs* non-faradaic response

Generally, impedance measurement is divided into two categories: faradaic and non-faradaic (Yang *et al.*, 2004). In electrochemical terminology, a faradaic process is one where the charge is physically transferred across an interface, usually in the form of an electron transfer from the electrode to an ion in solution or vice versa. However, transient currents can flow without actual charge transfer in non-faradaic processes (e.g. as in charging a capacitor). In the electrical domain, a perfect non-faradaic interface is represented by a capacitor, and a faradaic interface is represented by a resistor. Actual electrode-solution interfaces can have both faradaic and non-faradaic components. Faradaic requires a redox probe for impedance measurement, while non-faradaic measurement can be performed in the absence of a redox probe. In the absence of an added redox probe, the interfacial capacitance adopted at an

electrode immersed in electrolyte can be used as a sensitive function of surface change such as those associated with a binding event (Berggren *et al.*, 2001). Any target induced capacitance modulation arises from accompanying changes in dielectric constant, charge distribution, electrolyte or water penetration when it adsorbs, though practically simpler (in the sense that no redox probe needs to be added to the analytical solution), and thus more practical from an end user perspective. Impedance biosensor to detect *E.coli* O157:H7 using a high density microelectrode array without using any redox probe was reported (Radke and Alocilja, 2005). AFM1 detection in the ppt range was reported by non-faradaic impedance measurement (Vig *et al.*, 2009). The term capacitive biosensor usually designates a sensor based on such a non-faradaic scheme and usually refers to one that makes measurements at a single frequency.

1.9.2.4 Equivalent circuit analysis for EIS

The performance of an electrochemical cell is represented by an equivalent circuit that has the same behaviour as the real cell under a given excitation (Yang *et al.*, 2003). The electrical parameters generally used to design an equivalent circuit model for electrochemical curve fitting includes primarily electrolyte resistance (R_s) (bulk medium resistance) and double layer capacitance (C_{dl}) These factors contribute to the equivalent circuit model representing the experimental impedance data. In two electrode system, a simple equivalent circuit consisting of a resistor and a capacitor in series represents the behaviour of the impedance test when immersed in a conductive medium (Yang and Basir, 2008). The types of electrical components in the model and their interconnections control the shape of the equivalent circuit's impedance spectrum, and the circuit parameters control the size of each feature in the spectrum. Both of these factors affect the degree to which an equivalent circuit model represents the experimental impedance data, while more than one circuit model can fit the experimental data, a unique equivalent circuit is selected based on the circuit parameters best explaining the electrochemical cell's physical characteristics. A simple electrical equivalent circuit was reported for non-faradaic impedance measurement for the detection of *Salmonella typhimurium* (Yang *et al.*, 2003). In such a case, the non-faradaic path is active and no electrochemical reaction on the electrode surface occurs. For non-faradaic impedance measurement, a simple equivalent circuit consists of a series combination of medium resistance (R_s) and the double layer capacitance (C_{dl}) was presented as shown in Figure 1.7.

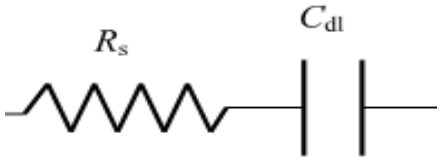

Figure 1.7 An equivalent circuit for non-faradaic impedance measurement.

1.9.2.4.1 Double-layer capacitance (C_{dl})

When a charged surface is in contact with an electrolyte, it attracts ions of opposite charge. This attractive tendency is opposed by the randomizing thermal motion of the ions, resulting in a build-up of ions with opposite charge near the surface. This local charge imbalance prevents the electric field generating from the charged surface from penetrating very far into solution. The characteristic length of this spatial decay of the electric field is called the Debye length. The locally-enhanced population of ions acts like the second plate of a capacitor, and the charge-voltage ratio is termed the double layer capacitance or diffuse layer capacitance.

1.9.2.4.2 Constant phase element (CPE)

The impedance results for a solid electrode/electrolyte interface often reveal a frequency dispersion that cannot be described by simple elements such as resistance and capacitance. The frequency dispersion is generally attributed to a "capacitance dispersion" expressed in terms of a constant-phase element (CPE). The CPE behaviour is generally attributed to distributed surface reactivity, surface inhomogeneity, roughness or fractal geometry, electrode porosity, and current and potential distributions associated with electrode geometry (Jorcin *et al.*, 2006). CPE was used to model double layer capacitance of electrodes. This is commonly favoured over the use of a simple capacitor (Gawad *et al.*, 2004). The complex impedance of a CPE is given by Equation 1.4.

$$Z_{CPE} = \frac{1}{(j\omega)^m A} \qquad (1.4)$$

Where A is analogous to a capacitance, ω is the frequency expressed in rad/sec, and m, is the CPE phase parameter. It can easily be seen that m=1 corresponds to a capacitor; m for capacitor modelling is typically between 0.85 and 0.98. Solid electrodes can be expected to have a certain amount of CPE behaviour, and thus modelling the electrode-solution interface as purely capacitive is simplistic and can reduce the quality of data fitting.

1.10 Summary of reported impedimetric biosensors

In this thesis, a miniaturized immunosensor was developed for various analytes with two electrode setup and a microfabricated device such as interdigitated electrodes and coil electrodes. Table 1.5 summarizes many researcher's efforts as published in the technical literature related to impedance biosensor.

Table 1.6 Summary of reported impedimetric biosensors

Electrode/ Measurement type	**Target**	**LOD**	**References**
ID-electrode, Non-faradaic	hIgG	50 ng mL^{-1}	Taylor *et al*., 1991
IDEs array, Non-faradaic	*E. coli*	7.4 × 04 CFU mL^{-1}	Varshney and Li, 2007
2-electrode, Non-faradaic	α-fetoprotein	50 ng mL^{-1}	Maupas *et al*., 1997
3-electrode, Faradaic	thrombin	3.6 ng mL^{-1}	Cai *et al*., 2006
3-electrode, Faradaic	Peanut protein Ara h 1	0.3 nM	Huang *et al*., 2008
3-electrode, Faradaic	AFM1	1 ng mL^{-1}	Dinçkaya *et al*., 2011
Biosensor chip, Faradiac	Prostate-Specific Antigen (PSA)	1 pg mL^{-1}	Chornokur *et al*., 2011
IDEA, Non-faradaic	*E. coli* O157:H7	3×10^{2} CFU mL^{-1}	Dastider *et al*., 2013
IDE, Non-faradaic	Atrazine	8.34 ± 1.37 μg L^{-1}	Valera *et al*., 2007
IDE, Non-faradaic	Sulfonamide	10 μg mL^{-1}	Bratov *et al*., 2008

1.11 Scope of research

Conventional techniques are available for quantification and identification of target analyte such as toxin, bacteria etc. These methods have some limitations such as low sensitivity, poor

detection limit and long analysis time. Moreover, it is not suitable for on-site monitoring. Therefore, the current research is focused on rapid, reliable, specific, sensitive and label-free methods of detecting a target analyte at low cost. It is also desired that the device should be simple and inexpensive to design and manufacture. Biosensor technology is claimed to satisfy these requirements. Electrochemical sensors are good choice due to their fast, simple, and low-cost detection capabilities for biological binding events.

In order to design and manufacture miniaturized biosensors, the transducer or the electrode needs to be small and portable. Shrinking electrode dimensions may lead to higher sensitivity (Grieshaber *et al*., 2008). Very less sample volume (on the order of microlitres or less) is required to detect when small electrodes are used (Farrell *et al*., 2004). Thus, it results in a reduction of both the time and cost of analysis. The miniaturization trend of biosensor instruments is adapted by miniaturization through microfabrication techniques, such as micro-electromechanical systems (MEMS). In this thesis, the effect of miniaturization has been demonstrated by reducing the size of electrodes (millimetre to micrometer) as well as electrochemical cell from custom made glass cell to 384 micro well plates. The sample volume was further reduced from 700 µL to 0.4 µL.

1.12 Gaps in existing research

In the light of literature survey, it is clear that;

1. There is a need for a simple biosensing approach that can be realized as sensitive yet low cost technique.
2. Bioelectronic based biosensor devices (such as IDEs) have emerged as potential tool for field applications based on signal transduction in antibody-antigen interactions, protein-protein interaction, intercellular reactions and many other complex biological reactions for qualitative and quantitative analysis. However, their application in field analysis is not much studied.
3. While significant progress has been demonstrated for few analyte detection using MEMS based biosensors, multianalyte multicomponent detection systems for biological applications using a single platform are yet to be explored (such as simultaneous analysis of a mixture of analytes within the given sample on a single device).

4. Reported biosensors need improvement in stability, sensitivity and better interface with biological substances.

1.13 Objectives of the present research

1. Development of novel miniaturized Ag wire based immunosensor for toxin detection.
2. Development of IDEs biosensor for sensitive detection of aflatoxins.
3. Development of a biochip based device for detection of glucose as model analyte.

1.14 Outline of thesis

The thesis comprises six chapters and each of these chapters has been described below:

Chapter 1 Introduction: About biosensors, classification of biosensors, affinity biosensor, transducers, electrochemical impedance spectroscopy (EIS), basics of EIS and faradaic and non-faradaic impedance biosensor. This chapter also discusses about gaps in the existing research and what more needs to be done, objective of the proposed doctoral work and thesis structure.

Chapter 2 Development of a novel two electrode based setup for quantification of antibody-antigen interaction: Brief description about biosensor construction, material selection, surface characterization of bare and modified electrode, electrochemical characterization of the modified electrode, sensing principle of the immunosensor, optimization of the immunosensor conditions and proof of concept of two electrode setup by EIS study of antibody- antigen interaction for AFM1 as model analyte.

Chapter 3 Development of impedimetric biosensors using two electrode setup for analysis of aflatoxins and bacteria: Importance of mycotoxins, aflatoxin M1 and B1, limits set by regulatory agencies, techniques for aflatoxins detection, validation of sensor operation, determination of AFM1 in milk and AFB1 in peanut by EIS techniques, equivalent circuit analysis, AFM1 detection in various milk product and *E.Coli* detection in water.

Chapter 4 Development of micro interdigitated electrodes (µ-IDEs) array impedimetric immunosensor for detection of AFM1: Introduction, comparison of macroelectrode and microelectrode, micro interdigitated electrodes, materials and geometry of IDEs, EIS study with IDEs, IDEs sensing principle, fabrication of IDEs, surface characterization, optimization

of IDEs immunosensor, IDEs immunosensor for analysis of AFM and proficiency test on developed IDEs device for unknown sample.

Chapter 5 Development of a novel coil microelectrode array (CMEA) biosensing device: Introduction, microelectrode material and geometry, reported work on microelectrode array, device fabrication in brief, measurement of ionic conductivity using the device by EIS technique, principle of glucose sensing, construction of monolithic glucose biochip, optimization of glucose biochip parameters, EIS study of glucose biochip, equivalent circuit analysis and analysis in real samples.

Chapter 6 Conclusions and future scope of work: This chapter presents a review of all the five chapter's conclusions and proposes the future scope of work**.** An outline of the different stages undertaken in this thesis to meet the aims and objectives is shown in the flowchart below (Figure 1.8).

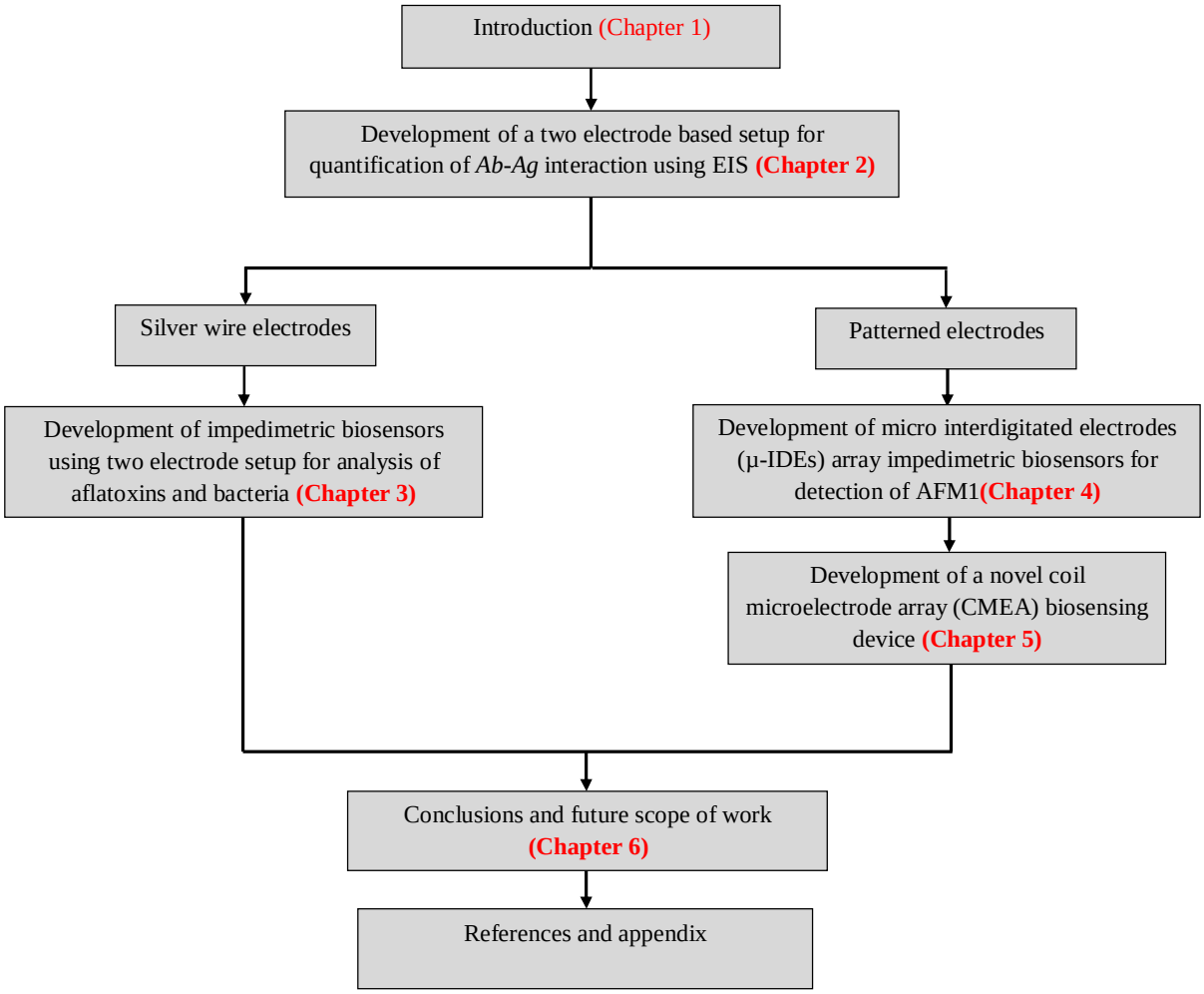

Figure 1.8 Flowchart detailing the different stages of the work in this thesis.

Chapter 2

Development of a novel two electrode based setup for quantification of antibody-antigen interaction

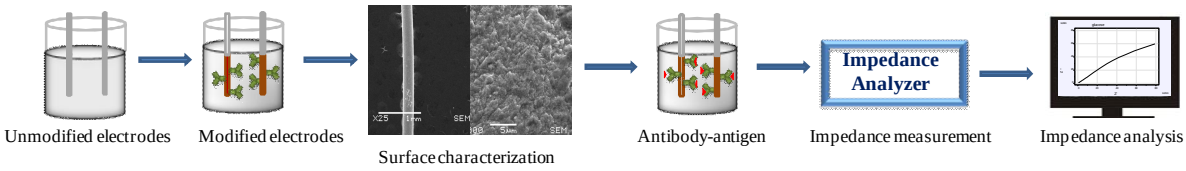

Graphical abstract of chapter content

2.1 Background

Electrochemical biosensors contain a biological recognition element such as enzymes, antibodies, nucleic acids, cells and tissues. These recognition elements also known as receptors selectively interact with the target analyte and produce an electrical signal that is related to the concentration of the analyte. Electrochemical biosensors are divided into two main categories based on the nature of the biological recognition process, i.e. biocatalytic and affinity biosensors as described in chapter 1. Biocatalytic devices incorporate enzymes, whole cells or tissue that recognize the target analyte and produce electro-active species. Affinity biosensors are based on selective interaction between the analyte and a biological component such as antibody or aptamer. Many biochemical analytes of interest are not amenable to detect by enzyme electrodes due to the lack of sufficiently selective enzymes being available for the analyte. Therefore, affinity biosensors have become an obvious choice. An affinity biosensor uses selective biomolecules such as antibodies, membrane receptors or oligonucleotides that strongly binds with a target analyte to produce a measurable electrical signal. Immunosensors are antibody based affinity biosensors, where the detection of a target analyte is brought about by its binding to a region of an antibody. Immunosensors are well known among analytical methods for their extremely low detection limits (Ronkainen-Matsuno *et al*., 2002). Immunosensors are extensively reported for both quantitative and qualitative detection at trace levels (Holford *et al*., 2012; Hervás *et al*., 2012).

This chapter presents construction and characterization of a two electrode based impedimetric immunosensor for quantification of antibody-antigen interaction considering AFM1 as model analyte.

2.2 Immunosensor construction

Design, construction methodology and materials science are closely linked with immunosensor development. This chapter describes the construction of a simple, sensitive and low cost impedimetric immunosensor based on EIS technique. An electrochemical biosensor usually consists of a transducer such as a pair of electrodes, an interface layer incorporating the biological recognition element and a protective coating. The surface of the biosensor device was characterized by SEM and FT-IR spectra. The selection of electrode material and modification of electrode is crucial for immunosensor function and performance.

2.3 Materials and instrumentation

All the chemicals used were of analytical grade and were used as received. Ag wire (diameter = 0.25 mm) was procured from ACROS Organics, USA. Anti AFM1 fractionated antiserum primary monoclonal antibody (mAb) raised from rat, Anti-rabbit (Rat) Fluorescein isothiocyanate (FITC) conjugated secondary antibody (pAb-FITC) were purchased from AbCam (UK). AFM1 standard, Tween20, 11-MUA, 1-ethyl-3-[3-dimethylaminopropyl] carbodiimide hydrochloride (EDC), N-hydroxy succinimide (NHS), certified reference material (CRM) ERM-BD 282 (AFM1 in whole milk powder <0.02 µg kg^{-1}) were purchased from Sigma–Aldrich, USA. Ethyl Alcohol 200 proof was purchased from TEDIA, USA. Hydrogen peroxide (H_2O_2) 30 % (w/v), acetonitrile (ACN) HPLC grade, di-sodium hydrogen phosphate (Na_2HPO_4), sodium di-hydrogen phosphate (NaH_2PO_4) from MERCK (Germany) and sodium hypochlorite (4 %) solution were purchased from Fisher Scientific (India). For sample handling, micropipettes (eppendorf ®, Germany) were used. Centrifugation of milk sample was done by minispin (eppendorf ®, Germany). Shaking and filtration of the samples were done by Spinix shaker (Tarsons, India). For the handling of AFM1 standard solution, glove box (Cole Parmer, USA) was used. For preparing all the solutions, water produced in a Milli-Q system (Millipore, Beford, MA, USA) was used. Certified ultra high pure nitrogen (99.9 %), pH meter (Seven Multi Mettler Toledo, 8603, Switzerland) was used. (FT-IR) spectra were recorded using FT/IR-4100 type A (JASCO, Japan) with attenuated total reflectance (ATR) attachment ATR PRO450-S. Fluorescence images were taken with an upright microscope (BX-51Olympus, Japan). Impedance measurements were carried out using IVIUM CompactStat impedance analyzer, Netherland. The surface morphology of the electrode was characterized by using a JEOL (JSM 6560 LV) SEM operated at an accelerating voltage of 20 kV.

2.4 Experimental setup

The measurement setup constitutes a pair of functionalized Ag and copper (Cu) wire electrode of diameter 0.25 mm, dipped in the analyte solution confined in cell by 10 mm, and separated by a distance of 1mm. The electrode setup and the glass cell were enclosed in a custom made Faraday cage. The monoclonal antibodies (mAb) was covalently coupled on Ag and Cu wire electrode through SAMs is described in chapter 3. The functionalized Ag and Cu wire electrodes were connected to IVIUM CompactStat impedance analyzer in 4-Electrode mode controlled through software (IVIUM soft) loaded on a laptop computer. In the 4-

Electrode mode, the first electrode was configured as working electrode (working and sense electrode combined together) and second electrode was reference electrode (reference and counter combined together).

2.5 Results and discussion

2.5.1 Selection of electrode material

In EIS, traditionally, macro sized metal rods or wires has been used as electrodes which are immersed in the medium to measure impedance (Towe and Pizziconi, 1997; Berggren *et al*., 1998). Therefore, the choice of electrode material is crucial in construction of impedimetric immunosensor for better performance in terms of sensitivity and selectivity. Metals such as Pt, Au (Kim *et al*., 2000), Ag (Brunelle, 2001) and stainless steel have been reported as electrode materials due to their excellent electrical and mechanical properties. Electrode materials such as, Ag and Cu wire has been tested for biosensor construction. The choice of materials was based on biocompatibility, low cost and ease of construction or fabrication of sensors. Figure 2.1 shows the impedance response of antibody attached to silver and copper wire electrode. It is clear from the figure that the impedance response of silver is higher than Cu electrode for same antibody dilution. A capacitive behaviour at low frequency was observed for Ag wire electrode from phase plot, shown in Figure 2.2. This is desirable for a non-faradaic impedance measurement. Hence, Ag wire was chosen as electrode material for the subsequent development of immunosensor.

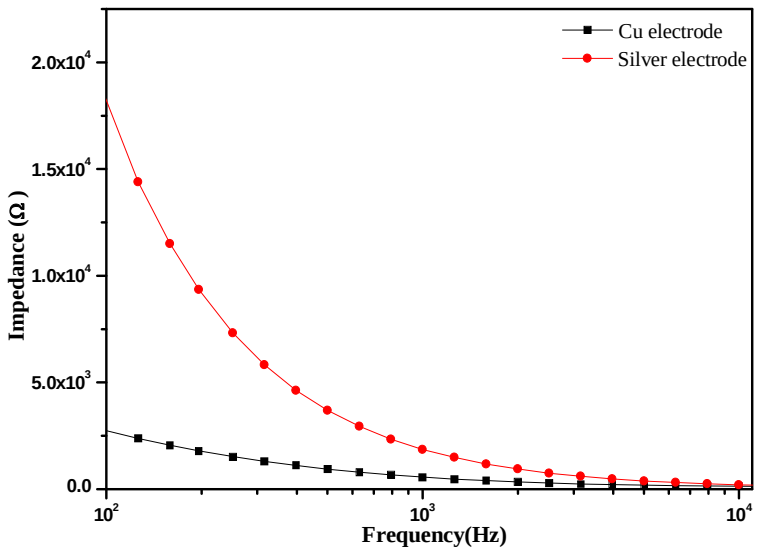

Figure 2.1 Impedance plot after antibody attachment for Ag and Cu wire electrode. EIS: 100 Hz to 10 kHz at 10 mV ac potential.

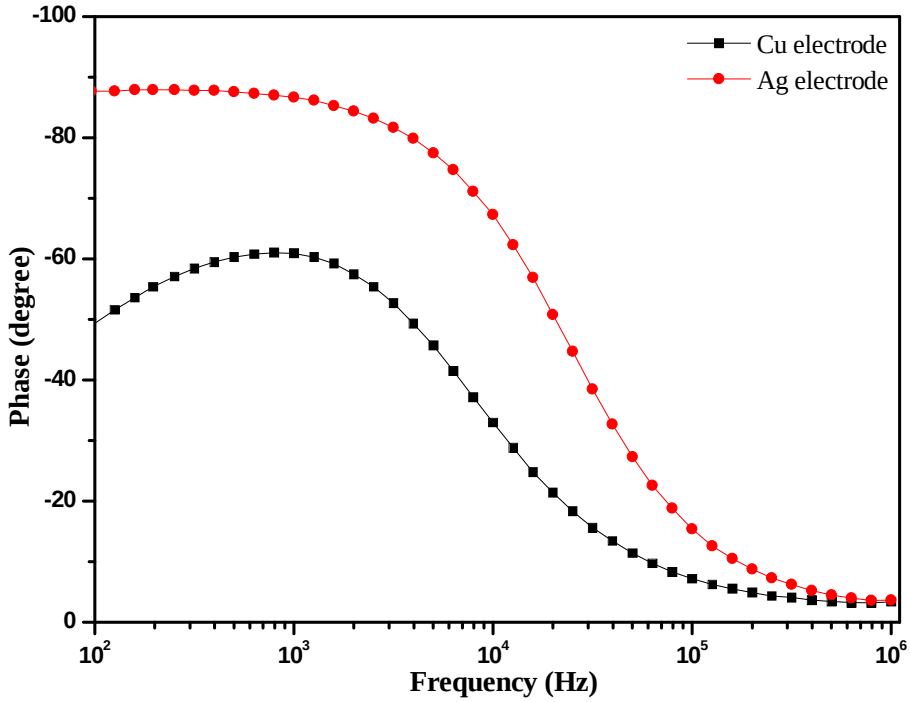

Figure 2.2 Phase plot after antibody attachment for Ag and Cu wire electrode. EIS: 100 Hz to 1 MHz at 10 mV ac potential.

2.5.2 Surface characterization of modified electrodes

To construct impedimetric immunosensor for various analytes, Ag wire electrode surface was modified with 11-MUA SAMs and 1° anti- mAb (specific antibody) was attached as a bio-recognition element. The modified surface was examined by SEM, FT-IR, and fluorescence to confirm the changes in surface morphology. Figure 2.3 (a) shows the SEM micrograph of the bare Ag wire electrode at magnification 25× and (b) shows the bare clean electrode surface at magnification 3000× (c) self assembly of 11-MUA on Ag wire electrode at magnification 3000× and (d) SEM after attachment of 1° anti-AFM1 mAb. It is clearly evident from Figure 2.3 (a) and (b) that the surface of the electrode was very clean before functionalization. Figure 2.3 (c) confirms the effective self assembly formation on the electrode surface. Further, it is also clear from Figure 2.3 (d) that 1° anti-AFM1 mAb were successfully attached to the electrode and was uniformly covered.

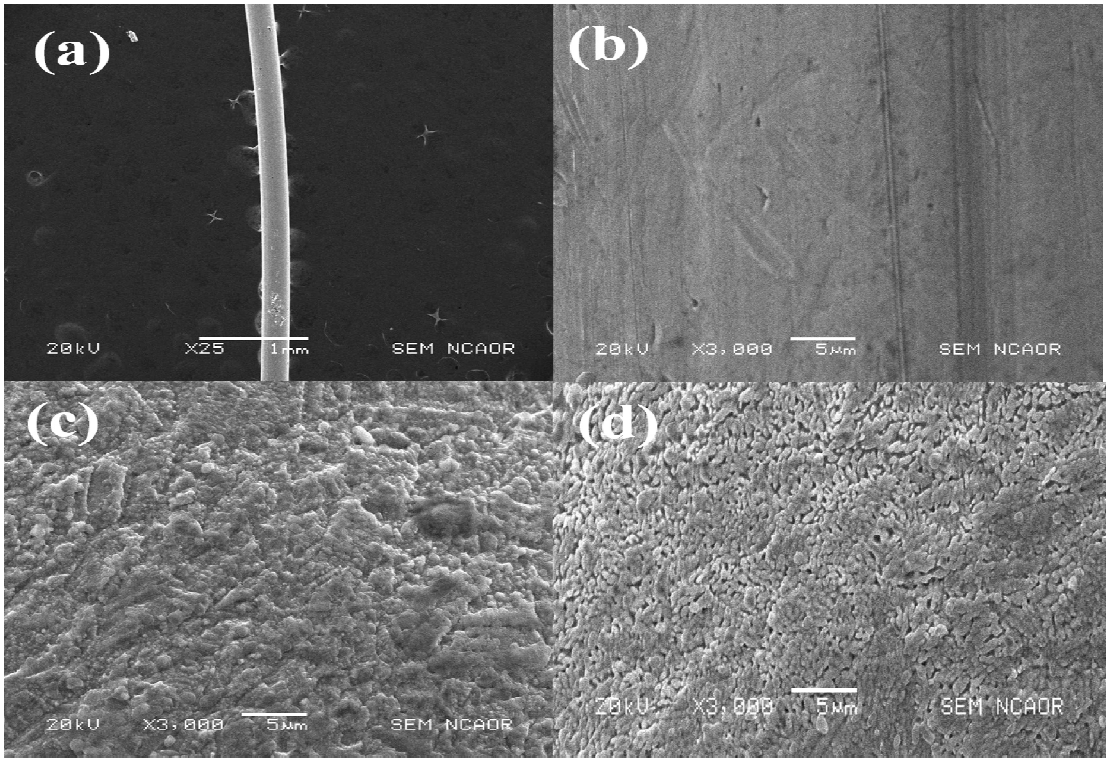

Figure 2.3 SEM micrograph Ag wire electrode (a) bare Ag wire electrode at magnification 25× (b) bare clean electrode surface at magnification 3000 × (c) self assembly of 11-MUA on Ag wire electrode at magnification 3000× and (d) SEM after attachment of 1° anti-AFM1 mAb.

Further, the carbodiimide cross-linking reaction to form the 11-MUA-mAb conjugated structure on Ag wire electrode surfaces was confirmed by ATR FT-IR. The spectra were acquired with 45° angle of incidence using 154 scans at 4 cm^{-1} resolution collected under vacuum conditions. The FT-IR spectra are shown in Figure 2.4. The FT-IR spectrum of the Ag wire treated with 11-MUA is shown in Figure 2.4 (i). It showed C-H stretches in asymmetric and symmetric modes at 2924 cm^{-1} and 2854 cm^{-1} respectively. The C=O stretch at 1734 cm^{-1}, associated with asymmetric (1647 cm^{-1}) and symmetric (1542 cm^{-1}) COO^- stretches, is characteristic of an organic carboxylic acid compound. The additional IR peaks at 1455 cm^{-1} and 1257 cm^{-1} is ascribed to C-H deformation and C-O stretch respectively. Upon immobilization of mAb in Figure 2.4 (ii) new absorption bands appeared; three IR bands at 1638 cm^{-1}, 1536 cm^{-1}, and 1263 cm^{-1} is ascribed to the absorption by the amide group that links mAb to 11-MUA functionalized Ag wire.

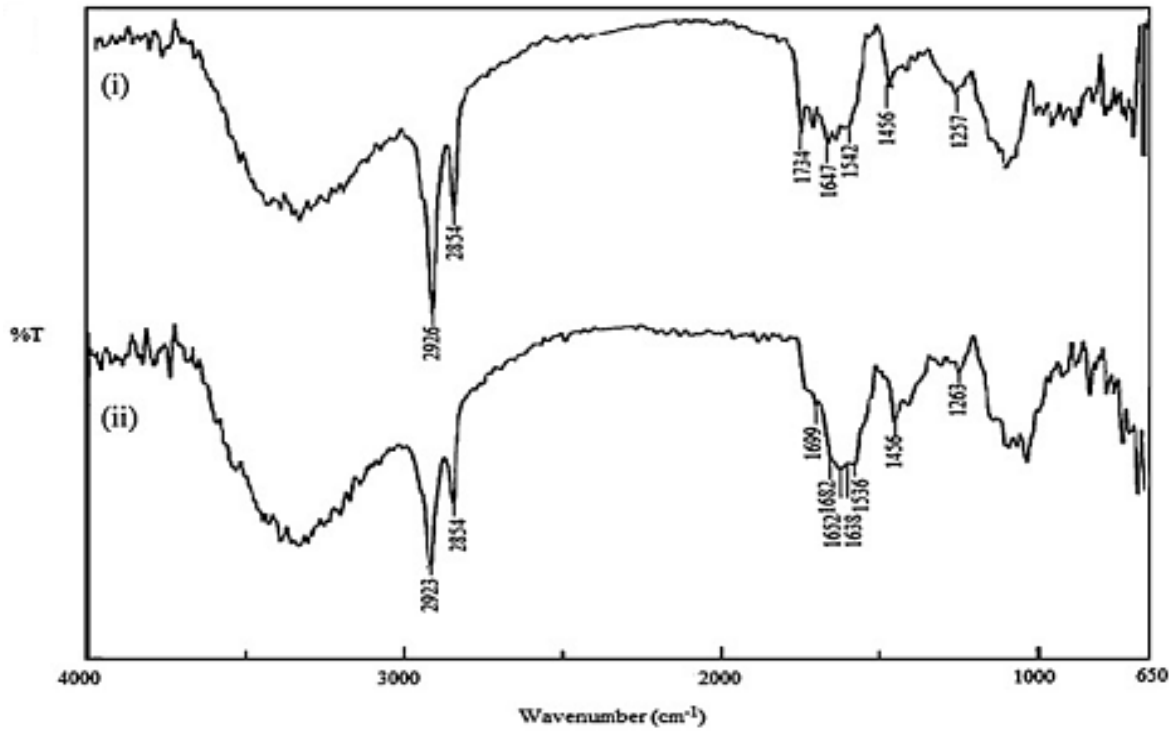

Figure 2.4 The ATR FT-IR spectrum of (i) the Ag wire treated with 11-MUA (ii) mAb coupled through 11-MUA functionalized Ag wire. Spectra were acquired with 45° angle of incidence using 154 scans at 4 cm^{-1} resolution collected under vacuum conditions.

The binding of mAb to Ag wire was also confirmed by fluorescence microscopy as shown in Figure 2.5. Two functionalized Ag wires (reference wire without mAb and sample wire coupled with mAb) were incubated with pAb-FITC (1: 64000) for 2 hrs at room temperature. Before excitation, both reference and the sample wire were rinsed with 0.01 M PBS to remove unbound pAb-FITC. Figure 2.5 (i) shows fluorescence image of reference and (ii) the sample Ag wire, after excitation. The binding of the pAb-FITC to the mAb of the thiolated Ag wire was clearly distinguished from the fluorescence images.

2.5.3 Electrochemical characterization of SAMs

Nyquist spectra for the bare Ag electrode and modified Ag electrode with 11-MUA is shown in Figure 2.6. The long-chain molecules of 11-MUA not only acted as the electron-transfer barrier but also as a capacitor. It was observed that the charge transfer resistance (R_{ct}) for 11-MUA modified electrode was larger than that of bare electrode, which was confirmed from larger semicircle response. This may be attributed due to the formation of the monolayer on the Ag surface that. It can also be seen that the semicircular diameter enlarged due to the –COOH terminated self assemblies, implying a high R_{ct}.

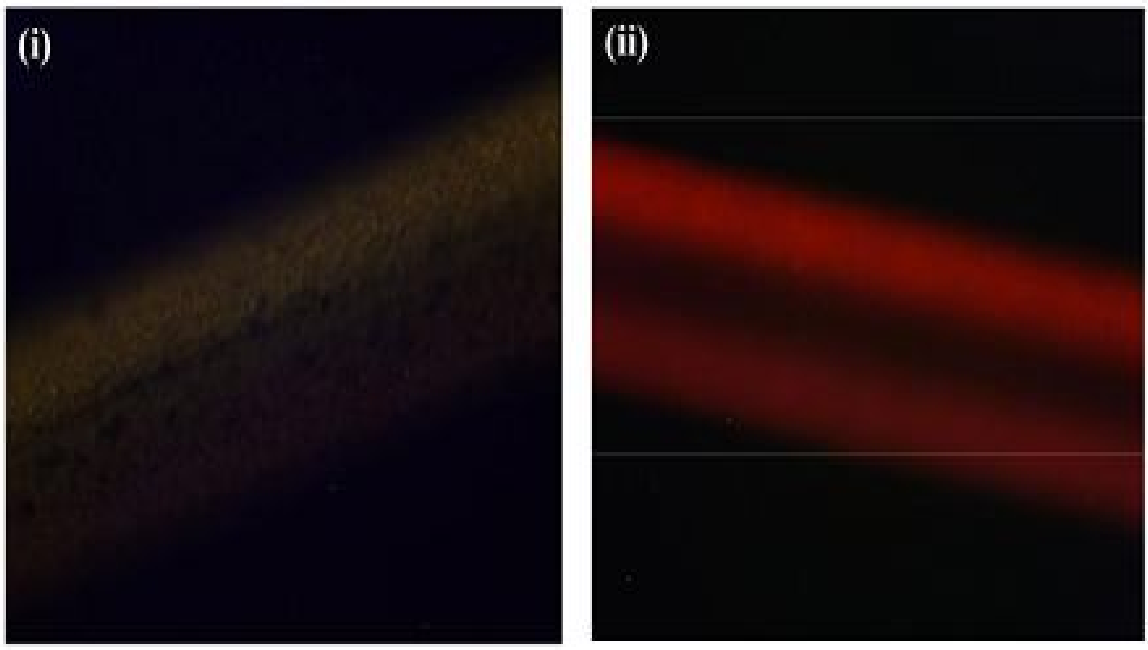

Figure 2.5 (i) Dark field image of the reference wire without mAb, (ii) fluorescence image of the sample wire coupled with mAb; captured using pAb-FITC (λ_{ex} 490 nm / λ_{em} 520 nm).

2.5.3.1 Effect of voltage on SAMs

The effect of voltage on SAMs was studied using EIS technique. Figure 2.7 represents the Nyquist plot of SAMs modified electrode at different time upon continuous applied voltage. It is evident from the figure that the semicircle diameter decreases, when voltage was applied for a longer time. This also indicates that the SAMs layer is distorted and also unable to provide insulation to the electrode upon continuous applied voltage.

2.5.3.2 Effect of electrode configuration

The effect of electrode configuration on functionalization of either (i) only one electrode or (ii) functionalizing both the electrodes, for non-faradaic impedance response was investigated using EIS. The comparison of Nyquist plot for both cases is shown as Figure 2.8. A large semicircle response was observed indicating large R_{leak}, when both the electrodes were functionalized as compared to single electrode for which a low response was recorded. This high R_{leak} is desirable for non-faradaic impedance measurements. Hence for immunosensor construction both electrodes were functionalized for further studies.

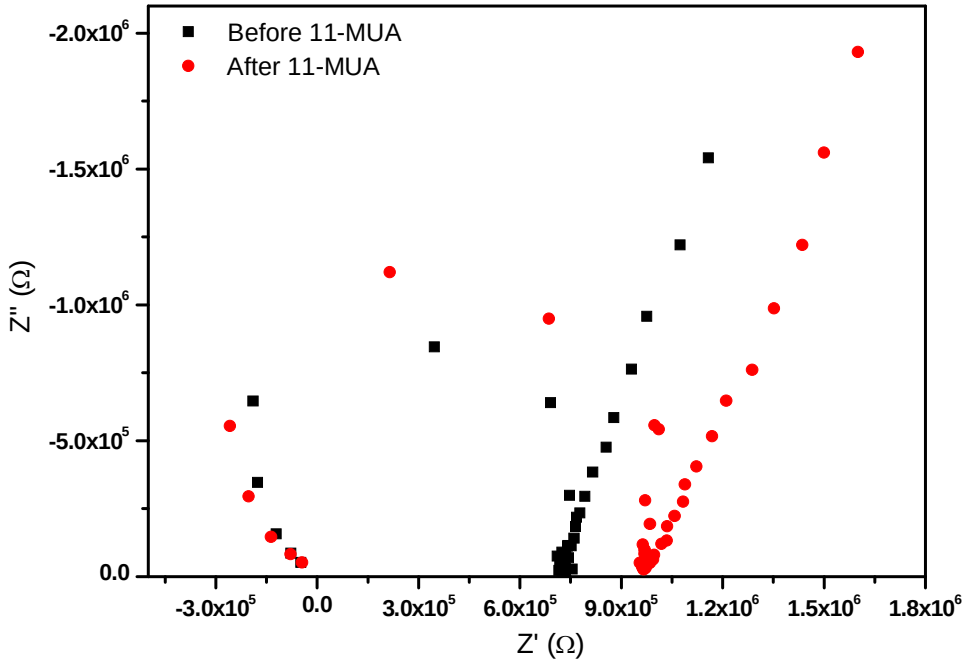

Figure 2.6 Nyquist plot of the electrodes before and after modification by 11-MUA in the frequency range (1 Hz to 100 kHz) in ethanolic medium at 10 mV ac potential in room temperature.

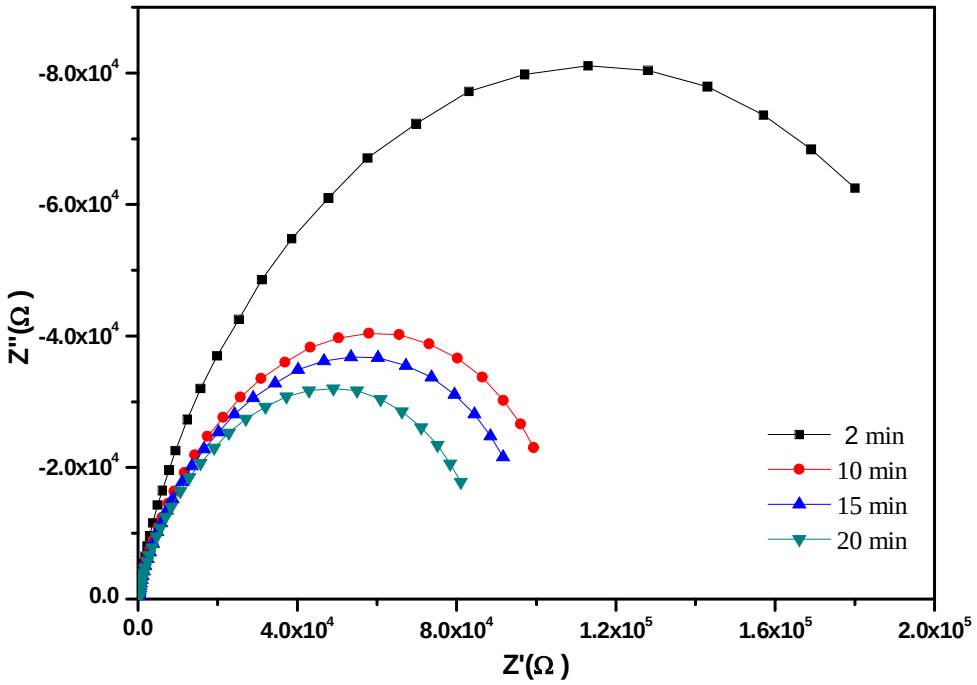

Figure 2.7 Nyquist plot of the electrodes after modification by 11-MUA in the frequency range (1 Hz to 100 kHz) in PBS medium at 10 mV ac potential.

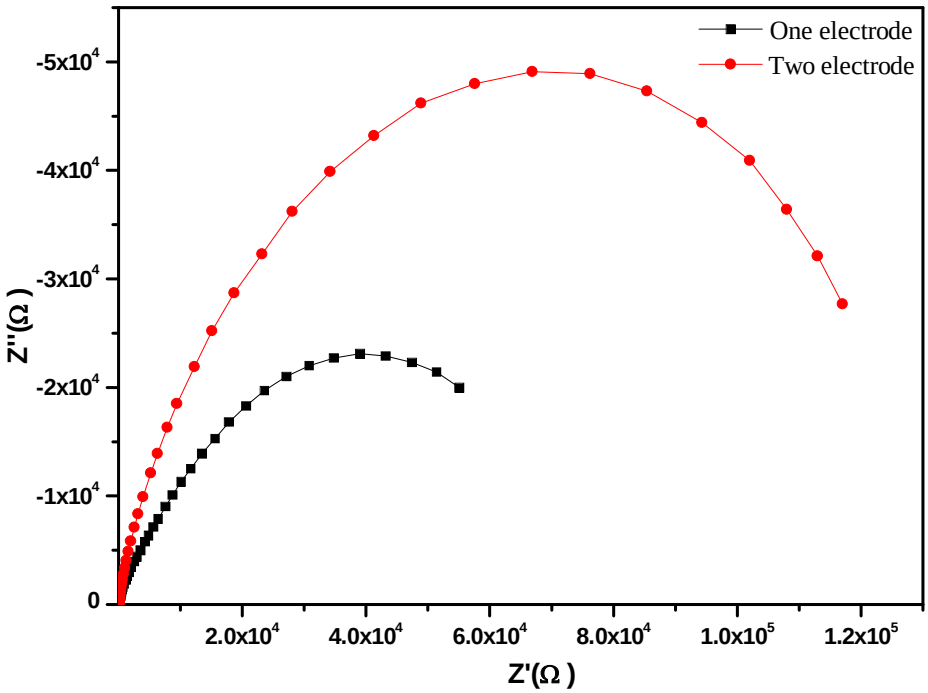

Figure 2.8 Nyquist plot for single and both electrodes modified by 11-MUA in the frequency range (1 Hz to 100 kHz) in PBS medium at 10 mV ac potential.

2.6 Validation of immunosensor

The signal generated in non-faradaic impedance biosensors are mainly due to capacitance changes, hence termed as a capacitive biosensor (Levine *et al*., 2009). Capacitive biosensors mainly focus on electrodes with impedimetric readout (Berggren *et al*., 2001). In their simplest configuration, the electrodes of a capacitance type sensor are two closely spaced parallel plates. The most common type of capacitive biosensors is based on electrode-solution interfaces as they provide a simple, rapid, label-free and inexpensive method for monitoring biological reactions. Impedance measurements are usually employed to exploit changes in dielectric properties and/or thickness of the dielectric layer at the electrode-solution interface due to the probe-target molecules binding. The capacitance at an electrode-solution interface can be described to be built-up of several capacitors in series. The first capacitor, C_{ins}, corresponds to the insulating layer. The second capacitor, C_{rec}, involves the contribution of the surface functionalization layer, the bound probe elements and the double layer. The third capacitor, C_d, represents the diffuse layer, which depend on analyte concentration. Binding of analyte resulted in capacitance change of the recognition layer C_{rec}. The total capacitance C_{tot} can then be described by Equation 2.1

$$\frac{1}{C_{tot}} = \frac{1}{C_{ins}} + \frac{1}{C_{rec}} + \frac{1}{C_d} \qquad (2.1)$$

The total capacitance is governed by the smallest capacitance of the three contributing layers. Therefore, the design of sensitive sensors demands careful selection of the insulating layer, which should have a high dielectric constant resulting in high C_{ins} capacitance values. To validate this concept, the impedance measurement was carried out for every step of biosensor development. Further, the electrode-electrolyte properties have investigated by capacitive sensing, which was extracted from the impedance measurement and shown in Figure 2.9. It is evident from the figure that three capacitances are in series, representing insulating layer, i.e. EDC/NHS, second capacitance was for antibody immobilization and the third capacitance was for antigen concentration. The decrease in total capacitance validates Equation.2.1.

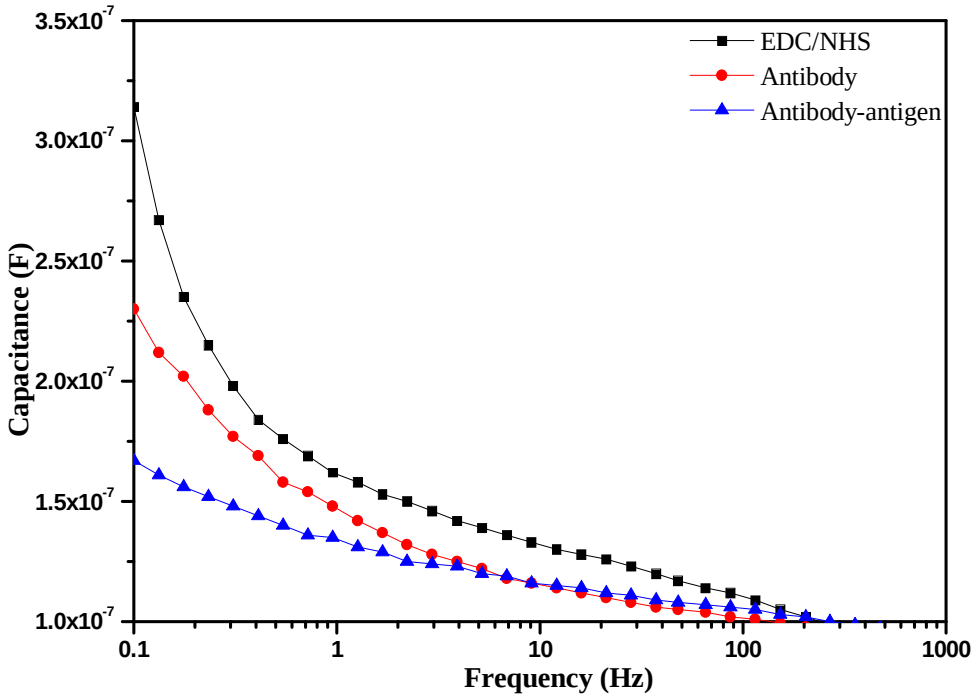

Figure 2.9 Capacitive response of developed biosensor. EIS: 10 mV ac potential, frequency range (0.1 Hz to 1 kHz).

2.7 Optimization of the immunosensor parameters

The impedance / capacitance response resulted from antibody-antigen interaction depends on various parameters such as antibody dilution, frequency range, applied voltage and incubation. The influence of these parameters on immunosensor performance was studied and optimized.

2.7.1 Antibody dilutions

The binding of antigen and antibody on the electrode surface directly affects the sensitivity of the immunosensor. The amount of antibody plays an important role in this process. The impedance response depends upon antibody- antigen binding and incubation time. Hence, the effect of various antibody dilutions were investigated and optimized. Various specific antibody dilution ratios such as 1: 8000, 1: 16000 and 1: 32000 were evaluated as shown in Figure 2.10. The choice of antibody dilution was based on the sensitivity towards the target antigen. The sensitivity was found to be 2.6 %, 1.4 % and 0.6 % respectively.

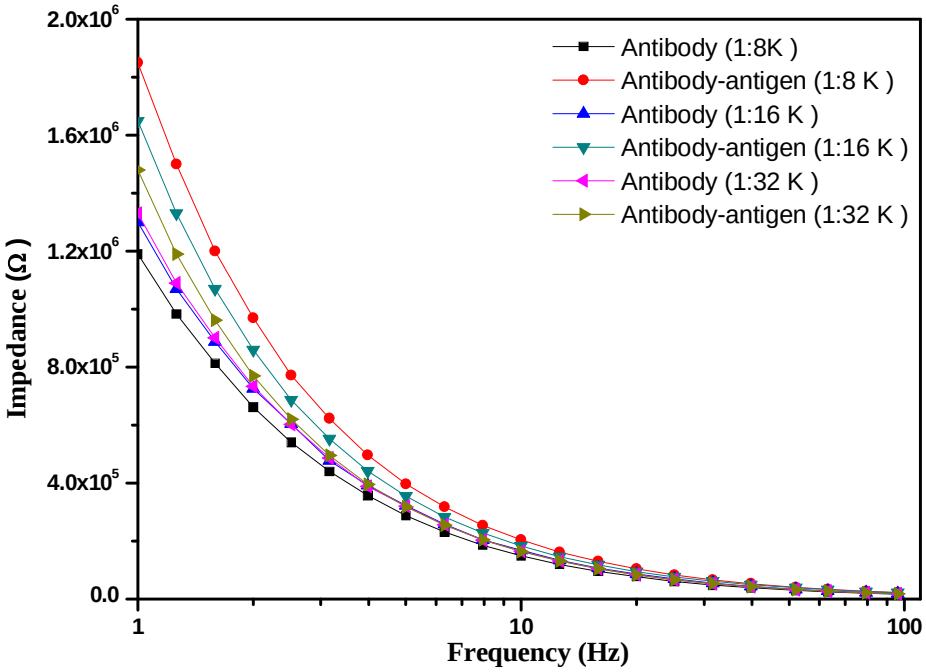

Figure 2.10 Impedance spectra for various antibody dilutions. EIS: 10 mV ac potential, frequency range (1 Hz to 100 Hz).

2.7.2 Incubation time

With the increase in incubation time, the impedance response also increased and reached to a saturation value after some finite time. The saturation level indicates that the possible binding of antibody and antigen is over. The time for binding depends on the matrix and transducers being used. Figure 2.11 shows the impedance response at different time for antibody- antigen interaction. It was found that after 20 min there was no further increase in the impedance response, thus 20 min was selected as an optimum incubation time for antibody-antigen interaction case.

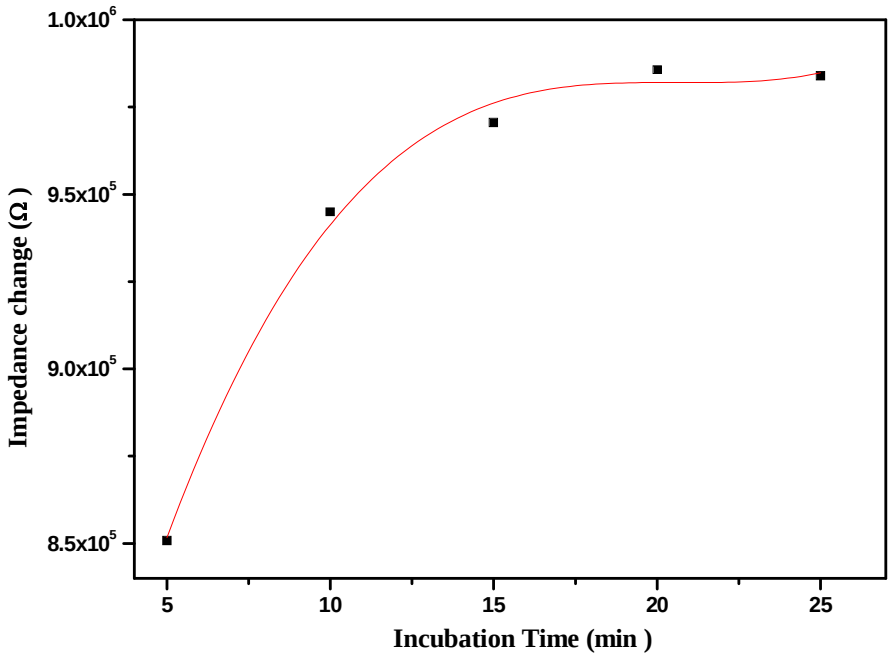

Figure 2.11 Optimization of incubation time for impedance measurement at 1 Hz.

2.7.3 Influence of frequency

For non-faradaic impedance measurement, the impedance or capacitance of the interface may be measured at a single frequency. The influence of applied frequency was also studied in the range, 1 Hz to 100 kHz. Six different frequencies of 1 Hz, 10 Hz, 96 Hz, 1 KHz, 10 kHz and 100 kHz were chosen to evaluate the impedance change during antibody-antigen interaction. The percentage impedance change was calculated against blank matrix presented as Figure 2.12. The maximum change in impedance during antibody-antigen interaction was observed about 35 % at 1 Hz. Thus, 1Hz was chosen for quantitative analysis for antibody-antigen interaction. The frequency of measurement may vary for specific application.

2.7.4 Influence of applied potential

In impedance biosensors, the applied voltage should be quite small, usually, 10 mV amplitude or less for several reasons. First, the current-voltage relationship is often linear only for small perturbations (Barbero *et al.*, 2005). A second reason is to avoid disturbing the probe layer; covalent bond energies are on the order of 1-3 eV but probe-target binding energies can be much less (and in some cases the probe is not covalently attached to the electrode), and applied voltages will apply a force on charged molecules. Figure 2.13 shows Nyquist plot recorded for different applied potential from (0.1 mV- 1 V). A stable response was obtained when applied potential was 10 mV and above. The impedance value at 1 Hz for

different applied potential is presented as Figure 2.14. Hence, potential of 10 mV was found suitable for measurement of impedance resulted from antibody-antigen interaction.

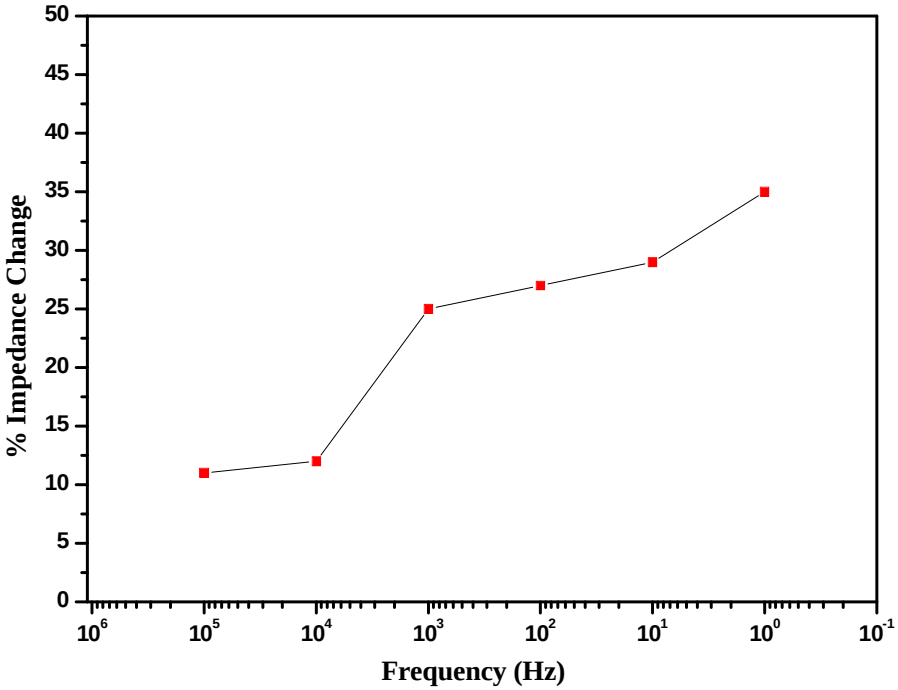

Figure 2.12 Percentage impedance change after antibody- antigen interaction recorded at different frequencies (1 Hz to 100 kHz) at 10 mV ac potential.

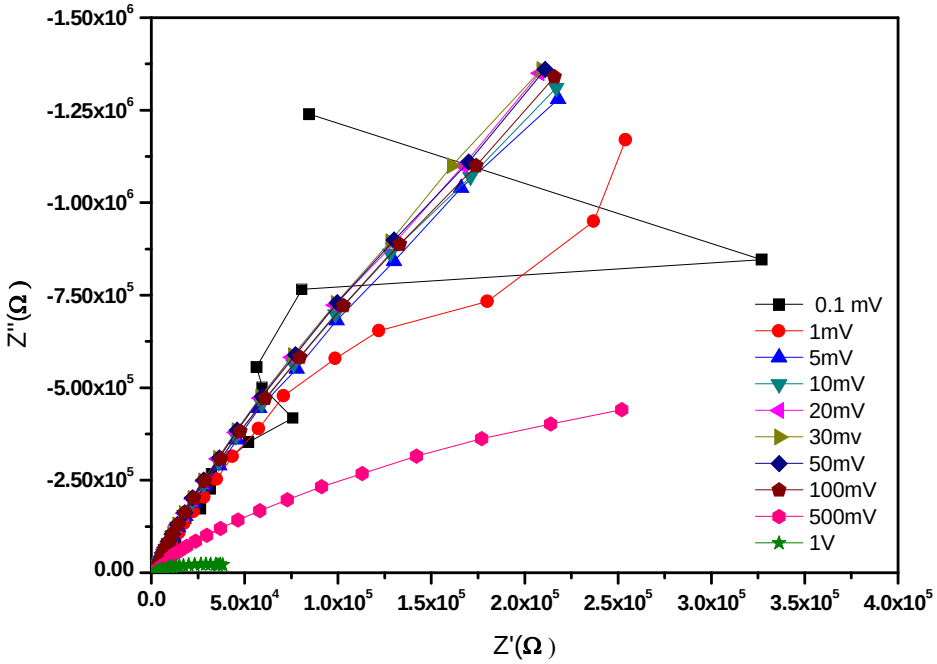

Figure 2.13 Nyquist plot recorded for antibody-antigen interaction at different applied potential.

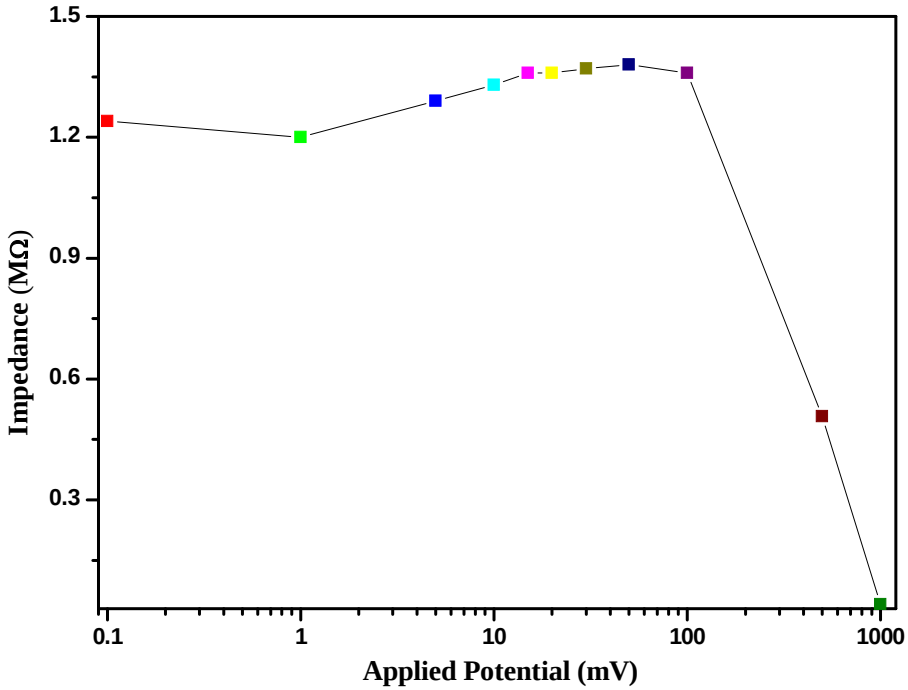

Figure 2.14 Impedance responses at different applied potential (0.01 mV-1 V) at 1 Hz frequency.

2.7.5 Sample volume

The response can be improved by increasing the analyte sample volume. However, antibody-antigen binding also depends on the amount of antibody immobilized on electrode surfaces. More analyte for the same amount of antibody may not increase the response. Therefore, a optimal sample volume should be determined. In this thesis various sample volumes from 0.4 µL to 700 µL were optimized for different biosensor applications.

2.8 EIS study of antibody-antigen interaction

The antibody-antigen interaction on the electrode surface was studied using EIS. For non-faradaic impedance measurement, the impedance/capacitance of the interface may be measured at a single frequency. The capacitance change is commonly used as an indicator of antibody-antigen interaction in non-faradaic biosensor (Daniels and Pourmand, 2007). Figure 2.15 shows the impedance response of antibody-antigen interaction on the electrode surface. In EIS measurement, antibody-antigen interactions create a new charged layer as a capacitance that is in series with the double layer capacitance. A decreased double layer capacitance and increased impedance were observed in the low frequency region. This confirms that the change in impedance was resulting from binding of the antigen to antibody.

It was observed that, impedance response in high frequency region (100 Hz to 100 kHz) remains almost constant while a significant change was observed in the low frequency region (1 Hz to 100 Hz) with highest impedance change at 1 Hz.

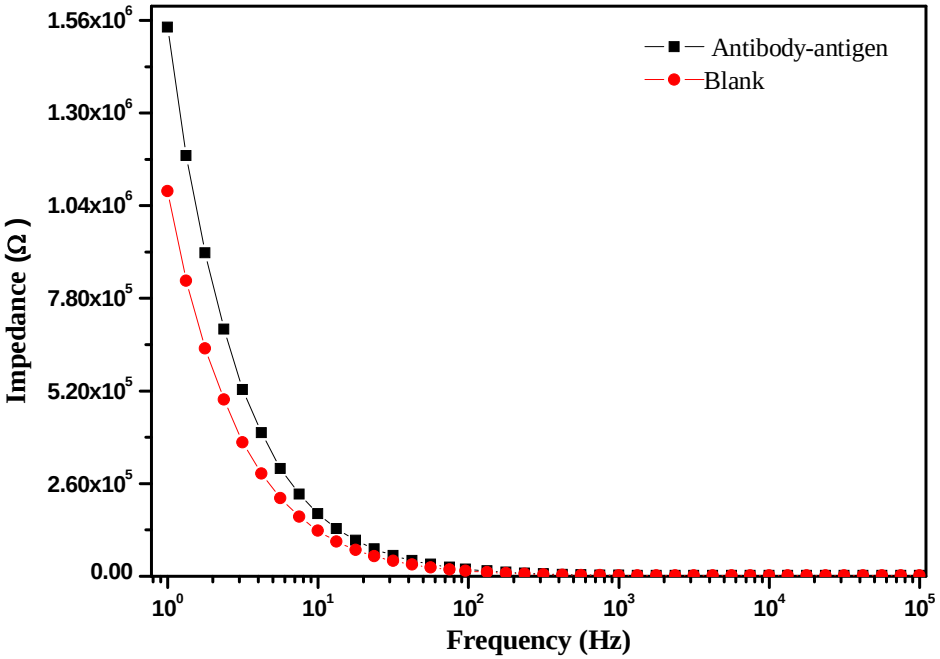

Figure 2.15 Impedance spectra of the immunosensor before and after interaction of antibody with antigen (25 pg mL^{-1} AFM1) at room temperature (0.01 M PBS medium, frequency range 1 Hz to 100 kHz at 10 mV ac potential).

2.9 Conclusions

This work illustrates the construction of immunosensor. Ag wire was selected as electrode material against Cu electrode. The surface of the modified electrode was studied by SEM, FT-IR and fluorescence to confirm the changes in surface morphology. The immunosensor operating parameters such as antibody dilution, applied potential, single frequency of measurement, incubation time and sample volume was optimized. The antibody dilution was selected based on the sensitivity towards the target antigen. A potential of 10 mV was found to be the appropriate voltage for impedance measurement. The maximum change in impedance was found at 1 Hz. The analysis time was found to be 20 min. This chapter also described and validated the sensing principle of immunosensor by EIS technique. The antibody- antigen interaction was demonstrated with a simple two electrode setup using EIS as a proof of concept for toxin (AFM1) as model analyte.

Chapter 3

Development of impedimetric biosensors using two electrode setup for analysis of aflatoxins and bacteria

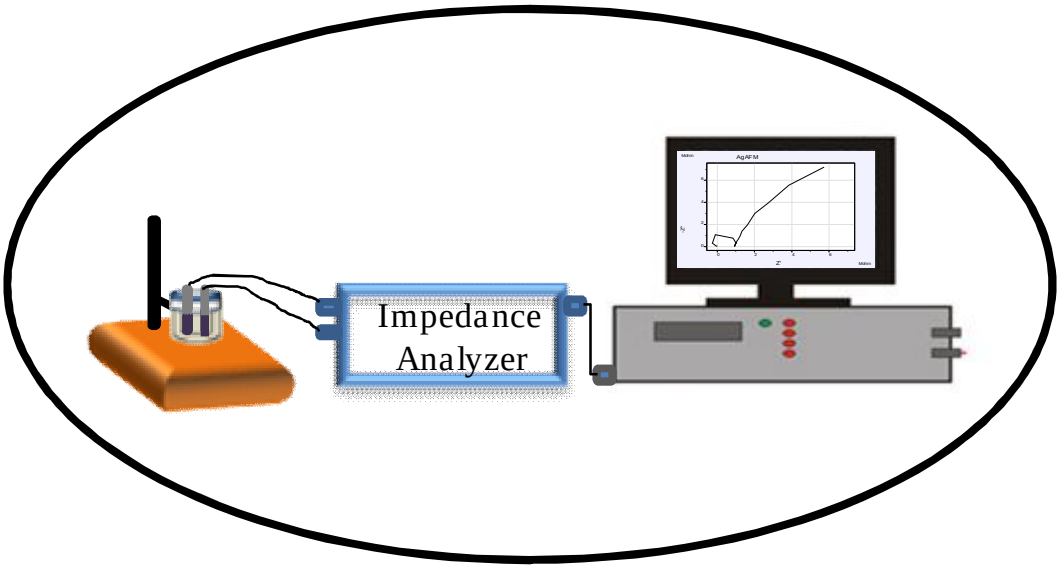

Graphical abstract of chapter content

3.1 Introduction

3.1.1 Importance of mycotoxins

The contamination of food by mycotoxins is responsible for many diseases (Richard, 2007). It is estimated that almost 25 % of the world's crops are affected by toxigenic fungi and become part of the food chain. High levels of mycotoxins in the diet can cause adverse acute and chronic effects on human health and a variety of species animals. Side effects may particularly affect the liver, kidney, nervous system, endocrine and immune systems (Kralj and Prosen, 2009).

3.1.2 AFB1 and AFM1

Aflatoxins are toxic metabolites produced by fungi, mainly *Aspergillus flavus* and A. *parasiticus* found in a large variety of food and animal feed. Naturally occurring aflatoxins are composed of B1, B2, G1, and G2. Aflatoxins are highly toxic, mutagenic, carcinogenic and teratogenic compounds (Oveisi *et al*., 2007; Sadeghi *et al*., 2009). AFB1 is found in abundance and is classed as a carcinogenic substance of group 1 by the International Agency for Research on Cancer (IARC) (IARC, 1993). When AFB1 is ingested with feed by cows, it is transformed into its hydroxylated metabolite product, AFM1, which is then secreted in the milk. Many grains and foodstuffs, including corn, peanuts, cottonseed, cereals, beans and rice have been found to be contaminated with aflatoxins. Moreover, humans are exposed to aflatoxins either directly by eating contaminated grains or indirectly via animal products. The contamination generally occurs in the field, during harvest and transportation, and during storage, under conditions where mold is allowed to grow. Since, aflatoxins are relatively heat stable, these are difficult to destroy once formed. The significant threat to human health posed by contamination has motivated extensive research in this toxin (Lee *et al*., 2004). The consumption of milk and milk products by human population is quite high, particularly in infants and children, thereby increasing the risk of exposure to AFM1. Evidence of hazardous human exposure to AFM1 through dairy products has been shown by several investigators (Fallah, 2010; Ghanem and Orfi, 2009). Recently, the need for ultra sensitive techniques for the special requirements such as those in infant food was highlighted with relatively lower analysis time for AFM1 (Shephard *et al*., 2012). Many international agencies had laid down specific regulations or detailed guidelines for the occurrence of mycotoxins in food. Table 3.1 summarizes the permissible limits of aflatoxins in food by different agencies such as;

European Union (EU), US Food and Drugs Administration (USFDA), CODEX and Food Safety and Standards Authority of India (FSSAI).

Table 3.1 Permissible limits for aflatoxins in different foods (Dors *et al.*, 2011)

Aflatoxins	**Product**	**Maximum permissible level**			
		EU	**USFDA**	**CODEX**	**FSSAI**
AFB1	Cereals for human consumption	2 µg/Kg	20 µg/Kg	Not specified	30 µg/Kg
AFB1	Groundnuts & dried fruits & their processed products for human consumption	2 µg/kg 4 µg/kg-Total	20 µg/kg-Total	15 µg/kg-Total	30 µg/kg
AFM1	Milk & Milk based products	50 pg mL^{-1}	500 pg mL^{-1}	500 pg mL^{-1}	0.5 µg/kg

3.1.3 Techniques for aflatoxins detection

3.1.3.1 Conventional techniques for aflatoxins detection

For better control of AFM1 in milk, various measurement techniques have been developed. Most of them require extraction of AFM1 from its source, purification by removing other substances, and finally quantification. AFM1 is generally quantified by ELISA (enzyme linked immunosorbent assay), TLC (thin layer liquid chromatography) and HPLC (high-performance liquid chromatography). Although the chromatographic methods are well-proven, they have some limitations. They are usually considered as laborious and time-intensive. Moreover, they require expensive equipment and materials. In addition to conventional techniques, Surface plasmon resonance (SPR) and quartz crystal microbalance (QCM) based biosensors have also been reported for analysis of aflatoxins. The reported conventional techniques for aflatoxin detection are presented as Table 3.2.

Table 3.2 Summary of reported conventional and other techniques for AFM1 and AFB1 detection

Detection technique	**Analytes**	**Matrix**	**Detection limit**	**Reference**
HPLC-FL	AFM1	Milk	0.006 μg/kg	Wang *et al*., 2012
TLC	AFM1	Cheese	0.65–0.80 μg/kg	Kamkar, 2006
ELISA	AFM1	Milk	0.005 pg mL^{-1}	Kanungo *et al*., 2011
HPLC-FL	AFB1	Cereals	0.003 ng/g	Fumani *et al*., 2011
UHPLC	AFB1	Peanut, corn	0.32 μg/kg	Fu *et al*., 2008
HPLC-ESIMS/ MS	AFB1	Peanuts and their derivative products	0.012-0.273 μg/kg	Huang *et al*., 2010
TLC-CCD	AFB1	Peanuts	0.4 ng/spot	Hoeltz *et al*., 2010
SPR	AFM1	Milk	0.6 pg mL^{-1}	Wang *et al*., 2009
SPR	AFB1	Acetonitrile–water	0.2 ng mL^{-1}	Van der Gaag *et al*., 2003
QCM	AFM1	Milk	0.01-10 ng mL^{-1}	Jin *et al*., 2009
QCM	AFB1	Grape juice	0.72 μg/kg	Wang and Xian-Xua , 2009

3.1.3.2 Electrochemical biosensors for aflatoxins

Electrochemical biosensors for aflatoxins detection are prominent due to their sensitivity, selectivity, low cost, simplicity, miniaturization, portability and ease of operation. Most of them are based on the high affinity interactions between antigen and specific antibodies. To convert the toxin interaction to an analytical signal, a variety of electrochemical techniques such as amperometric, potentiometric, conductimetric and impedimetric have been used. Among the reported biosensors, EIS has emerged as a sensitive technique for analysis of aflatoxins (Paniel *et al*., 2010; Vig *et al*., 2009). EIS is suitable to analyze the electrical

properties of the modified electrode, i.e. when an antibody coupled to the electrode reacts with the antigen of interest (Felice *et al*., 1999). Table 3.3 summarizes the reported electrochemical techniques for aflatoxin detection.

Table 3.3 Reported electrochemical techniques for AFM1 and AFB1 detection

Detection technique	**Analyte**	**Range of detection**	**LOD**	**Reference**
Impedimetric	AFM1	1-14 ng mL^{-1}	1 ng mL^{-1}	Dinckaya *et al*., 2011
Amperometric	AFM1	0.030–0.060 ng mL^{-1}	0.025 ng mL^{-1}	Parkar *et al*., 2009
Amperometric	AFM1	0.030–0.060 ng mL^{-1}	0.025 ng mL^{-1}	Micheli *et al*., 2005
Amperometric	AFM1	0.005–0250 ng mL^{-1}	0.001 ng mL^{-1}	Neagu *et al*., 2009
Potentiometric	AFM1	0.125–2 ng mL^{-1}	0.040 ng mL^{-1}	Rameil *et al*., 2010
Amperometric	AFB1	0.1-10 ng mL^{-1}	0.09 ng mL^{-1}	Ammida *et al*., 2006
Amperometric	AFB1	0.05-12 ng mL^{-1}	0.006 ng mL^{-1}	Tang *et al*., 2008
Impedimetric	AFB1	0.1-10 ng mL^{-1}	0.001 ng mL^{-1}	Zaijun *et al*., 2010
Impedimetric	AFB1	0.5-10 ng mL^{-1}	0.1 ng mL^{-1}	Liu *et al*., 2006

3.1.4 Impedance measurement using two electrode system

A significant progress in biosensor technology has been the miniaturization of electrochemical systems, which reduces sample and reagent volumes, reduces response time due to faster diffusion, makes the sensor more economical and is more favourable to portability. Most of the electrochemical sensors are often designed into a two electrode system for simplicity, miniaturization and low cost. To prove the concept of miniaturization, a two electrode silver wire based setup was developed to quantify various analytes throughout this chapter. Among the various electrochemical readout techniques, impedance spectroscopy (Kafka *et al*., 2008) is becoming an attractive tool to analyze fast and label-free interfacial changes originating from the biorecognition event at electrode surfaces.

This thesis work was focused on non-faradaic impedimetric biosensing due to its features of the simple, inexpensive and most direct transduction. In non-faradaic measurement, the capacitance at the electrode/electrolyte interface is measured, via the response to a small amplitude ac voltage. Measurements at low frequency, where the electrode/electrolyte interface capacitance dominates are the most sensitive to capture the small variations occurring at the electrode/electrolyte interface induced by biorecognition events. Capacitance method was reported for quantification of bacterial content in milk using two identical stainless steel electrodes by measuring capacitance at 1 kHz (Felice *et al.*, 1999).

3.1.5 Research gaps identified

Although other electrochemical techniques including cyclic voltammetry (CV) and amperometry have reported promising improvement in sensitivity, the low level detection signal in a low target concentration range is still a bottleneck. Among the reported biosensors, EIS has emerged as sensitive techniques for analysis of AFM1 (Paniel *et al.*, 2010; Vig *et al.*, 2009). One of the main advantages of EIS biosensors is no need of conjugating antibodies or mycotoxins with an enzyme to provide the electrochemical signal (Grieshaber *et al.*, 2008). A significant signal level can be obtained by EIS technique due to the inverse relation of the impedance with the current (Park and Park, 2009). Although, DNA based biosensor was developed to detect aflatoxin M1 in milk and dairy products using EIS technique (Dinckaya *et al.*, 2011). The reported biosensors lack portability with high sensitivity for AFM1 analysis in milk.

3.1.6 Objective

The aim was to develop a label-free silver wire based impedimetric immunosensor for detection of AFM1 in milk using two electrode systems.

3.1.7 Methodology

A practical and highly sensitive technique for ultra sensitive detection of AFM1 in milk with short analysis time was demonstrated. The developed impedimetric immunosensor is based on functionalized Ag wire electrode. Primary monoclonal antibody (mAb) specific to AFM1 was attached on the Ag wire through SAMs of 11-MUA. This imparts high specificity to the biosensor. The Ag wire setup provides additional features such as storage, ease of handling

and portability. The impedance change during antibody- antigen interaction was measured using EIS. After simple pre-treatment of milk samples, the immunosensor was optimized with regard interferences from milk matrix.

3.2 Materials and methods

3.2.1 Materials and instrumentation

Procourement of all reagents, chemicals and instruments for the AFM1 immunosensor development was described in Chapter 2.

3.2.2. Preparation of buffers

0.01 M phosphate buffered saline (PBS) was prepared by dissolving appropriate amount of Na_2HPO_4, NaH_2PO_4 containing 0.0027 M potassium chloride and 0.137 M sodium chloride. The pH of the buffer was adjusted to 7.4. PBS with Tween 20 (PBST) was prepared by adding 0.05 % Tween 20 (v/v) in PBS for washing purpose. All buffer solutions were stored at 4° C when not in use.

3.2.3 Preparation of AFM1 standard solutions

All the AFM1 solutions were prepared in a glove box in a maintained inert N_2 atmosphere. AFM1 stock solution (2.5 µg mL^{-1}) was prepared by dissolving the AFM1 powder in 5 % ACN (v/v) in PBS and stored at −20° C. Working AFM1 standard solutions in the range of 0.25-100 pg mL^{-1} were prepared by diluting the stock with 5 % ACN.

3.2.4 Preparation of AFM1 antibody solutions

The stock solution of rat monoclonal [1C6] mAb, 100 µg (1 mg mL^{-1}) was diluted with 50 µL of de-ionized water. It was divided into two fractions. The first fraction containing 40 µL was stored at −20° C. From the second fraction, working mAb solutions were prepared by serial dilution such as 1: 1000, and 1: 2000.

3.2.5 Preparation of standard milk based matrix

To assess the performance of the immunosensor, the milk samples were prepared by dissolving 1 g of ERM BD 282 whole milk powder (zero level AFM1) in 10 mL of 0.01 M PBS + 0.5 % (v/v) Tween20, preheated to 50° C (as indicated in the protocol). To minimize

the matrix effect, the solution was centrifuged for 10 min at 6000 rpm at 4° C, and the fatty layer was carefully removed and the supernatant was diluted (1/1, v/v) with PBS + 0.5 % (v/v) Tween20. For impedance studies, centrifuged milk samples were spiked with fixed amount of AFM1 (100 pg mL^{-1}, 75 pg mL^{-1}, 50 pg mL^{-1}, 25 pg mL^{-1}, 12.5 pg mL^{-1}, 6.25 pg mL^{-1}, 1 pg mL^{-1} and 0.25 pg mL^{-1}).

3.2.6 Cleaning procedure for the Ag wire electrode surface

Initially the surfaces of the bare Ag wire electrodes were washed ultrasonically in deionized water for 5 min to remove inorganic particles. Following this, the electrodes were immersed into piranha solution (H_2O_2/H_2SO_4, 30/70 v/v) for 30 s. The electrodes were washed with distilled water, followed by drying under the ultra pure nitrogen stream. This cleaning procedure was repeated before every electrode preparation step.

3.2.7 Immobilization of mAb on Ag wire electrode

All the glassware was soaked in piranha solution, rinsed thoroughly with distilled water and dried. The mAb was covalently coupled on Ag wire electrode through SAMs as described (Park *et al*., 2004) with some alteration. Firstly, the concentration of 11-MUA was optimized. Then a set of clean Ag wire electrodes were immersed overnight in 0.004 M ethanolic solution of 11-MUA under ambient condition. The electrodes covered by SAMs were gently washed with absolute ethanol to remove unbounded 11-MUA residues. The electrodes were dried with nitrogen stream before use. For coupling the mAb, the carboxyl group of SAMs on modified electrode was activated by 1:1 EDC/NHS (0.1 M each) mixture for 2 hrs. Subsequently, the electrode was washed with distilled water to remove excess EDC/NHS. Finally, mAb was attached to the electrode by carefully spreading mAb solution (1: 16000 in PBS) over the activated surface followed by overnight incubation at 4° C. The unused antibody coupled electrodes were washed and stored in 4° C for future use.

3.2.8 Experimental setup

The experimental setup constitutes a pair of pre-functionalized Ag wire electrode dipped into a custom made glass cell (capacity 750 µL) containing AFM1 spiked milk samples. The operation of presented sensor is based on the pair of Ag wire as an electrical transducer. The Ag wire surface was functionalized with analyte specific antibodies (anti-AFM1 mAb) attached using SAMs to form biological transducer. The binding of the analyte (AFM1) to the

biological transducer causes the impedance change, measured using two electrode setup. The electrode setup and the glass cell were enclosed in a custom made Faraday cage. The schematic of experimental setup is presented as Figure 3.1. In the presented setup, the two pre-functionalized Ag wire electrodes were separated by 1mm and dipped 10 mm in the cell. The functionalized Ag wire electrodes were connected to IVIUM CompactStat impedance analyzer. The impedance change caused by antibody-antigen interactions at the electrode surface was measured.

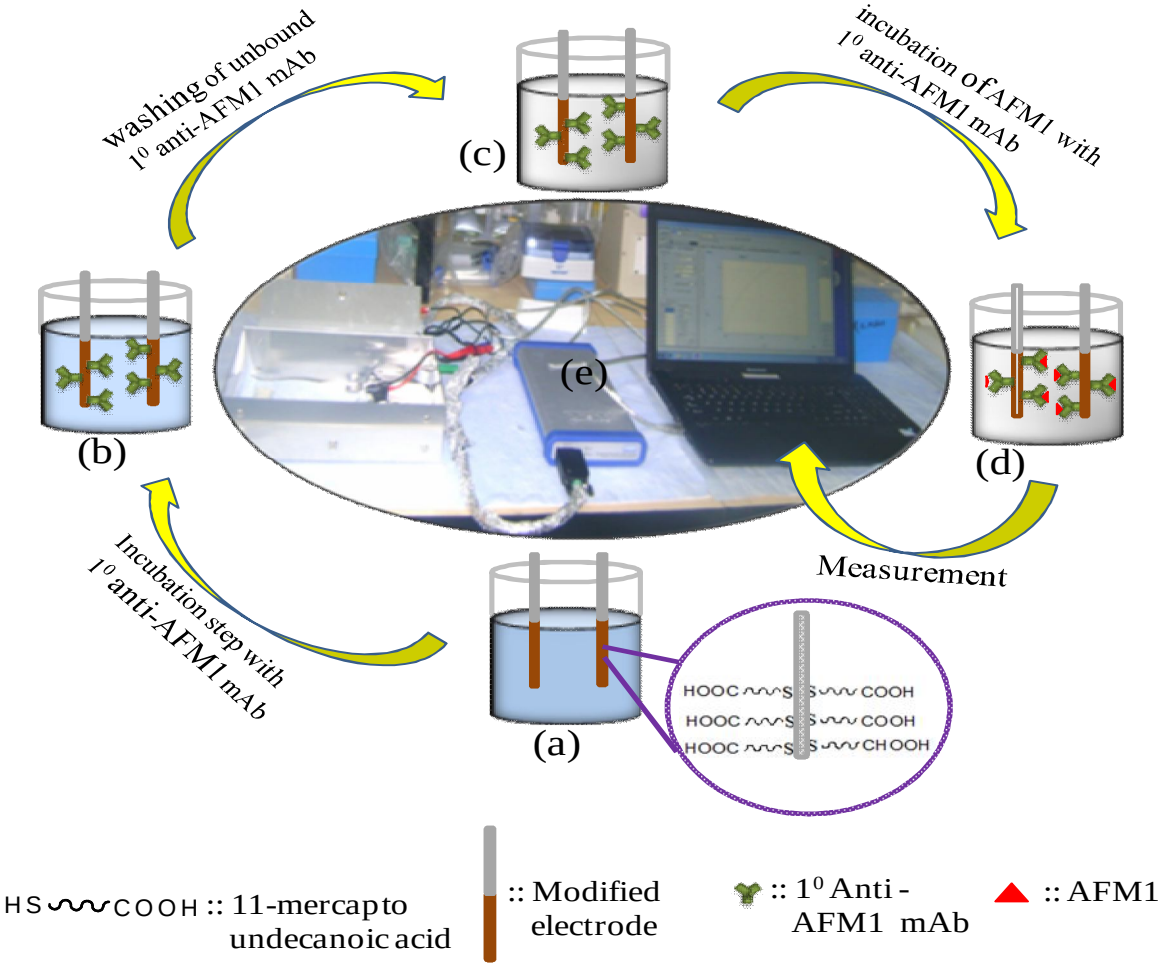

Figure 3.1 Schematic illustration of Ag wire electrode based impedimetric AFM1 immunosensor (a–d) with EIS measurement setup; (a) 11-MUA modified Ag wire electrode in microcell dipped in 0.01M PB, pH 7.4; (b) overnight incubation of mAb with modified electrode in PB; (c) washing of unbound mAb attached to electrode; (d) incubation of AFM1 with mAb attached electrode in milk based buffer; (e) experimental setup of Ag wire based immunosensor.

3.3 Results and discussion

3.3.1 Optimization of the immunosensor parameters

The binding of the AFM1 on the probe directly affects the sensitivity of the immunosensor. The parameter such as incubation time, frequency range, antibody dilution and applied voltage affects impedance measurements. The influence of these parameters for antibody-antigen interaction was studied using EIS (details in chapter 2). For AFM1 analysis, the optimized incubation time was found to be 20 min. The antibody dilution of 1:16000 was found to be optimum. The influence of applied potential and frequency ware also studied and found optimum as 10 mV and 1Hz.

3.3.2 Validation of sensor operation

The sensor was validated for quantitative AFM1 analysis. The EIS data was recorded for different concentrations of AFM1 (0.25-100 pg mL^{-1}). Figure 3.2 represents Nyquist plot obtained for the ac impedance analysis of mAb following exposure to various AFM1 concentrations. It was noted that both real components (Z′) and the imaginary component (Z″) of impedance increased with decreasing frequency. This confirms the interaction of mAb and AFM1. A significant increase in the impedance was observed in the lower frequency range (1 Hz to 10 Hz) when AFM1 concentrations were increased from 0.25 to 100 pg mL^{-1}.

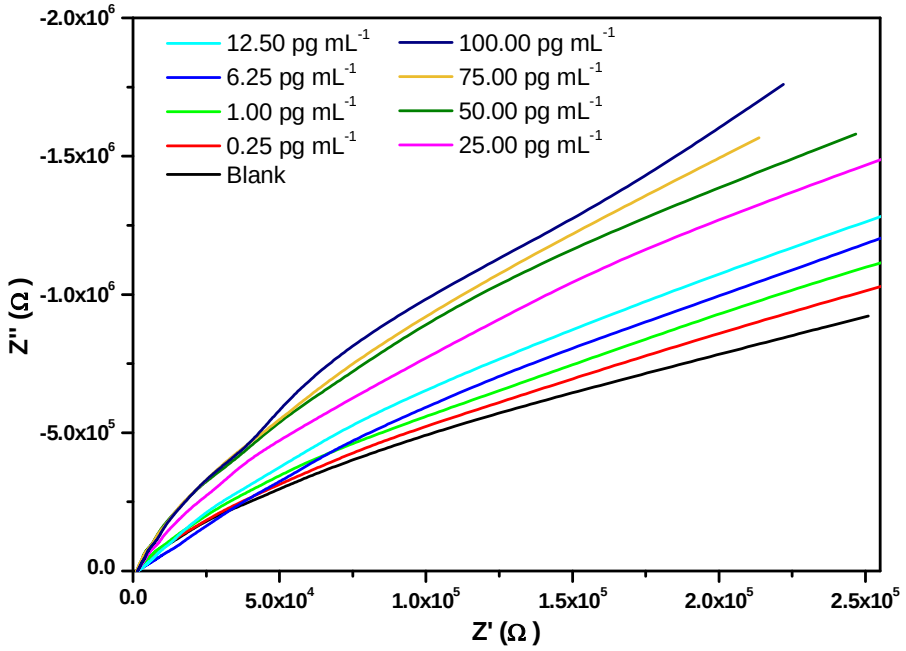

Figure 3.2 Nyquist plot recordings in presence of different concentration of AFM1 in milk based matrix (EIS: 1 Hz to 100 kHz, 10 mV ac potential).

3.3.3 Equivalent circuit analysis

In this work, various equivalent circuits were also evaluated to fit the obtained data obtained from mAb-AFM1 interaction. The proposed equivalent circuit with best fit results for the electrochemical cell using modified electrode is presented as Figure 3.3. The presented equivalent circuit represents a non-faradaic response at the electrode–electrolyte interface, since no redox species was present in the solution (Bart *et al.*, 2005). The proposed equivalent circuit consists of ohmic resistance of medium (R_s), double layer capacitance of outer layer ($C_{dl(ol)}$), double layer capacitance of inner layer ($C_{dl(il)}$) and resistance of inner layer (R_{dl}). $C_{dl(ol)}$ ($R_{dl}C_{dl(il)}$) represent the two layer structure for each electrode. $C_{dl(ol)}$ represents outer layer of the interface where the antibody- antigen interaction takes place. ($R_{dl}C_{dl(il)}$) sub-circuit represents the inner layer of the interface. R_{dl} which is parallel to $C_{dl(il)}$, resembles a part of SAMs. R_{dl} can be interpreted as the conductivity (by penetrating ions) of the SAMs (Bart *et al.*, 2005). Figure 3.4 shows Bode plot of experimental and fitted impedance spectra of AFM1. Fitting was done by using IVIUM equivalent circuit evaluator and optimized with phase, Z' and Z'' . The error weight is considered as equal for each point. The fitting has good agreement with experimental data, validating the equivalent circuit for developed immunosensor.

The binding of AFM1 mainly influenced the impedance at lower frequency i.e. at 1Hz, where R_s and $C_{dl(ol)}$ dominates the overall impedance. The value of impedance at 1Hz (1.54 MΩ) was over that at 1 kHz (2.66 kΩ). Since the double layer capacitance $C_{dl(ol)}$ became essentially resistive at low frequencies (<1 kHz), it became the main source that contributed to the total impedance, making the impedance value very high. The medium resistance could be ignored in this case. The double layer capacitive region in which the electrode impedance could be detected is indicated by $C_{dl(ol)}$. Whereas, in the high frequency range (>1 kHz), the capacitance almost offered no impedance, and the contribution of the double layer capacitance to the total impedance became zero. Thus, the only contribution to the total impedance was medium resistance (R_s) and was independent of the frequency. Therefore, the changes in the medium due to increase of AFM1 concentration could be detected by impedance measurement performed at different frequencies. The results of this study confirmed that at low frequency (<1 kHz), impedance can provide the information of the double layer capacitance.

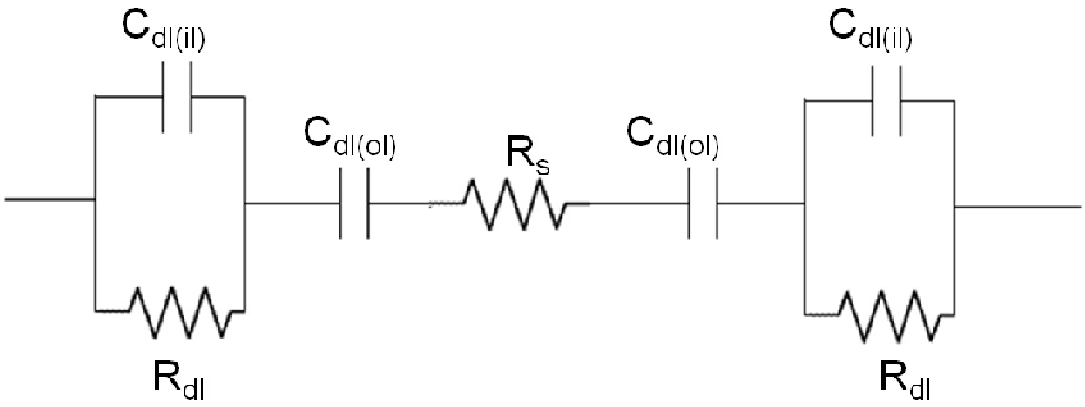

Figure 3.3 Equivalent circuit used to fit impedance of the AFM1 immunosensor in milk based buffer.

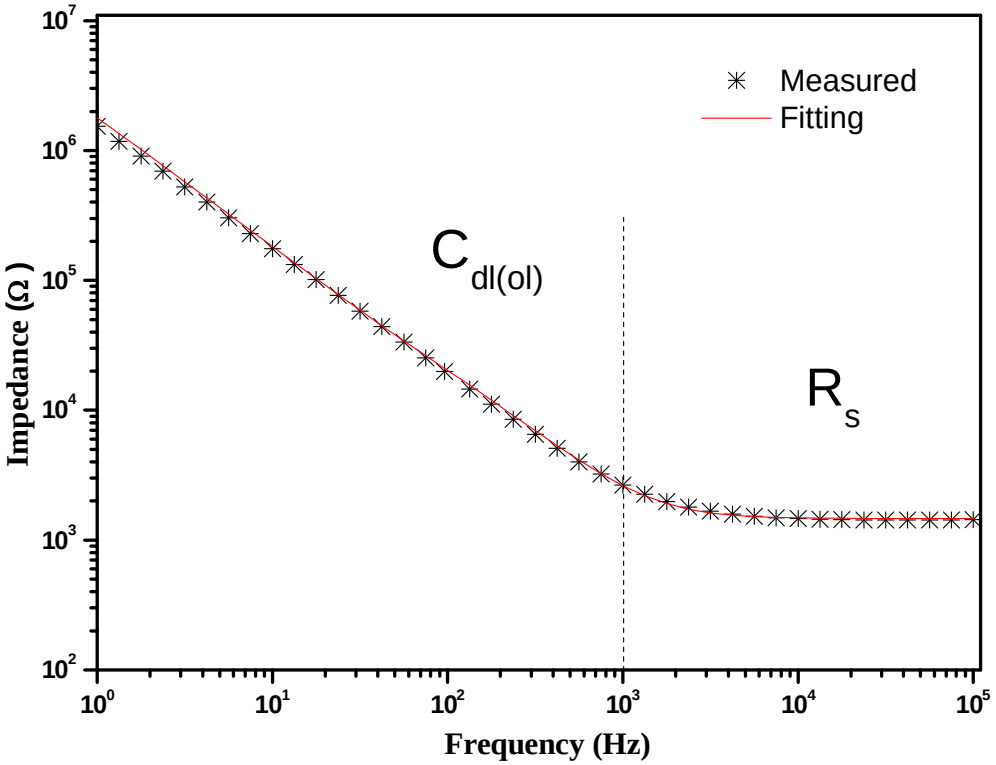

Figure 3.4 Impedance spectrum in the AFM1 environment with the fitting curve. ac applied potential: 10 mV, frequency range: 1 Hz to 100 kHz.

3.3.4 Calibration of sensor for AFM1 detection

Impedance data was collected for the functionalized electrodes after exposing it to increasing AFM1 concentration (0.25-100 pg mL^{-1}). The specific interaction of mAb and AFM1 gave rise to an overall increase in impedance from baseline response at the electrode/solution interface. The Nyquist plot of Z′ and Z″ components of the impedance at specific frequency

provided information for construction of the calibration curve, recorded by multiple interrogations (4 replicates each). The % impedance change was calculated using the Equation 3.1 for different concentrations of AFM1.

$$\% \text{ Impedance change} = (Z - Z_0) / Z_0 \times 100 \qquad (3.1)$$

Z_0 is the impedance for blank at 1 Hz.

Z is the impedance after exposing to AFM1 concentration at 1 Hz.

The linear calibration curve obtained for AFM1 is presented as Figure 3.5 and studied range as inset. A linear range of AFM1 detection in the range 6.25-100 pg mL^{-1} was achieved with SD = 1.13 and R^2 = 0.982. AFM1 concentration was directly proportional to % impedance change. This result is explained on the basis that the phenomenon of antibody-antigen interaction is a reversible process and thus adsorption and diffusion proceed simultaneously. Lower limit of quantitation (LOQ) defined as the AFM1 concentration producing a signal corresponding to AFM1-free milk minus 10 times of SD (Thompson *et al.*, 2002), was determined to be 6.25 pg mL^{-1} by analyzing four replicate sets of AFM1 fortified milk samples ranging from 1 to 100 pg mL^{-1}. Limit of detection (LOD) was calculated as the analyte concentration corresponding to the mean signal of blank (obtained by averaging the signal of four replicate sets) minus 3 times of SD (*Thompson et al.*, 2002). LOD was found to be 1 pg mL^{-1} with good sensitivity about 2.1 % impedance changes per decade. The linearity of calibration shows that this method is useful for ultra sensitive detection and quantification of AFM1 in milk or milk powder. Current AOAC approved method for sensitive AFM1 analysis in milk relies on ELISA, is usually based on a fluorophore or an enzyme labelled secondary antibody. The presented method does not require such additional labels and still competes well with the existing standard assay for milk analysis. The IC_{50} value for the presented label-free immunosensor was found at 57.62 pg mL^{-1} As against the desired 25 pg mL^{-1} detection limit for the baby food, the present method detects the concentration just at IC_{40} value. The signal inhibited in the presence of AFM1 in milk was calculated and a significantly low detection limit 1 pg mL^{-1} is achieved using the presented immunosensor with analysis time of 20 min. The summary of analytical figures of merit of AFM1 analysis with Ag wire setup is presented in Table 3.4.

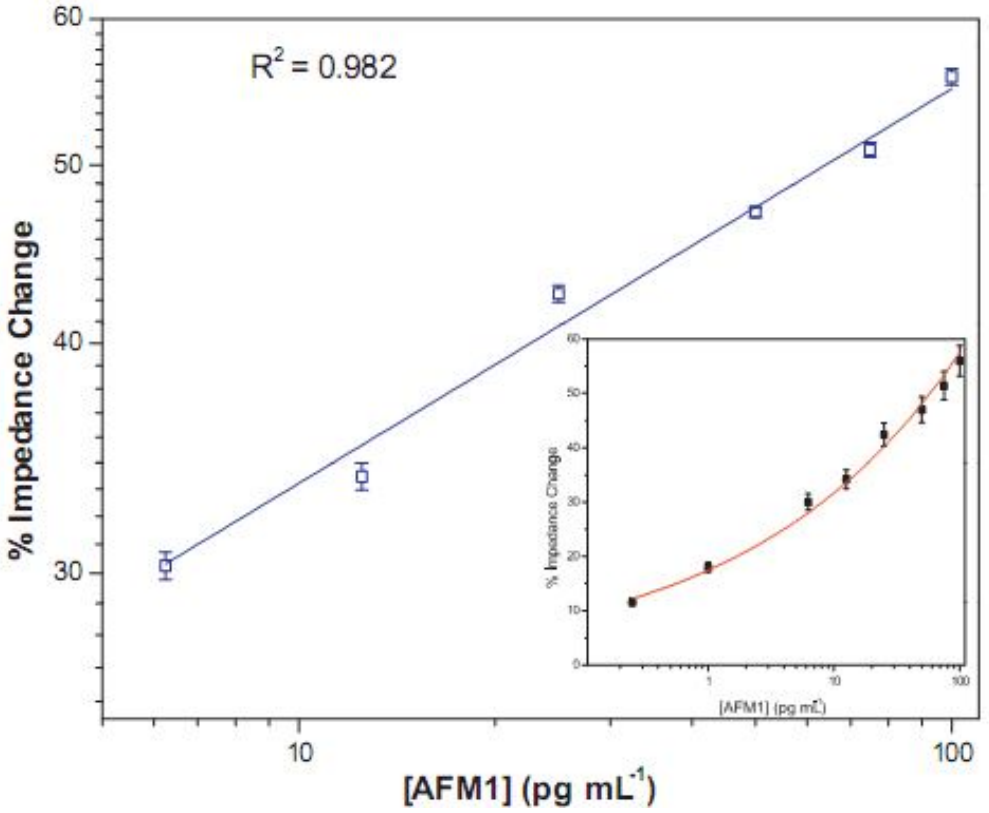

Figure 3.5 Calibration curve of label-free Ag wire AFM1 immunosensor.

Table 3.4 Summary of analytical figures of merit of AFM1 analysis in milk sample

Analytical parameters	**Experimental findings**
Dynamic Range	0.25–100 pg mL^{-1}
Linear Range	6.25–100 pg mL^{-1}
LOD	1 pg mL^{-1}
S.D	1.13
IC_{50}	57.62 pg mL^{-1}
R^2	0.982
Assay sample volume	700 µL
Analysis time	20 min

3.3.5 Sensor selectivity

The selectivity of the sensor towards AFM1 was studied in the frequency range 1 Hz to 100 kHz using EIS at 10 mV applied potential. In the optimized condition, the impedance response for AFM1 binding was measured in 20 min. The mAb deployed in the experiment was reported to partly cross-react with AFM2 (a structural analogue of AFM1). The cross-reactivity of mAb towards AFM1 and AFM2 was quantified experimentally using the presented setup at 25 pg mL^{-1}. As against the blank response, it is clearly seen that the sensor is highly selective towards AFM1 as against AFM2 as shown in Figure 3.6. The impedance change for AFM2 was found to be 4 %, whereas for AFM1 the change was 32 % at 1 Hz. The percent impedance change recorded for AFM1 binding was eightfold higher over AFM2 binding signifies good selectivity.

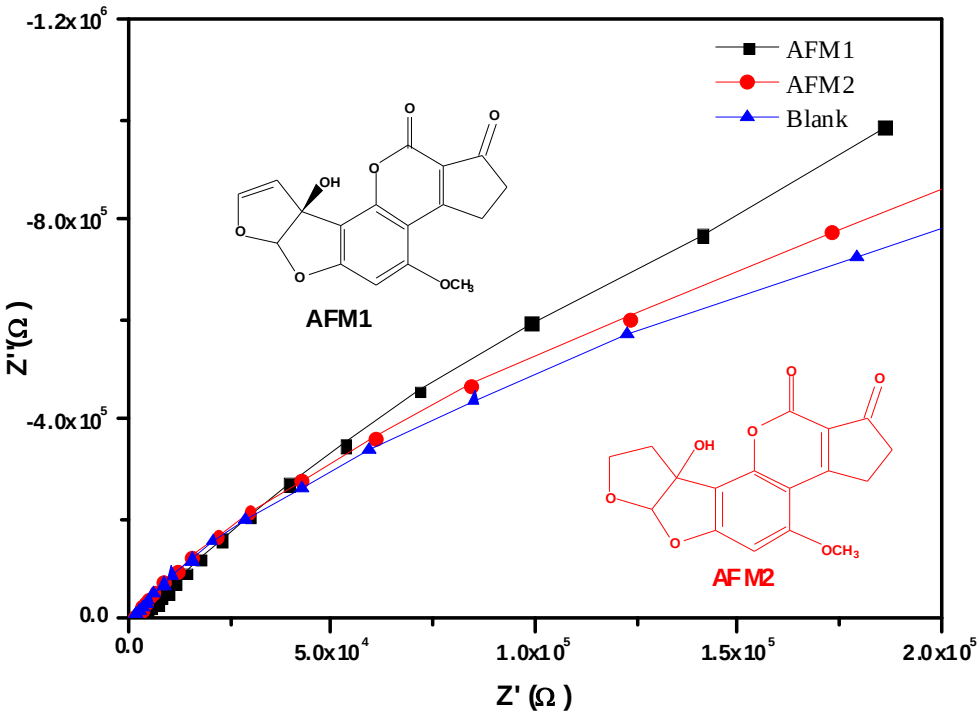

Figure 3.6 Nyquist plot in presence of 25 pg mL^{-1} of AFM1 and AFM2 (in milk based buffer) at electrode surface. EIS: 1 Hz to 100 kHz, 10 mV ac potential.

3.3.6 Conclusions

The development of a label-free silver wire based impedimetric immunosensor targeted towards AFM1 detection in milk was described here. A two electrode setup for impedance measurement in a custom made glass cell was optimized. The total assay volume of 700 µL was used in all the experiments.. The observed impedance changes indicated that the sensor has an approximate detection limit of 1 pg mL^{-1} and can detect various concentrations of

AFM1 up to 100 pg mL^{-1}. Sensor responses to antigen exposure were found to be concentration dependant with a linear correlation at least over the low concentration range between 6.25-100 pg mL^{-1}. The binding of antibody and antigen was also studied by an equivalent circuit with good fitting. An improved linear range with short analysis time of 20 min for AFM1 analysis, meeting EU standards in infant food has been achieved with good recoveries. The sensor showed excellent selectivity for AFM1 as against AFM2.

3.4 Need for AFM1 detection in various milk products

Contamination of milk with AFM1 and its ill effects on humans are well documented (Van Egmond, 2002; Gurbay *et al.*, 2006). Moreover from studies, it has been found that, AFM1 is relatively stable during milk pasteurization, storage as well as during the preparation of various dairy products (Badea *et al.*, 2004; Anfossi *et al.*, 2008). As a result, these can be found in various milk products such as yogurt, flavored milk, infant formula milk powder, cheese, and other milk-based confectioneries including chocolates, sweets and pastries etc. (Martins and Martins, 2000; Kamkar, 2006). Due to their carcinogenicity and severe toxicity, many international agencies have set maximum permissible limits of AFM1 in milk and related products (EC, 2006; FSSAI, F.No. 2-15015/30/2010). Therefore, it is important to determine AFM1 levels in milk and milk products in order to protect consumers in various age groups, meeting the stringent regulatory standards set by these international agencies.

3.4.1 EIS study of various milk products

Using an earlier developed label free EIS based immunosensor (Bacher *et al.*, 2012), the impedimetric analysis was further extended to study the effects of various milk products such as standard ERM BD-282 milk, flavored milk and drinking yogurt for quantitative analysis of AFM1. ERM BD-282 milk was re-constituted and spiked with known concentrations of AFM1. After the immobilization of mAb for AFM1, impedance measurements have been carried out with a 5 mV amplitude signal varying from 1Hz to 100 kHz (Kanungo *et al.*, 2014). AFM1 of 25 pg mL^{-1} was spiked in different milk samples and impedance data was recorded as depicted in Figure 3.7. For quantitative analysis, it is appropriate to measure changes in impedance at a single frequency. Figure 3.7 shows the change in impedance value at 1Hz for 25 pg mL^{-1} of AFM1 spiked in different milk samples. It is also evident from the Figure 3.7 that the similar impedance response is obtained for ERM-BD282 and flavored milk but large change in impedance was observed for yogurt. Since the impedance

spectroscopy allows the detection of capacitance changes at the interfaces. The change in capacitance can be derived from the imaginary part Z″, of the complex impedance spectra (Katz and Willner, 2003). The change of imaginary part of impedance, Z″ provides better correlation to analyte concentration than the real part of impedance (Bart *et al*., 2005).

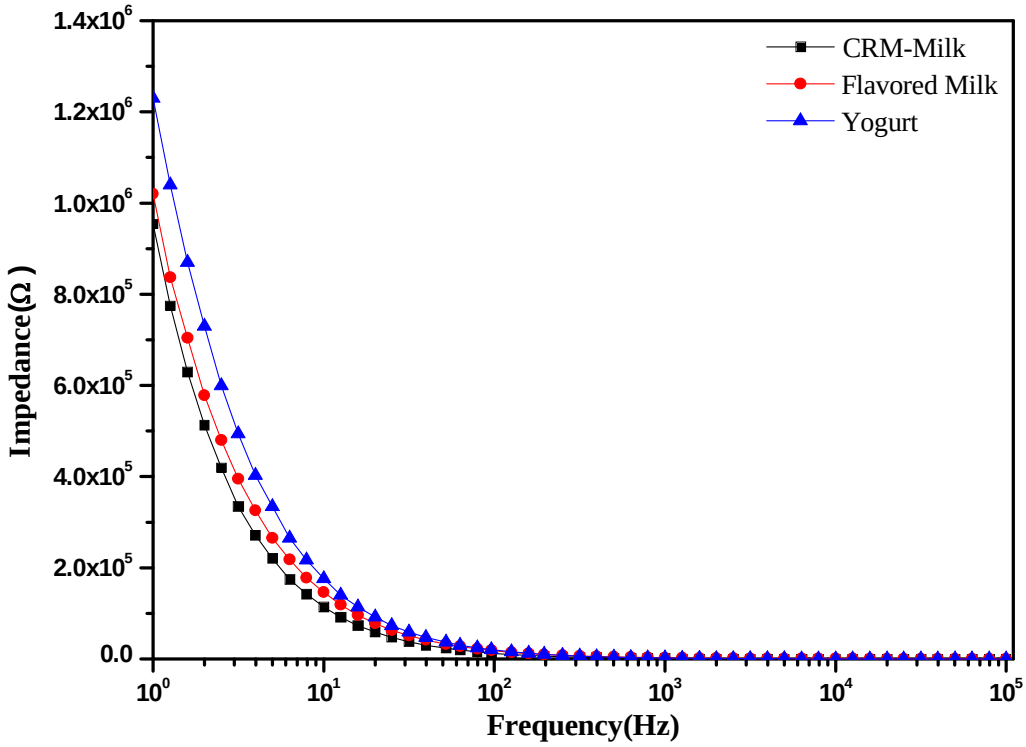

Figure 3.7 Impedance spectra of the immunosensor after interaction of mAb with 25 pg mL^{-1} AFM1 spiked in ERM-BD 282, flavored milk and drinking yogurt at room temperature (EIS: frequency range 1 Hz to 100 kHz at 5 mV ac potential).

The frequency to monitor the antibody-antigen interaction was chosen in such a way that the system exhibited near ideal capacitor behaviour (Berney *et al*., 2000). The influence of frequency was shown by Bode plot for various milk samples spiked with 25 page mL^{-1} of AFM1 and presented as Figure 3.8. The system exhibited near ideal capacitor behaviour in the region where the impedance curve was a straight line with a slope about -1 and the phase angle was as close to -90° as possible (Wu *et al*., 2005). This frequency was observed to be 52 Hz for ERM-BD282 milk and flavored milk and same was observed at 159 Hz for the yogurt sample as presented in Table 3.5. Thus, it was observed that the frequency shift occurs for the same concentration of analyte in various matrices. It was also observed that the developed immunosensor worked best for ERM-BD 282 and flavored milk, which were

almost similar in their constituents. But when drinking yogurt was tested, there was signal suppression, which might have attributed due to matrix interference.

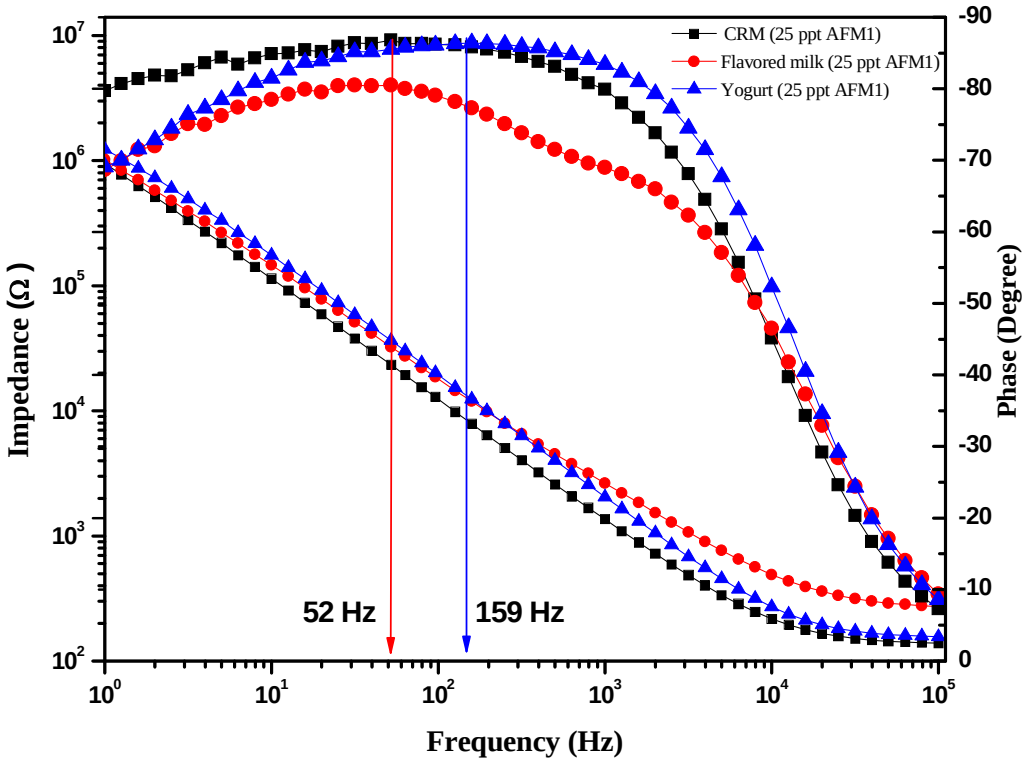

Figure 3.8 Bode plot of the immunosensor after interaction of mAb with 25 pg mL^{-1} AFM1 spiked in ERM-BD282, flavored milk and drinking yogurt at room temperature (EIS: frequency range 1 Hz to 100 kHz at 5 mV ac potential).

Table 3.5 Performance of immunosensor for various milk products

Matrix	**Impedance at 1Hz**	**Ideal capacitor behaviour**	
		Phase (°)	**Frequency**
ERM-BD282 milk	0.954 MΩ	86.8	52 Hz
Flavored milk	1.02 MΩ	80.5	52 Hz
Yougurt	1.23 MΩ	86.4	159 Hz

3.4.2 Conclusions

The immunosensor was tested for various milk matrices such as ERM-BD 282, flavoured milk and yogurt for AFM1 analysis. It was observed that the sensor response was similar for ERM-BD 282 and flavored milk, which are almost similar in their constituents. The ideal capacitor behaviour was found at same frequency i.e. 52 Hz for ERM-BD 282 and flavored milk but for yogurt it was 159 Hz. Suppression in signal was observed for drinking yogurt, this might be due to matrix interference.

3.5 Development of impedimetric immunosensor for detection of AFB1 in peanut

3.5.1 Introduction

AFB1, the most usual and most toxic of the aflatoxins, is the focus of many researchers due to the potent hepatotoxic and carcinogenic effects revealed in animal studies. Thus, there are reasonable economic and safety reasons for establishing highly sensitive, selective, cost-effective and rapid analytical methods for regular screening of AFB1 in a variety of specimens. To date, several methods such as HPLC, TLC, as well as ELISA have been used for detection of AFB1 in different specimens. However, there is still a need for more rapid and sensitive systems capable of early detection. AFB1 and the total aflatoxin level in peanut products are regulated with maximum residue levels (MRLs) that cannot be greater than 2 ng/g and 4 ng/g respectively (EC, 2001). The EIS technology has been used in the peanut research, such as estimation of mass ratio of the total kernels within a sample of in-shell peanuts using RF impedance method and non destructive moisture content determination for in-shell peanuts by capacitive sensing (Kandala *et al*., 2011). However, no report is available for ultrasensitive analysis of AFB1 in peanuts using EIS.

In this work, a simple, cost effective and label-free impedimetric immunosensor for detection of AFB1 in peanut matrix with the help of two electrode immersed in the single well of 384 micro well plates was developed. The immunosensor showed an excellent low limit of detection (0.01 pg mL^{-1}) for AFB1 with a short analysis time of 20 min. In this application, the volume reduction has also been achieved through usage of 384 microwell plates with working volume of 105 µL with the same concept of two electrode setup used in the previous section. The schematic representation of experimental set up is given in Figure 3.9. The functionalized electrode setup is usable under field conditions.

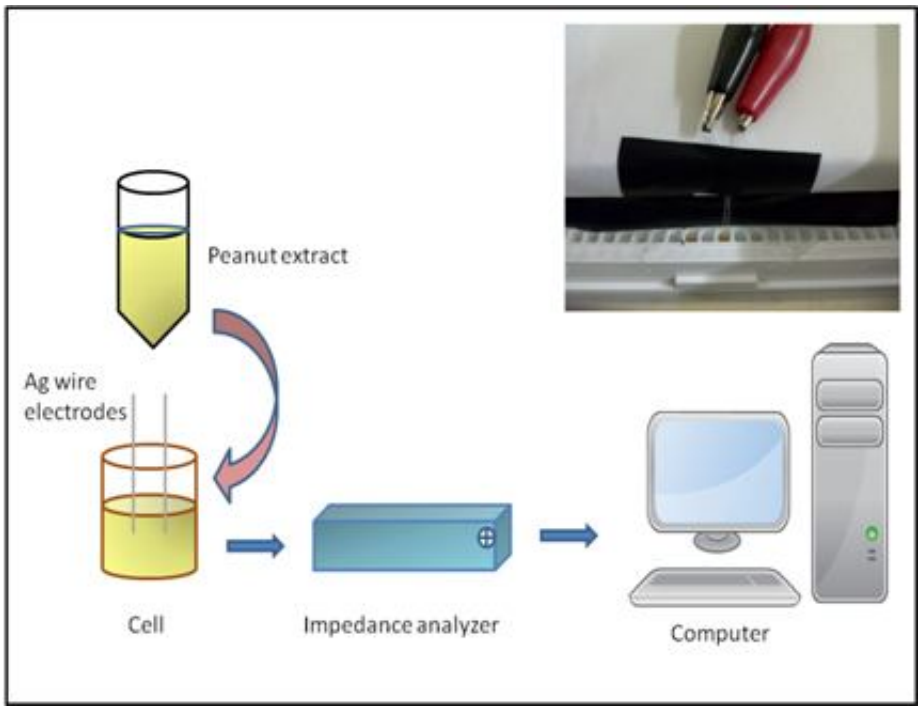

Figure 3.9 Schematic illustration of Ag wire electrode based impedimetric AFB1 immunosensor with EIS measurement setup; inset: Ag wire electrodes dipped into the 384 micro well plates.

3.5.2 Materials and methods

3.5.2.1 Materials and instrumentation

All the chemicals used were of analytical grade and used as received. Ag wire (diameter = 0.25 mm) and AFB1 were procured from ACROS Organics, USA. The diameter of wire was reduced to 0.18 mm by manual stretching. AFB1 primary polyclonal antibody (pAb) raised from rabbit, Tween20, 11-MUA, EDC and NHS were purchased from Sigma–Aldrich, USA. Ethyl Alcohol 200 proof was purchased from TEDIA, USA. Hydrogen peroxide (H_2O_2) 30 % (w/v), acetonitrile (ACN) HPLC grade, methanol, di-sodium hydrogen phosphate (Na_2HPO_4), sodium di-hydrogen phosphate (NaH_2PO_4) from MERCK (Germany) and sodium hypochlorite (4 %) solution were purchased from Fisher Scientific (India). For sample handling, micropipettes (eppendorf®, Germany) were used. Peanut samples were finely ground by a household mixer grinder. Shaking was done by Rotospin (Tarsons, India). Filtration was done by Whatman® filter paper 41 of 25 µm size. White 384 well polystyrene microtiter plates were purchased from Nunc (Denmark). For the handling of AFB1 standard solution, glove box (Cole Parmer, USA) was used. For preparing all the solutions, water

produced in a Milli-Q system (Millipore, Beford, MA, USA) was used. Certified ultra pure nitrogen (99.9 %), pH meter (Seven Multi Mettler Toledo, 8603, Switzerland) were used. Sonication of the sample was done on Toshcon ultrasonic cleaner (Toshniwal process instruments Pvt. Ltd., India). Impedance measurements were carried out using IVIUM™ CompactStat impedance analyzer, Netherland.

3.5.2.2 Preparation of AFB1 standard solutions

All the AFB1 solutions were prepared in a glove box in a maintained inert N_2 atmosphere. AFB1 stock solution 1000 µg /mL was prepared by dissolving the AFB1 crystalline in 5 % ACN (v/v) in PBS and stored at 4 $^{\circ}$C. Working AFB1 standard solutions were prepared in the following concentrations; 0.01, 0.1, 1, 10, 25, 50 & 100 pg mL^{-1} by diluting the stock with 5 % ACN.

3.5.2.3 Preparation of AFB1 antibody solutions

From the stock solution of rabbit polyclonal (pAb) [A8679-1ML], 1µL was taken and 999 µL of pyrogen free de-ionized water was added. From this 1:1000 dilution, working pAb solutions were prepared by serial dilution such as 1: 2000, 1: 4000, etc.

3.5.2.4 Peanut sample extraction procedure

Non contaminated peanuts were purchased from the local supermarket, Goa, India. The sample was extracted by the following method. Peanuts were finely ground by a household mixer grinder to a fine consistency. 10 g of this ground commodity was extracted with 50 mL of methanol/water mixture (80:20) by a rotospin shaker at 50 rpm for 15 min. The slurry was filtered through Whatman 41 filter paper and analyzed.

3.5.2.5 Immobilization of pAb on Ag wire electrode

The wires were washed with distilled water, followed by drying under the ultra pure nitrogen stream. This cleaning procedure was repeated before every electrode preparation step. Initially the surfaces of the bare Ag wire electrodes were washed ultrasonically in deionized water for 5 min to remove inorganic particles. Following this, the electrodes were immersed into piranha solution (H_2O_2/H_2SO_4, 30/70 v/v) for 30 s. The electrodes were dried with nitrogen stream before use. The clean and dried Ag wire electrodes were immersed overnight in 0.004 M ethanolic solution of 11-MUA under ambient condition. The electrodes covered

by SAMs were gently washed with absolute ethanol to remove unbounded 11-MUA residues. The electrodes were dried with nitrogen stream. The pAb was covalently coupled on Ag wire electrode through SAMs. For coupling the pAb, the carboxyl group of SAMs on modified electrode was activated by 1:1 EDC/NHS (0.1M each) mixture for 2 hrs. Subsequently, the electrodes were washed with distilled water to remove excess EDC/NHS. Finally, pAb was attached to the electrode by carefully spreading pAb solution (1: 64000 in coating buffer) over the activated surface followed by overnight incubation at 4° C. The unused antibody coupled electrodes were washed and stored at 4° C for future use.

3.5.2.6 Experimental

To conduct the experiment, 102 µL of the peanut extract solution was taken in 384 microwell plate. Then 3 µL AFB1 standard solutions (0.01, 0.1, 1, 10, 25, 50, 100 pg mL^{-1}) was spiked into it. The functionalized antibody coated antigen wires were dipped into the well by 10 mm and were separated by 1mm. EIS measurements were carried out at 5 mV applied potential with frequency range 1Hz to 100 kHz.

3.5.3 Results and discussion

3.5.3.1 Optimization of the immunosensor parameters

The parameters such as incubation time, frequency range, antibody dilution and applied voltage, influence the antibody-antigen binding. This parameter for antibody-antigen interaction using EIS was studied in detail in chapter 2. For AFB1 analysis, the optimized incubation time was found to be 20 min. The antibody dilution of 1: 64000 were found to be optimum. The influence of applied potential and frequency were also studied and found optimum as 5 mV and 1Hz.

3.5.3.2 Validation of sensor operation

The sensor was validated for quantitative AFB1 analysis. The EIS data were collected for different concentrations of AFB1 (0.01-100 pg mL^{-1}). Figure 3.10 represents Nyquist plot obtained from the ac impedance analysis of anti-AFB1 pAb following exposure to various AFB1 concentrations. The nature of the Nyquist plot confirms that the antibody-antigen interaction has occurred. A response corresponding to a change in the real component (Z´) accounts for the largest increase in impedance observed. The imaginary component (Z´´) increases to a larger extent at higher AFB1 concentrations were increased from 0.01-10 pg

mL^{-1}. The Intraday analysis of the presented immunosensor (n=4) showed a good repeatability with 5 % variance.

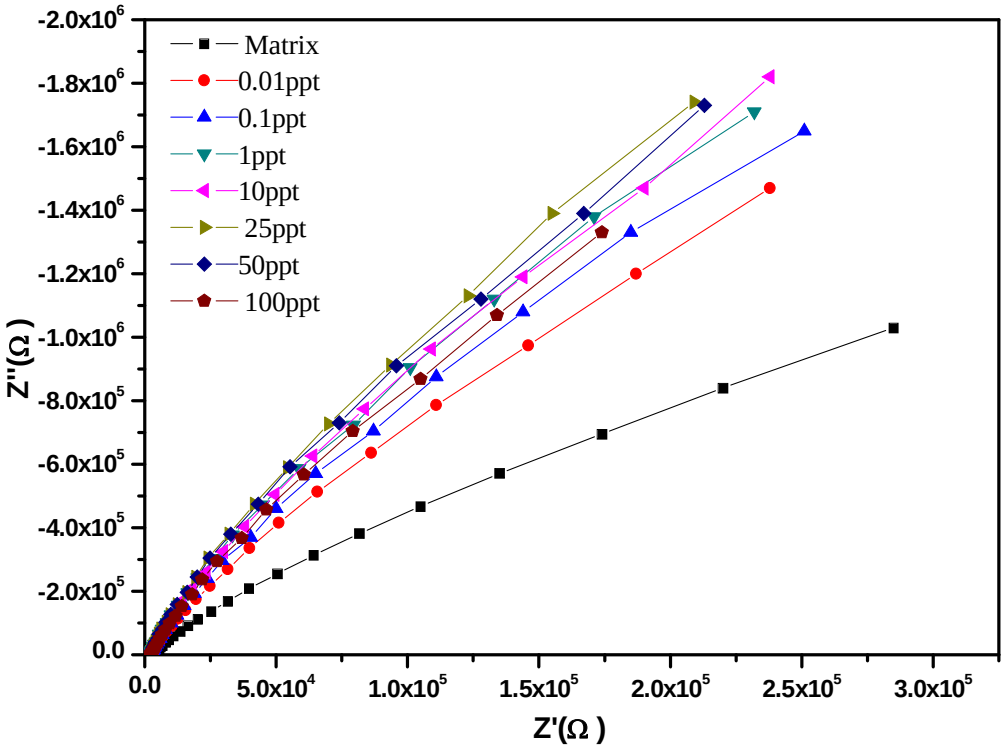

Figure 3.10 Nyquist plot in presence of different concentration of AFB1 (in peanut based matrix) at electrode surface. EIS: 1 Hz to 100 kHz, 5 mV ac potential.

3.5.3.3 Equivalent circuit analysis & validation

Various equivalent circuits have been evaluated to fit the obtained data for AFB1 analysis. The proposed equivalent circuit with best fit results for the electrochemical cell using modified electrode is presented as Figure 3.11. The presented equivalent circuit describes non-faradic phenomenon at the electrode-electrolyte interface. This equivalent circuit consists of ohmic resistance of medium (R_s), double layer capacitance of outer layer ($C_{dl(ol)}$), double layer capacitance of inner layer ($C_{dl(il)}$) and resistance of inner layer (R_{dl}) (Bacher *et al.*, 2012). $C_{dl(ol)}$ ($R_{dl}C_{dl(il)}$) represent the two layer structure for each electrode. $C_{dl(ol)}$ represents the outer layer of the interface where the antibody-antigen interaction takes place. ($R_{dl}C_{dl(il)}$) sub-circuit represents the inner layer of the interface. R_{dl} being parallel to $C_{dl(il)}$, resembles a part of SAMs. R_{dl} is interpreted as the conductivity (by penetrating ions) of the SAMs (Bart *et al.*, 2005). The best fit is obtained for $C_{dl(ol)}$ as constant phase element and modified as $CPE_{dl(ol)}$. Figure 3.12 shows Bode plot of experimental and fitted impedance spectra of

AFB1. Fitting was done by using IVIUM™ equivalent circuit evaluator and optimized with phase, Z´ and Z´´. The error weight is taken as equal for each point. It is evident from Figure 3.12 that for the presented immunosensor, the fitting has good agreement with experimental data, thereby validating the equivalent circuit.

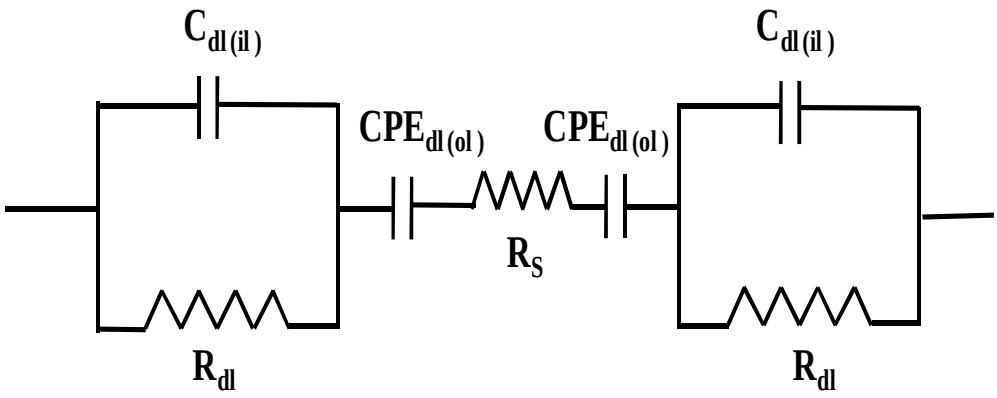

Figure 3.11 Equivalent circuit used to fit impedance of the AFB1 immunosensor in peanut based matrix.

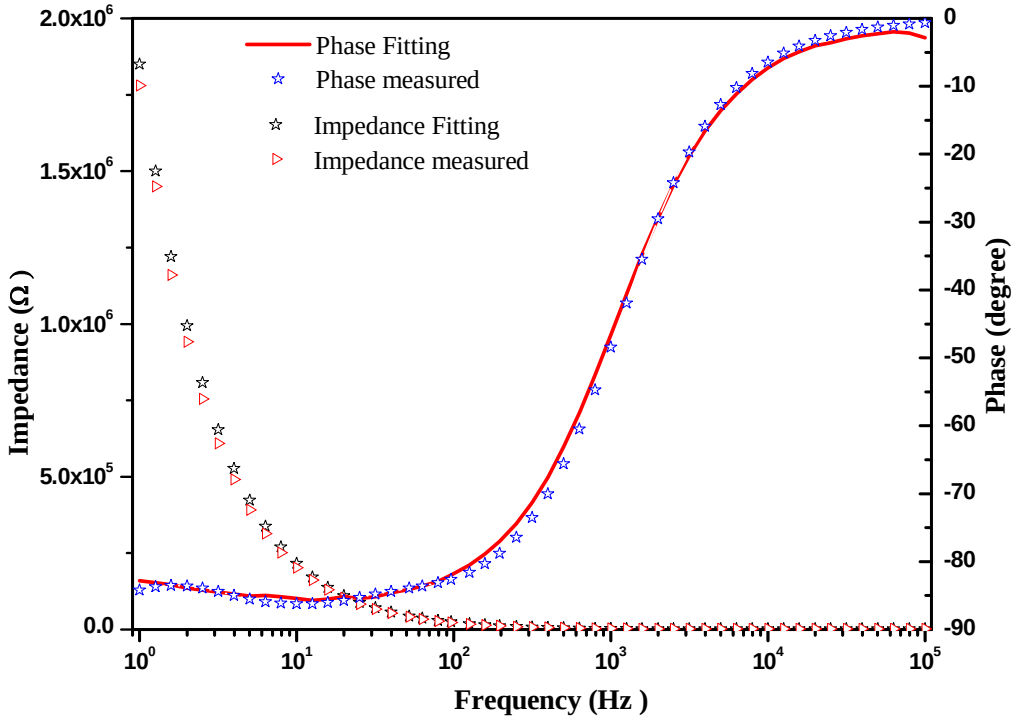

Figure 3.12 Bode plot of AFB1 analysis with the fitting curve. EIS: 5 mV ac potential, frequency range: 1 Hz to 100 kHz.

3.5.3.4 Calibration of sensor for AFB1 detection

Impedance data were recorded for the functionalized electrodes after exposing it to increasing AFB1 concentration (0.01-100 pg mL^{-1}). A frequency of 1Hz at applied ac potential 5 mV was selected for analysis, since at this frequency significant change in impedance response was observed. The specific interaction of anti-AFB1 and AFB1 gave rise to an overall increase in impedance change from baseline response at the electrode-solution interface for AFB1 concentration (0.01-10 pg mL^{-1}). The % impedance change was calculated corresponding to different concentrations of AFB1. The resulting calibration curve is presented in Figure 3.13. The analytical figure of merit of developed immunosensor for AFB1 analysis is presented as Table 3.6.

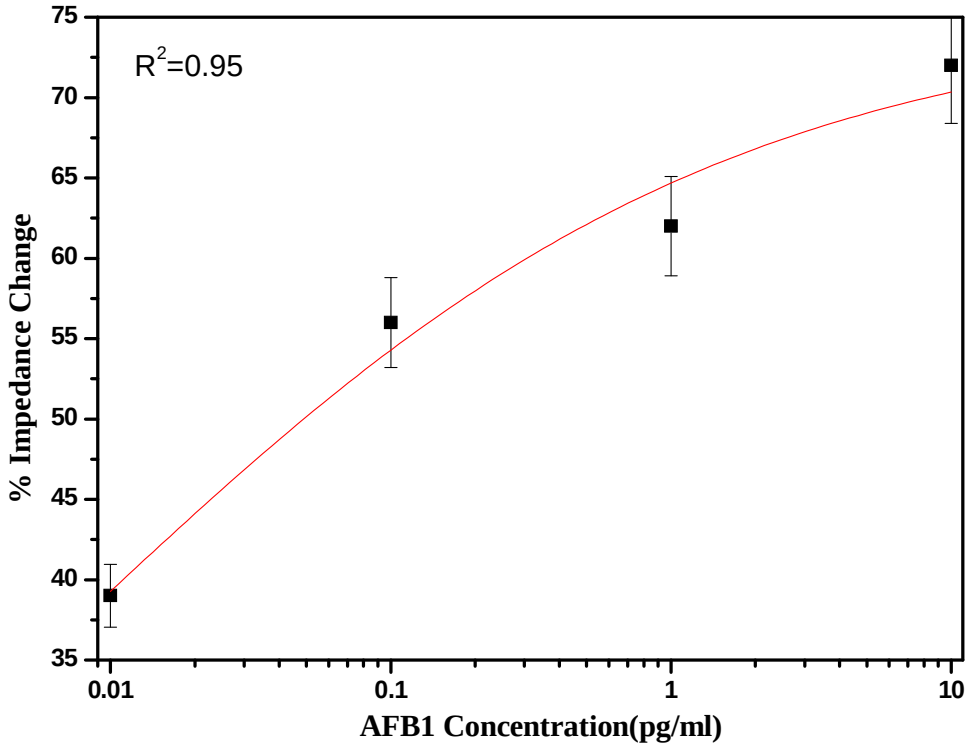

Figure 3.13 Calibration curve obtained for label-free immunosensor, anti-AFB1 pAb diluted to 1: 64000 in peanut matrix.

Table 3.6 Analytical figures of merit of the developed immunosensor for AFB1 analysis in peanut matrix

Analytical parameters	Experimental findings
Dynamic Range	0.01-100 pg mL^{-1}
Linear Range	0.01-10 pg mL^{-1}
LOD	0.01 pg mL^{-1}
S.D	0.16
R^2	0.954
Assay sample volume	105 µL
Analysis time	20 min

3.5.4 Conclusions

A highly sensitive and miniaturized label-free impedimetric immunosensor has been demonstrated for the analysis of AFB1 in peanut. A reduced sample volume of 105 µL was achieved with 384 microwell plate. The electrode diameter was reduced to 0.17 mm from 0.25 mm. The voltage for impedance measurement was optimized for 5 mV. The sensor could help screen the low level contamination of AFB1 in peanut samples. A linear range for AFB1 detection 0.1-10 pg mL^{-1} with SD= 0.16 and R^2= 0.954 was achieved. LOD was found to be 0.01 pg mL^{-1}. The immunosensor is simple to use and cost effective, thus it could be used in field conditions.

3.6 Development of impedimetric immunosensors for detection of *E. coli* in water

3.6.1 Introduction

The detection of contaminated water by pathogenic microorganism is an important concern for ensuring water safety, security and public health. A clean and treated water supply to each house may be the norm in Europe and North America, but in developing countries, access to both clean water and sanitation are not in the prime focus thus waterborne infections are common. *Escherichia coli (E.coli)* is a natural inhabitant of the intestinal tracts of humans and warm-blooded animals. The presence of this bacterium in water indicates that fecal

contamination may have occurred and consumers might be exposed to enteric pathogens when consuming water. Hence, *E. coli* is often preferred as an indicator organism because it is specifically stands for fecal contamination (Min and Baeumner, 2002). Rapid and reliable detection of *E.coli* is critical for the management of the waterborne diseases threatening human lives worldwide. Despite the potential public health threat from waterborne *E. coli*, there are no accepted methods for the rapid, accurate detection in surface waters. Current measures of microbial water quality rely exclusively on "indicators" of fecal pollution (e.g., fecal coliform bacteria or generic *E. coli*). However, there are no established correlations between the prevalence or concentration of these "indicators" and specific pathogens (Shelton *et al.*, 2006). Conventional methods for bacterial identification, usually involve various culturing techniques and different biochemical tests which are very time consuming and usually requires 2-4 days. Hence, there is a need for adequate monitoring technologies targeting representative pathogenic bacteria like *E. coli* at low levels within hours to prevent mortality and morbidity caused by waterborne outbreaks. Analysis time and sensitivity are the most important limitations related to the usefulness of bacterial testing. An extremely selective detection methodology is also required, because low numbers of pathogenic bacteria are often present in a complex biological environment along with many other non-pathogenic bacteria (Maalouf *et al.*, 2007). Biosensor techniques are particularly attractive for the detection and identification of pathogenic organism since they have potential sensitivity and selectivity. They are easy to use, provides results in few minutes, require minimal reagents, and can be deployed in the fields.

In recent years, several biosensors techniques have played important roles in the detection of pathogenic bacteria in different matrices. A variety of Immunosensors have been developed based on the antibody of the target bacteria, which utilizes fluorescence (Heyduk and Heyduk, 2010), EIS (Barreiros dos Santos *et al.*, 2013), QCM (Guo *et al.*, 2012) and SPR (Baccar *et al.*, 2010) However, these biosensors lack in practical applications because of their single use nature and instability of antibodies in unfavourable conditions. Moreover, DNA-based biosensors require efficient DNA extraction and need DNA amplification using PCR as bacterial cells contain a low copy number of DNA (Liao and Ho, 2009). Among the reported biosensors, EIS has emerged as sensitive techniques for bacterial detection due to multiple advantages, such as fast response, low cost and capability of miniaturization. Impedimetric biosensor was reported to detect whole *E. coli* bacterial cells in food and water (Radke and Alocilja, 2004). More recently, a label free DNA aptamer biosensor was reported,

incorporated in a biochip and used for in situ detection of *E. coli* outer membrane protein in water samples (Queirósa *et al*., 2013).

In the previous sections, the development of an impedimetric immunosensor for AFM1 and AFB1 using two electrode setup was described. In this section we demonstrate a simple, cost effective, label-free impedimetric immunosensor for detection of *E. coli* in water. To test the biosensor performance as a proof of concept for bacterial detection, a generic strain of *E.coli* MTCC-723 was used as a surrogate for the waterborne pathogen Enterotoxigenic *E.coli* (ETEC). The immunosensor is based on the use of anti-*E.coli* polyclonal antibodies immobilized on the Ag-wire electrode surface. The antibody immobilization and its ability to selectively graft *E.coli* on the sensing surface were fully characterized by fluorescence microscopy techniques. The developed immunosensor is highly sensitive, allowing for the detection of 10^2 - 10^8 CFU mL^{-1} of *E.coli* bacteria.

3.6.2 Experimental setup

The experimental setup consist of a pair of pre-functionalized Ag wire (0.25mm diameter) electrode immersed in the single well of Nunc 384 polystyrene well plate (capacity 120 µL/well) containing 90 µL bacterial suspensions of different concentration. The Ag-wire surface is functionalized with attached *pAb-E.coli* over the SAMs, to form a biological transducer. The electrode setup and the well plate were placed in a custom made Faraday cage. In the presented setup, the two pre-functionalized Ag wire electrodes were dipped in to the micro well plate. The functionalized Ag wire electrodes were connected to IVIUM CompactStat impedance analyzer. The schematic of experimental setup is presented as Figure 3.14.

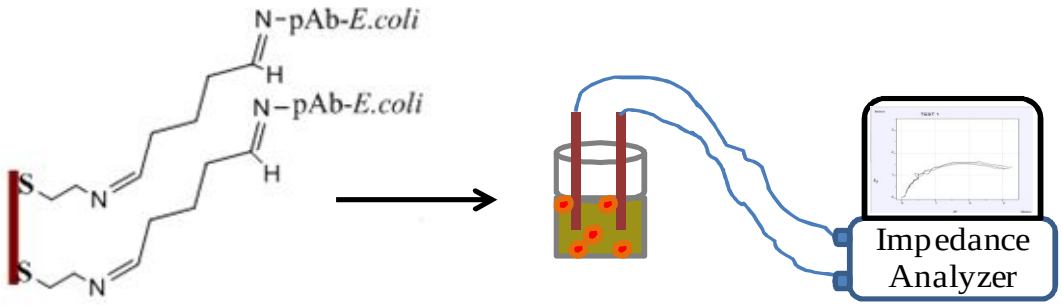

Figure 3.14 Schematic representation of Ag wire electrode based impedimetric immunosensor for detection of *E.coli*.

3.6.3 Results and discussion

3.6.3.1 Optimization of the immunosensor parameters

Various parameter were optimized which can influence the impedance measurement for *E.coli* analysis. The change in impedance of the immunosensor depends upon *E.coli* and *anti-E.coli* binding and incubation time. Hence, the effect of both the parameters has been investigated. Several *anti-E.coli* dilution ratios with PBS were evaluated (1:100, 1:1000 and 1:10000) and the maximum change in impedance was recorded for a dilution of 1:1000. Incubation time of 5 min was found to be optimal for impedance measurements. The influence of applied potential and frequency were also studied and found optimum as 10 mV and 10 Hz (Mishra *et al*., 2015).

3.6.3.2 EIS studies for *E. coli* binding

The antibody-antigen interaction of *pAb- E.coli* and *E.coli* Ag-wire electrode surface was studied using EIS. Figure 3.15 shows the impedance response for different concentrations of *E.coli* (10^2- 10^8 CFU mL^{-1}) in water resulted from the interaction of antibody-antigen on functionalized electrode surface. EIS is a useful technique to capture such interaction. This interaction results in a change of electrical properties such as capacitance and resistance at the electrode surface, allowing for label-free biosensing (Guan *et al*., 2004). In the EIS measurement, pAb-*E.coli* interactions create a new charged layer as a capacitance that is in series with the double layer capacitance. A decreased double layer capacitance and increased impedance were observed at the lower frequency. This confirms that the change in impedance is resulting from the binding of the antigen (*E.coli*). A decrease in impedance was observed with increasing frequency in the low frequency range from 10 Hz to 1 kHz, but in the high frequency range from1 kHz to 100 kHz, impedance was independent of frequency. At low frequencies (<1 kHz), the double layer capacitance offers essentially high impedance, it becomes the main component contributing to the total impedance, such that the medium resistance can be neglected. This region is defined as the double layer capacitive region in which the electrode impedance can be detected. When in the high frequency range (>1 kHz), the double layer capacitance almost offers no impedance, and its contribution to the total impedance nears zero. Thus, the only contribution to the total impedance at high frequencies is the medium resistance that is independent of the frequency. In the high frequency region (10 Hz to 100 kHz) it was observed that impedance remains constant. A

significant change was measured in the low frequency region (10 Hz to 1 kHz) with highest impedance change observed at 10 Hz.

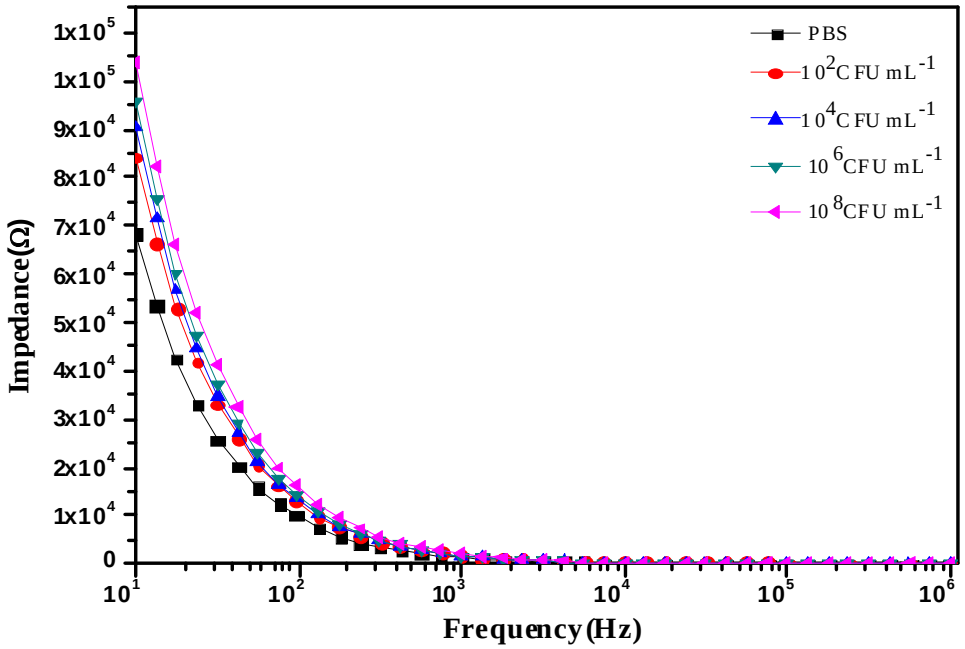

Figure 3.15 Impedance spectra for different concentrations of *E. coli* (10^2- 10^8 CFU mL^{-1}) in water. EIS: 10 Hz to 100 kHz applied frequency and 10 mV ac potential.

3.6.3.3 Calibration of sensor for *E. coli* detection in water

The *E.coli* bacterial samples were spiked in water samples to meet the calibration standards. Before spiking the standards, water was filtered through the bacteriological membrane filter (0.22 µ) and tested for the presence of any other *E. coli* strain i.e. *E.coli* O157:H7 using Singlepath® *E.coli* O157, a gold labeled immunosorbent assay (GLISA) rapid test (obtained from Merck-Millipore, Germany)**.** Impedance data was recorded for the functionalized electrodes after exposing it to increasing *E.coli* concentration (10^2-10^8 CFU mL^{-1}) in water. A frequency of 10 Hz at applied potential 10 mV was selected for analysis, since at this frequency significant change in impedance response was observed. The specific interaction of pAb-*E.coli* and *E.coli* gave rise to an overall increase in impedance change from baseline response at the electrode/solution interface for *E.coli* concentrations. The % impedance change was calculated corresponding to different concentrations of *E. coli*. The resulting calibration curve in water is shown as Figure 3.16. The analytical figures of merit of the developed immunosensor are presented in Table 3.7.

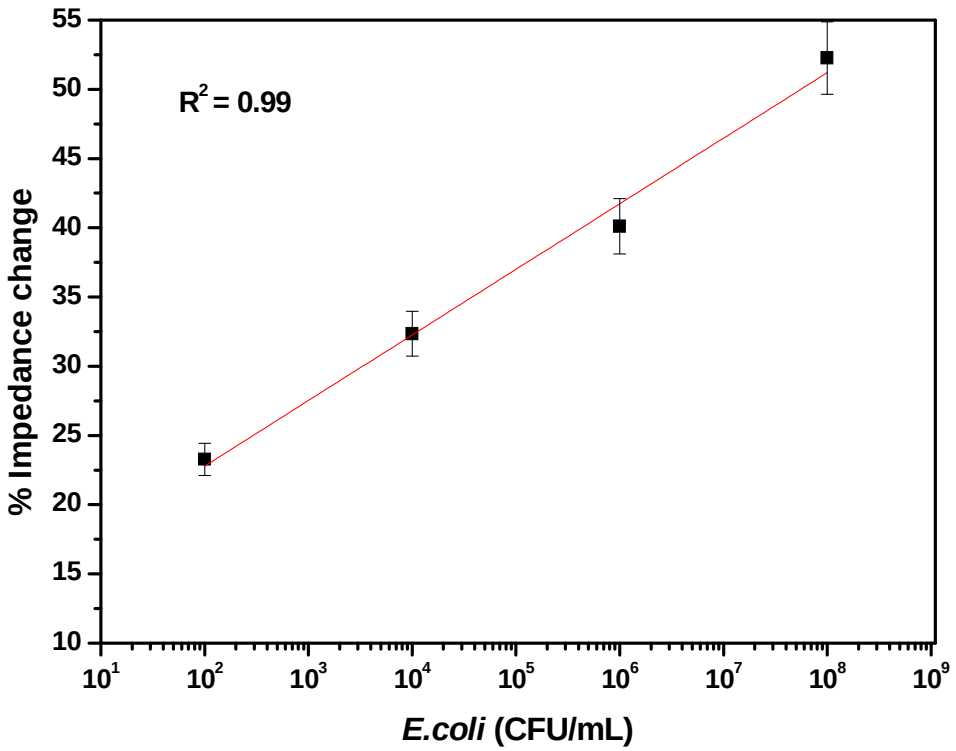

Figure 3.16 Calibration curve obtained for label-free impedimetric immunosensor for *E.coli* in water. EIS: 1 Hz to100 kHz applied frequency and at 10 mV ac potential.

Table 3.7 Analytical figures of merit of the developed immunosensor for *E.coli* MTCC 723 in water

Analytical parameters	**Experimental findings**
Dynamic Range	10^2-10^8 CFU mL^{-1}
Linear Range	10^2-10^8 CFU mL^{-1}
LOD	10^2 CFU mL^{-1}
S.D	0.80
R^2	0.99
Assay sample volume	90 µL
Analysis time	10 min

3.6.4 Conclusions

Using an anti E Coli antibody functionalized Ag wire, a label free impedimetric immunosensor for *E.coli* (MTCC-723) detection in water sample was demonstrated. Sensitivity and specificity of the developed immunosensor were examined by monitoring the changes in impedance of the Ag wire after bacterial cells were deposited on its surface. A linear trend of increasing impedance was obtained when the *E. coli* concentration increased from 10^2-10^8 CFU mL^{-1}. Presented immunosensor also supports that the label-free approaches may become practical for routine analysis of bacterial contamination in water.

Chapter 4

Development of micro interdigitated electrodes (µ-IDEs) array impedimetric immunosensor for detection of AFM1

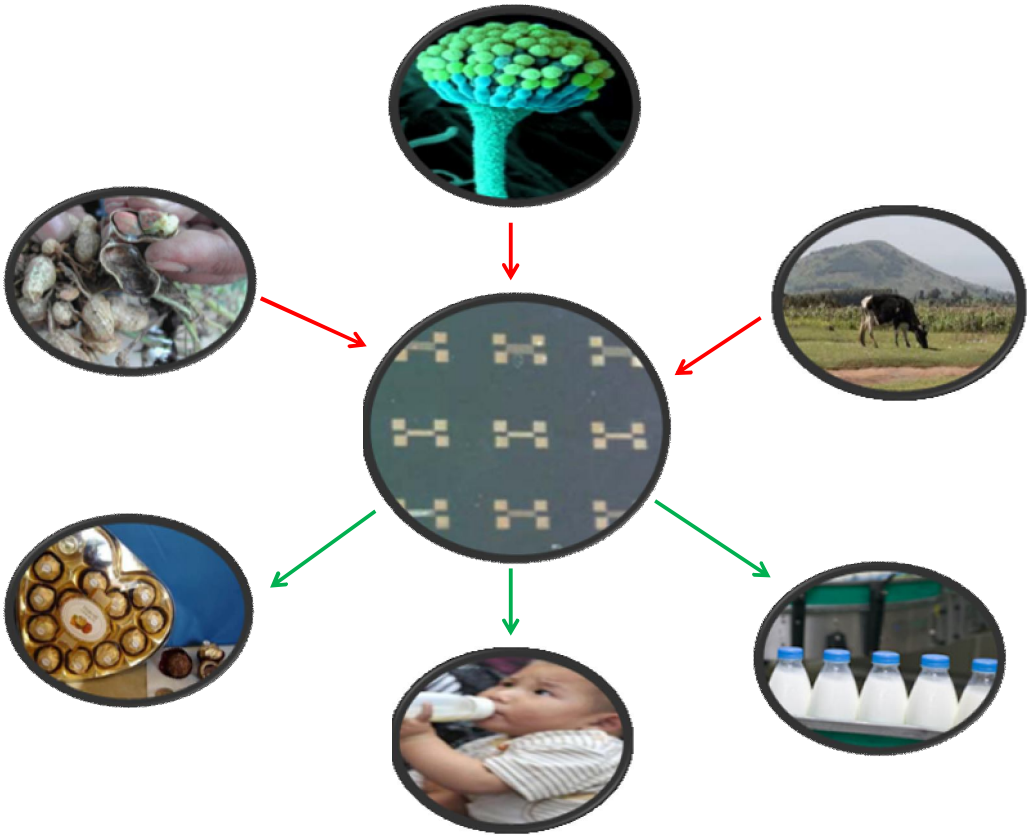

Graphical abstract of chapter content

Note: The work incorporated in this chapter of the thesis constitutes collaborative experimental work among BITS, Pilani & CARE IIT Delhi and had resulted in Intellectual Property, which is filed as an Indian Patent with application No. 1203/MUM/2013 and PCT International (PCT/IN2014/000176) and publication No. WO/2014/155391. Thus, due to non disclosure commitment to the funding agency (ICAR), some of the details are not disclosed.

4.1 Introduction

4.1.1 Background

In the previous chapter we have described the development of biosensor based on Ag wire electrode. The use of two electrode based impedance measurement setup for detection of aflatoxin in milk, peanut and bacteria in serum was demonstrated. In this thesis chapter, we have further miniaturized the two electrode by realizing the patterned electrode with the help of microfabrication technique. The process flow diagram of Microfabrication techniques is presented as Figure 4.1. We have also developed an application for aflatoxin analysis.

Miniaturized biosensors are necessary for many applications that need portable systems. The need for miniaturization arises from the need for increased throughput and reduced cost of analysis per sample. Miniaturized systems reduce reagent consumption by a factor of 10^3-10^4, (Figeys and Pinto, 2000). In impedance biosensor, impedance measurement requires macrosized metal rods or wires as electrodes to be immersed in the medium (Towe and Pizziconi, 1997). In an effort to miniaturize the sensor and to improve the sensitivity, microelectrodes are considered as promising candidate to combine with traditional detection systems.

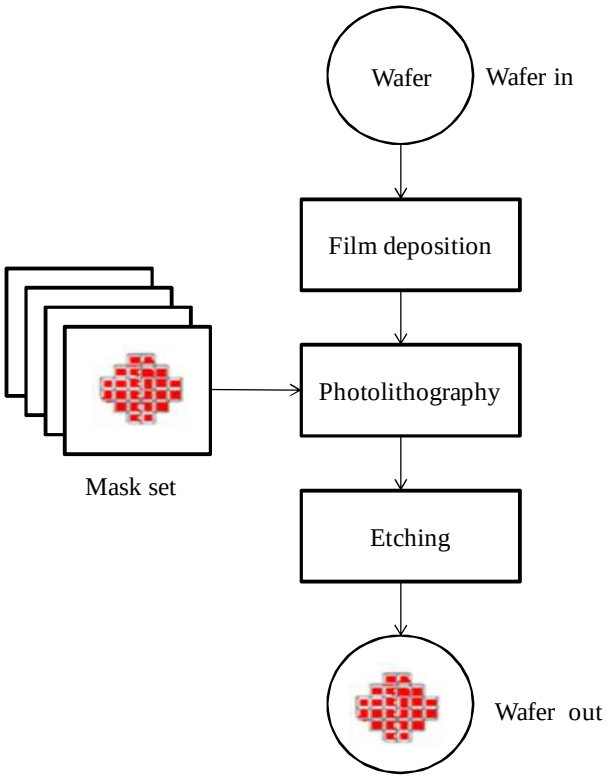

Figure 4.1 Process flow diagram of microfabrication technique.

4.1.2 Macroelectrode *vs* Microelectrode

In microelectrodes, the current is small and the current density is very high as compared to macroelectrodes. This high current density allows the microelectrode to be used in resistive media, including organic solvents. The enhanced diffusion allows steady state limiting currents to be achieved faster than macroelectrodes. Moreover, microelectrodes require lower concentrations of electro-active ions to form a double layer (Min and Baeumner, 2004). Thus, using microelectrodes, impedance measurement can be performed even in low conductivity solutions. Although microelectrodes offers many advantages over conventional electrodes, they suffer from a major disadvantage of very low resultant current which is difficult to measure. This can be addressed by using multiple microelectrodes connected in parallel to form an array of microelectrodes (Belmont *et al*., 1996).

4.1.3 Micro interdigitated electrodes (µ-IDEs)

Among the microelectrodes, micro interdigitated electrodes (µ-IDEs) present promising advantages in terms of low ohmic drop, fast establishment of steady-state, rapid reaction kinetics, and increased signal-to-noise ratio (Mauyama *et al*., 2006). µ-IDEs consists of a series of parallel microband electrodes in which alternating microbands are connected together, forming a set of interdigitating electrode fingers. Due to the proximity of cathodic and anodic electrodes, minute amounts of ionic species can be efficiently cycled between the electrodes, resulting in very large (>0.98) collection efficiencies (Thomas *et al*., 2004). In addition, µ-IDEs does not require a reference electrode and provide a simple means for obtaining a steady-state current response. This is relatively simpler to detect as compared to three or four electrode systems (Nebling *et al*., 2004).

4.1.4 µ-IDEs material and geometry

The use of µ-IDEs for the development of biosensors has been receiving growing interest. The fabrication of the µ-IDEs by means of lithography allows for the development of sensitive, low cost and miniaturized chemical sensors and biosensors. The µ-IDEs are usually fabricated by photolithography techniques on silicon (Si) and glass substrates and have a typical electrode width and spacing, which vary from nanometers (nm) to tens of microns. Au, Ti and Pt are some of the most commonly used metals for the fabrication of electrodes. A summary of µ-IDEs with various metals with dimensions is presented as Table 4.1.

The selection of materials for electrode fabrication depends on the specific application, ionic species, inertness of the material to the environment and their suitability to the fabrication process. They are fabricated on a variety of base materials, but the most commonly used ones are Si and quartz/glass (Kim *et al*., 2006). To avoid the complexity of the fabrication process, only one material is typically used for electrode fabrication. However, the effect of using different combinations of materials was also reported (Laczka *et al*., 2008).

Table 4.1 Summary of microfabricated μ-IDEs with various metals

Material	**Features size**	**Substrate**	**Fabrication techniques**	**Reference**
Gold (Au)	5 μm wide, pitch of 10 μm	Silicon	Photolithography	Chornokur *et al*., 2011
Gold (Au)	3 μm wide, 3μm space	Fused silica	Ion beam lithography	Rana *et al*., 2011
Titanium (Ti) , nickel(Ni) and gold(Au)	10 μm wide and 1.5 mm long.	Pyrex	Photolithography	Laczka *et al*., 2008
Platinum (Pt)	10 mm wide × 20 mm long × 0.5 mm thick, spacing are 20, 15, 10, and 5 μm	Borosilicate glass	Photolithography	Yang *et al*., 2011
Silver (Ag)	Length 6 mm, width 0.2 mm, electrode spacing 0.5 mm).	Epoxy-glass fiber PCB	Photolithography	Cortina *et al*., 2006
Aluminium (Al)	Width of 1.3 and spacing of 1.0 μm	Silicon	Photolithography	Moreno *et al*., 2007

4.1.5 Photolithography

The photolithography process can be broadly divided into the following steps; (a) wafer preparation (b) photoresist (PR) coating and pre-baking (c) exposure, PR developing, wafer inspection and post baking (d) etching of layer (e) removal of photoresist. The schematic diagram of standard photolithography process is shown in Figure 4.2. The PR developing is normally carried out in the same room where exposure unit is located. The photoresist is sensitive to the UV and blue-region of the light spectrum. For this reason, the photolithography area is provided with yellow lights.

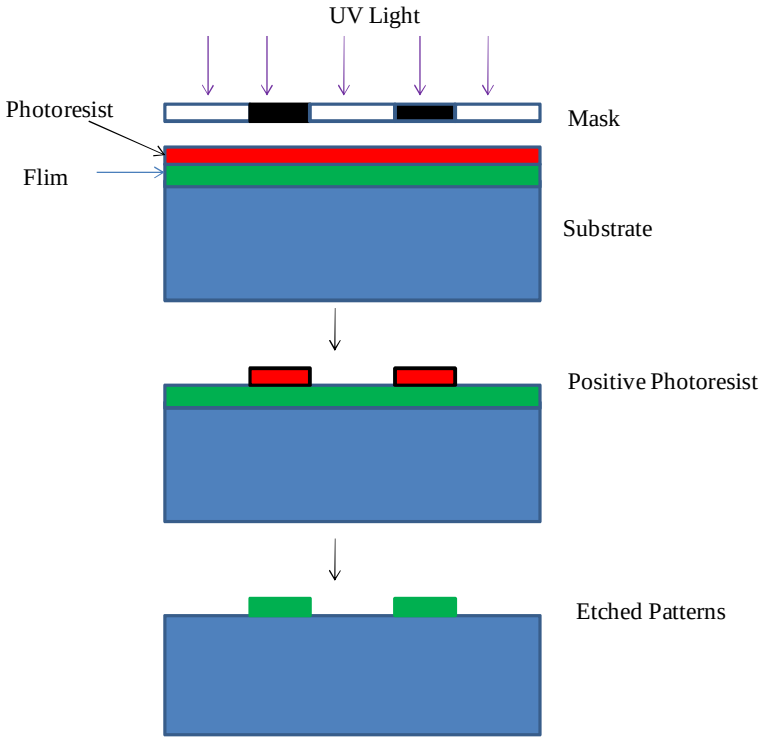

Figure 4.2 Process flow diagrams of photolithography technique.

4.1.6 EIS with µ-IDEs

EIS represents an important electrical transduction means of antibody-antigen interactions. EIS using µ-IDEs can directly sense detailed information about biological events occurring on an electrode surface (Yang and Guiseppi-Elie, 2008). The interaction is quantified in terms of induced capacitance and/or resistance changes, thus allowing for label-free detection and the study of biological systems. The EIS does not require multiple labelling and amplification steps associated with many other detection methods (Linderholm and Vannod, 2007). EIS technique with µ-IDEs has many biosensor applications. In the literature, several

µ-IDEs with EIS techniques are reported for the analysis of different analytes as presented in Table 4.2.

Table 4.2 Reported µ-IDEs with EIS for detection of different analyte

Analyte	**Detection technique**	**LOD**	**Reference**
Prostate-Specific Antigen (PSA)	EIS	1 pg ml^{-1}	Chornokur *et al.*, 2011
E. coli O157:H7	EIS	1.6×10^{2} cells	Varshney and Li, 2007
S. typhimurium	EIS	4.8×10^{0} $CFUml^{-1}$	Yang *et al*., 2004
C-reactive protein	EIS	0.1 ng mL^{-1}	Rossi *et al*., 2004
Myoglobin	EIS	100 ng mL^{-1}	Tweedie *et al*., 2006

4.1.7 Research gaps identified

Various sensor platforms have been used for electrochemical sensors, but these are mostly based on screen-printed technology (Paniel *et al*., 2010). Interest in the use of microelectrodes based on photolithography techniques, coupled with electrochemical detection methods is increasing. µ-IDEs have a greater advantage in terms of low ohmic drop, fast steady state response, rapid reaction kinetics and increased signal to noise ratio. For example, an impedimetric biosensor based on interdigitated electrode system was used to detect bacterial pathogens (Radke and Alocilja, 2005). More attractively, integration of EIS with µ-IDEs could provide sensitive label-free biosensing systems for detection of small molecules. A gold microelectrode array (MEA) was developed for detection of AFM1 (Parkar *et al.*, 2009). The microarray was characterized using cyclic voltammetry and measurement was carried out using a three electrode system. Though the sensor is sensitive, but uses electrochemical detection with HRP as the enzyme label. Thus, there is a need for simple, sensitive, robust, low cost and field-portable device for analysis of AFM1 in real sample. µ-IDEs are suitable to achieve all these characteristics for aflatoxin detection.

4.1.8 Objective

The aim was to develop a novel µ-IDEs device as impedimetric immunosensor for detection of AFM1.

4.1.9 µ-IDEs sensing principle

µ-IDEs resemble as parallel plate capacitor and work as an interdigitated capacitive sensor. Interdigitated electrodes are fabricated on a substrate and functionalized with probe biomolecules as shown in Figure 4.3. The interaction between the immobilized probes and target molecules may be monitored as a change in capacitance or impedance of the device. The capacitance of an µ-IDEs sensor is given by Equation 4.1 (Tsouti *et al.*, 2011).

$$C = n\,\varepsilon\,\frac{lt}{d} \qquad (4.1)$$

where ε is the permittivity of the sensitive coating film

n is number of electrode fingers,

l is the length of finger,

t is the thickness of the interdigitated electrodes and d is the distance between the electrodes.

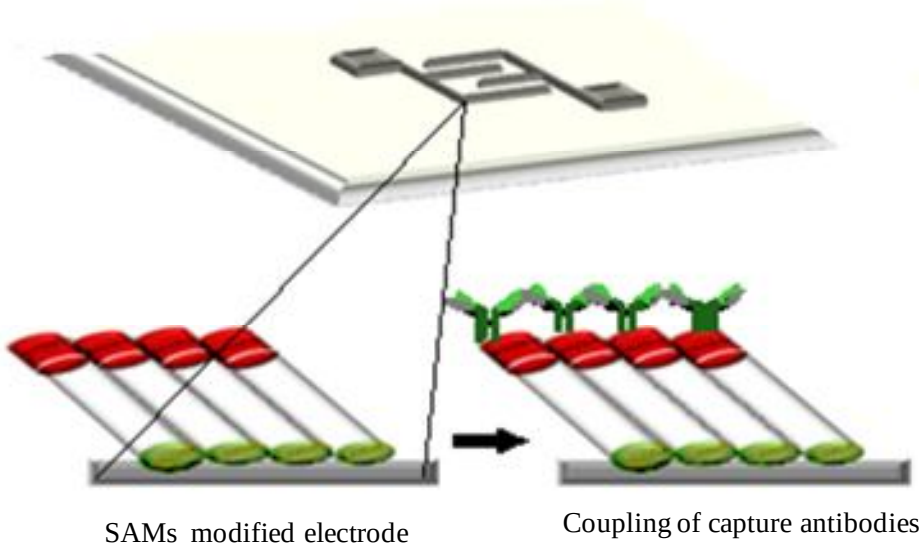

Figure 4.3 Schematic representation of immobilization of antibody on the functionalized patterned electrodes.

4.2 Novel µ-IDEs device fabrication

The novel µ-IDEs device was designed at BITS Pilani, Goa and fabricated at Centre for Applied Research in Electronics CARE, IIT Delhi. The fabrication of the µ-IDEs device includes following steps: (a) mask making (b) fabrication of µ-IDEs. The device was realized by depositing the desired electrode material and patterning of µ-IDEs structure using photolithography techniques. The optical photograph of the µ-IDEs device with zoomed images is shown Figure 4.4. The device as received was used for developing the aflatoxin analysis.

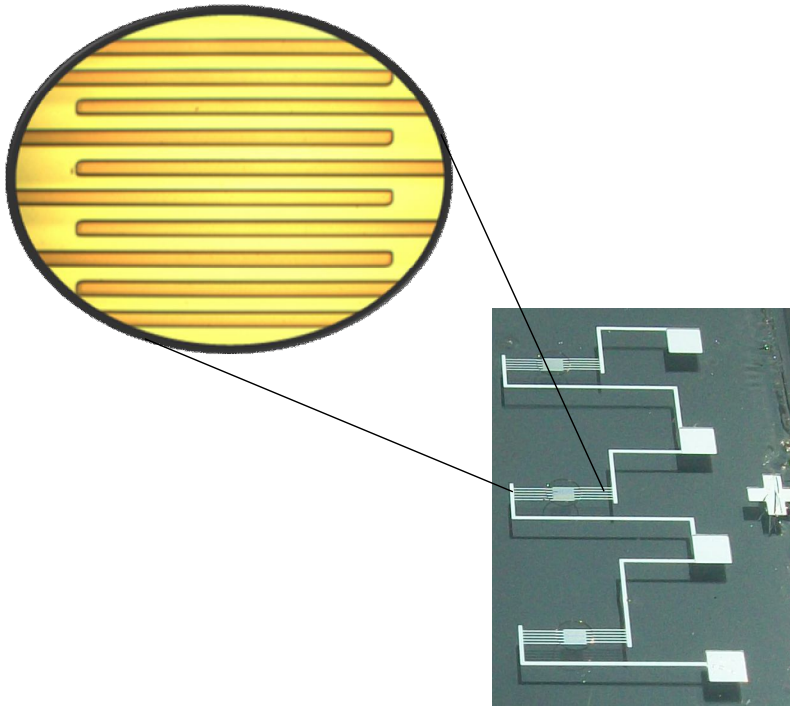

Figure 4.4 Optical photograph of µ-IDEs device with zoomed image.

4.3 Results and discussion

4.3.1 Optimization of µ-IDEs immunosensor parameters

The response of the µ-IDEs impedance biosensor greatly depends on the measurement conditions such as applied potential, frequency of measurement and sample volume, and mainly depends upon the analyte and the matrix being used. Therefore, these measurement parameters were optimized for µ-IDEs for analysis of aflatoxins. For the quantification of aflatoxins using EIS, various parameters were optimized such as applied potential and applied frequency. As the antibody and antigen binding was studied, care was taken so that

there was no disruption to the delicate antibody coating. Different voltages (0.1 mV, 0.5 mV, 1 mV and 5 mV) were applied for EIS measurement. An appropriate voltage was chosen to study antibody-antigen interaction through impedance measurement. The applied frequency was in the range from 1 Hz to 100 kHz. The single frequency for quantification depends upon analyte and the matrix used. The frequency was also optimized based on the analyte and matrix used. Sample volume was also varied and the optimum volume was found to be 20 µL.

4.3.2 Validation of µ-IDEs biosensor for AFM1

The µ-IDEs biosensor was validated for quantitative AFM1 analysis. The EIS data was recorded for various concentrations of AFM1 (1-100 pg mL^{-1}). Figure 4.5 shows the impedance spectra obtained for ac impedance analysis of mAb following exposure to various AFM1 concentrations. A significant increase in the impedance was observed in the lower frequency range, when AFM1 concentrations was increased from 1 to 100 pg mL^{-1}.

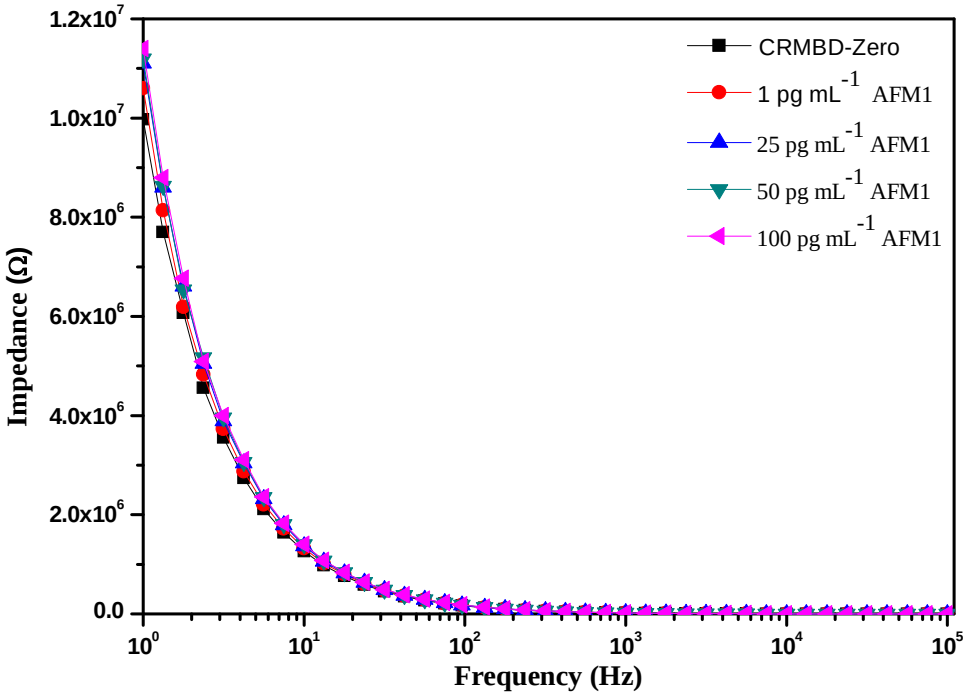

Figure 4.5 Impedance spectra of the µ-IDEs immunosensor after interaction of mAb with increasing concentration (1-100 pg mL^{-1}) of AFM1.

4.3.3 Calibration of µ-IDEs immunosensor for AFM1 in milk

Impedance data were recorded for the functionalized electrodes after exposing it to increasing AFM1concentration (1-100 pg mL^{-1}). The specific interaction of mAb and AFM1 gave rise to an overall increase in impedance change from baseline response at the electrode-solution

interface. The % impedance change was calculated as against blank and different concentrations of AFM1. The resulting calibration curve is shown in Figure 4.6. The calibration was found to be linear in the range of 25-100 pg mL^{-1} (R^2= 0.99). Limit of detection (LOD) was found to be 1 pg mL^{-1} and limit of quantitation (LOQ) was 100 pg mL^{-1}.

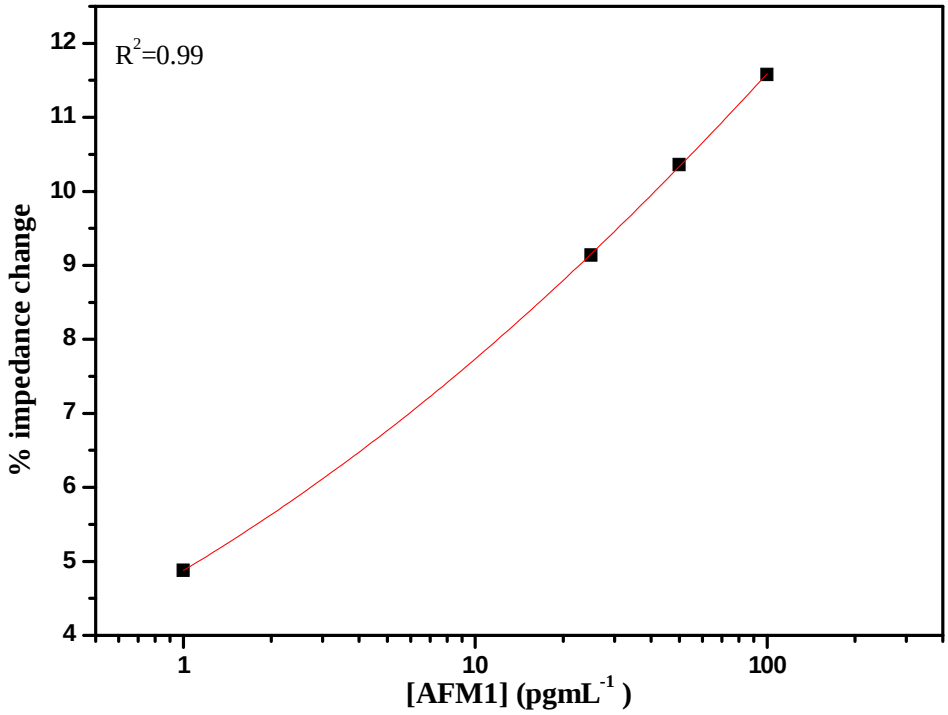

Figure 4.6 Calibration curve of µ-IDEs immunosensor for detection of AFM1.

4.4 Mycotoxin proficiency test in milk using µ-IDEs device

A proficiency test was conducted on the developed µ-IDEs device for AFM1 detection. The impedance measurement was carried out first using a standard kit solution and then with unknown sample. Impedance data were recorded for the functionalized electrodes after exposing it to increasing standard kit solution from (10 to 100 pg mL^{-1}) of AFM1. The resulting calibration curve is presented in Figure 4.7, for various concentrations of AFM1. The calibration was found to be linear in the range of 10-100 pg mL^{-1} (R^2= 0.99). Limit of detection (LOD) was found to be 10 pg mL^{-1} and limit of quantitation (LOQ) was 100 pg mL^{-1}. Similar impedance measurement was carried out for the unknown sample this is shown in Figure 4.8. From these figures it was clear that the unknown sample was detectable using the developed device.

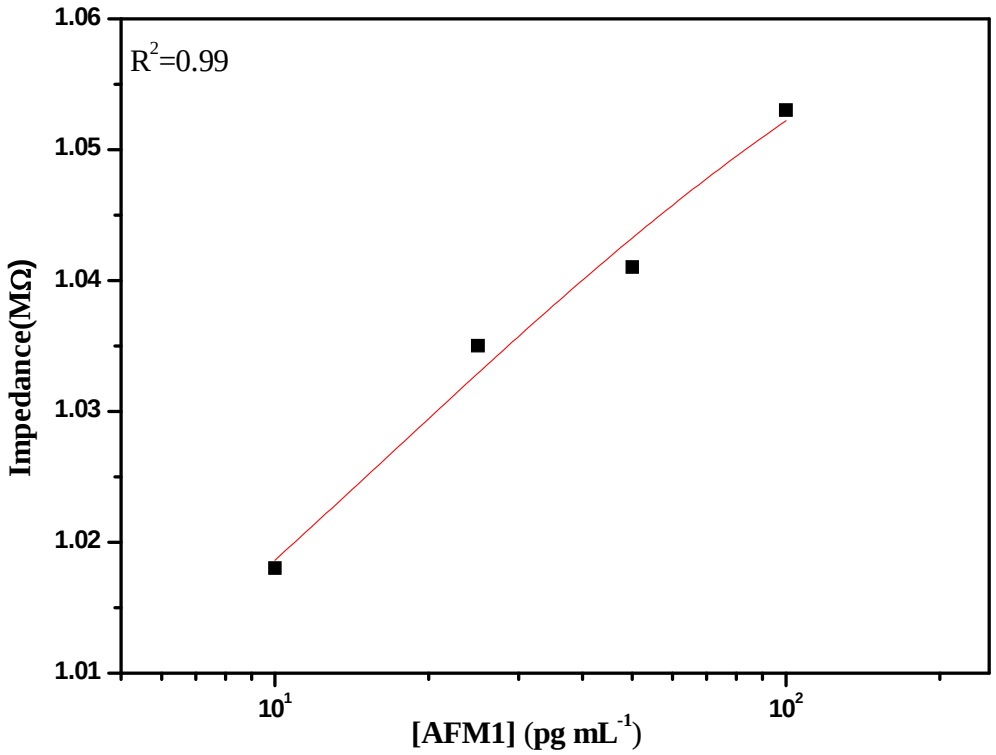

Figure 4.7 Calibration curve of μ-IDEs immunosensor after interaction of mAb with standard kit solution (10-100 pg mL^{-1} AFM1).

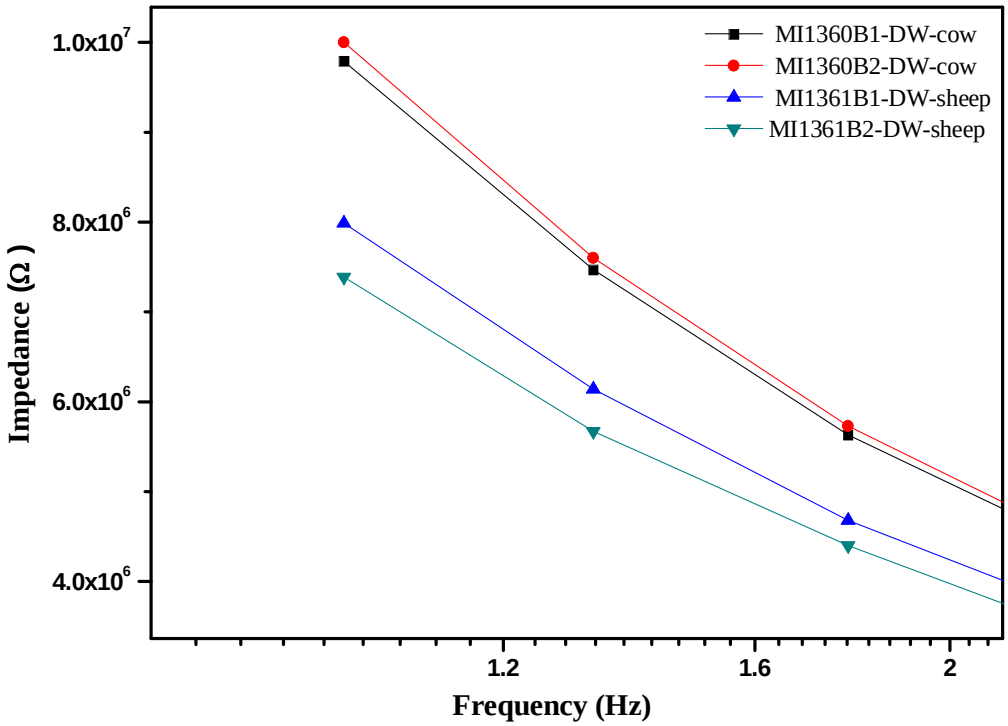

Figure 4.8 Impedance spectra of the μ-IDEs immunosensor after interaction of mAb with unknown AFM1 concentration. EIS: frequency range 1 Hz to 100 kHz at 5 mV ac potential .

4.5 Conclusions

Novel µ-IDEs devices with different material and dimensions were constructed. The label-free detection and analysis of AFM1 in milk was conducted on the developed µ-IDEs immunosensor using EIS technique. The µ-IDEs immunosensor operation parameters were optimized. The novel µ-IDEs device facilitates miniaturization of the assay and provides greater sensitivity with minimal sample volume. A linear range of detection 25-100 pg mL^{-1} has been achieved with excellent sensitivity and with a detection limit of 1 pg mL^{-1} for AFM1 in milk. Proficiency test was conducted with a developed µ-IDEs device for unknown samples. We have successfully detected the concentration of unknown samples using the developed device. This provides scope for on-line monitoring and sensitive analysis of aflatoxins and for tuning the device for different applications.

Chapter 5

Development of a novel coil microelectrode array (CMEA) biosensing device

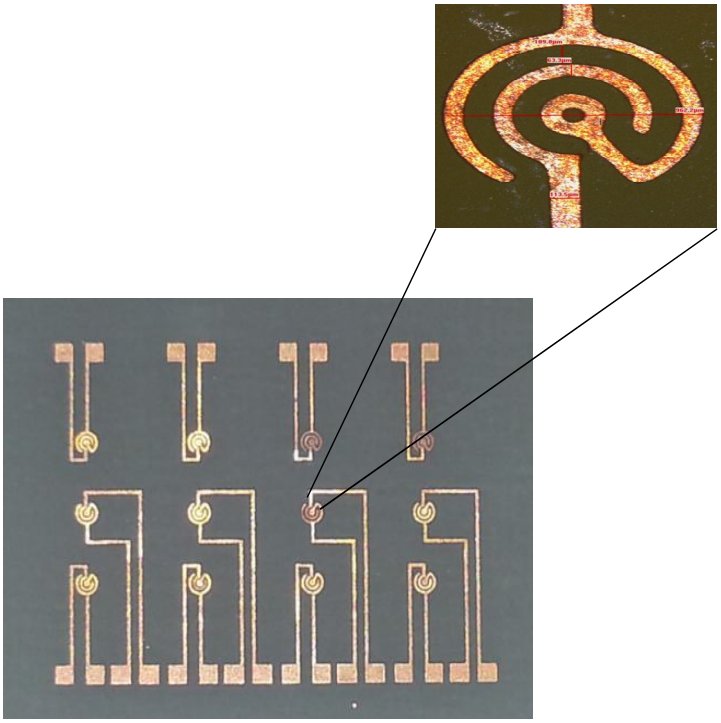

Graphical abstract of chapter content

**Note: The work incorporated in this chapter of the thesis constitutes collaborative experimental work between BITS, Pilani & Raja Ramanna Centre for Advanced Technology (RRCAT), Indore (India)*

5.1 Introduction

5.1.1 Background

The previous chapter (Chapter 4) described the development of a micro biosensor based on µ-IDEs with their application in food toxin analysis. This chapter presents the development of a biosensing platform based on monolithic device structure in the form of coil microelectrode arrays (CMEA). The use of advanced microfabrication technique was explored towards the development of monolithic strucutures and their application in diagnostics.

Micro-lithography is the technology that is used to create patterns with feature size ranging from a few µm to tens of mm. Lithography techniques are divided into two types based on the use of masks, and called masked lithography and maskless lithography. Masked lithography makes use of masks to transfer patterns over a large area simultaneously, thus, enabling a high-throughput fabrication up to several tens of wafers/hr. The forms of masked lithography include photolithography (Wagner and Harned, 2010), soft lithography (Qin *et al*., 2010), and nanoimprint lithography (Chen *et al*., 2010). Maskless lithography, such as electron beam lithography (Altissimo, 2010), focused ion beam lithography (Reyntjens and Puers, 2001), and scanning probe lithography (Han and Liu, 2011), fabricate arbitrary patterns by a serial writing without the use of masks.

Among the various lithography techniques photolithography is widely used in the semiconductor and IC industry (Pease and Chou, 2008). It has been deployed for pattern generation in manufacturing of ICs, microchips and MEMS devices. This technique utilizes an exposure of a light-sensitive polymer (photo-resist) to ultraviolet (UV) light to create a desired pattern. The use of UV and X-ray lithography is desirable for biochip fabrication. The UV lithographic photo-mask approach is compatible with standard clean room fabrication process, generating micro scale features (Suárez *et al*., 2010), whereas X-ray lithography is utilized for fabrication of microstructures with high aspect ratio and great structural height (Becker *et al*., 1986). Merging of microfabrication with electrochemical detection has led to the development of various handheld biosensor devices. Table 5.1 summarizes the various micro-devices developed using masked lithography techniques.

Table 5.1 Summary of reported lithography techniques for various micro devices

Device	**Lithography techniques**	**Applications**	**Reference**
Iridium microelectrodes array	Photolithography	Heavy metals	Belmont *et al*., 1996
Gold nanohole arrays	UV nanoimprint lithography	Chemical sensing	Chen and Shi, 2009
Silicon nanowire arrays	Nanoimprint lithography	pH sensing	Vu and Eschermann, 2009
Organic transistor	Photolithography	Glucose sensing	Shim and Bernards, 2009
Microwell	X-ray Lithography	Lab on a chip	Copic and Park, 2011
Microfluidic chip	Soft lithography	Binding kinetics between RNA and Mg^{2+}	YanáChang and NgoráAu, 2012

5.1.2 Microelectrode material and geometry

The development of miniaturized biosensor devices has received more attention over the past two decades. The small size of the biosensors leads to very small-scale experiments which results in very low sample volume; i.e. to the extent of microliters, or even nanoliters (Narakathu *et al*., 2010). The core component of electrochemical transducers i.e., electrodes have problems of limited sensitivity that can be improved by reducing the size of the transducer for facilitating rapid electron transport (Hintsche *et al*., 1994). In several previous studies, miniaturize electrochemical biosensors has been reported (Wang *et al*., 2005; Zou *et al*., 2007). Microelectrodes with various geometries are presented in Table 5.2. Among various shape of microelectrodes, the circular pattern electrode has been reported to be maximize the surface area of the sensing site while helping to minimize edge effects compared to various other patterned electrodes (Oldham, 2004). Among miniaturized devices, biochip is emerging fast, due to small sample volume, good reproducibility, easy

storage and potential for interrogating individual molecules (Craighead, 2006; Temiz *et al*., 2012).

Table 5.2 Summary of reported microelectrodes with various geometries

Electrode geometry	**Features size**	**Application**	**Reference**
Microdiscs array	50 µm diameter	Glucose sensing	Rahman *et al*., 2009
Ring shaped microelectrode	40 µm diameter 10 µm inner gap 15 µm outer gap	Cell-based biosensors	Hsiung *et al*., 2008
Bismuth microdiscs arrays	10 µm diameter	Trace metal	Kokkinos *et al*., 2012
Ring electrode	2 mm diameter	Immunosensor	Lee *et al*., 2013
Interdigitated double coils microelectrode	23 µm width, interval of 17 µm	Phosphate trace	Xue *et al*., 2012
Coil microelectrode	1mm width, 8 mm diameter	Erythromycin detection	Jacobs *et al*., 2013

Owing to fast, inexpensive and relatively ease in fabriction over conventional microfabrication, printed circuit board (PCB) has been widely reported in literature for microfabrication of electrode and microfludics device (Li *et al*., 2003; Tomazelli *et al*., 2011). Cu based electrode materials are of interest for the analysis of carbohydrates because of its superior capabilities in terms of the response range, detection limit, and particularly stability as compared to other reported materials (Ding *et al*., 2008; Tong *et al*., 2009). In this chapter, the development of novel monolithic miniaturized biochip device comprising coil microelectrode array (CMEA) was described.

5.1.3 Microelectrode array biochip

A biochip consists of an array of individual biosensors that can be individually monitored and generally are used for the analysis of multiple analytes (Song and Vo-Dinh, 2004). Biochip systems offer several advantages such as small size, better performance, ease of fabrication, simple analysis and low production cost (Vo-Dinh and Cullum, 2000). The small size of the

probes minimizes the sample requirement and reduce reagent and waste requirement. Table 5.3 presents the applications of microelectrode array biochip for detection of different analytes.

Table 5.3 Summary of reported applications of biochip

Biochip	**Analyte**	**Class**	**LOD**	**Reference**
Au Microelectrode Array	Hg^{2+}	Heavy metals	3.2 mg L^{-1}	Ordeig *et al*., 2006
Au Microelectrode Array	Tenascin C	Cancer marker	14 ng	Steude and Schmidt, 2011
IDAM chip	*E. coli* O157:H7	Pathogen	7.4×104 CFU mL^{-1}	Varshney and Li, 2007
IDAM chip	Oligonucleotides	Nucleic acid	0.5 ng L^{-1}	Elsholz *et al*., 2006
Interdigitated double-coil microelectrode chip	Phosphate	Chemical	0.5 μM	Xue *et al*., 2012

Microelectrode arrays have found new applications in several areas of electroanalysis, especially in the environmental and biomedical fields due to compact size, small sample volume, identical and geometrically well-defined elements, high sensitivity and low cost. Microelectrode arrays can be chemically modified like microelectrodes. These arrays are made by incorporating specific chemical groupings onto the surface, allows the properties of that reagent on the modified surface. The chosen modifying substances such as enzymes, monolayers etc. must exhibit selectivity to an analyte, such devices are based on the coupling of bioactive molecules with electrochemical transducers. Unmodified microelectrode arrays can determine heavy metals in environmental samples (Ordeig and del Campo, 2007). This chapter describes the fabrication of a CMEA platform and its application for the detection of different analytes, such as glucose and ionic liquid (KCl).

5.1.4 Research gaps identified

Various methods have been proposed for detection of glucose such as optical (Barone *et al*., 2005), colorimetric (Morris *et al*., 1992) and electrochemical (Shervedani and Hatefi-Mehrjardi, 2007). Several technological approaches have been used in various attempts to integrate electrochemical glucose biosensors into miniaturized formats. Reported electrochemical techniques for detection of glucose are presented in Table 5.4. Owing to the importance of reliable and fast clinical diagnostics, development of a novel glucose sensor with high sensitivity, fast response, excellent selectivity and low cost are desired (Newman and Turner, 2005; Wang, 2008).

Table 5.4 Reported electrochemical glucose biosensors

Electrode	**Target**	**Detection technique**	**Reference**
Pt electrode	Glucose	Amperemetric	Arslan *et al*., 2011
Conducting polymer electrode	Glucose	Potentiometric	Çiftçi *et al*., 2013
Ag Interdigitated array microelectrode	Glucose	Cyclic Voltametry	Haung *et al*., 2013
Ag electrode	Glucose	Impedimetric	Shervedani and Hatefi-Mehrjardi, 2007

5.1.5 Objective

The aim was to develop a miniaturized biochip device for multianalyte detection**.** Glucose and ionic liquid, Potassium Chloride (KCl) were chosen as model analyte.

5.1.6 Working principle of CMEA glucose biosensor

The biochip was realized through covalent immobilization of enzyme, glucose oxidase (GOD) as a model enzyme. The gluconate ions generated in the reaction were measured by the change in capacitance. In this case the degree of variation in capacitance was due to the

reaction of glucose and GOD. The schematic representation of GOD and glucose reaction is shown in Figure 5.1.

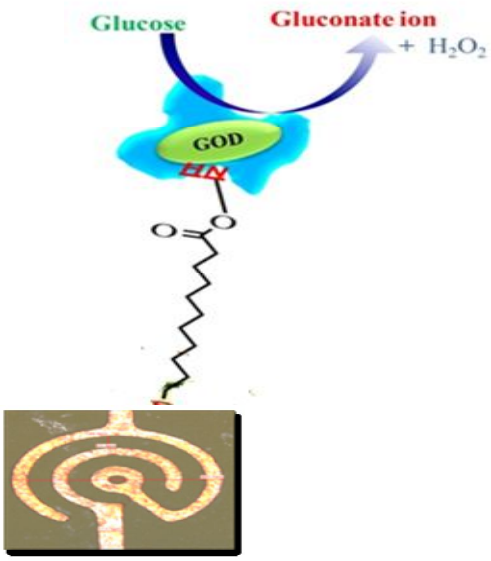

Figure 5.1 Schematic representation of glucose sensing using biochip.

5.2 Materials and methods

5.2.1 Materials and instrumentation

Glucose oxidase Type II-S (EC 1.1.3.4) from Aspergillus niger (GOD), 11-MUA, EDC and NHS were purchased from Sigma Chemical Co. (USA). Potassium Chloride (KCl), sodium phosphate dibasic (Na_2HPO_4), sodium phosphate monobasic (NaH_2PO_4), sodium chloride (NaCl) and other chemicals were of GR grade, Merck (Germany). Centrifugation, shaking and filtration of the samples were done by Spinwin mini centrifuge, Spinix shaker Tarsons (India). FT-IR spectra were recorded using IRAffinity-1 (SHIMADZU, Japan) with ATR attachment Specac Diamond ATR AQUA. Impedance measurement was carried out using IVIUM CompactStat impedance analyzer, Netherland. Certified ultra-high pure nitrogen (99.9 %), pH meter (Seven Multi Mettler Toledo, 8603, Switzerland) were used. SEM micrographs were recorded using Phillips XL 30 CP.

5.2.2 Fabrication of CMEA

CMEA devices were designed in BITS, Pilani-K. K. Birla Goa and fabricated at RRCAT, Indore. The CMEA device was fabricated using Cu-PCB as substrate material. The device was fabricated by the combination of UV and X-ray lithography. UV lithography was used to

create the coil microelectrode pattern and X-ray lithography was used to create circular sidewall structures around the coil microelectrode pattern. A high dpi laser monochrome print was used for the fabrication of coil microelectrode patterns and X-ray mask. To carry out UV and X-ray lithography, a suitable quality and low cost UV and X-ray masks were prepared. The fabrication process comprises three major steps towards CMEA; Step1: Coil microelectrode pattern fabrication, Step 2: X-ray mask for circular sidewall structure and Step 3: sidewall fabrication around coil microelectrode patterns. The fabrication process involving the above three steps is shown in Figure 5.2.

Step 1: a Cu laminate PCB was used as a substrate and UV photolithography was performed using UV mask for the fabrication of CMEA. After photolithography process, Cu was etched by dissolving in ferric chloride solution to obtain coil microelectrode patterns.

Step 2: a 100 μm thick Cu foil with significant absorption of X-ray below 10 keV was used as a base material to prepare X-ray masking patterns by step process of UV lithography followed by Cu etching.

Step 3: a cylindrical confinement on the coil microelectrode pattern was created using SU-8. SU-8 2150 was spin-coated and prebaked at 65° C and 95° C to achieve 400-500 μm resist thickness in a single step. The x-ray energy band of 2.5-9 keV and an exposure dose of 600 mAs were used to create vertical and steep sidewall structures. After the post exposure bake, SU-8 was developed in two bath Propylene glycol methyl ether acetate (PGMEA) developer solution to obtain monolithic CMEA structure.

The feature size of the developed device was determined using optical micrograph (Zetz-20 Noncontact 3-D profiler, ZETA Inc., USA). The measured average width of microelectrode was ~65 μm with a spacing of 110 μm. The total area occupied by Cu-CMEA in a circular sidewall was 0.192 mm^2 and the total length of the electrode was 2.94 mm. The diameter of the fabricated circular sidewall was measured as 962 μm. For aspect ratio (ratio of width and height) of 1, the circular well can be filled with 0.7 μL equivalent water solution.

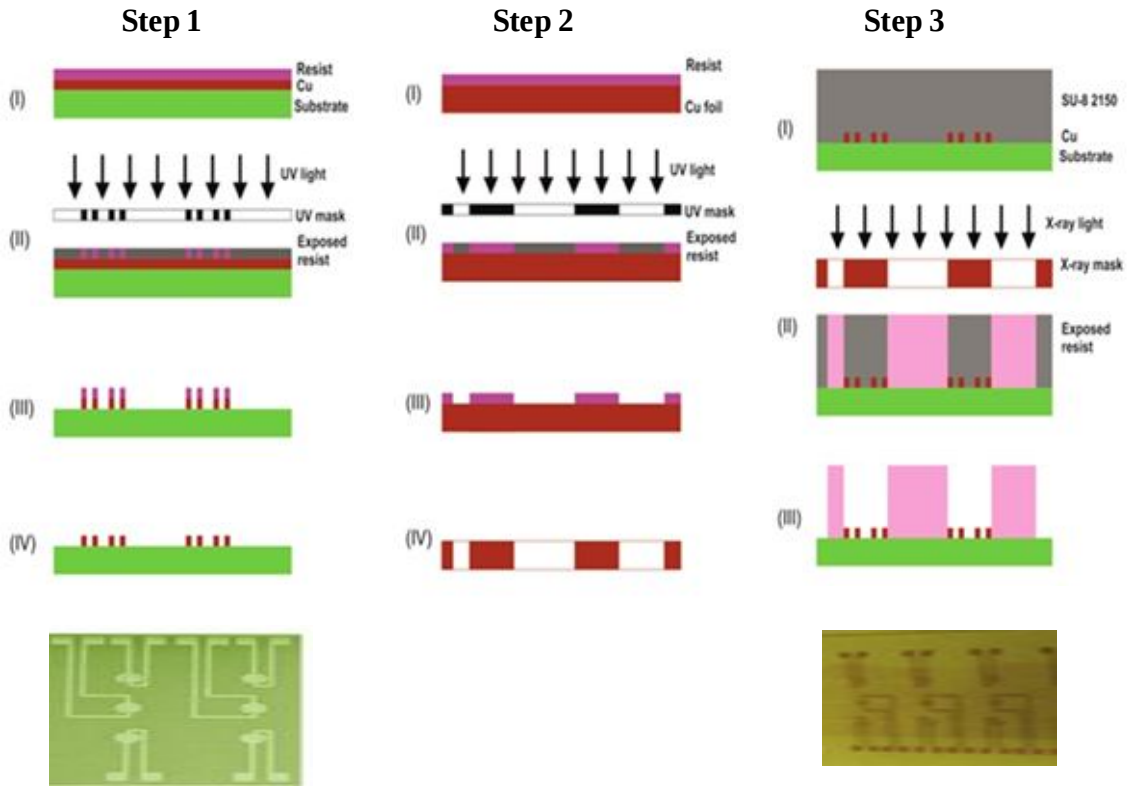

Figure 5.2 Schematic of fabrication process; Step 1: CMEA fabrication, Step 2: X-ray mask fabrication, Step 3: SU-8 microwell system over CMEA using X-ray lithography.

5.2.3 Solution preparation

Phosphate buffer (PB) 100 mM, pH 7.4 was prepared by mixing 100 mM of Na_2HPO_4 and 100 mM of NaH_2PO_4 in double distilled water (dd-H_2O). 100 mM Phosphate buffered saline (PBS) was prepared by dissolving appropriate amount of Na_2HPO_4, NaH_2PO_4 and NaCl and was used for incubation and washing. KCl (100 mM) was prepared by dissolving 74.55 mg in 100 mL in dd-H_2O. A stock solution of glucose (100 mM) was prepared by dissolving 0.180 g in 10 mL of PBS (100 mM, pH 7.4). Working solution of KCl and glucose was prepared freshly before daily use. Enzyme stock solutions were prepared in PB (100 mM, pH 7.4).

5.2.4 EIS measurements

Impedance measurements were carried out using IVIUM™ CompactStat impedance analyzer, Netherland in two electrode configuration. All the measurements were carried out in a Faraday cage to avoid the interference of the external field strength with the measured impedance signal. For the actual measurement two types of experiments were designed: (i) Calibration of the device for ionic conductance (using known and standard conductivity

solutions (ii) development of a glucose biosensor using covalently immobilized GOD.

5.2.5 Measurement of ionic conductivity using CMEA

The electrode surface was cleaned with ethanol and dried under a stream of highly pure nitrogen before use. For conductivity measurements, KCl solutions of known concentrations in the range 1M to 0.0001M were prepared. A known amount (0.70 µL) of different KCl solutions was dispensed on the device. The impedance measurements were recorded at 2.5 mV ac potential in the frequency range 1 Hz to 1 MHz. After each measurement, the sensor was washed with PBS and ethanol for further usage.

5.2.6 Construction of monolithic glucose biochip

The performance of developed CMEA biochip was realized using GOD as the model enzyme. An optimized amount of enzyme, i.e., 0.0625 IU/µL was physically adsorbed on CMEA surface. To achieve better performance, stability and reproducibility, a miniaturized glucose biochip was constructed based on efficient immobilization of enzyme GOD through SAMs. The glass containers used for monolayer preparation was cleaned with Piranha solution (a mixture of 98% H_2SO_4 and 30% H_2O_2, 7: 3, v/v; **caution**: piranha solution reacts exothermally and strongly reacts with organics) for 1 hr and rinsed exhaustively with dd-H_2O and ethanol. The device was washed with ethanol, and dried under a stream of high purity nitrogen before use. The enzymes were covalently coupled on the Cu electrode of CMEA through SAMs as described elsewhere (Bacher *et al*., 2012) with some alteration. These samples were immersed into 4 mM ethanolic solution of 11-MUA for 12 hrs (assembly time). After the assembly time the SAMs functionalized Cu electrode of CMEA were rinsed in ethanol followed by dd-H_2O and dried with a stream of dry nitrogen. For enzyme immobilization, the carboxylic acid-terminated SAMs were modified using an aqueous equimolar solution (100 mM) of EDC / NHS for 1 hr at room temperature. The resultant NHS ester monolayers were allowed to react for 4 hrs in a solution of GOD (0.0625 IU/µL) in PB. The enzyme (GOD) coupled Cu electrode of CMEAs was washed thoroughly with PB to remove non-specifically bound enzymes. For glucose measurement different concentration ranges from 10 nM to 20 mM were prepared. Glucose samples (0.4 µL) were dispensed on the device. All impedance measurements were performed in the frequency range 1 Hz to 10 kHz using 5 mV ac Voltage. The experimental setup and schematic illustration towards construction of glucose biochip is shown in Figure 5.3.

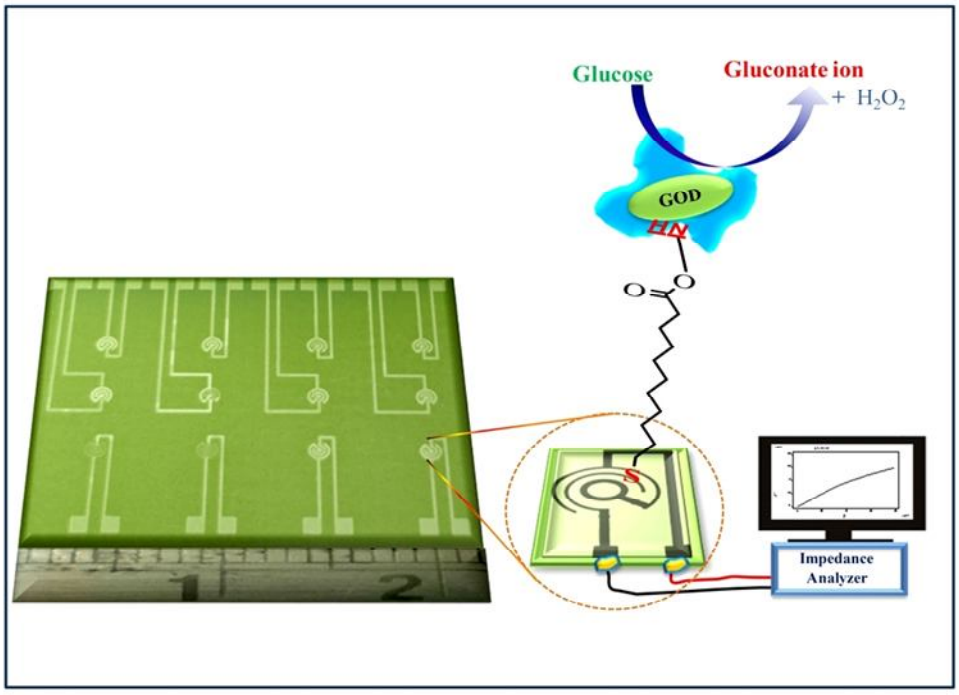

Figure 5.3 Experimental setup and schematic illustration towards construction of glucose biochip.

5.3 Results and discussion

5.3.1 Conductivity measurement

Different concentration of KCl solution such as 0.0001M, 0.001M, 0.01M, 0.1M and 1M were tested on the fabricated CMEA. Figure 5.4 shows the Nyquist plot for different concentrations of KCl with a frequency range of 1 MHz to 1 Hz. As the electron transfer mechanism was seen at higher frequency, hence the Nyquist plot was represented from 1 MHz to 1 Hz. The semicircle represents charge transfer resistance (R_{ct}), which was found to be decreasing with an increase in concentration. Figure 5.5 shows the measured impedance for various concentrations of KCl in the frequency ranges of 1 MHz to 1 Hz. It shows that the impedance decreases as the concentration of KCl increases. This characteristic supports the change in capacitance / resistance at conductive surface. An increase in the concentration of KCl solution causes an increase in the number of ions in the electrolyte. The decrease in the measured impedance of the sensor can be attributed to the change of concentration since the impedance of an electrolyte solution is related to ion concentration at the electrode-electrolyte interface. Conductivity measurement is further validated using a standard solution of conductivity standard 5 µS and 10 µS. Figure 5.6 shows the Nyquist plot for a standard solution of conductivity 5 µS and 10 µS. It was found that the solution with lower

conductivity has a larger semicircle (higher R_{ct}) and a small semicircle for higher conductivity (lower R_{ct}).

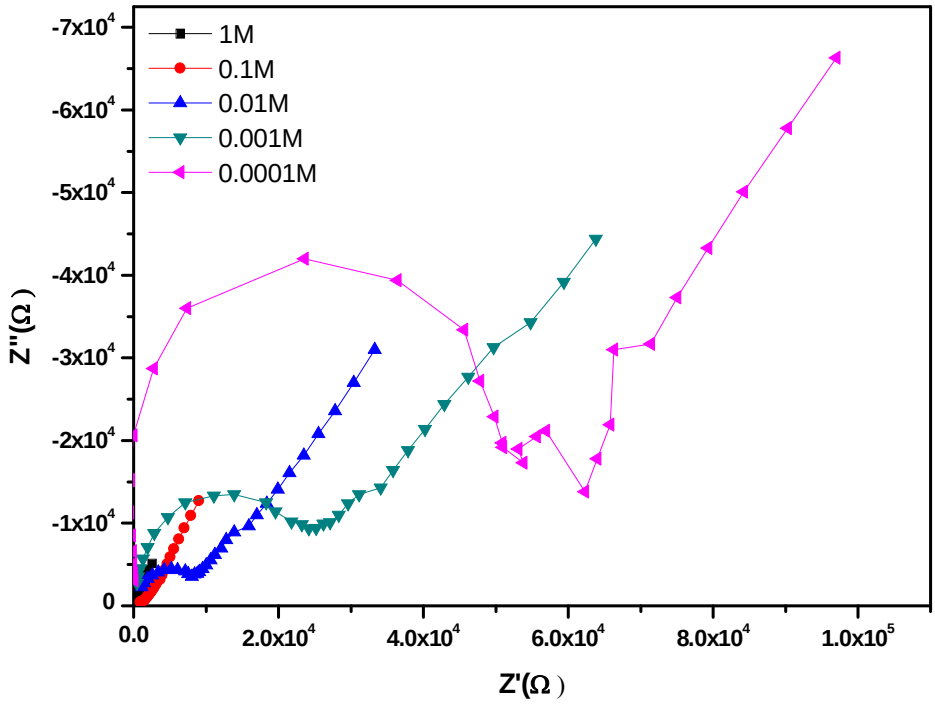

Figure 5.4 Nyquist plot recorded in presence of different concentration of KCl at electrode surface. EIS: 1 Hz to 1MHz, 2.5 mV ac potential.

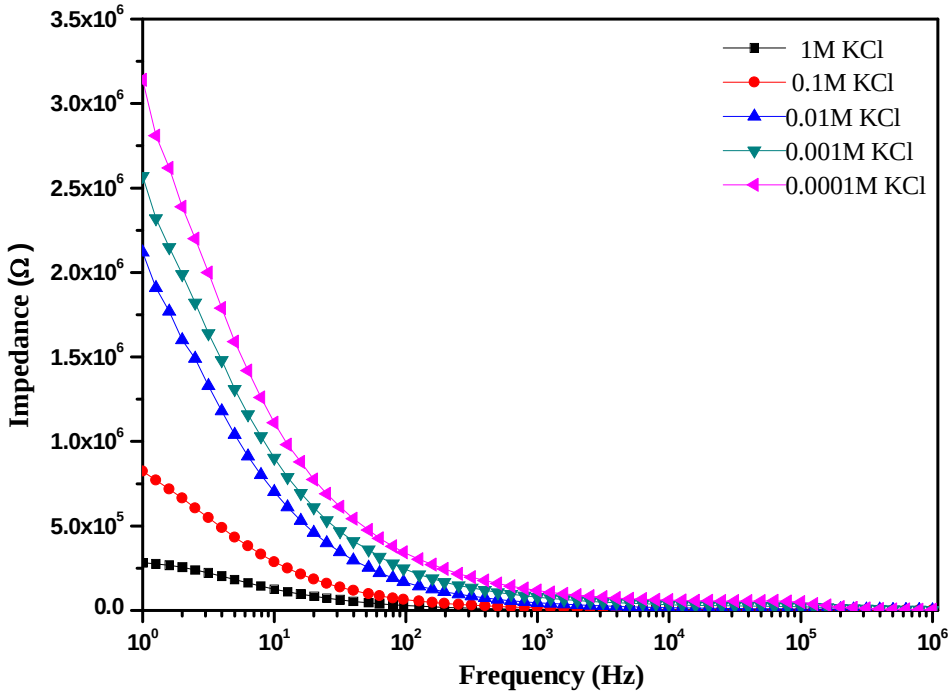

Figure 5.5 Impedance spectra for various concentrations of KCl. EIS: 1 Hz to 1 MHz, 2.5 mV ac potential.

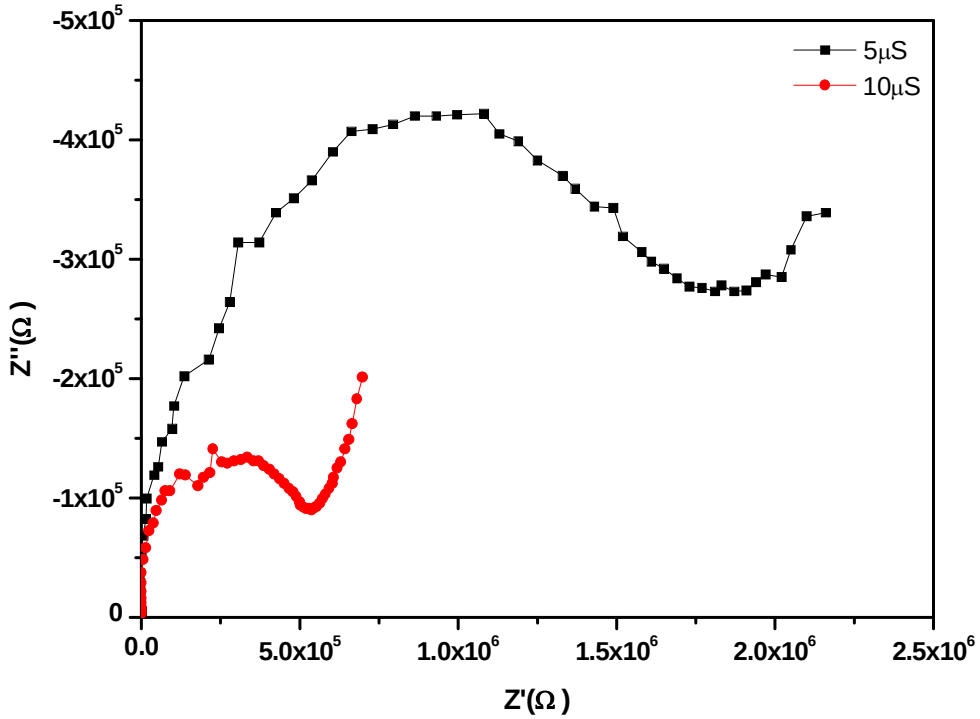

Figure 5.6 Nyquist plot recorded in presence of standard concentration of KCl (5 µS and 10 µS) at electrode surface. EIS: 1 Hz to 1 MHz, 2.5 mV ac potential.

5.3.2 Surface characterization of CMEA

Surface morphology studies: The surface of the Cu electrode of CMEA was characterized by Scanning electron microscope (SEM). Figure 5.7 (i) shows the SEM micrograph of the bare Cu electrode of CMEA at magnification 80× and Figure 5.7 (ii) and 5.7 (iii) show the electrode surface after surface modification by 11-MUA and after immobilization of enzymes at magnification 5000× respectively. After treating with 11-MUA, the Cu electrodes possessed a high rough surface topography. Whereas, after enzyme immobilization, the surface of the Cu electrodes were became relatively smooth than the surface treated with 11-MUA.

FT-IR studies: Further, the attachment of GOD to a SAMs of 11-MUA on the Cu electrode of CMEA surface was achieved using water soluble EDC/NHS as coupling agents. The carbodiimide cross-linking reaction to form the 11-MUA-GOD conjugated structure was confirmed by ATR FT-IR. The spectra were acquired with 128 scans at 4 cm^{-1} resolution. The FT-IR spectra are shown in Figure 5.8. Figure 5.8 (i) FT-IR spectrum of bare Cu electrode of CMEA. 11-MUA treated with Cu electrode of CMEA is shown in figure 5.8 (ii). It shows C-H stretches in asymmetric and symmetric mode at 2921 cm^{-1} and 2847 cm^{-1}

respectively. The C=O stretch at 1734 cm^{-1}, associated with asymmetric (1647 cm^{-1}) and symmetric (1542 cm^{-1}) COO^- stretches, is characteristic of an organic carboxylic acid compound. The additional IR peaks at 1455 cm^{-1} and 1257 cm^{-1} can be ascribed to C-H deformation and C-O stretch respectively. After immobilization of mAb in Figure 5.8 (iii) new absorption bands appeared; three IR bands at 1693 cm^{-1}, 1657 cm^{-1}, and 1263 cm^{-1} can be ascribed to the absorption by the amide group that links mAb to 11-MUA functionalized Cu electrode of CMEA.

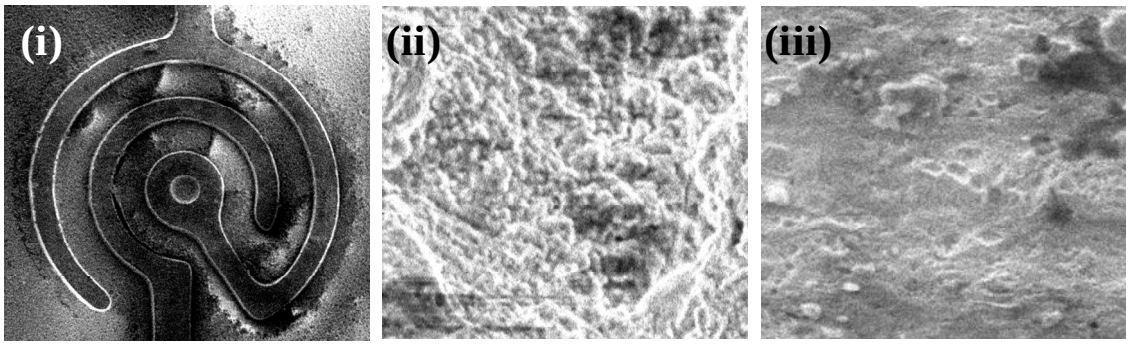

Figure 5.7 SEM micrograph of (i) bare Cu electrode of CMEA at magnification 80×; (ii) 11-MUA modified electrode surface at magnification 5000×; (iii) GOD immobilized electrode surface at magnification 5000×.

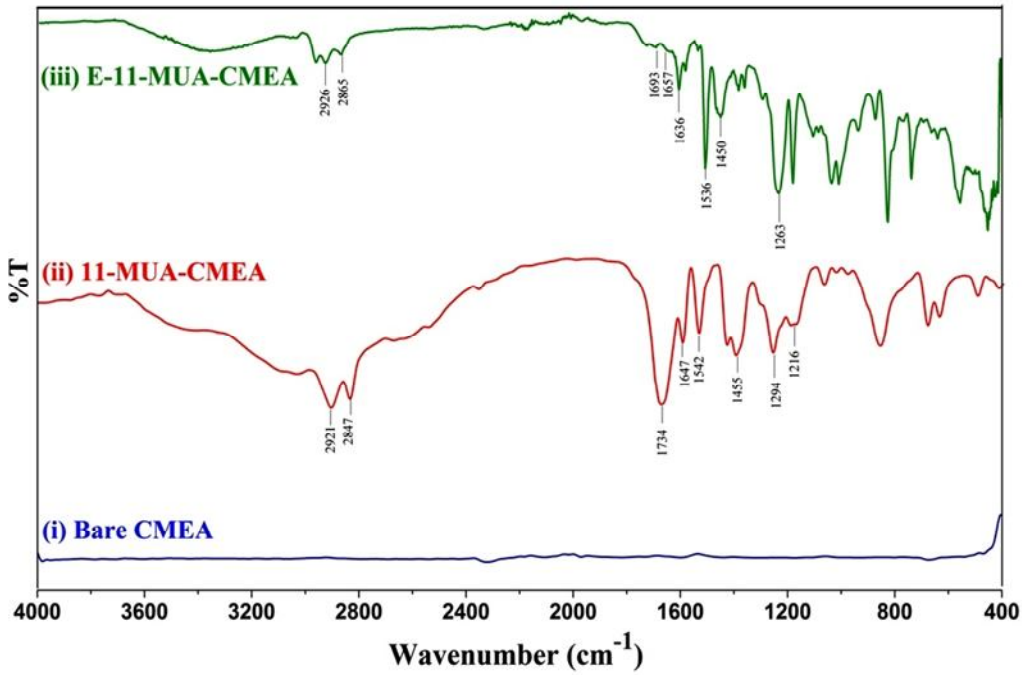

Figure 5.8 The ATR FT-IR spectrum of (i) Bare Cu electrode of CMEA (ii) the Cu electrode of CMEA treated with 11-MUA (iii) Enzyme coupled through 11-MUA functionalized on Cu electrode. Spectra were acquired 154 scans at 4 cm^{-1} resolution collected under vacuum conditions.

5.3.3 Optimization of CMEA biochip parameters

The response of the glucose sensor depends on the activity of GOD, which is related to concentration of GOD, applied potential, applied frequency and sample volume on CMEA. Thus, these parameters were optimized step wise.

5.3.3.1 Glucose oxidase (GOD) concentration

The reaction between amount of glucose and GOD directly affects the sensitivity of the glucose sensor. Since the concentration of GOD plays an important role in the reaction, various concentrations of GOD solutions were tested with Cu electrode of CMEA. The electrochemical signal depends upon Glucose-GOD interaction and reaction time. Hence, the effect of the concentration of GOD and reaction time was investigated. Various GOD concentrations such as 0.0081 IU/µL, 0.0165 IU/µL, 0.032 IU/µL, 0.0625 IU/µL, 0.13 IU/µL and 0.26 IU/µL was studied using 1 mM glucose. It was found that GOD concentration 0.0625 IU/µL was optimum as presented in Figure 5.9. As compared to other concentrations of GOD, concentration of 0.0625 IU/µL was showing enhanced impedance response. Further, the reaction time of GOD and the substrate was optimized as shown in Figure 5.9. The impedance response of the biochip gives a stable response upto a period of 5 min. There was a drop in response after 5 min, which can be attributed to the consumption of small amounts of electrolytes. The result confirmed that the catalyzed oxidation process of glucose was finished in 5 min. The maximum signal response was observed at 2 min. Thus, 2 min was chossen for further impedance measurements.

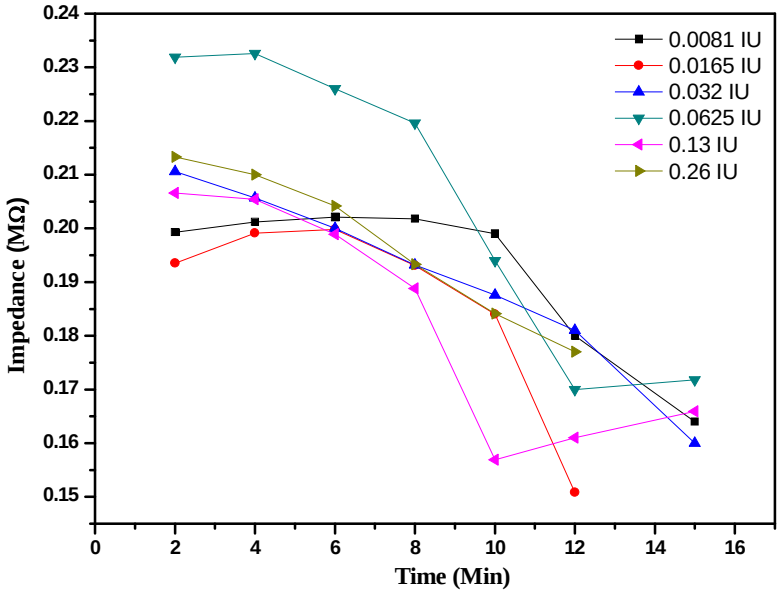

Figure 5.9 Impedance responses with time for various concentrations of GOD.

5.3.3.2 Influence of applied potential

The applied potential is an important parameter that influences the sensitivity of the modified sensor. Different potentials such as 0.1 mV, 0.5 mV, 1 mV, 2.5 mV and 5 mV were applied to the modified sensor. Voltage and current waveform was studied for impedance/capacitance measurement. It was found that, except 5 mV, at all other voltage less than 5 mV, a distorted current waveform was observed as shown in Figure 5.10. Therefore, 5 mV was chosen as the suaitable potential for impedance/capacitance measurement.

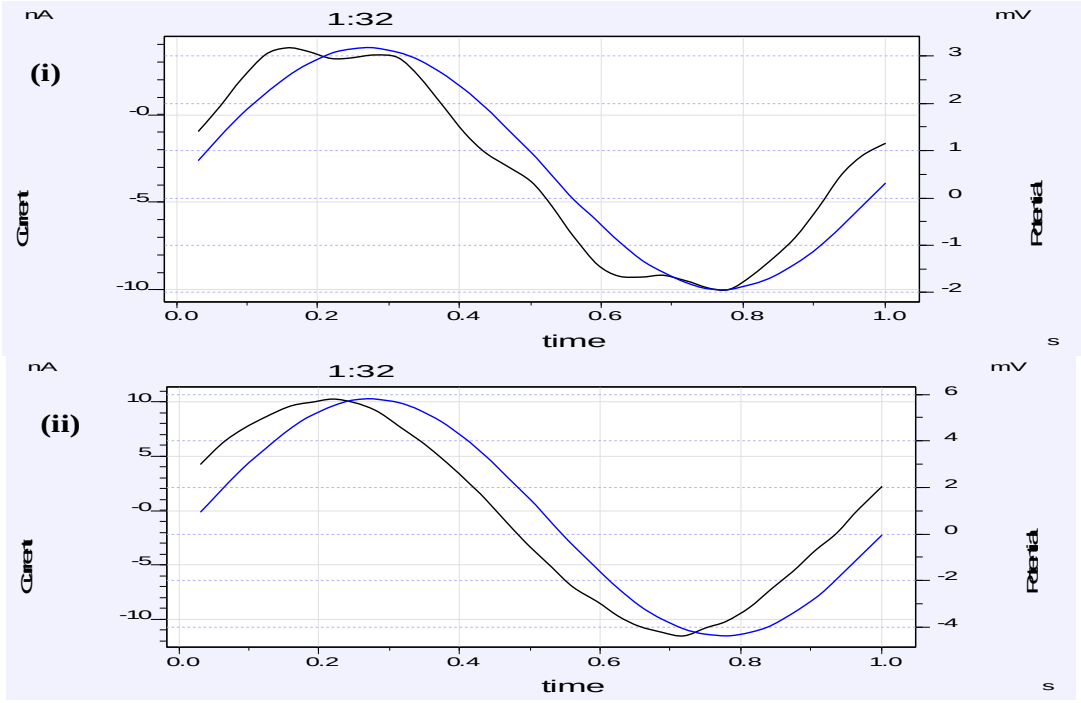

Figure 5.10 Voltage and current waveforms for (i) 2.5 mV and (ii) 5 mV ac potential. EIS: 1 Hz to 100 kHz.

5.3.3.3 Influence of frequency

The influence of applied frequency was also studied in the range 10 Hz to 1 kHz. Frequencies of 10 Hz, 100 Hz and 1 KHz were chosen for recording the impedance change during glucose-GOD interaction. Below 10 Hz, there was a distortion in the signal. At 10 Hz the impedance response was maximum as shown in Figure 5.11. Therefore, 10 Hz was chosen for glucose measurement.

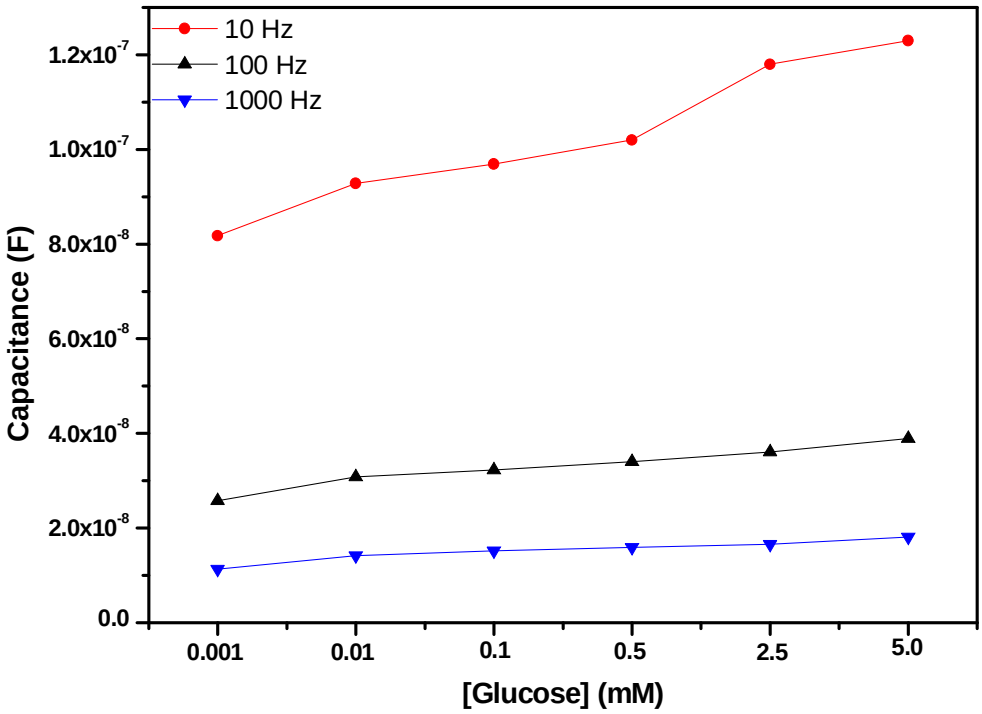

Figure 5.11 Optimization of single point frequency for various concentrations of glucose.

5.3.4 Effect of surface modification

The activity of enzyme GOD towards glucose was evaluated when enzymes were attached on the surface via covalent coupling as against the physically adsorbed GOD. The capacitive response of the reaction between GOD and various concentrations of glucose was evaluated at a frequency of 10 Hz, presented as Figure 5.12. The covalently attached enzyme exhibited significantly higher capacitance response over the physically adsorbed enzymes. The capacitance at 10 Hz was recorded for GOD functionalized Cu electrode of CMEA for glucose concentration of 1mM was found to be 0.707 µF (via thiolation) and 0.12 µF (*physisorped* i.e. non-specifically adsorbed GOD) respectively. The capacitance response was found to be almost 6 times higher for GOD immobilized on Cu electrode of CMEA via thiolation as against *physisorped GOD.* These important features of the presented biochip play an important role to enhance efficiency and specificity towards the rapid signal transfer rate and bio-recognition properties.

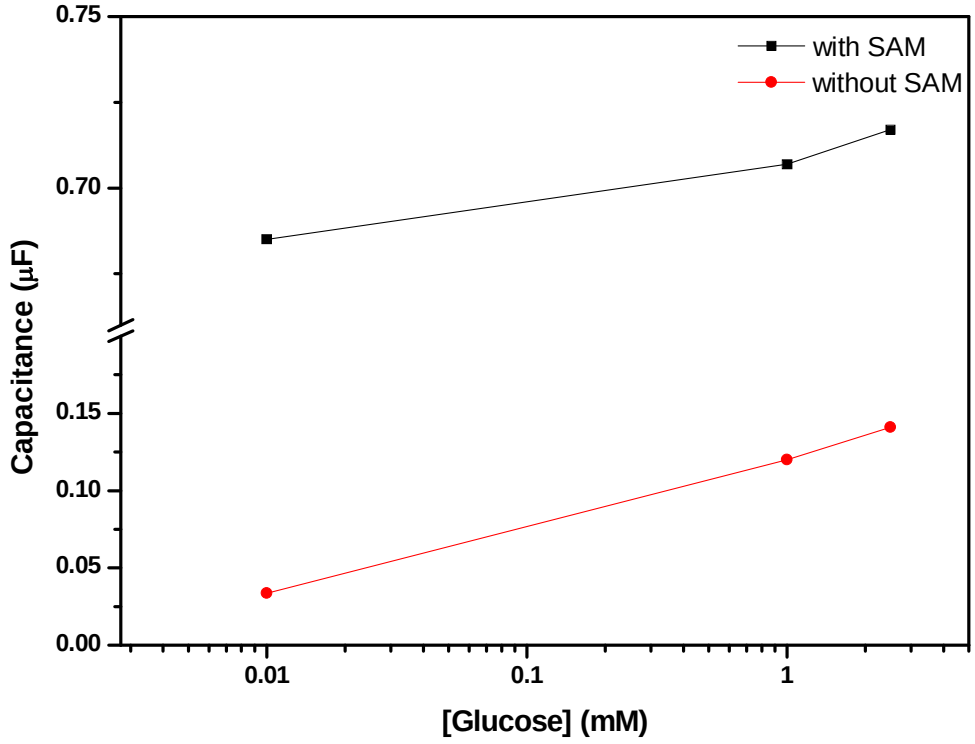

Figure 5.12 Capacitive response of different glucose concentration for modified and unmodified electrode.

5.3.5 EIS study of glucose biochip

For the analysis of glucose as a target analyte, enzyme GOD was immobilized on the modified CMEA by physical adsorption. Subsequently, a series of known concentration of glucose were sequentially injected on the surface of CMEA. The impedance was measured in the frequency range of 10 Hz to 10 kHz at the applied potential of 5 mV as shown in Figure 5.13. All the measurements were carried out in a grounded Faraday cage to avoid the interference of the external field strength with the measured impedance signal. The total impedance is contributed for interfacial electrode impedance and dominated by capacitance, as the measurement was non-faradaic. The capacitance, which is the imaginary part of the measured impedance is shown in Figure 5.14. In this case the degree of variation in capacitance is due to the reaction of glucose and GOD, resulting ions was observed at low frequency of 10 Hz. The decreasing impedance also confirms the higher current which is due to the presence of more gluconate ion generated during glucose and GOD reaction.

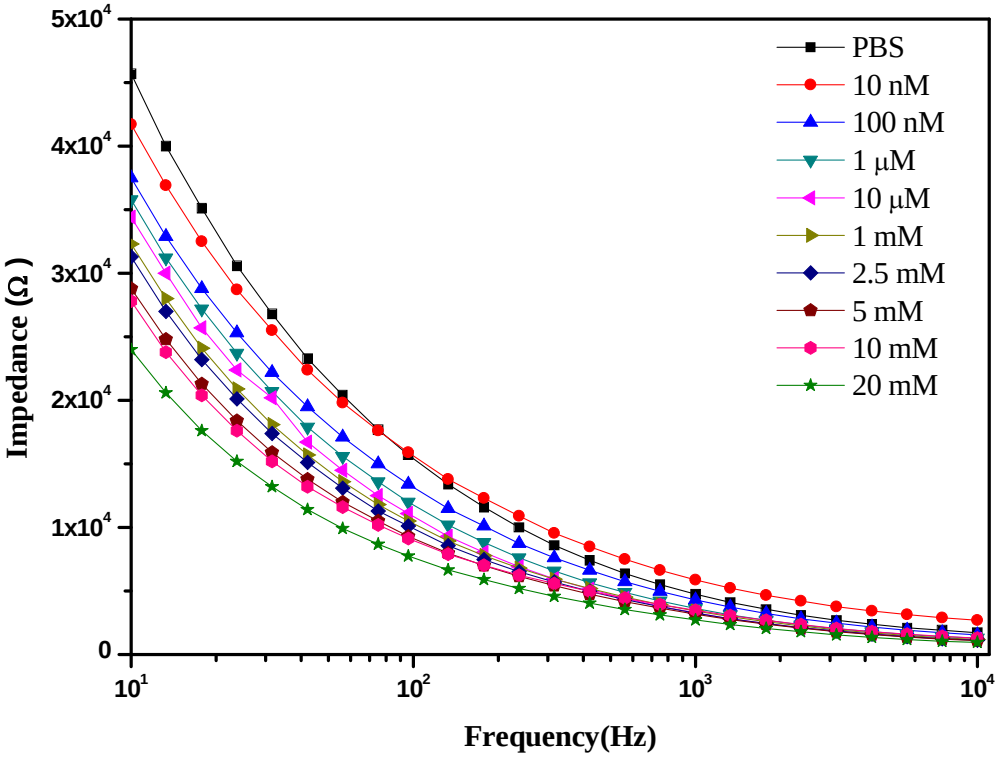

Figure 5.13 Impedance plot for different glucose concentration. EIS: 10 Hz to 10 kHz, 5 mV ac potential.

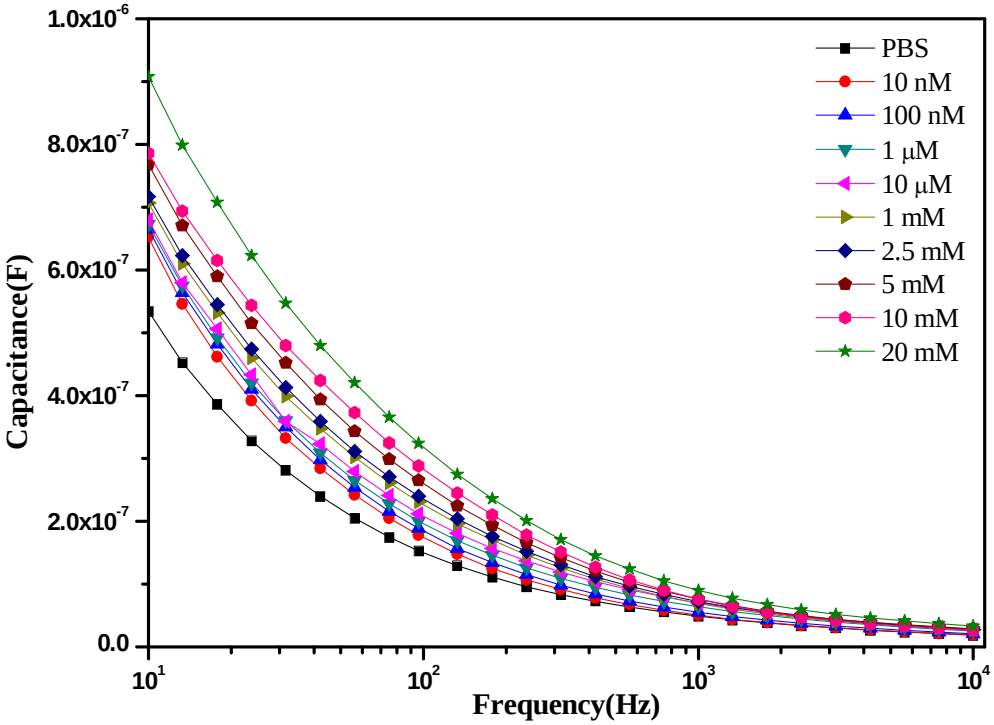

Figure 5.14 Capacitive spectra for various concentrations of glucose. EIS: 10 Hz to 10 kHz, 5 mV ac potential.

5.3.6 Equivalent circuit analysis

EIS is useful to study the sensor response based on frequency. The sensor can be modelled using an equivalent circuit (Lasseter *et al*., 2004). The electrical parameters generally used to design an equivalent circuit model for electrochemical curve fitting includes mainly, R_s (bulk medium resistance) and C_{dl}, etc. These factors affect the degree to which an equivalent circuit model represents the experimental impedance data. From the electric point of view, a simple equivalent circuit consisting of a resistor and a capacitor in series represents the behaviour of the impedance test systems when two electrodes are immersed into a conductive medium (Yang and Basir, 2008). The elements of an appropriate equivalent circuit represent the physical and chemical characteristics of the sensor, which can be used for understanding and optimization of the sensor response. A circuit model has been reported using immobilized glucose oxidase (GOD) on gold via mercaptopropionic acid SAMs (Shervedani and Hatefi-Mehrjardi, 2007). The simplified Randles model used as an equivalent circuit for the biosensor interface modified with 11-MUA and demonstrated for fluorescein/anti-fluorescein system (Wang, 2006).

Various equivalent circuits have been evaluated for fitting the measured data obtained from glucose analysis. The proposed equivalent circuit with best fit results for the electrochemical cell using modified CMEA is presented as Figure 5.15 (Inset). The presented circuit describes non-faradaic phenomenon at the electrode-electrolyte interface, since no species are present in the solution that undergo an electrochemical reaction. This equivalent circuit consists of ohmic resistance of the medium (R_s), double layer capacitance C_{dl} and resistance R_{dl}. R_{dl} being parallel to C_{dl}, resembles a part of SAMs. R_{dl} is interpreted as the conductivity (by penetrating ions) of the SAMs (Bart *et al.*, 2005). The best fit was obtained when C_{dl} replaced by constant phase element (CPE_{dl}). The double layer capacitance enhanced with the amount of absorbed ions resulting from glucose and GOD reaction. Figure 5.15 shows Bode plot of experimental and fitted impedance spectra of Glucose. Fitting was done by using IVIUM™ equivalent circuit evaluators and optimized with phase, Z´ and Z´´. The error weight was taken as equal for each point. It is evident from Figure 5.15 that for the presented glucose sensor, the fitting has a good agreement with experimental data, thereby validating the equivalent circuit.

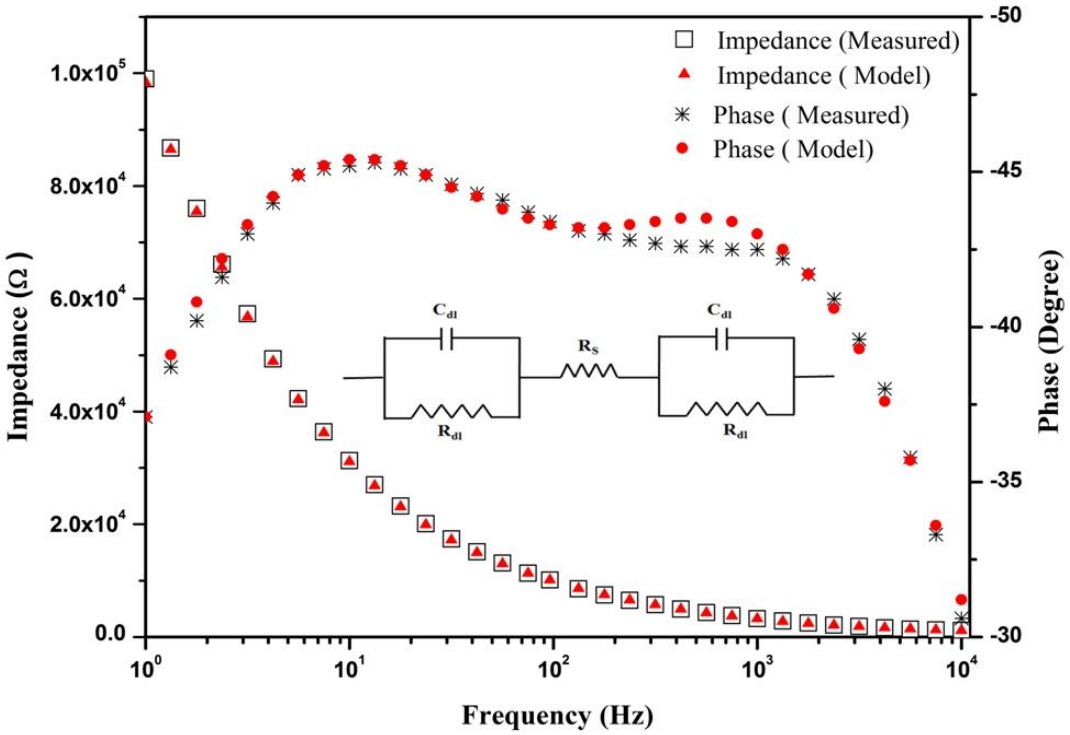

Figure 5.15 Impedance spectrum in the glucose environment with the fitting curve. EIS: ac applied potential: 5 mV; frequency range: 1 Hz to 10 kHz. **Inset:** Equivalent circuit used to fit impedance of the glucose sensor in buffer.

5.3.7 Calibration of glucose biochip

Capacitance data was recorded for the functionalized CMEAs after exposing it to increasing glucose concentration (10 nM - 20 mM). A frequency of 10 Hz at applied ac potential 5mV was selected for analysis since at this frequency significant change in capacitance was observed. The electrochemical reaction between glucose and GOD gave rise to an overall increase in capacitance change from baseline response at the electrode-solution interface for glucose concentration. The resulting calibration curve is presented in Figure 5.16. The calibration was found to be linear in the range of 100 nM-10 mM (R^2 = 0.99, n = 5) with a relative standard deviation (R.S.D.) of 2.31±0.2 for the GOD functionalized Cu electrode of CMEA. The linear equation was; y = 0.71069 + 0.01262x (mM). LOD was found to be 10 nM and limit of quantitation (LOQ) was 100 nM. The analytical figures of merits of the assay are presented in Table 5.5.

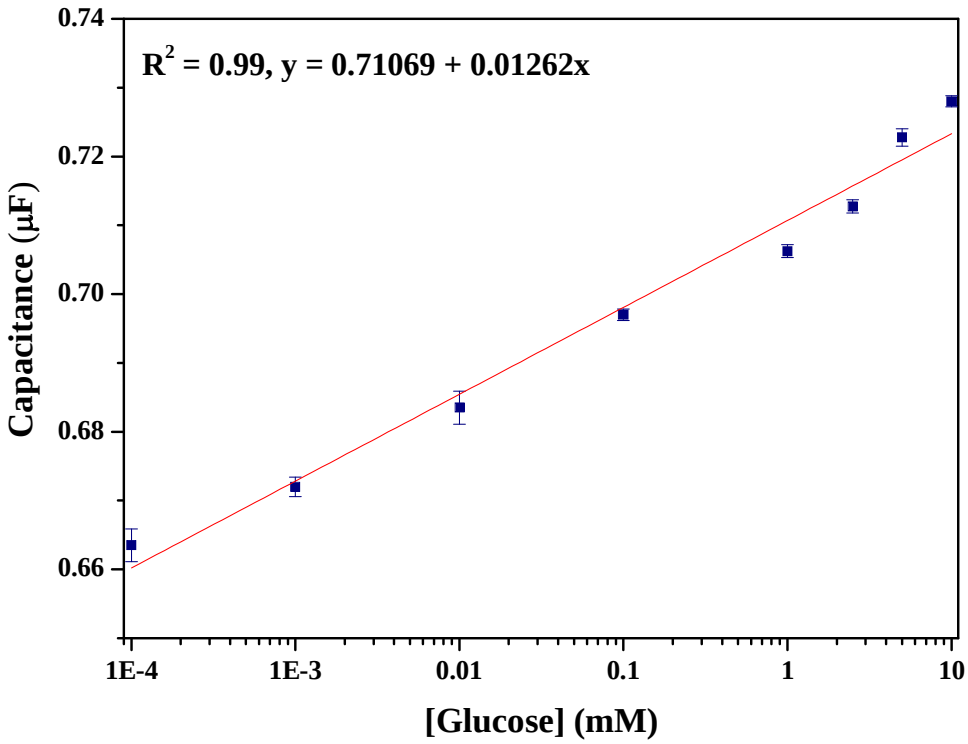

Figure 5.16 Calibration curve for different glucose concentrations obtained for enzyme coupled via 11-MUA.

Table 5.5 Analytical figures of merit of the developed CMEA biochip for glucose analysis in buffer

Analytical parameters	**Experimental findings**
Dynamic Range	10 nM-20 mM
Linear Range	100 nM-10 mM
LOD	10 nM
R.S.D	0.713%
R^2	0.99
Assay sample volume	0.4 µL
Analysis time	2 min

5.3.8 Biochip performance

5.3.8.1 Storage stability

The storage stability of the developed CMEA biochip was examined at 4° C and measured thrice every day with washing steps over a week. A loss of 8.3 % of the initial response after 1 week was observed when GOD was immobilized via 11-MUAwith the retention of more than about 90 % of the initial values for 1 mM glucose concentration; whereas, for the physisorped enzyme the activity reduced to 46.1 % within two days of use. The loss of activity in case of physisorped enzymes can be attributed due to the washing steps.

5.3.8.2 Reproducibility

The intra batch device performance (N= 5) was evaluated for the developed glucose biochip. The resulting data is presented as Table 5.5. An excellent reproducibility with almost no loss of enzyme activity was obtained with an R.S.D. of 0.713 % and 0.684 % against 2.5 mM and 5.0 mM glucose respectively as shown in Figure 5.17. These results suggested that the glucose biochip showed acceptable reproducibility. Analytical data for capacitive response of intra batch device performance (N= 5) with respect to 2.5 mM and 5.0 mM are presented in Table 5.6.

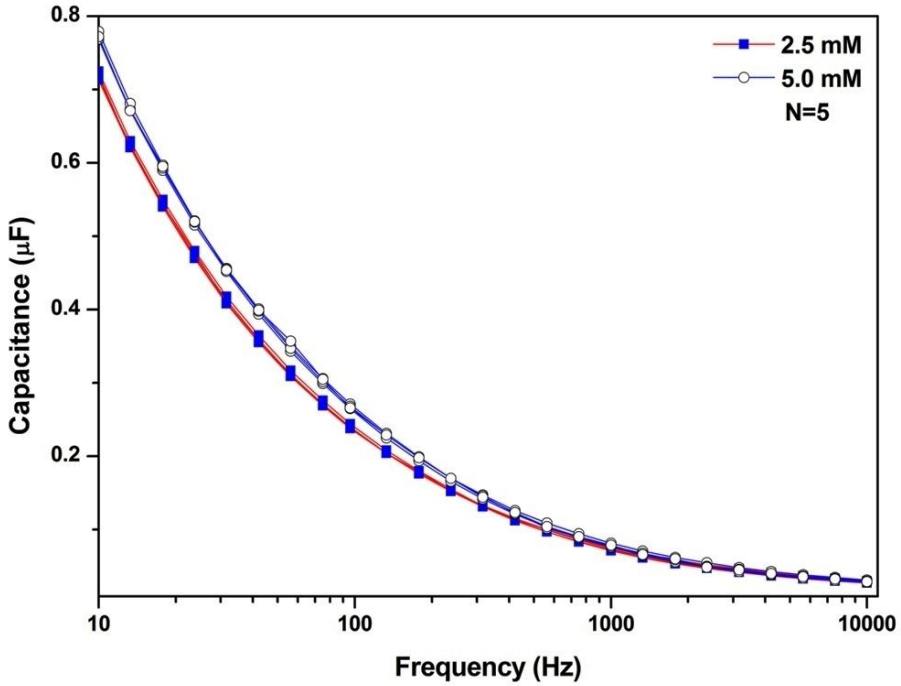

Figure 5.17 Capacitive response for intra batch device performance (N = 5) for the developed glucose biosensor; [Glucose] = 2.5 mM and 5.0 mM.

Table 5.6: Analytical data for capacitive response of intra batch device performance (N = 5) with respect to 2.5 mM and 5.0 mM

[Glucose](mM)	Biochip	Capacitive response at 10 Hz (µF)	Mean ± standard deviation (µF)	R.S.D. (%)
2.5	CMEA-1	0.7214	0.7179± 0.0051	0.713
	CMEA-2	0.7129		
	CMEA-3	0.7169		
	CMEA-4	0.7247		
	CMEA-4	0.7134		
5.0	CMEA-6	0.7787	0.7731 ± 0.0053	0.684
	CMEA-7	0.7679		
	CMEA-8	0.7686		
	CMEA-9	0.7787		
	CMEA-10	0.7717		

5.3.8.3 Reusability

The reusability of the biochip was also examined by measuring its response to a 5 mM glucose solution for five times as shown in Figure 5.18. In this process, the electrode was regenerated by sonicating (10 s) and followed by immersing in dd-water. Subsequent to this, the sensor can be reused with minimal loss of sensitivity (< 5% deviation in sensitivity).

5.4 Analysis of real samples

Since the normal human blood glucose concentration ranges from 4.0 - 6.0 mM, the linear range achieved using this CMEA biochip will be of great significance in clinical diagnosis. The CMEA biochip was used for determination of glucose in real serum samples to verify the practical application of the developed method. Four serum samples were tested for glucose detection in serum with CMEA biochip. The measured values were compared with a commercial blood glucose monitoring system. The glucose concentration detected in the serum samples is in the range of 1-10 mM. The recovery of glucose was evaluated by standard addition of pure glucose into solutions containing the serum samples. The

corresponding results are presented in Table 5.6. The proposed sensor gives a good recovery (95 %). The results demonstrated here reveal the potential applications of the CMEA sensor for determination of glucose in real samples.

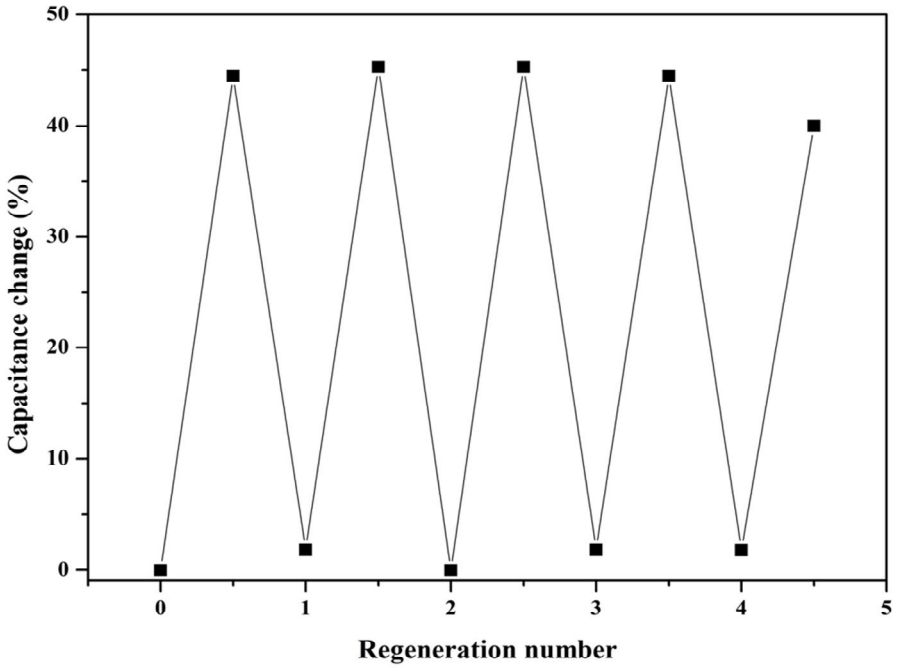

Figure 5.18 Sensor regeneration by 10 s sonication, followed by immersing in dd-water; % change in capacitance values recorded in absence and presence of 5.0 mM glucose.

Table 5.7 Sample analysis by standard addition method using developed CMEA biochip and comparison with commercial glucometer

Serum samples	**Glucose added (mM)**	**Glucose found (mM)**		**Analytical figures of merit using CMEA**		
		CMEA	**Commercial glucometer**	**R.S.D. (%)**	**R.E. (%)**	**Recovery (%)**
Sample 1	10	9.68	10.56	1.12	3.2	96.8
Sample 2	5	5.19	4.95	0.77	3.8	103.8
Sample 3	2.5	2.39	2.44	1.56	4.4	95.6
Sample 4	1	0.97	N.D.	1.75	3.0	97.0

5.5 Conclusions

A monolithic coil-microelectrode biochip device that was fabricated using UV and an X-ray lithography technique was presented. The application of the developed CMEA biochip for use in conductivity measurement and glucose biosensing was demonstrated. A linear range of detection for glucose (100 nM-10 mM) was achieved using GOD immobilized CMEA biochip. Excellent sensitivity and detection limit of 10 nM were recorded. The present biochip has the potential to detect glucose and has an analysis time of 2 min and requires a low sample volume of 0.4 µL. An important feature of the biochip device is its reusability that makes it an attractive feature over existing disposable devices. An excellent reproducibility was achieved for intra batch device performance.

Chapter 6

Conclusions

The research work presented in this thesis has been focused on the development of novel impedimetric biosensor and their miniaturization in bio-analysis. The developed novel devices were demonstrated in various applications, such as analysis of aflatoxins, bacteria and glucose. Through this work, the use of two electrode setup and its miniaturization was achieved successfully towards the development of simple yet sensitive biosensors. Here, we briefly revisit the significant contributions of this work.

Two electrode based setup was developed to quantify antibody- antigen interaction in terms of impedance/capacitance signal using the EIS technique as a proof of concept. As electrode material, Ag wire was found to be suitable over Cu wire for non-faradaic impedance measurement. The choice of material was based on electrochemical performance. The immunosensor construction, i.e. surface modification of electrode and the attachment of capture antibody to the electrode was confirmed using SEM and FT-IR. Extensive experiments were carried out for optimizing various parameters such as antibody dilution, applied potential, single frequency of measurement, incubation time and sample volume. These parameters were directly associated with immunosensor performance, when impedance was measured. The antibody dilution was optimized based on the sensitivity towards the target antigen. A potential of 10 mV was found to be the appropriate voltage for impedance analysis. The maximum change in impedance due to antibody-antigen interaction was found at 1Hz. The optimal analysis time was found to be 20 min with a sample volume of 700 µL (Chapter 2).

In an effort towards assay miniaturization, we have demonstrated two electrode setup for impedance measurement in a custom made glass cell with reduced assay volume of 700 µL.The developed two electrode based setup was used for the detection of aflatoxins (AFM1 and AFB1) and bacteria such as *E.Coli* by EIS technique. A label-free Ag wire based impedimetric immunosensor targeted towards AFM1 detection in milk was developed. In milk samples, an excellent LOD of 1 pg mL^{-1} was achieved with good sensitivity about 2.1 % impedance changes per decade. An improved linear range with short analysis time of 20 min for AFM1 analysis meeting EU standards in infant food was achieved. The developed immunosensor was validated with the simple equivalent circuit with double layer capacitance

for experimental data fitting. The fitting showed good agreement with experimental data. The immunosensor also showed excellent selectivity for AFM1 as against AFM2 (Chapter 3).

Matrix effects of various milk products such as ERM-BD 282, flavored milk and yogurt for analysis of AFM1 was also studied using EIS. The similar impedance response was obtained from ERM-BD 282 and flavored milk, but a large change in impedance was observed for yogurt from impedance analysis. This change in impedance may be due to matrix interference. The ideal capacitive behaviour was observed at different frequency when different milk matrices were used. For ERM-BD 282 and flavored milk, ideal capacitive behaviour was observed at a frequency of 52 Hz, wherein for yogurt it was 159 Hz (Chapter 3).

Further, miniaturization of two electrode setup was carried out in 384 micro well plates with application focussed on AFB1 analysis in peanut. The total assay volume was 105 µL. A highly sensitive and miniaturized label-free impedimetric immunosensor was developed for the analysis of AFB1 in peanut. EIS measurements were carried out with an optimal potential of 5 mV and frequency range was 1 Hz to 100 kHz. A lower limit of detection of 0.01 pg mL^{-1} for AFB1 in peanut was achieved. The immunosensor is simple and can be used under field conditions. The developed immunosensor was validated with equivalent circuit and found good fitting with experimental data when constant phase element were used instead of capacitor. This method can be extended for monitoring the quality of groundnut under storage conditions when the toxin is just beginning to grow (Chapter 3).

Subsequently, the Ag wire based immunosensor concept was extended to investigate bacterial contamination of water. A label-free impedimetric immunosensor for *E.coli* (MTCC-723) detection in water sample was developed. Under the optimal conditions, a linear increasing impedance trend was obtained when the *E. coli* concentration increased from 10^2 to 10^8 CFU mL^{-1}. The immunosensor showed a detection limit of 10^2 CFU mL^{-1} for *E.coli* in water sample (Chapter 3).

For better sensitivity, the use of a microfabricated electrode as an alternative transducer for the electrochemical immunosensor was investigated. The design and fabrication of µ-IDEs device were achieved followed by its application to detect toxin in various food matrices at ultra trace levels. The developed immunosensor showed a linear range of detection 25-100 pg mL^{-1} with a detection limit of 1 pg mL^{-1} for AFM1 in milk. The

developed µ-IDEs immunosensor was also tested against unknown samples. This work also demonstrated the quantification of unknown samples, hence the scope for on-line monitoring and sensitive analysis of aflatoxins and tuning the device for different applications (Chapter 4).

A monolithic coil-microelectrode array biochip device was designed and fabricated using a combination of UV and X-ray lithography techniques. The developed device was tested for measurement of conductivity of standard solution. The conductivity of KCl solution was tested and limit of detection was found to be 0.1 mM. The device was also tested for measurement of ions and extended for use as biochip device, where gluconate ions were measured for quantitative analysis of glucose using EIS techniques. Lower detection limit of 10 nM was achieved with excellent sensitivity. The biochip could detect glucose with an analysis time of 2 min with low sample volume of 0.4 µL. The performance of the biochip was also studied. It was found that the biochip can be reused with minimal loss of sensitivity. The biochip was also used for determination of glucose in real serum samples to verify the practical application. A good recovery of 95 % was obtained from the developed glucose sensor. The results showed the potential applications of the biochip for determination of glucose in real samples (Chapter 5).

Significant contribution

1. A systematic study of aflatoxins (AFM1 and AFB1) and *E.coli* analysis has been carried out using a simple yet sensitive impedimetric immunosensor. The sensor comprising two electrode setup. The sensor has been validated against existing commercial kit and the utility of developed sensor for practical use in analysis of milk, milk powder, yogurt, peanut extract and *E.coli* has been successfully demonstrated.
2. The proof of concept for quantification of antibody-antigen interaction using EIS technique has been extensively studied and optimized for real sample analysis.
3. Using microfabrication technology, a novel miniaturize biosensing platform has been developed for ultra sensitive detection of toxin, which has resulted in the intellectual property as international patent.
4. The use of hybrid microfabrication technology coupled with the synchrotron radiation source has been exploited to develop a high aspect ratio miniaturized biosensing platform for enhanced sensitivity.

Future scope of work

The overall results achieved from the immunosensors developed in this work (Ag wire two electrode setup and µ-IDEs) were very promising as these devices could meet the most stringent standards for detection of target analytes such as AFM1, AFB1 and *E.Coli* determination in milk, peanuts and water samples respectively. The developed sensors are cost effective, easy to use, ultra sensitive and field portable. However, there is ample scope to take this work forward to ultimately benefit the society. The future scope in this direction will aim at product specific design and field trials of the sensor. The development of two electrode based impedimetric immunosensor for AFM1, AFB1 and *E.coli* detection using EIS has been successfully demonstrated. This work is being further explored to develop reliable field portable sensor for bacterial contamination in drinking water.

- The developed miniaturized two electrode based impedimetric immunosensor for analysis of AFM1 in milk can be taken up for translational research to enable screening of milk samples at milk collection centres.
- The developed wire based two electrode setup has potential for further miniaturization using micro/nanotechnology, which can be further exploited for enhanced sample throughput and reproducibility. The developed wire based two electrode setup can easily be extended for the analysis of different analytes such as Ochratoxin A, Fumonisin B1 and etc. This is being explored in collaboration with RRCAT, Indore.
- µ-IDEs immunosensor developed for the detection of AFM1 using EIS has been very sensitive, robust, easy to use, and require less time of analysis. Further investigation will focus on development of multi-analyte biosensing system.
- Coil microelectrode array biochip device showed promising results for conductivity measurement and glucose sensing. This sensing platform will be further extended to other clinical analyses such as creatinine, urea etc.

References

Alocilja E. C., Radke S. M. Market analysis of biosensors for food safety. *Biosensors and Bioelectronics*, 2003, 18: 841-846.

Altissimo M. E-beam lithography for micro-/nanofabrication. *Biomicrofluidics*, 2010, 4: 3-6.

Amine A., Mohammadi H., Bourais I., Palleschi G. Enzyme inhibition-based biosensors for food safety and environmental monitoring. *Biosensors and Bioelectronics*, 2006, 21: 1405-1423.

Ammida N., Micheli L., Piermarini S., Moscone D., Palleschi G. Detection of aflatoxin B1 in barley: Comparative study of immunosensor and HPLC. *Analytical Letters*, 2006, 39: 1559-1572.

Anfossi L., Calderara M., Baggiani C., Giovannoli C., Arletti E., Giraudi G. Development and Application of Solvent-free Extraction for the Detection of Aflatoxin M1 in Dairy Products by Enzyme Immunoassay. *Journal of Agricultural and Food Chemistry*, 2008, 56: 1852-1857.

Arduini F., Errico I., Amine A., Micheli L., Palleschi G., Moscone D. Enzymatic spectrophotometric method for aflatoxin B detection based on acetylcholinesterase inhibition. *Analytical Chemistry*, 2007, 79: 3409-3415.

Arora K., Chand S., Malhotra B. D. Recent developments in bio-molecular electronics techniques for food pathogens. *Analytica Chimica Acta*, 2006, 568: 259-274.

Arslan F., Ustabaş S., Arslan H. An amperometric biosensor for glucose determination prepared from glucose oxidase immobilized in polyaniline-polyvinylsulfonate film. *Sensors*, 2011, 11: 8152-8163.

Arya S. K., Solanki P. R., Datta M., Malhotra B. D. Recent advances in self-assembled monolayers based biomolecular electronic devices. *Biosensors and Bioelectronics*, 2009, 24: 2810-2817.

Baccar H., Mejri M. B., Hafaiedh I., Ktari T., Aouni M., Abdelghani A. Surface plasmon resonance immunosensor for bacteria detection. *Talanta*, 2010, 82: 810-814.

Baccar H., Mejri M., Prehn R., del Campo R., Baldrich E. Interdigitated Microelectrode Arrays Integrated in Microfluidic Cell for Biosensor Applications. *Journal of Nanomedicine & Nanotechnology*, 2014, 5: 243.

Bacher G., Pal S., Kanungo L., Bhand S. A label-free silver wire based impedimetric immunosensor for detection of aflatoxin M1 in milk. *Sensors and Actuators* B. 2012, 168: 223-230.

Badea M., Micheli L., Messia M. C., Candigliota T., Marconi E., Mottram T., Velasco-Garcia M., Moscone D., Palleschi G. Aflatoxin M1 determination in raw milk using a flow-injection immunoassay system. *Analytica Chimica Acta*, 2004, 520: 141-148.

Banada P. P., Guo S. L. Optical forward-scattering for detection of Listeria monocytogenes and other Listeria species. *Biosensors and Bioelectronics*, 2007, 22: 1664-1671.

Banica F. G. Chemical Sensors and Biosensors: Fundamentals and Applications. Wiley, Chichester, 2012.

Barbero G. A., Alexe-Ionescu L., Lelidis I. Significance of small voltage in impedance spectroscopy measurements on electrolytic cells. *Journal of Applied Physics*, 2005, 98: 113703-5.

Barlen B., Mazumdar S. D., Lezrich O., Kämpfer P., Keusgen M. Detection of Salmonella by surface plasmon resonance. *Sensors*, 2007, 7: 1427-1446.

Barone P. W., Parker R. S., Strano M. S. In vivo fluorescence detection of glucose using a single-walled carbon nanotube optical sensor: design, fluorophore properties, advantages, and disadvantages. *Analytical Chemistry*, 2005, 77: 7556-7562.

Barreiros dos Santos M., Agusil J. P., Prieto-Simón B., Sporer C., Teixeira V., Samitier J. Highly sensitive detection of pathogen *Escherichia coli* O157:H7 by electrochemical impedance spectroscopy. *Biosensors and Bioelectronics*, 2013, 45: 174-180.

Bart M., Stigter E., Stapert H., De Jong G., Van Bennekom W. On the response of a label-free interferon-γ immunosensor utilizing electrochemical impedance spectroscopy. *Biosensors and Bioelectronics*, 2005, 21: 49-59.

Bartlett P. N. Bioelectrochemistry Fundamentals, Experimental Techniques and Applications. John Wiley & Sons, West Sussex, England, 2008.

Becker E. W., Ehrfeld W., Hagmann P., Maner A., Münchmeyer D. Fabrication of microstructures with high aspect ratios and great structural heights by synchrotron radiation lithography, galvanoforming, and plastic moulding (LIGA process). *Microelectronic Engineering*, 1986, 4: 35-56.

Belmont C., Tercier M.-L., Buffle J., Fiaccabrino G. C., Koudelka-Hep M. Mercury-plated iridium-based arrays of microelectrodes for trace metals detection by voltammetry: optimum conditions and reliability. *Analytica Chimica Acta*, 1996, 329: 203-214.

Benavides G. L., Bieg L. F., Saavedra M. P., Bryce E. A. High aspect ratio meso-scale parts enabled by wiremicro-EDM. *Microsystem Technologies*. 2002, 8: 395-401

Berggren C., Bjarnason B., Johansson G. An immunological interleukine-6 capacitive biosensor using perturbation with a potentiostatic step. *Biosensors and Bioelectronics*, 1998, 13: 1061-1068.

Berggren C., Bjarnason B., Johansson G. Capacitive Biosensors. *Electroanalysis*, 2001, 13: 173-180.

Berney H., West J., Haefele E., Alderman J., Lane W., Collins J. K. A DNA diagnostic biosensor: development, characterisation and performance. *Sensors and Actuators* B. 2000, 68: 100-108.

Bogomolova A., Komarova E., Reber K., Gerasimov T., Yavuz O., Bhatt S., Aldissi M. Challenges of electrochemical impedance spectroscopy in protein biosensing. *Analytical Chemistry*, 2009, 81: 3944-3949.

Boubour E., Lennox R. B. Stability of ω-functionalized self-assembled monolayers as a function of applied potential. *Langmuir*, 2000, 16: 7464-7470.

Bourgeois W., Romain A.-C., Nicolas J., Stuetz R. M. The use of sensor arrays for environmental monitoring: interests and limitations. *Journal of Environmental Monitoring*, 2003, 5: 852-860.

Bratov A., Ramon-Azcon J., Abramova N., Merlos A., Adrian J., Sanchez-Baeza F., Marco M. P., Dominquez C. *Biosensors and Bioelectronics*, 2008, 118: 84-89.

Brunelle S. Electroimmunoassay technology for foodborne pathogen detection. *IVD Technology*, 2001, 7: 55-66.

Cai H., Lee T. M.-H., Hsing I. M. Label-free protein recognition using an aptamer-based impedance measurement assay. *Sensors and Actuators* B. 2006, 114: 433-437.

Campbell G. A., Mutharasan R. A method of measuring *Escherichia coli* O157: H7 at 1 cell/mL in 1 liter sample using antibody functionalized piezoelectric-excited millimeter-sized cantilever sensor. *Environmental Science & Technology*, 2007, 41: 1668-1674.

Campuzano S., Pedrero M., Montemayor C., Fatás E., Pingarrón J. M. Characterization of alkanethiol-self-assembled monolayers-modified gold electrodes by electrochemical impedance spectroscopy. *Journal of Electroanalytical Chemistry*, 2006, 586: 112-121.

Cardoso P., Davim, J. P. A brief review on micromachining of materials. *Reviews on Advanced Materials Science*. 2012, 30: 98-102.

Chen J., Shi J. Gold nanohole arrays for biochemical sensing fabricated by soft UV nanoimprint lithography. *Microelectronic Engineering*, 2009, 86: 632-635.

Chen J., Shi J., Cattoni A., Decanini D., Liu Z., Chen Y., Haghiri-Gosnet A. M. A versatile pattern inversion process based on thermal and soft UV nanoimprint lithography techniques. *Microelectronic Engineering*, 2010, 87: 899-903.

Cheng F., Gamble L. J., Castner D. G. XPS, TOF-SIMS, NEXAFS, and SPR Characterization of Nitrilotriacetic Acid-Terminated Self-Assembled Monolayers for Controllable Immobilization of Proteins. *Analytical Chemistry*, 2008, 80: 2564-2573.

Chornokur G., Arya S. K., Phelan C., Tanner R., Bhansali S. Impedance-Based Miniaturized Biosensor for Ultrasensitive and Fast Prostate-Specific Antigen Detection. *Journal of Sensors*, 2011, 1-7.

Chowdhury A. D., De A., Chaudhuri C. R., Bandyopadhyay K., Sen P. Label free polyaniline based impedimetric biosensor for detection of *E.coli* O157:H7 Bacteria. *Sensors and Actuators* B. 2012, 171-172: 916-923.

Çiftçi H., Tamer U., Teker M. Ş., Pekmez N. Ö. An enzyme free potentiometric detection of glucose based on a conducting polymer poly (3-aminophenyl boronic acid-co-3-octylthiophene). *Electrochimica Acta*, 2013, 90: 358-365.

Copic D., Park S. J. Fabrication of high-aspect-ratio polymer microstructures and hierarchical textures using carbon nanotube composite master molds. *Lab on a Chip*, 2011, 11**:** 1831-1837.

Cortina M., Esplandiu M. J., Alegret S., del Valle M. Urea impedimetric biosensor based on polymer degradation onto interdigitated electrodes. *Sensors and Actuators* B. 2006, 118: 84-89.

Craighead H. Future lab-on-a-chip technologies for interrogating individual molecules. *Nature*, 2006, *442*: 387-393.

Daniels J. S., Pourmand N. Label-Free Impedance Biosensors: Opportunities and Challenges. *Electroanalysis*, 2007, 19: 1239-1257.

Dannenberger O., Weiss K., Woll C., Buck M. Reactivity of self-assembled monolayers: formation of organized amino functionalities. *Physical Chemistry Chemical Physics*, 2000, 2: 1509-1514.

Dastider S. G., Barizuddin S., Wu Y., Dweik M., Almasri M. Impedance biosensor based on interdigitated electrode arrays for detection of low levels of *E.coli* O157:H7. IEEE 26th International Conference on Micro Electro Mechanical Systems (MEMS), 2013, 955-958.

Dávila D., Esquivel J. P., Sabaté N., Mas J. Silicon-based microfabricated microbial fuel cell toxicity sensor. *Biosensors and Bioelectronics*, 2011, 26: 2426-2430.

Davis F., Nabok A. V., Higson S. P. J. Species differentiation by DNA-modified carbon electrodes using an ac impedimetric approach, *Biosensors and Bioelectronics*, 2005, 20: 1531-1538

de Groot M. T., Evers T. H., Merkx M., Koper M. T. M. Electron Transfer and Ligand Binding to Cytochrome c‘ Immobilized on Self-Assembled Monolayers. *Langmuir*, 2006, 23: 729-736.

Dinckaya E., Kinik O., Sezginturk M. K., Altug C., Akkoca A. Development of an impedimetric aflatoxin M1 biosensor based on a DNA probe and gold nanoparticles. *Biosensors and Bioelectronics*, 2011, 26: 3806-3811.

Ding H.-Y., Zhou Y., Zhang S.-J., Yin X.-B., Li Y.-J., He X.-W. Preparation of nano-copper modified glassy carbon electrode and its catalytic oxidation to glucose. *Chinese Journal of Analytical Chemistry*, 2008, 36: 839-842.

Dors G. C., Caldas S. C., Feddern V., Bemvenuti R., Hackbart H. C. D. S., De Souza M. M., Oliveira M. D. S., Buffon J. G., Primel E. G., Furlong E. B. Aflatoxins: Contamination, Analysis and Control, Aflatoxins-Biochemistry and Molecular Biology, InTech, 2011. DOI: 10.5772/24902. ISBN: 978-953-307-395-8.

E U Commission, Commission Regulation (EC) No. 466/2001 of 8 March 2001 setting maximum levels for certain contaminants in foodstuffs. *Official Journal European Communities*, 2001, L77.

Elsholz B., Wörl R., Blohm L., Albers J., Feucht H., Grunwald T., Jürgen B., Schweder T., Hintsche R. Automated Detection and Quantitation of Bacterial RNA by Using Electrical Microarrays. *Analytical Chemistry*, 2006, 78: 4794-4802.

European Commission (EC). Commission Regulation (EC) No 1881/2006 of 19 December 2006 setting maximum levels for certain contaminants in foodstuffs. *Official Journal of the European Union*, 2006, L364: 5-24.

Fallah A. Assessment of aflatoxin M1 contamination in pasteurized and UHT milk marketed in central part of Iran. *Food and Chemical Toxicology*, 2010, 48: 988-991.

Fang C., He J., Chen Z. A disposable amperometric biosensor for determining total cholesterol in whole blood. *Sensors and Actuators* B. 2011, 155: 545-550.

Farrell S., Ronkainen-Matsuno N. J., Halsall H. B., Heineman W. R. Bead-based immunoassays with microelectrode detection. *Analytical and Bioanalytical Chemistry*, 2004, 379: 358-367.

Felice C. J., Madrid R. E., Olivera J. M., Rotger V. I., Valentinuzzi M. E. Impedance microbiology: quantification of bacterial content in milk by means of capacitance growth curves. *Journal of Microbial Methods*, 1999, 35: 37-42.

Ferrara L. A., Fleischman A. J., Togawa D., Bauer T. W., Benzel E. C., Roy S. An in vivo Biocompatibility Assessment of MEMS Materials for Spinal Fusion Monitoring. *Biomedical Microdevices*, 2003, 5: 297-302.

Figeys D., Pinto D. Lab-on-a-Chip: A Revolution in Biological and Medical Sciences. *Analytical Chemistry*, 2000, 72: 330 A-335 A.

Food safety and standards (contaminants, toxins and residues) regulations, 2011, F.No. 2-15015/30/2010.

Fragoso A., Laboria N., Latta D., O'Sullivan C.K. Electron Permeable Self-Assembled Monolayers of Dithiolated Aromatic Scaffolds on Gold for Biosensor Applications. *Analytical Chemistry*, 2008, 80: 2556-2563.

Fu Z., Huang X., Min S. Rapid determination of aflatoxins in corn and peanuts. *Journal of Chromatography* A, 2008, 1209: 271-274.

Fumani N. S., Hassan J., Yousefi S. R. Determination of aflatoxin B1 in cereals by homogeneous liquid–liquid extraction coupled to high performance liquid chromatography-fluorescence detection. *Journal of Separation Science*, 2011, 34: 1333-1337.

Gawad S., Cheung K., Seger U., Bertsch A., Renaud P. Dielectric spectroscopy in a micromachined flow cytometer: theoretical and practical considerations. *Lab on a Chip*, 2004, 4: 241-251.

Ghanem I., Orfi M. Aflatoxin M1 in raw, pasteurized and powdered milk available in the Syrian market. *Food Control*, 2009, 20: 603-605.

Grieshaber D., MacKenzie R., Voros J., Reimhult E. Electrochemical Biosensors-Sensor Principles and Architectures. *Sensors*, 2008, 8: 1400-1458.

Guan J.-G., Miao Y.-Q., Zhang Q.-J. Impedimetric biosensors. *Journal of Bioscience and Bioengineering*, 2004, 97: 219-226.

Guo X., Lin C.-S., Chen S.-H., Ye R., Wu V. C. H. A piezoelectric immunosensor for specific capture and enrichment of viable pathogens by quartz crystal microbalance sensor, followed by detection with antibody-functionalized gold nanoparticles. *Biosensors and Bioelectronics*, 2012, 38: 177-183.

Gurbay A., Aydın S., Girgin G., Engin A. B., Sahin G. Assessment of aflatoxin M1 levels in milk in Ankara, Turkey. *Food Control*, 2006, 17: 1-4.

Haab B. B. Methods and applications of antibody microarrays in cancer research. *Proteomics*, 2003, 3: 2116-2122.

Hakim M. M., Lombardini M., Sun K., Giustiniano F., Roach P. L., Davies D. E., Howarth P. H., de Planque M. R., Morgan H., Ashburn P. Thin film polycrystalline silicon nanowire biosensors. *Nano Letters*, 2012, 12: 1868-1872.

Han Y., Liu C. Pneumatically actuated active polymer pen lithography. *Sensors and Actuators* A. 2011, 167: 433-437.

Hervás M., López M. A., Escarpa A. Electrochemical immunosensing on board microfluidic chip platforms. *TrAC Trends in Analytical Chemistry*, 2012, 31: 109-128.

Heyduk E., Heyduk T. Fluorescent homogeneous immunosensors for detecting pathogenic bacteria. *Analytical Biochemistry*, 2010, 396: 298-303.

Hintsche R., Paeschke M., Wollenberger U., Schnakenberg U., Wagner B., Lisec T. Microelectrode arrays and application to biosensing devices. *Biosensors and Bioelectronics*, 1994, 9: 697-705.

Hoeltz M., Welke J. E., Dottori H. A., Noll I. B. Photometric procedure for quantitative analysis of aflatoxin B1 in peanuts by thin-layer chromatography using charged coupled device detector. *Química Nova*, 2010, 33: 43-47.

Holford T. R. J., Davis F., Higson S. P. J. Recent trends in antibody based sensors. *Biosensors and Bioelectronics*, 2012, 34: 12-24.

Hollenberg B. A., Richards C. D., Richards R., Bahr D. F., Rector D. M. A MEMS fabricated flexible electrode array for recording surface field potentials. *Journal of Neuroscience Methods*, 2006, 153: 147-153.

Hou Y., Tlili C., Jaffrezic-Renault N., Zhang A., Martelet C., Ponsonnet L., Errachid A., samitier J., Bausells J. Study of mixed Langmuir–Blodgett films of immunoglobulin G/amphiphile and their application for immunosensor engineering. *Biosensors and Bioelectronics*, 2004, 20: 1126-1133.

Hsiung L.-C., Yang C.-H., Chiu C.-L., Chen C.-L., Wang Y., Lee H., Cheng J.-Y., Ho M.-C., Wo A. M. A planar interdigitated ring electrode array via dielectrophoresis for uniform patterning of cells. *Biosensors and Bioelectronics*, 2008, 24: 869-875.

Huang B., Han Z., Cai Z., Wub Y., Ren Y. Simultaneous determination of aflatoxins B1, B2, G1, G2, M1 and M2 in peanuts and their derivative products by ultra-high-performance liquid chromatography–tandem mass spectrometry. *Analytica Chimica Acta*, 2010, 662: 62-68.

Huang H.-M., Huang P.-K., Kuo W.-H., Ju Y.-H., Wang M.-J. Sol–gel immobilized enzymatic glucose biosensor on gold interdigitated array (IDA) microelectrode. *Journal of Sol-Gel Science and Technology*, 2013, 67: 492-500.

Huang Y., Bell M. C., Suni I. I. Impedance Biosensor for Peanut Protein Ara h 1. *Analytical Chemistry*, 2008, 80: 9157-9161.

International Agency for Research on Cancer. IARC monograph on the Evaluation of Carcinogenic Risk to Humans; IARC: Lyon, France, 1993, 56.

Ivnitski D., Sitdikov R., Ivnitski N. Non-invasive electrochemical hand-held biosensor as diagnostic indicator of dental diseases. *Electrochemistry Communications*, 2003, 5: 225-229.

Jacobs M., Nagaraj V. J., Mertz T., Selvam A. P., Ngo T., Prasad S. An electrochemical sensor for the detection of antibiotic contaminants in water. *Analytical Methods*, 2013, 5: 4325-4329.

Jang L. S., Keng H. K. Modified fabrication process of protein chips using a short-chain self-assembled monolayer. *Biomedical Microdevices*, 2008, 10: 203-211.

Jin X., Jin X., Liu X., Chen L., Jiang J., Shen G. Biocatalyzed deposition amplification for detection of aflatoxin B1 based on quartz crystal microbalance. *Analytica Chimica Acta*, 2009, 645: 92-97.

Jorcin J.-B., Orazem M. E., Pébère N. CPE analysis by local electrochemical impedance spectroscopy. *Electrochimica Acta*, 2006, 51: 1473-1479.

Kafi A. K. M., Lee D.-Y., Park S.-H., Kwon Y.-S. Development of a peroxide biosensor made of a thiolated-viologen and hemoglobin-modified gold electrode. *Microchemical Journal*, 2007, 85: 308-313.

Kafka J., Pänke O., Abendroth B., Lisdat F. A label-free DNA sensor based on impedance spectroscopy. *Electrochimica Acta*, 2008, 53: 7467-7474.

Kamkar A. A study on the occurrence of aflatoxin M1 in Iranian Feta cheese. *Food Control*, 2006, 17: 768-775.

Kandala C. V., Sundaram J., Govindarajan K., Subbiah J. Nondestructive analysis of in-shell peanuts for moisture content using a custom built NIR Spectrometer. *Journal of Food Engineering*, 2011, 2: 1-7.

Kanungo L., Bacher G., Bhand S. Flow-Based Impedimetric Immunosensor for Aflatoxin Analysis in Milk Products. *Applied Biochemistry and Biotechnology*, 2014, 174: 1157-1165.

Kanungo L., Pal S., Bhand S. Miniaturized hybrid immunoassay for high sensitivity analysis of aflatoxin M1 in milk. *Biosensors and Bioelectronics*, 2011, 26: 2601-2606.

Katz E., Willner I. Probing Biomolecular Interactions at Conductive and Semiconductive Surfaces by Impedance Spectroscopy: Routes to Impedimetric Immunosensors, DNA-Sensors, and Enzyme Biosensors. *Electroanalysis*, 2003, 15: 913-947.

Kaushik A., Solanki P. R., Sood K. N., Ahmad S., Malhotra B. D. Fumed silica nanoparticles–chitosan nanobiocomposite for ochratoxin-A detection. *Electrochemistry Communications*, 2009, 11: 1919-1923.

Kim I.-D., Rothschild A., Lee B. H., Kim D. Y., Jo S. M., Tuller H. L. Ultrasensitive Chemiresistors Based on Electrospun TiO_2 Nanofibers. *Nano Letters*, 2006, 6: 2009-2013.

Kim J. H., Cho J. H., Cha G. S. Conductimetricmembrane strip immunosensor with polyaniline-bound gold colloids as signal generator. *Biosensors and Bioelectronics*, 2000, 14: 907-915.

Kokkinos C., Economou A., Raptis I. Microfabricated disposable lab-on-a-chip sensors with integrated bismuth microelectrode arrays for voltammetric determination of trace metals. *Analytica Chimica Acta*, 2012, 710: 1-8.

K'Owino I. O., Sadik O. A. Impedance Spectroscopy: A Powerful Tool for Rapid Biomolecular Screening and Cell Culture Monitoring. *Electroanalysis*, 2005, 17: 2101-2113.

Kralj Cigić I., Prosen H. An Overview of Conventional and Emerging Analytical Methods for the Determination of Mycotoxins. *International Journal of Molecular Sciences*, 2009, 10: 62-115.

Laczka O., Baldrich E., Muñoz F. X., del Campo F. J. Detection of Escherichia coli and Salmonella typhimurium Using Interdigitated Microelectrode Capacitive Immunosensors: The Importance of Transducer Geometry. *Analytical Chemistry*, 2008, 80: 7239-7247.

Lai R. Y., Seferos D. S., Heeger A. J., Bazan G. C., Plaxco K. W. Comparison of the Signaling and Stability of Electrochemical DNA Sensors Fabricated from 6- or 11-Carbon Self-Assembled Monolayers†. *Langmuir*, 2006, 22: 10796-10800.

Lasseter T. L., Cai W., Hamers R. J. Frequency-dependent electrical detection of protein binding events. *Analyst*, 2004, 129: 3-8.

Lee G.-Y., Choi Y.-H., Chung H.-W., Ko H., Cho S., Pyun J.-C. Capacitive immunoaffinity biosensor based on vertically paired ring-electrodes. *Biosensors and Bioelectronics*, 2013, 40: 227-232.

Lee H., Sun E., Ham D., Weissleder R. Chip–NMR biosensor for detection and molecular analysis of cells. *Nature Medicine*, 2008, 14: 869-874.

Lee N. A., Wang S., Allan R. D., Kennedy I. R. A rapid aflatoxins B1 ELISA: Development and validation with reduced matrix effects for peanuts, corn, pistachio, and soybeans. *Journal of Agricultural and Food Chemistry*, 2004, 52: 2746-2755.

Levine P. M., Gong P., Levicky R., Shepard K. L. Real-time, multiplexed electrochemical DNA detection using an active complementary metal-oxide-semiconductor biosensor array with integrated sensor electronics. *Biosensors and Bioelectronics*, 2009, 24: 1995-2001.

Li C.-W., Cheung C. N., Yang J., Tzang C. H., Yang M. PDMS-based microfluidic device with multi-height structures fabricated by single-step photolithography using printed circuit board as masters. *Analyst*, 2003, 128: 1137-1142.

Li X., Toyoda K., Ihara I. Coagulation process of soymilk characterized by electrical impedance spectroscopy. *Journal of Food Engineering*, 2011, 105: 563-568.

Liao W.-C., Ho J.-a. A. Attomole DNA Electrochemical Sensor for the Detection of *Escherichia coli* O157. *Analytical Chemistry*, 2009, 81: 2470-2476.

Lin J., He C., Zhang L., Zhang S. Sensitive amperometric immunosensor for α-fetoprotein based on carbon nanotube/gold nanoparticle doped chitosan film. *Analytical Biochemistry* 2009, 384: 130-135.

Linderholm P., Vannod J. Bipolar resistivity profiling of 3D tissue culture. *Biosensor and Bioelectronics*, 2007, 22: 789-796.

Lisdat F., Schäfer D. The use of electrochemical impedance spectroscopy for biosensing. *Analytical and Bioanalytical Chemistry*, 2008, 391: 1555-1567.

Liu Y., Qin Z., Wu X., Jiang H. Immune-biosensor for aflatoxin B1 based bio-electrocatalytic reaction on micro-comb electrode. *Biochemical Engineering Journal*, 2006, 32: 211-217.

Lorenz W., Schulze K. D. Zur anwendung der transformations—impedanzspektrometrie. *Journal of Electroanalytical Chemistry and Interfacial Electrochemistry*, 1975, 65: 141-153.

Love J. C., Estroff L. A., Kriebel J. K., Nuzzo R. G., Whitesides G. M. Self-Assembled Monolayers of Thiolates on Metals as a Form of Nanotechnology. *Chemical Reviews*, 2005, 105: 1103-1170.

Maalouf R., Fournier-Wirth C., Coste J., Chebib H., Saïkali Y., Vittori O., Errachid A., Cloarec J.-P., Martelet C., Jaffrezic-Renault N. Label-Free Detection of Bacteria by Electrochemical Impedance Spectroscopy: Comparison to Surface Plasmon Resonance. *Analytical Chemistry*, 2007, 79: 4879-4886.

Macdonald J. R. Impedance Spectroscopy. Wiley Interscience Publication, NY, 1987.

Madou M. J. Fundamentals of Microfabrication and Nanotechnology. 3rd ed. CRC Press, Boca Raton, 2012.

Martins M. L., Martins H. M. Aflatoxin M1 in raw and ultra high temperature-treated milk commercialized in Portugal. *Food Additives and Contaminants*, 2000, 17: 871-874.

Maruyama K., Ohkawa H., Ogawa S., Ueda A., Niwa O., Suzuki K. Fabrication and Characterization of a Nanometer-Sized Optical Fiber Electrode Based on Selective Chemical Etching for Scanning Electrochemical/Optical Microscopy. *Analytical Chemistry*, 2006, 78: 1904-1912.

Maupas H., Soldatkin A. P., Martelet C., Jaffrezic-Renault N., Mandrand B. Direct immunosensing using differential electrochemical measurements of impedimetric variations. *Journal of Electroanalytical Chemistry*, 1997, 421: 165-171.

McNaught AD, Wilkinson A. IUPAC. *Compendium of Chemical Terminology, 2nd ed.* (The "Gold Book"). Blackwell Scientific Publications, Oxford, UK, 1997.

Micheli L., Grecco R., Badea M., Moscone D., Palleschi G. An electrochemical immunosensor for aflatoxin M1 determination in milk using screen-printed electrodes. *Biosensors and Bioelectronics*, 2005, 21: 588-596.

Min J., Baeumner A. J. Characterization and Optimization of Interdigitated Ultramicroelectrode Arrays as Electrochemical Biosensor Transducers. *Electroanalysis*, 2004, 16: 724-729.

Min J., Baeumner A. J**.** Highly Sensitive and Specific Detection of Viable *Escherichia coli* in Drinking Water**.** *Analytical Biochemistry*, 2002, 303: 186-193.

Mishra G. K., Bacher G., Roy U., Bhand S. A label free impedemetric immunosensor for detection of *Escherichia coli* in water. *ScienceJet*, 2015, 4: 76.

Mishra G. K., Mishra R. K., Bhand S. Flow injection analysis biosensor for urea analysis in adulterated milk using enzyme thermistor. *Biosensors and Bioelectronics*, 2010, 26: 1560-1564.

Mizutani F. Biosensors utilizing monolayers on electrode surfaces. *Sensors and Actuators* B. 2008, 130: 14-20.

Mohd Syaifudin A. R., Jayasundera K. P., Mukhopadhyay S. C. A low cost novel sensing system for detection of dangerous marine biotoxins in seafood. *Sensors and Actuators* B. 2009, 137: 67-75.

Moreno-Hagelsieb L., Foultier B., Laurent G., Pampin R., Remacle J., Raskin J. P., Flandre D. Electrical detection of DNA hybridization: Three extraction techniques based on interdigitated Al/Al_2O_3 capacitors. *Biosensors and Bioelectronics*, 2007, 22: 2199-2207.

Morris N., Cardosi M., Birch B., Turner A. An electrochemical capillary fill device for the analysis of glucose incorporating glucose oxidase and ruthenium (III) hexamine as mediator. *Electroanalysis*, 1992, 4: 1-9.

Muramatsu H., Dicks J. M., Tamiya E., Karube I. Piezoelectric crystal biosensor modified with Protein-A for determinationa of immunoglobins. *Analytical Chemistry*, 1987, 59: 2760-2763.

Narakathu B. B., Atashbar M. Z., Bejcek B. E. Improved detection limits of toxic biochemical species based on impedance measurements in electrochemical biosensors. *Biosensors and Bioelectronics*, 2010, 26: 923-928.

Neagu D., Perrino S., Micheli L., Palleschi G., Moscone D. Aflatoxin M1 determination and stability study in milk samples using a screen-printed 96-well electrochemical microplate. *International Dairy Journal*, 2009, 19: 753-758.

Nebling E., Grunwald, T., Albers J., Schäfer P., Hintsche R. Electrical detection of viral DNA using ultramicroelectrode arrays. *Analytical Chemistry*, 2004, 76: 689-696.

Newman J. D., Turner A. P. Home blood glucose biosensors: a commercial perspective. *Biosensors and Bioelectronics*, 2005, 20: 2435-2453.

Nicu L., Leichlé T. Micro-and Nanoelectromechanical Biosensors. John Wiley & Sons., 2014.

Oldham K. B. Electrode "edge effects" analyzed by the Green function method. *Journal of Electroanalytical Chemistry*, 2004, 570: 163-170.

Olkhov R. V., Shaw A. M. Label-free antibody-antigen binding detection by optical sensor array based on surface-synthesized gold nanoparticles. *Biosensors and Bioelectronics*, 2008, 23: 1298-1302.

Ordeig O., Banks C. E., del Campo J., Muñoz F. X., Compton R. G. Trace Detection of Mercury (II) Using Gold Ultra-Microelectrode Arrays. *Electroanalysis*, 2006, 18: 573-578.

Ordeig O., del Campo J. Electroanalysis Utilizing Amperometric Microdisk Electrode Arrays. *Electroanalysis*, 2007, 19:1973-1986.

Oveisi M.-R., Jannat B., Sadeghi N., Hajimahmoodi M., Nikzad A. Presence of aflatoxin M1 in milk and infant milk products in Tehran, Iran. *Food Control*, 2007, 18: 1216-1218.

Paniel N., Radoi A., Marty J-L. Development of an electrochemical biosensor for the detection of aflatoxin M1 in milk. *Sensors*, 2010, 10: 9439-9448.

Park I-S., Kim D-K., Adanyi N., Varadi M., Kim N. Development of a direct-binding chloramphenicol sensor based on thiol or sulfide mediated self-assembled antibody monolayers. *Biosensors and Bioelectronics*, 2004, 19: 667-674.

Park J. Y., Park S. M. DNA hybridization sensors based on electrochemical impedance spectroscopy as a detection tool. *Sensors*, 2009, 9: 9513-9532.

Parker C. O., Lanyon Y. H., Manning M., Arrigan D. W. M., Tothill I. E. Electrochemical immunochip sensor for aflatoxin M1 detection. *Analytical Chemistry*, 2009, 81: 5291-5298.

Patel P. D. Biosensors for measurement of analytes implicated in food safety: a review. *TrAC Trends in Analytical Chemistry*, 2002, 21: 96-115.

Pease R. F., Chou S. Y. Lithography and other patterning techniques for future electronics. *Proceedings of the IEEE*, 2008, 96: 248-270.

Pemberton R. M., Cox T., Tuffin R., Sage I., Drago G. A., Biddle N., Griffiths J., Pittson R., Johnson G., Xu J., Jackson S. K., Kenna G., Luxton R., Hart J. P. Microfabricated glucose biosensor for culture welloperation. *Biosensors and Bioelectronics*, 2013, 42: 668-677.

Poirier G. E., Tarlov M. J., Rushmeier H. E. Two-dimensional liquid phase and the px. sqroot. 3 phase of alkanethiol self-assembled monolayers on Au (111). *Langmuir*, 1994, 10: 3383-3386.

Qi H., Wang C., Cheng N. Label-free electrochemical impedance spectroscopy biosensor for the determination of human immunoglobulin G. *Microchimica Acta*, 2010, 170: 33-38.

Qin D., Xia Y., Whitesides G. M. Soft lithography for micro- and nanoscale patterning. *Nature Protocols*, 2010, 5: 491-502.

Queirós R. B., de-los-Santos-Álvarez N., Noronha J. P., Sales M. G. F. A label-free DNA aptamer-based impedance biosensor for the detection of *E. coli* outer membrane proteins. *Sensors and Actuators* B. 2013, 181: 766-772.

Radke S. M., Alocilja E. C. A high density microelectrode array biosensor for detection of *E. coli* O157:H7. *Biosensors and Bioelectronics*, 2005, 20: 1662-1670.

Radke S. M., Alocilja E. C. Design and fabrication of a microimpedance biosensor for bacterial detection. *Sensors Journal, IEEE*, 2004, 4: 434-440.

Rahman A. R. A., Justin G., Guiseppi-Elie A. Towards an implantable biochip for glucose and lactate monitoring using microdisc electrode arrays (MDEAs). *Biomedical Microdevices*, 2009, 11: 75-85.

Rameil S., Schubert P., Grundmann P., Dietrich R., Märtlbauer E. Use of 3-(4-hydroxyphenyl) propionic acid as electron donating compound in a potentiometric aflatoxin M1-immunosensor. *Analytica Chimica Acta*, 2010, 661: 122-127.

Rana S., Page R. H., McNeil C. J. Impedance spectra analysis to characterize interdigitated electrodes as electrochemical sensors. *Electrochimica Acta*, 2011, 56: 8559-8563.

Reynaerts D., Heeren P.-H. s., Van Brussel H.. Microstructuring of silicon by electro-discharge machining (EDM)-part I: theory. *Sensors and Actuators* A. 1997, 60: 212-218.

Reyntjens S., Puers R. A review of focused ion beam applications in microsystem technology. *Journal of Micromechanics and Microengineering*, 2001, 11: 287-300.

Ricci F., Volpe G., Micheli L., Palleschi G. A review on novel developments and applications of immunosensors in food analysis. *Analytica Chimica Acta*, 2007, 605: 111-129.

Ricciardi C., Castagna R., Ferrante I., Frascella F., Luigi Marasso S., Ricci A., Canavese G., Lorè A., Prelle A., Gullino Lodovica M., Spadaro D. Development of a microcantilever-based immunosensing method for mycotoxin detection. *Biosensors and Bioelectronics*, 2013, 40: 233-239.

Richard J. L. Some major mycotoxins and their mycotoxicoses—An overview. *International Journal of Food Microbiology*, 2007, 119: 3-10.

Rogers K. R., Mascini M. Biosensors for field analytical monitoring. *Field Analytical Chemistry and Technology*, 1999, 2: 317-331.

Ronkainen N. J., Halsall H. B., Heineman W. R. Electrochemical biosensors. *Chemical Society Reviews*, 2010, 39: 1747-1763.

Ronkainen-Matsuno N. J., Thomas J. H., Halsall H. B., Heineman W. R. Electrochemical immunoassay moving into the fast lane. *TrAC Trends in Analytical Chemistry*, 2002, 21: 213-225.

Rossi L., Quach A., Rosenzweig Z. Glucose oxidase–magnetite nanoparticles bioconjugate for glucose sensing. *Analytical and Bioanalytical Chemistry*, 2004, 380: 606-613.

Sadeghi N., Oveisi M. R., Jannat B., Hajimahmoodi M., Bonyani H., Jannat F. Incidence of aflatoxin M1 in human breast milk in Tehran, Iran. *Food Control*, 2009, 20: 75-78.

Sassolas A., Blum L. J., Leca-Bouvier B. D. Immobilization strategies to develop enzymatic biosensors. *Biotechnology Advances*, 2012, 30: 489-511.

Sharma A., Rogers K. R. Biosensors. *Materials Science and Technology*, 1994, 5: 461-472.

Shelton D. R., Karns J. S., Higgins J. A., Van Kessel J. A. S., Perdue M. L., Belt K. T., Russell-Anelli J., DebRoy C. Impact of microbial diversity on rapid detection of enterohemorrhagic Escherichia coli in surface waters. *FEMS Microbiology Letters*, 2006, 261: 95-101.

Shen G., Cai C., Yang J. Fabrication of an electrochemical immunosensor based on a gold–hydroxyapatite nanocomposite–chitosan film. *Electrochimica Acta*, 2011, 56: 8272-8277.

Shephard G. S., Berthiller F., Burdaspal P.A., Crews C., Jonker M. A., Krska R., MacDonald S., Malone R. J., Maragos C., Sabino M., Solfrizzo M., Van Egmond H. P., Whitaker T. B. Developments in mytoxin analysis: an update for 2010–2011. *World Mycotoxin Journal*, 2012, 1: 3-30.

Shervedani R. K., Hatefi-Mehrjardi A. Electrochemical characterization of directly immobilized glucose oxidase on gold mercaptosuccinic anhydride self-assembled monolayer. *Sensors and Actuators* B. 2007, 126: 415-423.

Shim, N. Y., Bernards D. A. All-plastic electrochemical transistor for glucose sensing using a ferrocene mediator. *Sensors*, 2009, 9: 9896-9902.

Skládal P. Advances in electrochemical immunosensors. *Electroanalysis*, 1997, 9: 737-745.

Song J. M., Vo-Dinh T. Miniature biochip system for detection of *Escherichia coli* O157: H7 based on antibody-immobilized capillary reactors and enzyme-linked immunosorbent assay. *Analytica Chimica Acta*, 2004, 507: 115-121.

Spinella K., Mosiello L., Palleschi G., Vitali F. Development of a QCM (Quartz Crystal Microbalance) Biosensor to the Detection of Aflatoxin B1. *Open Journal of Applied Biosensor*, 2013, 2: 112-119.

Steude A., Schmidt S. An electrode array for electrochemical immuno-sensing using the example of impedimetric tenascin C detection. *Lab on a Chip*, 2011, 11: 2884-2892.

Suárez G., Keegan N., Spoors J. A., Ortiz P., Jackson R. J., Hedley J., McNeil C. J. Biomolecule patterning on analytical devices: a microfabrication-compatible approach. *Langmuir*, 2010, 26: 6071-6077.

Suni I. I. Impedance methods for electrochemical sensors using nanomaterials. *TrAC Trends in Analytical Chemistry*, 2008, 27: 604-611.

Tang J., Gao M., Deng C., Zhang X. Recent development of multi-dimensional chromatography strategies in proteome research. *Journal of Chromatography* B. 2008, 866: 123-132.

Taylor R. F., Marenchic I. G., Spencer R. H. Antibody-based and receptor based biosensors for detection and process control. *Analytica Chimica Acta*, 1991, 249: 67-70.

Temiz Y., Ferretti A., Leblebici Y., Guiducci C. A comparative study on fabrication techniques for on-chip microelectrodes. *Lab on a Chip*, 2012, 12: 4920-4928.

Thevenot D. R., Toth K., Durst R. A., Wilson G. S. Electrochemical Biosensors: Recommended Definitions and Classification. *Pure and Applied Chemistry*, 1999, 71: 2333-2348.

Thevenot D. R., Toth K., Durst R. A., Wilson G. S. Electrochemical biosensors: recommended definitions and classification. *Biosensors and Bioelectronics*, 2001, 16: 121-131.

Thomas J. H., Kim S. K., Hesketh P. J., Halsall H. B., Heineman W. R. Microbead-based electrochemical immunoassay with interdigitated array electrodes. *Analytical Biochemistry*, 2004, 328:113-122.

Thompson M., Ellison S. L. R., Wood R. Harmonized guidelines for single-laboratory validation of methods of analysis (IUPAC Technical Report). *Pure and Applied Chemistry*, 2002, 74: 835-855.

Tomazelli Coltro W. K., Fracassi da Silva J. A., Carrilho E. Rapid prototyping of polymeric electrophoresis microchips with integrated copper electrodes for contactless conductivity detection. *Analytical Methods*, 2011, 3: 168-172.

Tong S., Jin H., Zheng D., Wang W., Li X., Xu Y., Song W. Investigations on copper–titanate intercalation materials for amperometric sensor. *Biosensors and Bioelectronics*, 2009, 24: 2404-2409.

Towe B. C., Pizziconi V. B. A microflow amperometric glucose biosensor. *Biosensors and Bioelectronics*, 1997, 12: 893-899.

Tsouti V., Boutopoulos C., Zergioti I., Chatzandroulis S. Capacitive microsystems for biological sensing. *Biosensors and Bioelectronics*, 2011, 27: 1-11.

Turner A. P. F. Biochemistry: Biosensors – Sense and Sensitivity. *Science*, 2000, 290: 1315-1317.

Tweedie M., Subramanian R., Lemoine P., Craig I., McAdams E. T., McLaugh-lin J. A., Maccraith B., Kent N. Fabrication of impedimetric sensors for label-freepoint-of-care immunoassay cardiac marker systems, with passive microfluidicdelivery. *Conference Proceedings–IEEE Engineering in Medicine and Biology Society*, 2006, 4610-4614.

Valera E., Ramón-Azcón J., Rodríguez Á. Impedimetric immunosensor for atrazine detection using interdigitated μ-electrodes (IDμE's). *Sensors and Actuators* B. 2007, 125: 526-537.

Van der Gaag B., Spath S., Dietrich H., Stigter E., Boonzaaijer G., van Osenbruggen T., Koopal K. Biosensors and multiple mycotoxin analysis. *Food Control*, 2003, 14: 251-254.

Van Egmond H. P. Worldwide regulations for mycotoxins. Mycotoxins and Food Safety, Kluwer Academic/Plenum Publishing: New York, 2002, 504: 257-269.

Van Emon J. M. Immunoassay and Other Bioanalytical Methods, ed. CRC Press, Boca Raton, FL, USA, 2007.

Varshney M., Li Y. Interdigitated array microelectrode based impedance biosensor coupled with magnetic nanoparticle–antibody conjugates for detection of *Escherichia coli* O157:H7 in food samples. *Biosensors and Bioelectronics*, 2007, 22: 2408-2414.

Vig A., Muñoz-Berbel X., Radoi A., Cortina-Puig M., Marty J.-L. Characterization of the gold-catalyzed deposition of silver on graphite screen-printed electrodes and their application to the development of impedimetric immunosensors. *Talanta*, 2009, 80: 942-946.

Vig A., Radoi A., Mu˜noz-Berbel X., Gyemant G., Marty J-L. Impedimetric aflatoxin M1 immunosensor based on colloidal gold and silver electrodeposition. *Sensors and Actuators* B. 2009, 138: 214-220.

Vo-Dinh T., Cullum B. Biosensors and biochips: advances in biological and medical diagnostics. *Fresenius' Journal of Analytical Chemistry*, 2000, 366: 540-551.

Vu X. T., Eschermann J. F. Top-down processed silicon nanowire transistor arrays for biosensing. *Physica Status Solidi*, 2009, 206: 426-434.

Wagner C., Harned N. EUV lithography: Lithography gets extreme. *Natutre Photonics*, 2010, 4: 24-26.

Wanekaya A. K., Chen W., Mulchandani A. Recent biosensing developments in environmental security. *Journal of Environmental Monitoring*, 2008, 10: 703-712.

Wang J. Electrochemical biosensors: towards point-of-care cancer diagnostics. *Biosensors and Bioelectronics*, 2006, 21: 1887-1892.

Wang J. Analytical Electrochemistry. John Wiley & Sons, VCH, Hoboken, New Jersey, USA, 2006.

Wang J. Electrochemical glucose biosensors. *Chemical Reviews*, 2008, 108: 814-825.

Wang J., Carmon K. S., Luck L. A., Suni I. Electrochemical Impedance Biosensor for Glucose Detection Utilizing a Periplasmic *E. coli* Receptor Protein. *Electrochemical and Solid State Letters*, 2005, 8: H61-H64.

Wang L., Xian-Xue G. Biomolecule-functionalized magnetic nanoparticles for flow-through quartz crystal microbalance immunoassay of aflatoxin B1. *Bioprocess and Biosystems Engineering*, 2009, 32: 109-116.

Wang Y., Dostálek J., Knoll W. Long range surface plasmon-enhanced fluorescence spectroscopy for the detection of aflatoxin M1 in milk. *Biosensors and Bioelectronics*, 2009, 24: 2264-2267.

Wang Y., Liu X., Xiao C., Wang Z., Wan J., Xiao H., Cui L., Xiang Q., Yue T. HPLC determination of aflatoxin M1 in liquid milk and milk powder using solid phase extraction on OASIS HLB. *Food Control*, 2012, 28: 131-134.

Wang Y., Xu H., Zhang J., Li G. Electrochemical sensors for clinic analysis. *Sensors*, 2008, 8: 2043-2081.

Wu Z.-S., Li J.-S., Deng T., Luo M.-H., Shen G.-L., Yu R.-Q. A sensitive immunoassay based on electropolymerized films by capacitance measurements for direct detection of immunospecies. *Analytical Biochemistry*, 2005, 337: 308-315.

Xue Q., Bian C., Tong J., Sun J., Zhang H., Xia S. Fabrication of a 3D interdigitated double-coil microelectrode chip by MEMS technique. *Microchimica Acta*, 2012, 177: 491-496.

YanáChang Y., NgoráAu S. W. Measuring rapid kinetics by a potentiometric method in droplet-based microfluidic devices. *Chemical Communications*, 2012, 48: 1601-1603.

Yang L., Bashir R. Electrical/electrochemical impedance for rapid detection of foodborne pathogenic bacteria. *Biotechnology Advances*, 2008, 26:135-150.

Yang L., Guiseppi-Elie A. Impedimetric biosensors for nano and microfluidics, in Encyclopedia of microfluidics and nanofluidics, ed. by D. Li. Springer-Verlag GmbH, Berlin Heidelberg, 2008, 2: 811-823.

Yang L., Guiseppi-Wilson A., Guiseppi-Elie A. Design considerations in the use of interdigitated microsensor electrode arrays (IMEs) for impedimetric characterization of biomimetic hydrogels. *Biomedical Microdevices*, 2011, 13: 279-289.

Yang L., Li Y., Erf G. F. Interdigitated Array Microelectrode-Based Electrochemical Impedance Immunosensor for Detection of *Escherichia coli* O157: H7. *Analytical Chemistry*, 2004, 76: 1107-1113.

Yang L., Li Y., Griffis C. L., Johnson M. G. Interdigitated microelectrode (IME) impedance sensor for the detection of viable *Salmonella typhimurium*. *Biosensors and Bioelectronics*, 2004, 19: 1139-1147.

Yang L., Ruan C., Li Y. Detection of viable Salmonella typhimurium by impedance measurement of electrode capacitance and medium resistance, *Biosensors and Bioelectronics*, 2003, 19: 495-502.

Young-Min S., Gamzina D., Barnett L.R., Yaghmaie F., Baig A., Luhmann N. C. UV Lithography and Molding Fabrication of Ultrathick Micrometallic Structures Using a KMPR Photoresist. *Journal of Microelectromechanical Systems*. 2010, 19: 683-689.

Zaijun L., Zhongyun W., Xiulan S., Yinjun F., Peipei C. A sensitive and highly stable electrochemical impedance immunosensor based on the formation of silica gel–ionic liquid biocompatible film on the glassy carbon electrode for the determination of aflatoxin B1 in bee pollen. *Talanta*, 2010, 80: 1632-1637.

Zamfir L.-G., Geana I., Bourigua S., Rotariu L., Bala C., Errachid A., Jaffrezic-Renault N. Highly sensitive label-free immunosensor for ochratoxin A based on functionalized magnetic nanoparticles and EIS/SPR detection. *Sensors and Actuators* B. 2011, 159: 178-184.

Zou Z., Kai J., Rust M. J., Han J., Ahn C. H. Functionalized nano interdigitated electrodes arrays on polymer with integrated microfluidics for direct bio-affinity sensing using impedimetric measurement. *Sensors and Actuators* A. 2007, 136: 518-526.

List of Publications

Patent applications

1. Co-inventor in Indian Patent Application "A device for analysis of aflatoxins", Application No. 1203/MUM/2013, Ownership-ICAR, Govt. Of India. Inventors: Sunil Bhand, Sudhir Chandra, Hardik Pandya, Gautam Bacher, Lizy Kanungo (output from chapter 4)
2. Co-inventor in PCT International Application "A device for analysis of aflatoxins", Application (PCT/IN2014/000176), Ownership-ICAR, Govt. Of India. Inventors: Sunil Bhand, Sudhir Chandra, Hardik Pandya, Gautam Bacher, Lizy Kanungo (Output from chapter 4).

List of publications counted in thesis

1. Bacher G., Pal S., Kanungo L., Bhand S. A label-free silver wire based impedimetric immunosensor for detection of aflatoxin M1 in milk. *Sensors and Actuators* B. 2012, 168: 223-230. (Output from chapter 3).
2. Bacher G.*, Kanungo L.*, Bhand S. Miniaturized label-free impedimetric immunosensor for analysis of Aflatoxin B1 in peanut. *Sensing Technology* (ICST), *Sixth International Conference* on, IEEE. 2012, 29-35. (Output from chapter 3).
3. Kanungo L., Bacher G., Bhand S. Flow-Based Impedimetric Immunosensor for Aflatoxin Analysis in Milk Products. *Applied Biochemistry and Biotechnology*, 2014, 174:1157-1165. (Output from chapter 3).
4. International Application Published under the Patent Cooperation Treaty PCT: A device for detection and analysis of Mycotoxins", Application (PCT/IN2014/000176), Ownership-ICAR, Govt. Of India. Inventors: Sunil Bhand, Sudhir Chandra, Hardik Pandya, Gautam Bacher, Lizy Kanungo , WO/2014/155391, October 02, 2014. (Output from chapter 4).
5. Mishra G. K.*, Bacher G.*, Roy U., Bhand S. A label free impedemetric immunosensor for detection of *Escherichia coli* in water. *ScienceJet*, 2015,4: 76 (Output from chapter 3).
6. Bacher G.*, Dhamgaye V.*, Pal S.*, Lodha G.S., Bhand S. A miniaturized reusable biochip device-application in glucose biosensing. Manuscript to be submitted (Output from chapter 5).

[#] Authors with equal contribution

Participated in Conferences and Workshop

1. Presented a poster at at 2nd International Conference on Bio-Sensing Technology organized by Elsevier, Oct 10- 12, 2011, Amsterdam, The Netherlands, entitled "A simple and sensitive impedimetric biosensor for analysis of Aflatoxin M1" Gautam Bacher, Souvik Pal, Sunil Bhand.

2. Oral Presentation at 6th International Conference on Sensing Technology ICST 2012" with focus on sensors in agriculture organized by CDAC Kolkata and Massay University, New Zealand, Dec 18-21, 2012 Kolkata, India, entitled "Miniaturized label-free impedimetric immunosensor for analysis of Aflatoxin B1 in peanut" Gautam Bacher, Lizy Kanungo, Sunil Bhand.

3. Presented a poster at Indo- UK International Workshop On Advanced Materials And Their Applications In Nanotechnology (AMAN 2014) Organized by BITS Pilani, KK Birla Goa Campus (May 17- 19, 2014) entitled "Impedemetric immunosensor for bacterial detection" Geetesh K. Mishra, Gautam Bacher, Utpal Roy and Sunil Bhand (2nd prize in poster presentation).

4. Attended BITSSA Global Meet and presented a poster on "A field portable device for analysis of Aflatoxin M1 in milk'', 3-5th January 2014 at BITS Hyderabad**.**

5. Attended SERC School on Electrochemical Systems, 16-28 May, 2011, IIT Bombay.

6. Attended the ISEAC International Symposium cum workshop on Electrochemistry organized by Indian Society for Electroanalytical Chemistry, Dec. 7-10th 2011, Goa.

7. Attended the National Symposium cum workshop on Carbon materials, Jan 20-21, 2012, Govt. College of Arts, science & Commerce, Sanquelim, Goa.

8. Attended the Fifth SERC School on "New Developments in Microfabrication with Focus on Synchrotron Radiation based Deep X-ray Lithography" October 29-November 03, 2012 Raja Ramanna Centre for Advanced Technology (RRCAT), Indore.

9. Attended interaction meeting on “x-ray lithography and microfabrication” Dec 5-6, 2013 at Raja Ramanna Centre for Advanced Technology (RRCAT), Indore.

Abstract accepted in conferences

1. L. Kanungo, G. Bacher, S. Pal, S. Bhand. Ultrasensitive Micro-Biosensors for Analysis of Aflatoxins. Emerging Technologies from micro to nano (ETMN-2013). BITS, Pilani-K.K. Goa Campus.

2. Abstract accepted for oral presentation: Geetesh K Mishra, Gautam Bacher, Utpal Roy, and Sunil Bhand. A micro biosensor for label-free detection of *Salmonella* in water at national conference on Nano Functional Materials (NFM2014), BITS, Pilani India, 2014.

Brief Biography of the candidate

Name	Gautam G. Bacher
Date of Birth	21-07-1975
Education	M. Tech (Instrumentation), 2003
	NIT Kurukshetra, Kurukshetra (HR), India
	MBA (Finance & Marketing), 2001
	Nagpur University, Nagpur (M.S.) India
	BE (Electronics and Power), 1997
	Nagpur University, Nagpur (M.S.) India
Email ID	ggb@goa.bits-pilani.ac.in

Research Publications

01 Indian Patent filed, 01 PCT International Filed, 04 publications in international journal, 01 manuscript submitted.

Work Experience

1. Working as a Lecturer, Department of Electrical, Electronics & Instrumentation Engineering, BITS Pilani K K Birla Goa Campus, Goa (April 2007 till date).
2. Worked as Lecturer, Department of Electrical Engineering, St.Vincent Palloti college of Engineering, Nagpur (MS) (Feb 2005 to March 2007).
3. Worked as Lecturer, Department of Electrical Engineering Rajiv Gandhi College of Engineering Research and Technology, Chandrapur (MS) (Dec 1997 to July 2001 and July 2003 to Jan. 2005)

Award and Honors

2nd Prize in poster presentation at Indo- UK International Workshop on Advanced Materials and Their Applications in Nanotechnology (AMAN 2014).

Brief Biography of the Supervisor

Name	Prof. Sunil Bhand
Date of Birth	17.03.1969
Present Position	Professor, Department of Chemistry,
	BITS, Pilani-KK Birla Goa Campus
Address	C-201 BITS, Pilani-KK Birla Goa Campus
	NH17B Bypass, Zuari Nagar Goa 403726 India
Email	sunilbhand@goa.bits-pilani.ac.in, sunil17_bhand@yahoo.com
Education	Ph.D., 1996
	M.Sc., 1990 (First in University Merit)

Post-Doctoral Experience

Department of Pure and Applied Biochemistry
Lund University Sweden 2001-2002,
Short term visits 2003, 2004, 2005, 2007, 2008

No. of Sponsored Research Projects

(a) Completed projects

i. Joint Indo-Swedish Project on Biosensors for Environmental analysis 2003-2005 funded by Swedish Research Council (Prof. B. Danielsson and Prof. Sunil Bhand as joint PIs) 35 lakhs.

ii. CSIR Project 2006-2009 on biosensors for analysis of pesiticides in sea water 14.6 lakhs.

iii. Consortium PI for NAIP, ICAR New Delhi funded project on "Development of biosensors and micro techniques for analysis of pesticide residues, aflatoxin, heavy metals and bacterial contamination in milk.729 lakhs, in collaboration with IITD, NDRI and PU Patiala.

iv. Consortium Co-PI, NAIP project on "Detection and mitigation of dairy pathogens and detection of adulterants using chemical biology" 45 lakhs.

(b) Ongoing Project

i. Multi-institute Consortium Project entitled "Imprinted polymer for sensing and removal of selected antibiotic and pesticide residue" Project no. NFBSFARA/PHT-4007/2013-14. Funding Agency: National Funds for Basic and Strategic Research in Frontier Areas of Agricultural Science, ICAR, New Delhi, 125.25511 Lakh.

ii. Centre of Research Excellence in Water, Waste water and Energy Management (CORE WWEM) funded by BITS, Pilani. Subproject title: Development of Field Deployable biosensor for analysis of bacterial contaminant in potable water, Rs. 41 Lakh.

Honors and awards

i. Invited as Opponent to a Ph.D. Thesis for Linkoeping University Sept. 2011.

ii. Best Poster award "Biosensors for arsenic analysis" 7th Intl Conference on Biogeochemistry of trace elements 2003 Uppsala Sweden.

iii. UV Rao memorial awards for young scientists by Indian Chemical Society 1998.

Publications

i. 06 Patents (03 International including 02 PCT and 01 Australian and 03 Indian) and 37 publications in international journals.

ii. Membership of societies: Affiliate member IUPAC since 2000 IAEAC Switzerland, AAAS, USA, 2012.

Reviewer for international journals

Biosensors and Bioelectronics, Analytical Letters, Int Journal of Env Anal Chemistry, Applied Biochemistry and Biotechnology, J Agri food Chemistry.

No of Ph.D. Students

Completed 03, Registered 06,

No of Conferences organized: 03

Appendix iv

Reprint of Publications

Sensors and Actuators B 168 (2012) 223–230

Contents lists available at SciVerse ScienceDirect

Sensors and Actuators B: Chemical

journal homepage: www.elsevier.com/locate/snb

A label-free silver wire based impedimetric immunosensor for detection of aflatoxin M1 in milk

Gautam Bacher[a,b,1], Souvik Pal[a,1], Lizy Kanungo[a], Sunil Bhand[a,*]

[a] Biosensor Lab., Department of Chemistry, BITS, Pilani-K.K. Birla Goa Campus, Goa 403726, India
[b] Department of EEE&I, BITS, Pilani-K.K. Birla Goa Campus, Goa 403726, India

ARTICLE INFO

Article history:
Received 5 February 2012
Received in revised form 31 March 2012
Accepted 4 April 2012
Available online 11 April 2012

Keywords:
Immunosensor
Aflatoxin M1
Silver wire electrode
Electrochemical impedance spectroscopy
Label-free detection
Milk

ABSTRACT

A highly sensitive and selective label-free impedimetric immunosensor based on silver (Ag) wire electrode for the detection aflatoxin M1 (AFM1) in milk is presented. The sensor was constructed by functionalizing Ag wire coupled with selective monoclonal antibodies of AFM1 through self assembled monolayers. The antigen–antibody interaction was quantified by measuring impedance in the frequency range (1–100 Hz) at 10 mV applied ac potential. A linear working range (6.25–100 pg mL^{-1}) for AFM1 was obtained with 20 min analysis time. The sensor sensitivity was found to be about 2.1% impedance change per decade with limit of quantitation 6.25 pg mL^{-1} and limit of detection 1 pg mL^{-1}. Good recoveries were obtained with SD = 1.13 and R^2 = 0.982 in spiked milk samples. The proposed method is useful for sensitive analysis of AFM1 in milk.

1. Introduction

Aflatoxins are highly toxic, mutagenic, carcinogenic, and teratogenic compounds [1–3]. The consumption of milk and milk products by human population is quite high, particularly in infants and children thereby increasing the risk of exposure to aflatoxin M1 (AFM1). Evidence of hazardous human exposure to AFM1 through dairy products has been shown by several investigators [4–6]. Recent review report confirms the immense interest in the development of enzyme linked immunosorbent assay (ELISA) for analysis of AFM1 in milk and milk products. Recently, the need for ultra sensitive techniques for the special requirements such as those in infant food was highlighted with relatively lower analysis time for AFM1 [7].

According to the US Food and Drug Administration (USFDA), AFM1 in milk should not exceed 500 pg mL^{-1}. AFM1 level in milk has been set more restrictively to 50 pg mL^{-1} by the European Union (EU) for adult consumption. In baby-food products this level should not exceed 25 pg mL^{-1}. Rastogi et al. reported that out of 87 samples of milk analyzed, 87.3% were found to be contaminated with AFM1. In India, almost 99% of the contaminated milk samples exceeded the European Community/Codex Alimentarius recommended limits and 9% samples exceeded the prescribed limit of USFDA regulations [8].

For better control of AFM1 in milk, various measurement techniques have been developed. AFM1 is generally quantified by ELISA [9], thin layer chromatography (TLC) [10] and high performance liquid chromatography (HPLC) [11]. These methods have some limitations such as low sensitivity, detection limit and long analysis time [12]. In addition to conventional techniques, surface plasmon resonance (SPR) [13] and quartz crystal microbalance (QCM) [14] based biosensors have also been reported for analysis of aflatoxins.

Among the reported biosensors, electrochemical impedance spectroscopy (EIS) has emerged as sensitive techniques for analysis of AFM1 [15,16]. The reported biosensors lack portability with high sensitivity for AFM1 analysis in milk.

In EIS, traditionally, macro sized metal rods or wires were used as electrodes immersed in the medium to measure impedance [17,18]. Felice et al. reported a capacitance method for quantification of bacterial content in milk using two identical stainless steel electrodes by measuring capacitance at 1 kHz. EIS is suitable to analyze the electrical properties of the modified electrode, i.e. when an antibody coupled to the electrode reacts with the antigen of interest [19]. In such a case, the adsorption/desorption process was the rate-determining step. This step is controlled through the appropriate choice of electrical potential. This confirmed that the antigen–antibody interaction was largely influenced by the applied potential. EIS is also a suitable technique to understand the

* Corresponding author. Tel.: +91 832 2580332; fax: +91 832 2557030/33.
E-mail addresses: sunil17_bhand@yahoo.com, sunilbhand@bits-goa.ac.in (S. Bhand).
[1] These authors contributed equally to this work.

0925-4005/$ – see front matter © 2012 Elsevier B.V. All rights reserved.
http://dx.doi.org/10.1016/j.snb.2012.04.012

adsorption and charge transfer process for modified electrode [20]. In an EIS technique, an equivalent circuit of the electrode set-up is used to curve fit the experimental data and extract the necessary information about the electrical parameters responsible for the impedance change [21].

Self-assembled monolayers (SAMs) provide a means for the molecular design on a bio-inert surface with specific functions. SAMs provide a promising basis for immobilizing biomolecules via the functional group [22]. More significantly, it is possible to apply different functionalized SAMs to cross-link with targeted molecules. This causes little disruption or destabilization of the SAMs selected in specific applications [23–26]. SAMs with gold nanoparticles have been reported to improve the sensitivity of an impedimetric sensor [27].

The purpose of the present study is to demonstrate a practical and highly sensitive technique for ultra sensitive detection of AFM1 in milk with short analysis time. The presented impedimetric immunosensor is based on functionalized Ag wire electrode. Primary monoclonal antibody (mAb) specific to AFM1 was attached on the Ag wire through SAMs of 11-marcaptoundecanoic acid (11-MUA). This imparts high specificity to the biosensor. The Ag wire set-up provides additional features such as storage, ease of handling and portability. The impedance change during antigen–antibody interaction was measured using EIS. After simple pre-treatment of milk samples, the immunosensor was optimized with regard interferences from milk matrix. Present work demonstrates a simple, cost effective, label-free impedimetric immunosensor for detection of AFM1 in milk with the help of two electrode system. The immunosensor showed an astoundingly low limit of detection (1 pg mL^{-1}) for AFM1 with a short analysis time of 20 min. In the presented biosensor set-up, the volume reduction has also been achieved through custom made glass cell. The method with pre-functionalized electrodes is usable under field conditions.

2. Materials and methods

2.1. Materials and instrumentation

All the chemicals used were of analytical grade and were used as received. Ag wire (diameter = 0.25 mm) was procured from ACROS Organics, USA. Anti AFM1 fractionated antiserum primary monoclonal antibody (mAb) raised from rat, Anti-rabbit (Rat) Fluorescein isothiocyanate (FITC) conjugated secondary antibody (pAb-FITC) were purchased from AbCam (UK). AFM1 standard, Tween20, 11-mercaptoundecanoic acid (11-MUA), 1-ethyl-3-[3-dimethylaminopropyl] carbodiimide hydrochloride (EDC), N-hydroxy succinimide (NHS), certified reference material ERM-BD 282 (AFM1 in whole milk powder <0.02 μg kg^{-1}) were purchased from Sigma–Aldrich, USA. Ethyl Alcohol 200 proof was purchased from TEDIA, USA. Hydrogen peroxide (H_2O_2) 30% (w/v), acetonitrile (ACN) HPLC grade, di-sodium hydrogen phosphate (Na_2HPO_4), sodium di-hydrogen phosphate (NaH_2PO_4) from MERCK (Germany) and sodium hypochlorite (4%) solution were purchased from Fisher Scientific (India). For sample handling, micropipettes (eppendorf®, Germany) were used. Centrifugation of milk sample was done by minispin (eppendorf®, Germany). Shaking and filtration of the samples were done by Spinix shaker (Tarsons, India). For the handling of AFM1 standard solution, glove box (Cole Parmer, USA) was used. For preparing all the solutions, water produced in a Milli-Q system (Millipore, Beford, MA, USA) was used. Certified ultra high pure nitrogen (99.9%), pH meter (Seven Multi Mettler Toledo, 8603, Switzerland) were used. Fourier Transform InfraRed (FT-IR) spectra were recorded using FT/IR-4100typeA (JASCO, Japan) with attenuated total reflectance (ATR) attachment ATR PRO450-S. Fluorescence images were taken on upright microscope (BX-51Olympus, Japan). Impedance measurements were carried out using IVIUM CompactStat impedance analyzer, Netherland. Surface morphology of the electrode was characterized by using a JEOL (JSM 6560 LV) Scanning Electron Microscope (SEM) operated at an accelerating voltage of 20 kV.

2.2. Preparation of buffers

0.01 M phosphate buffered saline (PBS) was prepared by dissolving appropriate amount of Na_2HPO_4, NaH_2PO_4 containing 0.0027 M potassium chloride and 0.137 M sodium chloride. The pH of the buffer was adjusted to 7.4. PBS with Tween20 (PBST) was prepared by adding 0.05% Tween20 (v/v) in PBS for washing purpose. All buffer solutions were stored at 4 °C when not in use.

2.3. Preparation of AFM1 standard solutions

All the AFM1 solutions were prepared in a glove box in a maintained inert N_2 atmosphere. AFM1 stock solution (2.5 μg mL^{-1}) was prepared by dissolving the AFM1 powder in 5% ACN (v/v) in PBS and stored at −20 °C. Working AFM1 standard solutions in the range of 0.25–100 pg mL^{-1} were prepared by diluting the stock with 5% ACN.

2.4. Preparation of AFM1 antibody solutions

The stock solution of rat monoclonal [1C6] mAb, 100 μg (1 mg mL^{-1}) was diluted with 50 μL of de-ionized water. It was divided into two fractions. The first fraction containing 40 μL was stored at −20 °C. From the second fraction, working mAb solutions were prepared by serial dilution such as 1:1000, and 1:2000.

2.5. Preparation of standard milk based matrix

To assess the performance of the immunosensor, the milk samples were prepared by dissolving 1 g of ERM BD 282 whole milk powder (zero level AFM1) in 10 mL of 0.01 M PBS + 0.5% (v/v) Tween20, preheated to 50 °C (as indicated in the protocol). To minimize the matrix effect, the solution was centrifuged for 10 min at 6000 rpm at 4 °C, and the fatty layer was carefully removed and the supernatant was diluted (1/1, v/v) with PBS + 0.5% (v/v) Tween20. For impedance studies, centrifuged milk samples were spiked with fixed amount of AFM1 (100 pg mL^{-1}, 75 pg mL^{-1}, 50 pg mL^{-1}, 25 pg mL^{-1}, 12.5 pg mL^{-1}, 6.25 pg mL^{-1}, 1 pg mL^{-1} and 0.25 pg mL^{-1}).

2.6. Cleaning procedure for the Ag wire electrode surface

Initially the surfaces of the bare Ag wire electrodes was washed ultrasonically in deionized water for 5 min to remove inorganic particles. Following this, the electrodes were immersed into piranha solution (H_2O_2/H_2SO_4, 30/70 v/v) for 30 s. The electrodes were washed with distilled water followed by drying under ultra pure nitrogen stream. This cleaning procedure was repeated before every electrode preparation step.

2.7. Immobilization of mAb on Ag wire electrode

All the glassware were soaked in piranha solution, rinsed thoroughly with distilled water and dried. The mAb was covalently coupled on Ag wire electrode through SAMs as described [27] with some alteration. Firstly, the concentration of 11-MUA was optimized. Then a set of clean Ag wire electrode were immersed overnight in 0.004 M ethanolic solution of 11-MUA under ambient condition. The electrodes covered by SAMs were gently washed with absolute ethanol to remove unbounded 11-MUA residues. The

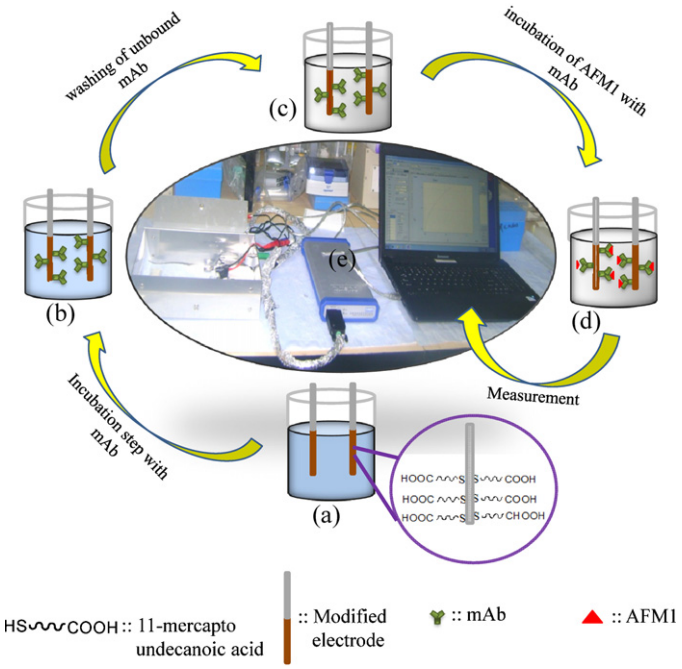

Fig. 1. Schematic illustration of Ag wire electrode based impedimetric AFM1 immunosensor (a–d) with EIS measurement setup (e). (a) 11-MUA modified Ag wire electrode in microcell dipped in 0.01 M PB, pH 7.4; (b) overnight incubation of mAb with modified electrode in PB; (c) washing of unbound mAb attached to electrode; (d) incubation of AFM1 with mAb attached electrode in milk based buffer; (e) experimental set-up of Ag wire based immunosensor.

electrodes were dried with nitrogen stream before use. For coupling the mAb, the carboxyl group of SAMs on modified electrode was activated by 1:1 EDC/NHS (0.1 M each) mixture for 2 h. Subsequently, the electrode was washed with distilled water to remove excess EDC/NHS. Finally, mAb was attached to the electrode by carefully spreading mAb solution (1:16,000 in PBS) over the activated surface followed by overnight incubation at 4 °C. The unused antibody coupled electrodes were washed and stored at 4 °C for future use.

2.8. Experimental set-up

The experimental set-up constitutes a pair of pre-functionalized Ag wire electrode dipped into a custom made glass cell (capacity 750 μl) containing AFM1 spiked milk samples. The operation of presented sensor is based on the pair of Ag wire as an electrical transducer. The Ag wire surface is functionalized with analyte specific antibodies (anti-AFM1 mAb) attached using SAMs to form biological transducer. The binding of the analyte (AFM1) to the biological transducer causes the impedance change. This is measured using two electrode set-up. The electrode set-up and the glass cell were enclosed in a custom made Faraday cage. The schematic of experimental set-up is presented as Fig. 1. In the presented set-up, the two pre-functionalized Ag wire electrodes were dipped in the cell. The functionalized Ag wire electrodes were connected to IVIUM CompactStat impedance analyzer in 4-Electrode mode controlled through software (IVIUM soft) loaded on a laptop computer. In the 4-Electrode mode, the first electrode was configured as working electrode (working and sense electrode combined together) and second electrode was reference electrode (reference and counter combined together). The impedance change caused by antigen–antibody interactions at the electrode surface was measured.

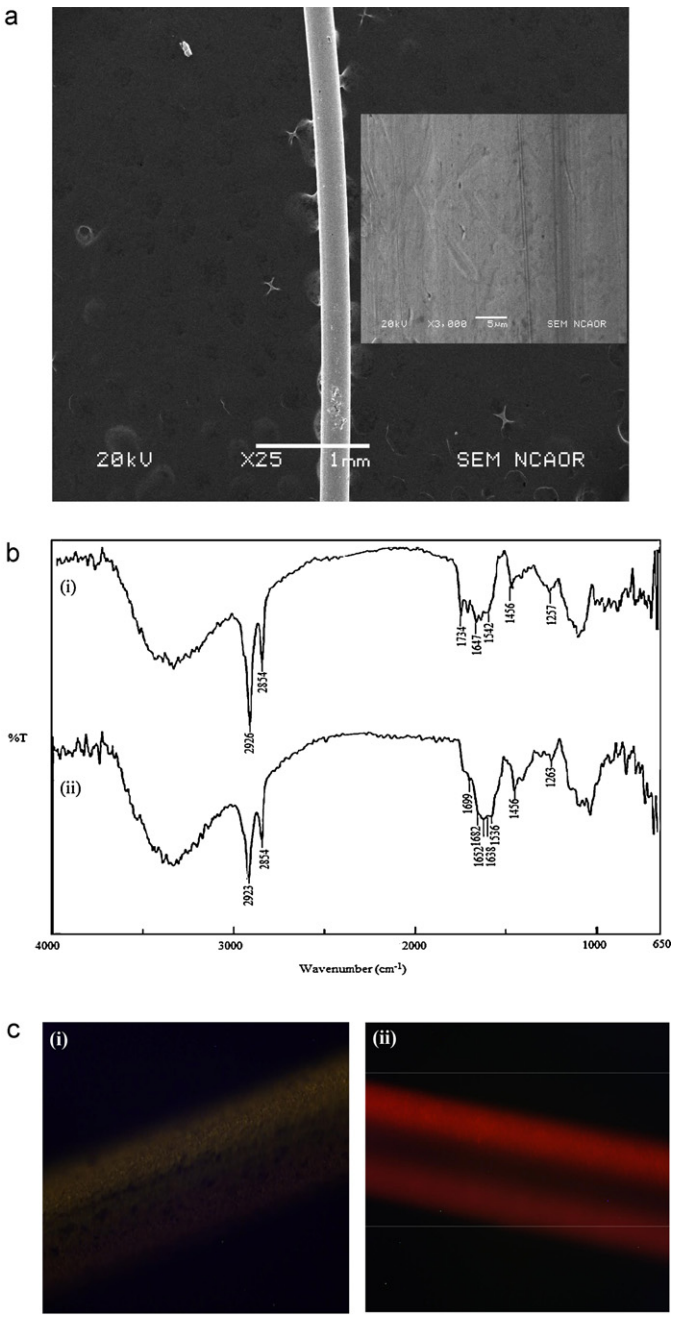

Fig. 2. (a) Shows the SEM micrograph of the bare Ag wire electrode at magnification 25× and (inset) shows the bare clean electrode surface at magnification 3000×. (b) The ATR FT-IR spectrum of (i) the Ag wire treated with 11-MUA (ii) mAb coupled through 11-MUA functionalized Ag wire. Spectra were acquired with 45° angles of incidence using 154 scans at 4 cm^{-1} resolution collected under vacuum conditions. (c) (i) Dark field image of reference wire without mAb, (ii) fluorescence image of the sample wire coupled with mAb; captured using pAb-FITC (λ_{ex} 490 nm/λ_{em} 520 nm).

2.9. Safety caution

While handling the highly toxic AFM1, all necessary precautionary measures must be taken to prevent contamination. As the substance is photosensitive [28,29], solutions should not be exposed to daylight. Safety goggles, respiratory mask and lab coats must be used throughout the experiment. All laboratory glassware and consumables contaminated with AFM1 must be soaked in 4% Sodium hypochlorite.

Piranha solution is highly corrosive in nature; it should be handled with extreme caution using proper safety equipments.

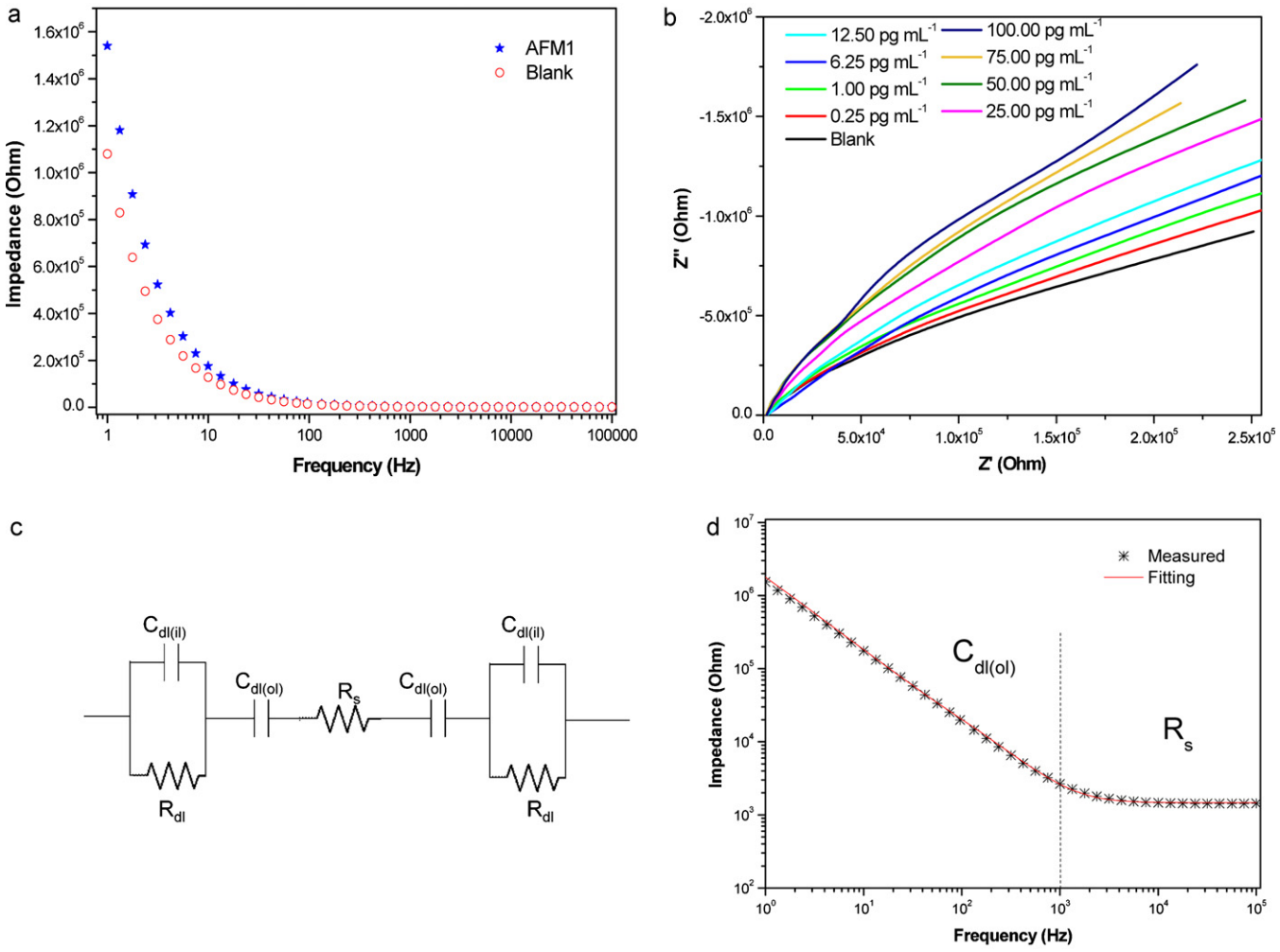

Fig. 3. (a) Impedance spectra of the immunosensor before and after interaction of mAb with 25 pg mL^{-1} AFM1 at room temperature (0.01 M PBS medium, frequency range 1 Hz to 100 KHz at ac potential 10 mV). (b) Analytical signal (Nyquist plot) recordings in presence of different concentration of AFM1 in milk based matrix (EIS: 1 Hz to 100 KHz, 10 mV AC potential). (c) Equivalent circuit used to fit impedance of the AFM1 immunosensor in milk based buffer. R_s: ohmic resistance of medium; $C_{dl(ol)}$: double layer capacitance of outer layer where the antigen–antibody takes place; $C_{dl(il)}$: double layer capacitance of inner layer; R_{dl}: resistance of inner layer which is parallel to $C_{dl(il)}$ representing ion penetration to the SAM. (d) Impedance spectrum in the AFM1 environment with the fitting curve. ac applied potential: 10 mV; frequency range: 1 Hz to 100 KHz.

It should not be stored in closed container. For handling piranha solution, glass containers must be used.

3. Results and discussion

3.1. Optimization of the immunosensor conditions

Since the binding of the AFM1 on the probe directly affects the sensitivity of the immunosensor, the influence of the incubation time on probe impedance was investigated. With increasing incubation time, the impedance response increased and reached to a constant value after 20 min (Supplementary material, Fig. S1). For all the impedance measurements, a sine modulated ac potential of 10 mV was optimized with analysis time 20 min. The influence of applied frequency was also studied in the applied frequency range (1 Hz to 100 KHz). Impedance spectra were recorded as Nyquist plot (real impedance vs. imaginary impedance).

3.2. Surface characterization of Ag wire electrodes

The surface of the Ag wire electrode was characterized by SEM. Fig. 2(a) shows the SEM micrograph of the bare Ag wire electrode at magnification 25× and (inset) shows the bare clean electrode surface at magnification 3000×.

The carbodiimide cross-linking reaction to form the 11-MUA—mAb conjugated structure on Ag wire electrode surfaces was confirmed by ATR FT-IR. The spectra were acquired with 45° angles of incidence using 154 scans at 4 cm^{-1} resolution collected under vacuum conditions. The FT-IR spectra are shown in Fig. 2(b). Fig. 2(b) (i) is the FT-IR spectrum of the Ag wire treated with 11-MUA. It showed C—H stretches in asymmetric and symmetric modes at 2924 cm^{-1} and 2854 cm^{-1} respectively. The C=O stretch at 1734 cm^{-1}, associated with asymmetric (1647 cm^{-1}) and symmetric (1542 cm^{-1}) COO^- stretches, is characteristic of an organic carboxylic acid compound. The additional IR peaks at 1455 cm^{-1} and 1257 cm^{-1} is ascribed to C—H deformation and C—O stretch respectively. Upon immobilization of mAb in Fig. 2(b) (ii) new absorption bands appeared; three IR bands at 1638 cm^{-1}, 1536 cm^{-1}, and 1263 cm^{-1} is ascribed to the absorption by the amide group that links mAb to 11-MUA functionalized Ag wire.

The binding of mAb to Ag wire was also confirmed by fluorescence microscopy. Two functionalized Ag wires (reference wire without mAb and sample wire coupled with mAb) were incubated with pAb-FITC (1:64,000) for 2 h at room temperature. Before excitation, both reference and the sample wire were rinsed with 0.01 M

PBS to remove unbound pAb-FITC. Fig. 2(c) (i) shows fluorescence image of reference and (ii) the sample Ag wire, after excitation. The binding of the pAb-FITC to the mAb of the thiolated Ag wire is clearly distinguished from the fluorescence images.

3.3. EIS study of AFM1 binding on sensor electrode

In the present work, the antigen–antibody interaction of mAb and AFM1 on the Ag wire electrode surface was studied using EIS. EIS is a useful technique to capture such interaction. This interaction results in change of electrical properties such as capacitance and resistance at the electrode surface allowing for label-free biosensing [30]. The capacitance change is commonly used as indicator of antigen–antibody interaction for non-faradaic biosensor [31]. Fig. 3(a) presents the interaction of antigen–antibody on functionalized electrode surface. In the EIS measurement, mAb–AFM1 interactions create a new charged layer as a capacitance that is in series with the double layer capacitance. A decreased double layer capacitance and increased impedance was observed at the lower applied frequency. This confirms that the change in impedance is resulting from binding of the antigen (AFM1). In the higher frequency region (100 Hz to 100 kHz) it was observed that impedance remains constant. A significant change was measurable in the low frequency region (1–100 Hz) with highest impedance change observed at 1 Hz.

3.4. Validation of sensor operation

The sensor was validated for quantitative AFM1 analysis. The EIS data were collected for different concentrations of AFM1 (0.25–100 pg mL^{-1}). Fig. 3(b) represents Nyquist plot obtained for the ac impedance analysis of mAb following exposure to various AFM1 concentrations. It is evident that both real component (Z') and the imaginary component (Z'') of impedance increased with decreasing frequency. The nature of Nyquest plot also confirms that the interaction of mAb and AFM1 has occurred. A significant increase in the impedance was observed in the lower frequency range (1–10 Hz), when AFM1 concentrations were increased from 0.25 to 100 pg mL^{-1}.

3.5. Equivalent circuit analysis and validation

The performance of an electrochemical cell is represented by an equivalent circuit that has the same behaviour as the real cell under a given excitation [32]. The electrical parameters generally used to design an equivalent circuit model for electrochemical curve fitting includes primarily, electrolyte resistance (bulk medium resistance) and double layer capacitance. These factors contribute to the equivalent circuit model representing the experimental impedance data. For two electrode system, a simple equivalent circuit consisting of a resistor and a capacitor in series represent the behaviour of the impedance test when immersed into a conductive medium [33]. Faradaic EIS requires the addition of a redox-active species and DC bias conditions, whereas for non-faradaic impedance spectroscopy, no additional reagent is required [31]. Yang et al. presented a simple electrical equivalent circuit for non-faradaic impedance measurement for detection of *Salmonella typhimurium*. In such a case, non-faradic path is active and no electrochemical reaction on the electrode surface occurs [32]. In the present work, various equivalent circuits were evaluated to fit the obtained data resulting from mAb–AFM1 interaction. The proposed equivalent circuit with best fit results for the electrochemical cell using modified electrode is presented as Fig. 3(c). The presented equivalent circuit indicates a non-faradaic response phenomenon at the electrode–electrolyte interface, since no redox species is present in the solution [34]. The proposed equivalent circuit consists of ohmic resistance of medium (R_s), double layer capacitance of outer layer ($C_{dl(ol)}$), double layer capacitance of inner layer ($C_{dl(il)}$) and resistance of inner layer (R_{dl}). $C_{dl(ol)}$ ($R_{dl}C_{dl(il)}$) represent the two layer structure for each electrode. $C_{dl(ol)}$ represents outer layer of the interface where the mAb–AFM1 interaction takes place. ($R_{dl}C_{dl(il)}$) sub-circuit represent the inner layer of the interface. R_{dl} is parallel to $C_{dl(il)}$, resembles a part of SAMs. R_{dl} is interpreted as the conductivity (by penetrating ions) of the SAMs [34]. Fig. 3(d) shows Bode plot of experimental and fitted impedance spectra of AFM1 binding. Fitting was done by using IVIUM equivalent circuit evaluator and optimized with phase, Z' and Z''. The error weight is equal for each point. It is evident from Fig. 3(d) that for the presented immunosensor, the fitting has good agreement with experimental data, thereby validating the equivalent circuit. The Nyquest plot is also validated with proposed equivalent circuit (Supplementary material, Fig. S2). The binding of AFM1 caused the impedance change at lower frequency of 1 Hz, where R_s and $C_{dl(ol)}$ dominates the overall impedance. The value of impedance at 1 Hz (1.54 MΩ) was over that at 1 kHz (2.66 KΩ).

Since the double layer capacitance $C_{dl(ol)}$ became essential resistive at low frequencies (<1 kHz), it became the main source that contributed to the total impedance, making the impedance value high. The medium resistance is ignored in this case. The double layer capacitive region in which the electrode impedance is detected, is indicated by $C_{dl(ol)}$ of Fig. 3(d). Whereas, in the high frequency range (>1 kHz), the capacitance almost offered no impedance and hence the contribution of the double layer capacitance to the total impedance became zero. Thus, the contribution to the total impedance was medium resistance (R_s) and was independent of the frequency. Therefore, with increasing AFM1 concentration, the change in the medium resistance is detected by impedance measurement at different frequencies. The results of this study confirms that at low frequency (<1 kHz), impedance provides the information of the double layer capacitance of the presented electrode.

3.6. Storage stability of the sensor

The storage stability of Ag wire electrodes functionalized with mAb were tested by storing them at 4 °C in PBS medium. A good consistency on storage of electrodes was observed. For intra batch measurements, the impedance response of the sensor was reduced by 5.8 ± 0.3% (n = 6) when stored for two weeks (measured against 57.62 pg mL^{-1} AFM1; ac potential of 10 mV and applied frequency range from 1 Hz to 100 KHz). This confirms the stability of SAMs procedure as well as antibody coupling.

3.7. Sensor selectivity

The selectivity of the sensor towards AFM1 was studied in the frequency range 1 Hz to 100 KHz using EIS at 10 mV applied potential. In the optimized condition, the response signal for AFM1 binding was measurable in 20 min. The mAb deployed in the experiment is reported to partly cross-react with AFM2 (a structural analogue of AFM1). The cross-reactivity of mAb towards AFM1 and AFM2 was quantified experimentally using the presented set-up at 25 pg mL^{-1}. As against the blank response, it is clearly evident that the sensor is highly selective towards AFM1 as against AFM2 (Supplementary material, Fig. S3). The impedance change for AFM2 was found to be 4% whereas for AFM1 the change was 32% at 1 Hz. The percent impedance change recorded for AFM1 binding was eight fold higher over AFM2 binding.

3.8. Calibration of sensor for AFM1 detection

In immunosensor, the dilution of mAb is usually a compromise over the high dilution required to achieve a low detection limit

Table 1
Comparison of limit of detection in reported electrochemical immunosensor for AFM1. R.S.D (relative standard deviation) % = (standard deviation/mean) × 100; $n = 4$.

Method of detection	Electrode material	Range	LOD achieved	Reference
Impedimetric immunosensor	Silver electrodes (two electrode system)	1–100 pg mL^{-1}	1 pg mL^{-1}	This work
Electrochemical biosensor	Screen printed carbon electrode	5–500 pg mL^{-1}	10 pg mL^{-1}	[15]
Impedimetric aflatoxin M1 immunosensor	Colloidal gold and silver electrodeposition	15–1000 pg mL^{-1}	15 pg mL^{-1}	[16]
Impedimetric aflatoxin M1 biosensor	Gold electrode (three electrode method)	1000–14,000 pg mL^{-1}	1000 pg mL^{-1}	[36]
Electrochemical immunosensor	Screen printed carbon electrode(three electrode method)	39–1000 pg mL^{-1}	39 pg mL^{-1}	[37]

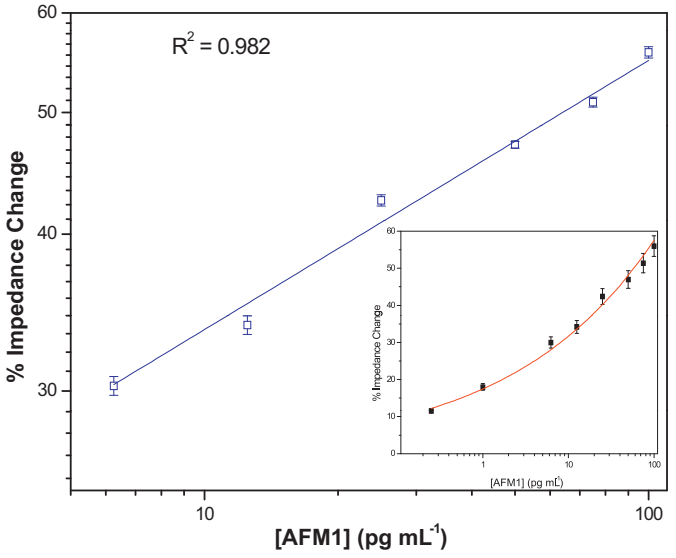

Fig. 4. Calibration curve of label-free Ag wire AFM1 immunosensor for linear range 6.25–100 pg mL^{-1} with SD = 1.13 and $R^2 = 0.982$. LOQ = 6.25 pg mL^{-1} and LOD = 1 pg mL^{-1} with sensitivity about 2.1% impedance change per decade; mAb diluted to 1:16,000 in PB, incubation time 20 min. (Inset) Calibration curve obtained for the whole studied range (0.25–100 pg mL^{-1}); IC_{50} = 57.62 pg mL^{-1}.

and that needed to produce a sufficiently high signal. Thus, various mAb dilutions in the range 1:4000 to 1:64,000 were tested. The impedance change corresponding to 1:16,000 dilution was found optimum. Under this conditions, a 1:16,000 dilution of mAb was shown to give a relative standard deviation of 0.55% for $n = 4$. To assess the performance for the determination of AFM1, a calibration was obtained by incubating various concentrations of AFM1 with 1:16,000 dilution of mAb.

Impedance data was collected for the functionalized electrodes after exposing it to increasing AFM1 concentration (0.25–100 pg mL^{-1}). The specific interaction of mAb and AFM1 gave rise to an overall increase in impedance change from baseline response at the electrode/solution interface. The Nyquist plot of Z' and Z'' components of the impedance at a specific frequency provided information for construction of calibration curve recorded by multiple interrogations (4 replicates each). The % impedance change was calculated corresponding to different concentrations of AFM1.

The linear calibration curve obtained for AFM1 is presented as Fig. 4 and studied range as inset. A linear range for AFM1 detection in the range 6.25–100 pg mL^{-1} was achieved with SD = 1.13 and $R^2 = 0.982$. It is evident from Fig. 4 that AFM1 concentration is directly proportional to % impedance change as the concentration increases. This result is explained on the basis that phenomenon of antigen–antibody interaction is a reversible process and thus adsorption and diffusion proceed simultaneously. Lower limit of quantitation (LOQ) defined as the AFM1 concentration producing a signal corresponding to AFM1-free milk minus 10 times of SD [35], was determined to be 6.25 pg mL^{-1} by analyzing four replicate sets of AFM1 fortified milk samples ranging from 1 to 100 pg mL^{-1}. Limit of detection (LOD) was calculated as the analyte concentration corresponding to the mean signal of blank (obtained by averaging the signal of four replicate sets) minus three times of SD [35]. LOD was found to be 1 pg mL^{-1} with good sensitivity about 2.1% impedance changes per decade. The linearity of calibration shows that this method is useful for ultra sensitive detection and quantification of AFM1 in milk or milk powder. Current AOAC approved method for sensitive AFM1 analysis in milk relies on ELISA, is usually based on a fluorophore or an enzyme labelled secondary antibody. The presented method does not require such additional labels and still competes well with the existing standard assay for milk analysis. The IC_{50} value for the presented label-free immunosensor was found at 57.62 pg mL^{-1}. As against the desired 25 pg mL^{-1} detection limit for the baby food, the present method detects the concentration just at IC_{40} value. The signal inhibited in the presence of AFM1 in milk was calculated and a significantly low detection limit 1 pg mL^{-1} is achieved using the presented immunosensor with analysis time of 20 min. The presented wire electrode based label free immunosensor is a highly sensitive method for AFM1 analysis, comparable with other established methods (Table 1).

Table 2
Recovery of AFM1 from certified reference material ERM-BD282, milk samples. R.E. (relative error) % = [(measured value − true value)/true value] × 100.

[AFM1] added (pg mL^{-1})	[AFM1] found (pg mL^{-1})	R.S.D %	R. E. %	Recovery %
0.25	0.24	2.6	−4.0	96.0
1.00	0.96	0.3	−4.0	96.0
6.25	6.14	0.2	−1.8	98.2
12.50	12.42	0.1	−0.7	99.3
25.00	24.64	2.7	−0.8	99.2
50.00	46.70	1.9	−1.4	98.6
75.00	74.57	0.8	−0.6	99.4
100.00	93.70	0.9	−6.2	93.8

3.9. Recovery of AFM1 from spiked and CRM milk samples

The developed immunosensor was validated with certified reference material (ERM-BD282, zero level of AFM1) for milk powder. The milk powder was reconstituted as described elsewhere [22]. The fortified (0.5% fat) milk samples with 100, 75, 50, 25, 12.5, 6.25, 1 and 0.25 pg mL^{-1} of AFM1 were interpolated from the calibration curve using reconstituted CRM.

The precision and reliability of the developed assay is notable from the data presented in Table 2. The resultant data showed an excellent recovery. The reported recoveries in Table 2 are quite consistent with average recovery above 95% for concentrations up to 75 pg mL^{-1} with average recoveries 98.1 ± 1.5, except for the 100 pg mL^{-1} (93%).

The precision was determined by calculating the relative standard deviation (R.S.D. %) for the replicate measurements and the accuracy (R.E. %) was calculated by assessing the agreement

between measured and nominal concentration of the fortified samples.

4. Conclusion

A label-free silver wire based impedimetric immunosensor has been successfully developed for ultra sensitive determination of AFM1 in milk samples. A linear range of detection 6.25–100 pg mL^{-1} has been achieved with excellent sensitivity and detection limit of 1 pg mL^{-1}. The mAb–AFM1 interaction causing change in capacitance was quantified using EIS. The equivalent circuit for the presented immunosensor comprises R_s, $C_{dl(ol)}$ ($R_{dl}C_{dl(il)}$). The binding of AFM1 caused the change in impedance at lower frequency of 1 Hz, where R_s and $C_{dl(ol)}$ dominates the overall impedance. An improved linear range with short analysis time of 20 min for AFM1 analysis meeting EU standards in infant food has been achieved with good recoveries. The sensor demonstrated excellent selectivity for AFM1 as against AFM2. The bio-functionalized Ag-wire electrodes are used up to two weeks when stored at 4 °C.

Acknowledgements

This work is funded by National Agriculture Innovation Project (NAIP) No. C4/C10125, ICAR and The World Bank. SP acknowledges to NAIP for the award of Research Associate Fellowship. Authors express sincere thanks to Dr. Rahul Mohan, NCAOR, Goa for SEM, NIO, Goa for Fluorescence imaging, M/s ANATEK services, India for ATR FT-IR. GB is thankful to Director, BITS, Pilani-K.K. Birla Goa Campus, India. The authors are thankful to the Editor for valuable suggestions to improve the manuscript.

Appendix A. Supplementary data

Supplementary data associated with this article can be found, in the online version, at http://dx.doi.org/10.1016/j.snb.2012.04.012.

References

[1] M.-R. Oveisi, B. Jannat, N. Sadeghi, M. Hajimahmoodi, A. Nikzad, Presence of aflatoxin M1 in milk and infant milk products in Tehran, Iran, Food Control 18 (2007) 1216–1218.
[2] N. Sadeghi, M.R. Oveisi, B. Jannat, M. Hajimahmoodi, H. Bonyani, F. Jannat, Incidence of aflatoxin M1 in human breast milk in Tehran, Iran, Food Control 20 (2009) 75–78.
[3] M. Badea, L. Micheli, M.C. Messia, T. Candigliota, E. Marconi, T. Mottram, M. Velasco-Garcia, D. Moscone, G. Palleschi, Aflatoxin M1 determination in raw milk using a flow-injection immunoassay system, Analytica Chimica Acta 520 (2004) 141–148.
[4] A.A. Fallah, Assessment of aflatoxin M1 contamination in pasteurized and UHT milk marketed in central part of Iran, Food and Chemical Toxicology 48 (2010) 988–991.
[5] A.A. Fallah, T. Jafari, A. Fallah, M. Rahnama, Determination of aflatoxin M1 levels in Iranian white and cream cheese, Food and Chemical Toxicology 47 (2009) 1872–1875.
[6] I. Ghanem, M. Orfi, Aflatoxin M1 in raw, pasteurized and powdered milk available in the Syrian market, Food Control 20 (2009) 603–605.
[7] G.S. Shephard, F. Berthiller, P.A. Burdaspal, C. Crews, M.A. Jonker, R. Krska, S. MacDonald, R.J. Malone, C. Maragos, M. Sabino, M. Solfrizzo, H.P. Van Egmond, T.B. Whitaker, Developments in mytoxin analysis: an update for 2010–2011, World Mycotoxin Journal 1 (2012) 3–30.
[8] S. Rastogi, P.D. Dwivedi, S.K. Khanna, M. Das, Detection of aflatoxin M1 contamination in milk and infant milk products from Indian markets by ELISA, Food Control 15 (2004) 287–290.
[9] E.K. Kim, D.H. Shon, D. Ryu, J.W. Park, H.J. Hwang, Y.B. Kim, Occurrence of aflatoxin M1 in Korean dairy products determined by ELISA and HPLC, Food Additives and Contaminants 17 (2000) 59–64.
[10] A. Kamkar, A study on the occurrence of aflatoxin M1 in Iranian Feta cheese, Food Control 17 (2006) 768–775.
[11] M. Bognanno, L. La Fauci, A. Ritieni, A. Tafuri, A. De Lorenzo, P. Micari Di, L. Renzo, S. Ciappellano, V. Sarullo, F. Galvano, Survey of the occurrence of aflatoxin M1 in ovine milk by HPLC and its confirmation by MS, Molecular Nutrition and Food Research 50 (2006) 300–305.
[12] P. Rosi, A. Borsari, G. Lasi, S. Lodi, A. Galanti, A. Fava, S. Girotti, E. Ferri, Aflatoxin M1 in milk: reliability of the immunoenzymatic assay, International Dairy Journal 17 (2007) 429–435.
[13] Y. Wang, J. Dostálek, W. Knoll, Long range surface plasmon-enhanced fluorescence spectroscopy for the detection of aflatoxin M1 in milk, Biosensors and Bioelectronics 24 (2009) 2264–2267.
[14] X. Jin, X. Jin, X. Liu, L. Chen, J. Jiang, G. Shen, et al., Biocatalyzed deposition amplification for detection of aflatoxin B1 based on quartz crystal microbalance, Analytica Chimica Acta 645 (2009) 92–97.
[15] N. Paniel, A. Radoi, J-L Marty, Development of an electrochemical biosensor for the detection of aflatoxin M1 in milk, Sensors 10 (2010) 9439–9448.
[16] A. Vig, A. Radoi, X. Muñoz-Berbel, G. Gyemant, J-L Marty, Impedimetric aflatoxin M1 immunosensor based on colloidal gold and silver electrodeposition, Sensors Actuators B 138 (2009) 214–220.
[17] B.C. Towe, V.B. Pizziconi, A microflow amperometric glucose biosensor, Biosensors Bioelectronics 12 (1997) 893–899.
[18] C. Berggren, B. Bjarnason, G. Johansson, An immunological interleukine-6 capacitive biosensor using perturbation with a potentiostatic step, Biosensors Bioelectronics 13 (1998) 1061–1068.
[19] C.J. Felice, R.E. Madrid, J.M. Olivera, V.I. Rotger, M.E. Valentinuzzi, Impedance microbiology: quantification of bacterial content in milk by means of capacitance growth curves, Journal of Microbial Methods 35 (1999) 37–42.
[20] K-S Ma, H. Zhou, J. Zoval, M. Madou, DNA hybridization detection by label free versus impedance amplifying label with impedance spectroscopy, Sensors Actuators B 114 (2006) 58–64.
[21] L. Yang, Y. Li, G.F. Erf, Interdigitated array microelectrode-based electrochemical impedance immunosensor for detection of *Escherichia coli* O157:H7, Analytical Chemistry 76 (2004) 1107–1113.
[22] L. Kanungo, S. Pal, S. Bhand, Miniaturised hybrid immunoassay for high sensitivity analysis of aflatoxin M1 in milk, Biosensors and Bioelectronics 26 (2011) 2601–2606.
[23] A. Ulman, Formation, Structure of self-assembled monolayers, Chemical Reviews 96 (1996) 1533–1554.
[24] C.M.A. Brett, S. Kresak, T. Hianik, A.M. OliveiraBrett, Studies on self-assembled alkanethiol monolayers formed at applied potential on polycrystalline gold electrodes, Electroanalysis 15 (2003) 557–565.
[25] N.K. Chaki, K. Vijayamohanan, Self-assembled monolayers as a tunable platform for biosensor applications, Biosensors and Bioelectronics 17 (2002) 1–12.
[26] B.G. Keselowsky, D.M. Collard, A.J. García, Surface chemistry modulates fibronectin conformation and directs integrin binding and specificity to control cell adhesion, Journal of Biomedical Materials Research 66A (2003) 247–259.
[27] I-S Park, D-K Kim, N. Adanyi, M. Varadi, N. Kim, Development of a direct-binding chloramphenicol sensor based on thiol or sulfide mediated self-assembled antibody monolayers, Biosensors and Bioelectronics 19 (2004) 667–674.
[28] M.L. Rodríguez Velasco, M.M. Calonge Delso, D. Ordónez Escudero, ELISA and HPLC determination of the occurrence of aflatoxin M1 in raw cow's milk, Food Additives and Contaminants 20 (2003) 276–280.
[29] Aflatoxin M1 in Liquid Milk, AOAC Official Method (2000.08).
[30] J.-G. Guan, Y.-Q. Miao, Q.-J. Zhang, Impedimetric biosensors, Journal of Bioscience and Bioengineering 97 (2004) 219–226.
[31] J.S. Danielsa, N. Pourmand, Label-free impedance biosensors: opportunities and challenges, Electroanalysis 19 (2007) 1239–1257.
[32] L. Yang, C. Ruan, Y. Li, Detection of viable *Salmonella typhimurium* by impedance measurement of electrode capacitance and medium resistance, Biosensors and Bioelectronics 19 (2003) 495–502.
[33] L. Yang, R. Basir, Electrical/electrochemical impedance for rapid detection of foodborne pathogenic bacteria, Biotechnology Advances 26 (2008) 135–150.
[34] M. Bart, E.C.A. Stigter, H.R. Stapert, G.J. de Jong, W.P. van Bennekom, On the response of a label-free interferon-(immunosensor utilizing electrochemical impedance spectroscopy, Biosensors and Bioelectronics 21 (2005) 49–59.
[35] M. Thompson, S.L.R. Ellison, R. Wood, Harmonized guidelines for single-laboratory validation of methods of analysis (IUPAC Technical Report), Pure and Applied Chemistry 74 (2002) 835–855.
[36] E. Dinçkaya, Ö. Kınık, M.K. Sezgintürk, Ç. Altuğ, A. Akkoca, Development of an impedimetric aflatoxin M1 biosensor based on a DNA probe and gold nanoparticles, Biosensors and Bioelectronics 26 (2011) 3806–3811.
[37] C.O. Parker, I.E. Tothill, Development of an electrochemical immunosensor for aflatoxin M1 in milk with focus on matrix interference, Biosensors and Bioelectronics 24 (2009) 2452–2457.

Biographies

Gautam Bacher is pursuing Ph.D. in the Department of EEE&I, BITS, Pilani-K.K. Birla Goa Campus, Goa 403726, India. He received his M.Tech. degree in instrumentation from NIT Kurukshetra, India in 2003. His current research is on the development of micro and nano biosensor devices.

Souvik Pal is pursuing Ph.D. in the Department of Chemistry, BITS, Pilani-K.K. Birla Goa Campus, Goa, India. He received his M.Sc., degree in chemistry from Assam

University, Silchar, India in 2008. His current research is on the development of novel micro and nano-biosensor techniques for environmental analysis.

Lizy Kanungo is pursuing Ph.D. in the Department of Chemistry, BITS, Pilani-K.K. Birla Goa Campus, Goa, India. She received her M.Sc., degree in bioinformatics from Orissa University of Agriculture and Technology, Bhubaneswar, India in 2004. Her current research is on the development of sensitive biosensor technique for aflatoxins.

Sunil Bhand is Associate Professor at the Department of Chemistry, BITS, Pilani-K.K. Birla Goa Campus, Goa, India, leading the biosensor group. He received his Ph.D. 1996 in chemistry from Devi Ahilya University, Indore, India. He was guest researcher at the Department of Pure and Applied Biochemistry, Lund University, Sweden, during 2000–2003, 2005, 2007 and 2011. His research interest is biosensors and environmental nanochemistry.

Miniaturized label-free impedimetric immunosensor for analysis of Aflatoxin B1 in peanut

Gautam Bacher[#,$,@], Lizy Kanungo[$] , Sunil Bhand*
[#] Department of EEE & I, Biosensor Lab., Dept. of Chemistry
BITS, Pilani- K. K. Birla Goa Campus, Goa- 403726
[$] Authors with equal contribution, [@] *IEEE* Member, student, *Author for correspondence
E-mail ids: ggb@bits-goa.ac.in, lizy_kanungo@yahoo.co.in, sgbhand@gmail.com

Abstract— **A highly sensitive and selective label-free impedimetric immunosensor based on silver (Ag) wire electrode for the detection aflatoxin B1 (AFB1) in peanut is presented. The sensor was constructed by functionalizing Ag wire coupled with polyclonal antibodies of AFB1 through self assembled monolayers. The antigen–antibody interaction was analyzed by measuring impedance in the frequency range (1–100 KHz) at 5mV applied ac potential in a 384 micro well plate with assay volume 105µL. A working range (0.01–100pg/mL) for AFB1 was obtained with 20min analysis time with limit of detection 0.01pg/mL. The obtained SD and R^2 values were 0.16 and 0.95 respectively.**

Keywords- AFB1; electrochemical impedance spectroscopy; label free; peanut; immunosensor

I. INTRODUCTION

Aflatoxins are toxic metabolites produced by fungi, mainly *Aspergillus flavus* and *A. parasiticus* found in a large variety of food and animal feed. Naturally occurring aflatoxins are composed of B1, B2, G1, and G2. AFB1 is found in abundant and is classified as a carcinogenic substance of group 1 by the International Agency for Research on Cancer (IARC) [1]. Many grains and foodstuffs, including corn, peanuts, cottonseed, cereals, beans, and rice, have been found to be contaminated with aflatoxins. Moreover, humans are exposed to aflatoxins either directly by eating contaminated grains or indirectly via animal products. The contamination generally occurs in the field, during harvest and transportation, and during storage, under conditions where mold is allowed to grow. Since, aflatoxins are relatively heat stable, these are difficult to destroy once formed. The significant threat to human health posed by contamination has motivated extensive research in this toxin [2]. In the European Union, the AFB1 and the total aflatoxin level in peanut products are regulated with maximum residue levels (MRLs) that cannot be greater than 2ng/g and 4ng/g respectively [3].

Several methods for the detection of AFB1 have been established, including thin layer chromatography (TLC), high performance liquid chromatography (HPLC), and enzyme linked immunosorbent assay (ELISA) [4-6]. TLC is a relatively economical method that requires little equipment. HPLC is often coupled with different cleanup procedures such as solid phase extraction, supercritical fluid extraction, immunoaffinity chromatography, and matrix solid phase dispersion [5–8]. Although sensitive and accurate, chromatographic methods require expensive equipment and extended cleanup steps. Immunoassays offer advantages over chromatographic procedures since they are faster and cheaper [7]. Immunosensors based on the optical waveguide lightmode spectroscopy (OWLS) technique, the impedimetric responses, and electrochemical arrays [8-10] have also emerged during recent years. Electrochemical sensors are good choice due to their fast, simple, and low-cost detection capabilities for biological binding events [11-12].

Among the reported biosensors, electrochemical impedance spectroscopy (EIS) has emerged as sensitive technique for analysis of aflatoxins [13-14]. EIS is suitable to analyze the electrical properties of the modified electrode, i.e. when an antibody coupled to the electrode reacts with the antigen of interest [15]. In such a case, the adsorption/desorption process is the rate-determining step. This remarkable step is controlled through the appropriate choice of electrical potential. This confirms that the antigen–antibody interaction is largely influenced by the applied potential. EIS is also a suitable technique to

978-1-4673-2248-5/12/$31.00 ©2012 IEEE

understand the adsorption and charge transfer process for modified electrode [16]. In an EIS technique, an equivalent circuit of the electrode set-up is used to curve fit the experimental data and extract the necessary information about the electrical parameters responsible for the impedance change [17]. The EIS technology has been used in the peanut research for the following purposes such as estimation of mass ratio of the total kernels within a sample of in-shell peanuts using RF impedance method [18] and non destructive moisture content determination for in-shell peanuts by capacitive sensing [19]. However, no report is available on ultrasensitive analysis of AFB1 in peanuts using EIS.

Self-assembled monolayers (SAMs) provide a means for the molecular design on a bio-inert surface with specific functions. SAMs provide a promising basis for immobilizing biomolecules via the functional group [20]. More significantly, it is possible to apply different functionalized SAMs to cross-link with targeted molecules. This causes little disruption or destabilization of the SAMs selected in specific applications [21-24]. SAMs with gold nanoparticles have been reported to improve the sensitivity of an impedimetric sensor [25].

The objective of the present study is to demonstrate a practical and highly sensitive technique for ultra sensitive detection of AFB1 in peanut with short analysis time of 20min. The presented impedimetric immunosensor is based on functionalized Ag wire electrode. Primary polyclonal antibody (pAb) specific to AFB1 were attached on the Ag wire through SAMs of 11-marcaptoundecanoic acid (11-MUA). This imparts high specificity to the biosensor. The Ag wire set-up provides extra features such as storage, ease of handling and portability. The impedance change during antigen–antibody interaction is measured using EIS.

Herein we present a simple, cost effective, label-free impedimetric immunosensor for detection of AFB1 in peanut matrix with the help of two electrodes immersed in the single well of 384 micro well plate. The immunosensor showed an excellent low limit of detection (0.01pg/mL) for AFB1 with a short analysis time of 20min. In the presented biosensor setup, the volume reduction has also been achieved through usage of 384 microwell plate with working volume of 105µl. The schematic representation of experimental set up is given in Fig. 1. The functionalized electrode setup is usable under field conditions.

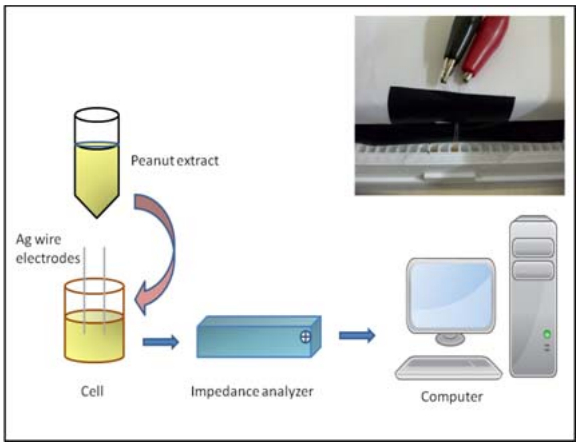

Figure 1: Schematic illustration of Ag wire electrode based impedimetric AFB1 immunosensor with EIS measurement setup; inset: Ag wire electrodes dipped into the 384 micro well plate.

II. MATERIALS AND METHODOLOGY

All the chemicals used were of analytical grade and used as received. Ag wire (diameter = 0.25mm) and AFB1 were procured from ACROS Organics, USA. The diameter of wire was reduced to 0.18mm by manual stretching. AFB1 primary polyclonal antibody (pAb) raised from rabbit, Tween20, 11-mercaptoundecanoic acid (11-MUA), 1-ethyl-3-[3-dimethylaminopropyl] carbodiimide hydrochloride (EDC), N-hydroxy succinimide (NHS) were purchased from Sigma–Aldrich, USA. Ethyl Alcohol 200 proof was purchased from TEDIA, USA. Hydrogen peroxide (H_2O_2) 30% (w/v), acetonitrile (ACN) HPLC grade, methanol, di-sodium hydrogen phosphate (Na_2HPO_4), sodium di-hydrogen phosphate (NaH_2PO_4) from MERCK (Germany) and sodium hypochlorite (4%) solution were purchased from Fisher Scientific (India). For sample handling, micropipettes (eppendorf®, Germany) were used. Peanut samples were finely ground by a household mixer grinder. Shaking was done by Rotospin (Tarsons, India). Filtration was done by Whatman® filter paper 41 of 25µm size. White 384 well polystyrene microtiter plates were purchased from Nunc (Denmark). For the handling of AFB1 standard solution, glove box (Cole Parmer, USA) was used. For preparing all the solutions, water produced in a Milli-Q system (Millipore, Beford, MA, USA) was used. Certified ultra pure nitrogen (99.9%), pH meter (Seven Multi Mettler Toledo, 8603, Switzerland) were used. Sonication of the sample was done on Toshcon ultrasonic cleaner (Toshniwal process instruments Pvt. Ltd., India). Impedance measurements were carried out using IVIUM™ CompactStat impedance analyzer, Netherland.

A. Preparation of buffers

Buffers were made by the following method. For coating purpose, a 0.05M carbonate buffer (CB) was prepared. The pH was adjusted to 9.6. As CB changes composition over time, it was made fresh each time. 0.01M phosphate buffered saline (PBS) was used for incubation and washing purpose. The pH was adjusted to 7.4. Buffer (PBST) was made by adding 0.05% Tween 20 (v/v) in 0.01M phosphate buffered saline. All buffer solutions were stored at 4^0C when not in use.

B. Preparation of AFB1 standard solutions

All the AFB1 solutions were prepared in a glove box in a maintained inert N_2 atmosphere. AFB1 stock solution 1000µg/mL was prepared by dissolving the AFB1 crystalline in 5% ACN (v/v) in PBS and stored at 4^0C. Working AFB1 standard solutions were prepared in the following concentrations; 0.01, 0.1, 1. 10, 25, 50 & 100pg/mL by diluting the stock with 5% ACN.

C. Preparation of AFB1 antibody solutions

From the stock solution of rabbit polyclonal (pAb) [A8679-1ML], 1µl was taken and 999µl of pyrogen free de-ionized water was added. From this 1:1000 dilution, working pAb solutions were prepared by serial dilution such as 1:2000, 1:4000 etc.

D. Peanut sample extraction procedure

Non contaminated peanuts were purchased from the local supermarket, Goa, India. The sample was extracted by the following method. Peanuts were finely ground by a household mixer grinder to a fine consistency. 10g of this ground commodity was extracted with 50mL of methanol/water mixture (80:20) by a rotospin shaker at 50rpm for 15min. The slurry was filtered through Whatman 41 filter paper and analyzed.

E. Immobilization of pAb on Ag wire electrode

The wires were washed with distilled water followed by drying under ultra pure nitrogen stream. This cleaning procedure was repeated before every electrode preparation step. Initially the surfaces of the bare Ag wire electrodes was washed ultrasonically in deionized water for 5min to remove inorganic particles. Following this, the electrodes were immersed into piranha solution (H_2O_2/H_2SO_4, 30/70 v/v) for 30s. The electrodes were dried with nitrogen stream before use. The clean and dried Ag wire electrodes were immersed overnight in 0.004M ethanolic solution of 11-MUA under ambient condition. The electrodes covered by SAMs were gently washed with absolute ethanol to remove unbounded 11-MUA residues. The electrodes were dried with nitrogen stream. The pAb was covalently coupled on Ag wire electrode through SAMs. For coupling the pAb, the carboxyl group of SAMs on modified electrode was activated by 1:1 EDC/NHS (0.1M each) mixture for 2h. Subsequently, the electrodes were washed with distilled water to remove excess EDC/NHS. Finally, pAb was attached to the electrode by carefully spreading pAb solution (1:64000 in coating buffer) over the activated surface followed by overnight incubation at 4^0C. The unused antibody coupled electrodes were washed and stored at 4^0C for future use.

F. Experimental

To conduct the experiment, 102µl of the peanut extract solution was taken in 384 microwell plate. Then 3µl AFB1 standard solution (0.01, 0.1, 1, 10, 25, 50, 100pg/mL) was spiked into it. The functionalized ab coated Ag wires were dipped into the well by 1cm and were separated by 1mm. EIS measurements were carried out at 5mV applied potential with frequency range 1Hz-100KHz.

G. Safety

AFB1 is a extremely potent carcinogen, therefore great care should be taken to avoid personal exposure. It is necessary to wear lab coat, safety mask and gloves when doing experiments. The waste should be treated with hypochlorite before disposal.

III. RESULTS & DISCUSSIONS

A. Optimization of the immunosensor

1) antibody dilutions: The binding of the AFB1 and anti-AFB1 antibody on the electrodes directly affects the sensitivity of the immunosensor. The amount of anti-AFB1 antibody plays an important role in this process. The electrochemical signal depends upon antigen- antibody binding and incubation time. Hence, the effect of the concentration of anti-AFB1 antibody and incubation time were investigated. Of the various anti-AFB1 dilution ratios evaluated, 1:64000 was found to be optimum as presented in Fig. 2a for impedance signal and sensitivity. Incubation time of 20min was found to be optimal for impedance measurements.

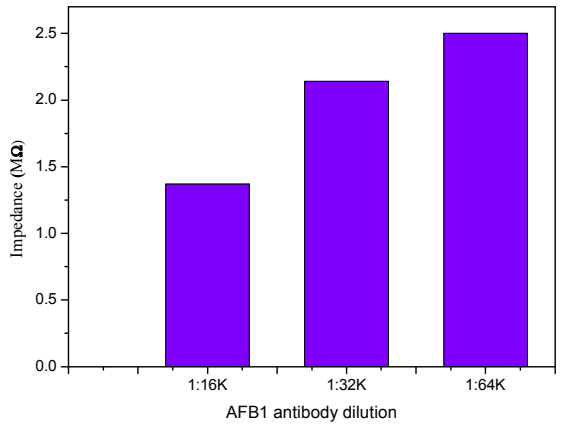

Figure 2a: Optimization of antibody dilution for AFB1 analysis

2) Influence of applied frequency: The influence of applied frequency was also optimized in the range 1Hz to 100KHz. Six frequencies of 1Hz, 10Hz, 96Hz, 1KHz, 10KHz and 100KHz were chosen for recording the impedance change during antigen-antibody interaction. The percentage impedance change was calculated against blank matrix and is presented as Fig. 2b. The maximum change in impedance during antigen-antibody interaction was observed about 35% at 1Hz. Thus, 1Hz was chosen for quantitative analysis of AFB1.

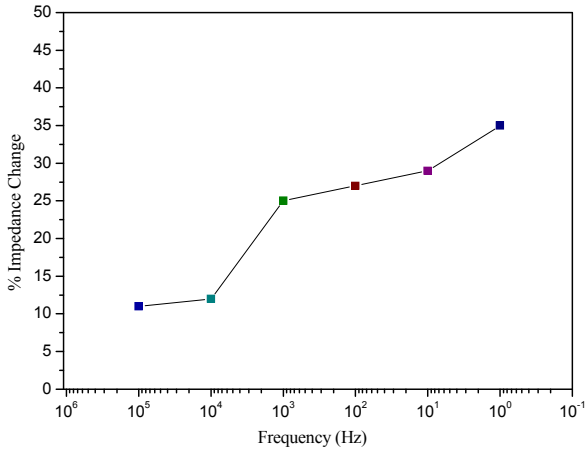

Figure 2b: Percentage impedance change after antigen-antibody interaction recorded at different frequencies (1Hz- 100KHz) at 5mV applied potential.

3) Influence of applied potential: In impedance immunosensor the applied voltage should be quite small, usually 10mV or lesser since the current-voltage relationship is often linear for small perturbations [26]. Fig. 2c shows the Nyquist plot recorded for different applied potential from 0.1mV to 1V. It is also clear from Fig. 2c that the stable response is obtained when applied potential was 5mv and above. At 0.1mV, 1mV, 0.5V and 1V applied potential the response signal was not satisfactory. Fig. 2d investigates the impedance value at 1Hz at various applied potential. It is confirmed from Fig. 2d that a potential of 5mV is optimum for monitoring the impedance resulted from antigen-antibody interaction.

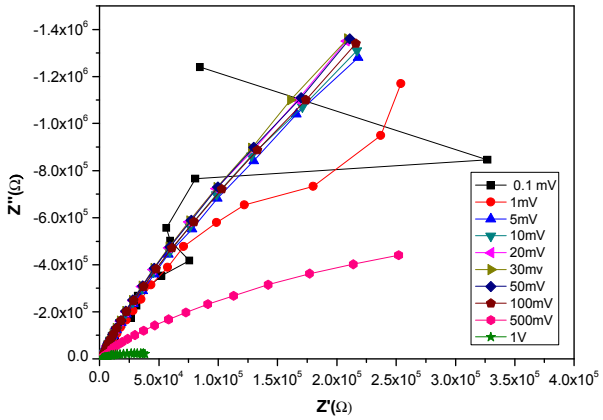

Figure 2c: Nyquist plot recorded for 10pg/mL AFB1 in peanut based matrix at different applied potential.

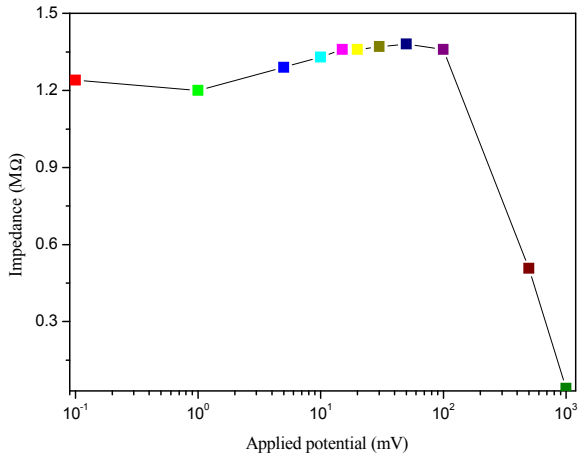

Figure 2d: Measured impedance change at different applied potential (0.01mV-1V) at 1Hz frequency.

B. EIS study of AFB1 binding on sensor electrode

The interaction of antigen-antibody on functionalized electrode surface is presented as Fig. 3. These interactions create a new charged layer as a capacitance that is in series with the double layer capacitance. A decreased double layer capacitance and increased impedance was observed at the lower applied frequency of 1Hz for lower concentration (0.01-10pg/mL) and decreased impedance was observed at higher concentration (25-100pg/mL). The change in impedance confirmed binding of the antigen (AFB1). The decrease in impedance is

attributed to the limiting value of available binding sites on the electrode. As regards applied frequency, it was observed that impedance remains constant in the higher frequency region (100Hz-100kHz). A significant change was measurable in the low frequency region (1-100Hz). Since the maximum changes in impedimetric response were recorded at 1Hz, all measurements were carried out at this frequency.

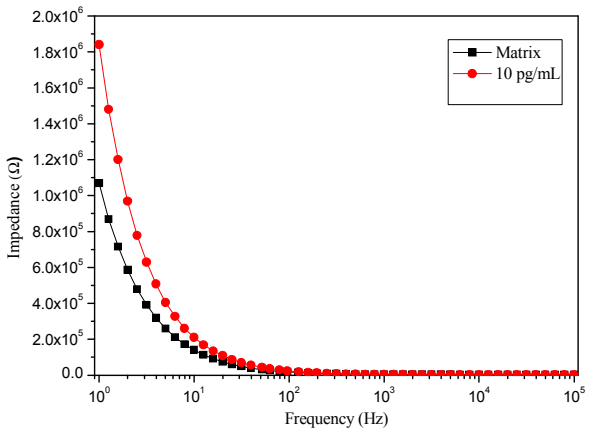

Figure 3: Impedance plot of the immunosensor before and after interaction of anti-AFB1 pAb with two different AFB1concentrations at room temperature in methanol/water (80:20) medium, frequency range 1Hz to 100KHz at applied ac potential 5mV.

B. Validation of sensor operation

The sensor was validated for quantitative AFB1 analysis. The EIS data were collected for different concentrations of AFB1 (0.01-100pg/mL). Fig. 4 represents Nyquist plot obtained for the ac impedance analysis of anti-AFB1 pAb following exposure to various AFB1 concentrations.

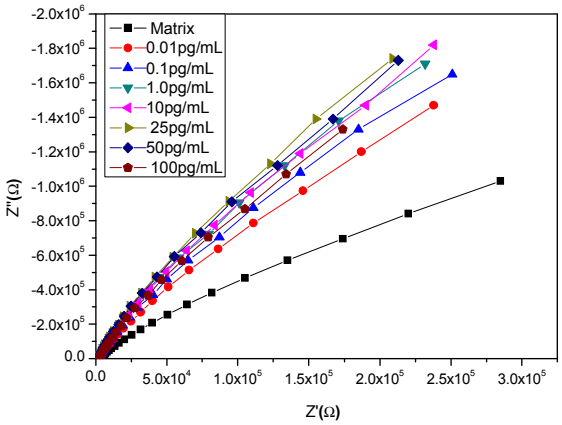

Figure 4: Analytical signal (Nyquist plot) recordings in presence of different concentration of AFB1 (in peanut based matrix) at electrode surface. EIS: 1Hz to 100KHz, 5mV ac potential.

It is evident that both Z′ and Z′′ component of impedance increased with decreasing frequency. The nature of Nyquist plot also confirms that the antigen-antibody interaction has occurred. A response corresponding to a change in the real component (Z′) accounts for largest increase in impedance observed. The imaginary component (Z′′) increases to a larger extent at higher AFB1 concentrations were increased from 0.01-10pg/mL. The intraday analysis of the presented immunosensor (n=4) showed a good repeatability with 5 % variance.

C. Equivalent circuit analysis & validation

The performance of an electrochemical cell is represented by an equivalent circuit that has the same behavior as the real cell under a given excitation [27]. The electrical parameters generally used to design an equivalent circuit model for electrochemical curve fitting includes mainly, electrolyte resistance (bulk medium resistance) and double layer capacitance etc. These factors affect the degree to which an equivalent circuit model represents the experimental impedance data. From the electric point of view, a simple equivalent circuit consisting of a resistor and a capacitor in series represents the behavior of the impedance test systems when two electrodes are immersed into a conductive medium [28]. Herein various equivalent circuits have been evaluated to fit the obtained data for AFB1 analysis. The proposed equivalent circuit with best fit results for the electrochemical cell using modified electrode is presented as Fig. 5 and has been chosen for further investigation.

Figure 5: Equivalent circuit used to fit impedance of the AFB1 immunosensor in peanut based matrix.

The presented circuit describes non-faradic phenomenon at the electrode–electrolyte interface, since no species are present in the solution that undergo an electrochemical reaction. This equivalent circuit consists of ohmic resistance of medium (R_s), double layer capacitance of outer layer ($C_{dl(ol)}$), double layer capacitance of inner layer ($C_{dl(il)}$) and resistance of inner layer (R_{dl}) [12]. $C_{dl(ol)}$ ($R_{dl}C_{dl(il)}$) represent the two layer structure for each electrode.

$C_{dl(ol)}$ represents outer layer of the interface where the antigen-antibody interaction takes place. ($R_{dl}C_{dl(il)}$) sub-circuit represents the inner layer of the interface. R_{dl} being parallel to $C_{dl(il)}$, resembles a part of SAMs. R_{dl} is interpreted as the conductivity (by penetrating ions) of the SAMs [29]. The best fit is obtained for $C_{dl(ol)}$ as constant phase element and modified as $CPE_{dl(ol)}$. Fig. 6 shows Bode plot of experimental and fitted impedance spectra of AFB1. Fitting was done by using IVIUM™ equivalent circuit evaluator and optimized with phase, Z′ and Z′′. The error weight is taken as equal for each point. It is evident from Fig. 6 that for the presented immunosensor, the fitting has good agreement with experimental data, thereby validating the equivalent circuit.

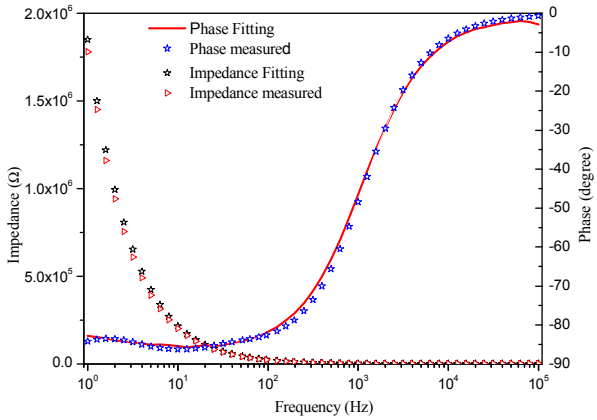

Figure 6: Bode plot of AFB1 analysis with the fitting curve. ac applied potential: 5mV; frequency range: 1Hz to 100KHz.

D. Calibration of sensor for AFB1 detection

Impedance data were recorded for the functionalized electrodes after exposing it to increasing AFB1 concentration (0.01 - 100pg/mL). A frequency of 1Hz at applied ac potential 5mV was selected for analysis since at this frequency significant change in impedance response was observed. The specific interaction of anti-AFB1 and AFB1 gave rise to an overall increase in impedance change from baseline response at the electrode/solution interface for AFB1 concentration (0.01-10pg/mL). The % impedance change was calculated corresponding to different concentrations of AFB1. The resulting calibration curve is presented in Fig. 7. A linear range for AFB1 detection 0.1-10pg/mL with SD=0.16 and R^2=0.954 was achieved. Limit of detection (LOD) was found to be 0.01pg /mL.

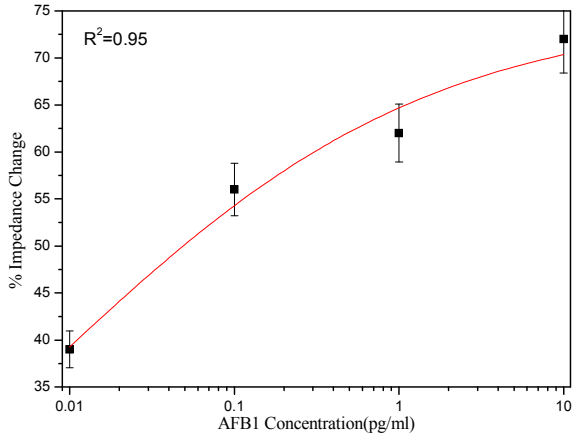

Figure 7: Calibration curve obtained for label free immunosensor, anti-AFB1 pAb diluted to 1:64000 in peanut matrix, incubation time 20min ; Linear range for AFM1 detection 1-100pg/mL with SD = 0.16 and R^2 = 0.95.

IV. CONCLUSION

A highly sensitive and miniaturized label-free impedimetric immunosansor has been demonstrated for the analysis of AFB1 in peanut. The sensor could help screen the low level contamination of AFB1 in peanut samples. The immunosensor is simple to use and cost effective, thus it could be used in field conditions. Future work involves in detection of other mycotoxins using same principle.

ACKNOWLEDGEMENT

This work is financially supported under NAIP Project No. C4/C10125 funded by ICAR (India) and the World Bank. LK is thankful to NAIP for award of Senior Research Fellowship. GB is thankful to Director, BITS, Pilani-K.K. Birla Goa Campus.

REFERENCES

[1] International Agency for Research on Cancer. IARC monograph on the Evaluation of Carcinogenic Risk to Humans; IARC: Lyon, France, 1993; vol. 56.

[2] N. A. Lee, S. Wang, R. D. Allan, and I. R. Kennedy, "A rapid aflatoxins B1 ELISA: Development and validation with reduced matrix effects for peanuts, corn, pistachio, and soybeans," J. Agric. Food Chem., vol. 52, pp. 2746-2755, 2004.

[3] E U Commission, Commission Regulation (EC) No. 466/2001 of 8 March 2001 setting maximum levels for certain contaminants in foodstuffs, Official Journal European Communities L77 (2001) 1.

[4] J. Jaimez, C.A. Fente, B.I. Vazquez, C.M. Franco, A. Cepeda, G. Mahuzier, and P. Prognon, "Application of the assay of aflatoxins by liquid chromatography with fluorescence detection in food analysis," J. Chromatogr. A, vol. 882, pp. 1–10, 2000.

[5] J. Stroka, R.V. Otterdijk, and E. Anklam, "Immunoaffinity column clean-up prior to thin-layer chromatography for the determination of aflatoxins in various food matrices," J. Chromatogr. A, vol. 904, pp. 251–256, 2000.

[6] N.A. Lee, S. Wang, R.D. Allan, and I.R. Kennedy, "A rapid aflatoxin B1 ELISA: Development and validation with reduced matrix effects for peanuts, Corn, pistachio, and soybeans," J. Agric. Food Chem, vol. 52, pp. 2746–2755, 2004.

[7] A. Korde, U. Pandey, S. Banerjee, H.D. Sarma, S. Hajare, M. Venkatesh, A.K. Sharma, and M.R.A. Pillai, "Development of a radioimmunoassay procedure for aflatoxin B1 measurement," J. Agric. Food Chem, vol. 51, pp. 843–846, 2003.

[8] S. Piermarini, L. Micheli, N.H.S. Ammida, G. Palleschi, D. Moscone, "Electrochemical immunosensor array using a 96-well screen-printed microplate for aflatoxin B1 detection," Biosens. Bioelectron, vol. 22, pp. 1434–1440, 2007.

[9] N. Adanyi, I.A. Levkovets, S. Rodriguez, A. Ronald, M. Varadi, and I. Szendro, "Development of immunosensor based on OWLS technique for determining aflatoxin B1 and ochratoxin A," Biosens. Bioelectron, vol. 22, pp. 797–802, 2007.

[10] J.H.O. Owino, A. Ignaszak, A. Al-Ahmed, P.G.L. Baker, H. Alemu, J.C. Ngila, and E.I. Iwuoha, "Modelling of the impedimetric responses of an aflatoxin B1 immunosensor prepared on an electrosynthetic polyaniline platform," Anal. Bioanal. Chem., vol. 388, pp. 1069–1074, 2007.

[11] E. Bakker, and Y. Qin, "Electrochemical sensors," Anal. Chem., vol. 78, pp. 3965–3983, 2006.

[12] G. Bacher, S. Pal., L. Kanungo, and S. Bhand, "A label-free silver wire based impedimetric immunosensor for detection of aflatoxin M1 in milk," Sens. Actuat. B, vol. 168, pp. 223- 230, 2012.

[13] N. Paniel, A. Radoi, and J-L Marty, "Development of an electrochemical biosensor for the detection of aflatoxin M1 in milk," Sensors, vol. 10, pp. 9439–9448, 2010.

[14] A. Vig, A. Radoi, X. Mu˜noz-Berbel, G. Gyemant, and J-L Marty, "Impedimetric aflatoxin M1 immunosensor based on colloidal gold and silver electrodeposition," Sens. Actuat. B, vol. 138, 214–220, 2009.

[15] C.J. Felice, R.E. Madrid, J.M. Olivera, V.I. Rotger, and M.E. Valentinuzzi, "Impedance microbiology: quantification of bacterial content in milk by means of capacitance growth curves," J. Microbial Methods, vol. 35, pp. 37–42, 1999.

[16] K. S. Ma, H. Zhou, J. Zoval, and M. Madou, "DNA hybridization detection by label free versus impedance amplifying label with impedance spectroscopy," Sens. Actuat. B, vol. 114, pp. 58–64, 2006.

[17] L. Yang, Y. Li, and G.F. Erf, "Interdigitated array microelectrode-based electrochemical impedance immunosensor for detection of Escherichia coli O157:H7," Anal. Chem., vol., 76, pp. 1107–1113, 2004.

[18] C. V. Kandala, and J. Sundaram, "Estimation of mass ratio of the total kernels within a sample of in-shell peanuts using RF Impedance Method," J. of Elect. And Engg, vol. 2010, Article ID 375430, DOI: 10.1155/2010/375430.

[19] C. V. Kandala, J. Sundaram, K. Govindarajan, and J. Subbiah, "Nondestructive analysis of in-shell peanuts for moisture content using a custom built NIR Spectrometer," J. Food Engg., vol. 2, pp. 1-7, 2011.

[20] L. Kanungo, S. Pal, and S. Bhand, "Miniaturised hybrid immunoassay for high sensitivity analysis of aflatoxin M1 in milk," Biosens. Bioelectron, vol. 26, pp. 2601–2606, 2011.

[21] A. Ulman, "Formation, Structure of self-assembled monolayers," Chem. Rev., vol. 96, pp. 1533–1554, 1996.

[22] C.M.A. Brett, S. Kresak, T. Hianik, and A.M. OliveiraBrett," Studies on self-assembled alkanethiol monolayers formed at applied potential on polycrystalline gold electrodes," Electroanal., vol. 15, pp. 557–565, 2003.

[23] N.K. Chaki, and K. Vijayamohanan," Self-assembled monolayers as a tunable platform for biosensor applications," Biosens. Bioelectron, vol. 17, pp. 1–12, 2002.

[24] B.G. Keselowsky, D.M. Collard, and A.J. Garcia, "Surface chemistry modulates fibronectin conformation and directs integrin binding and specificity to control cell adhesion," J. Biomed. Mater. Res., A, vol. 66, pp. 247–259, 2003.

[25] I. S. Park, D. K. Kim, N. Adanyi, M. Varadi, and N. Kim," Development of a direct-binding chloramphenicol sensor based on thiol or sulfide mediated self-assembled antibody monolayers," Biosens. Bioelectron, vol. 19, pp. 667–674, 2004.

[26]G. Barbero, A. L. Alexe-Ionescu, and I. Lelidis, "Significance of small voltage in impedance spectroscopy measurements on electrolytic cells," *Journal of Applied Physics,* vol. 98, pp. 113703, 2005.

[27] L. Yang, C. Ruan, and Y. Li, "Detection of viable Salmonella typhimurium by impedance measurement of electrode capacitance and medium resistance," Biosens. Bioelectron.,vol. 19, pp. 495-502, 2003.

[28] L. Yang, and R. Basir, "Electrical/ Electrochemical impedance for rapid detection of foodborne pathogenic bacteria," Biotechnol. Adv., vol. 26, pp. 135-150, 2008.

[29] M. Bart, E.C.A. Stigter, H.R. Stapert, G.J. de Jong, and W.P. van Bennekom, "On the response of a label-free interferon-γ immunosensor utilizing electrochemical impedance spectroscopy," Biosens. Bioelectron., vol. 21, pp. 49-59, 2005.

Flow-Based Impedimetric Immunosensor for Aflatoxin Analysis in Milk Products

Lizy Kanungo, Gautam Bacher & Sunil Bhand

Applied Biochemistry and Biotechnology
Part A: Enzyme Engineering and Biotechnology

ISSN 0273-2289
Volume 174
Number 3

Appl Biochem Biotechnol (2014)
174:1157-1165
DOI 10.1007/s12010-014-0995-y

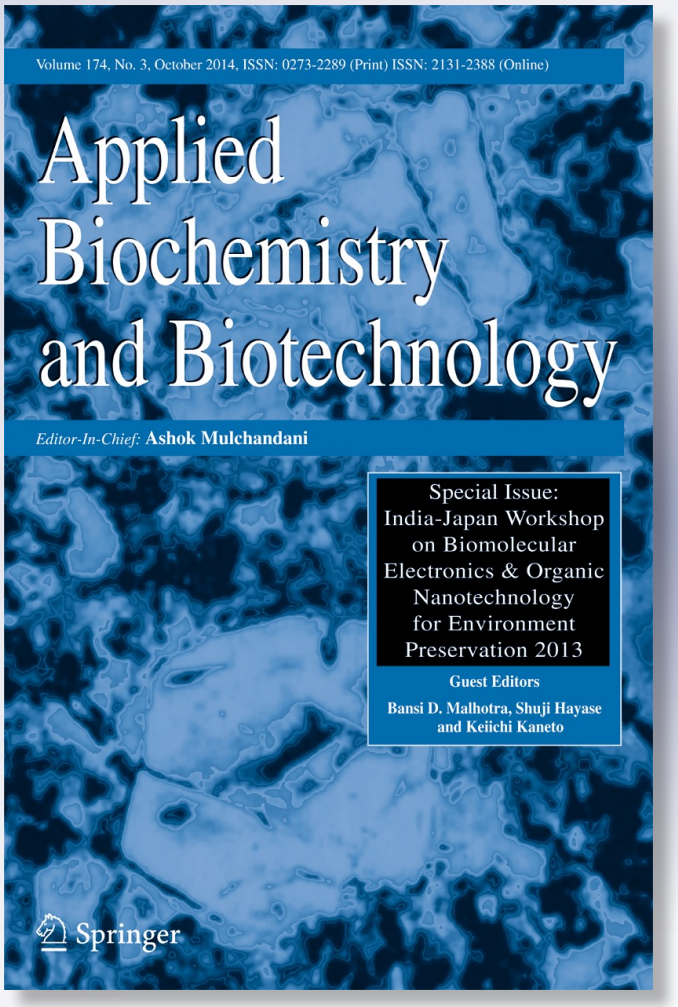

Springer

Appl Biochem Biotechnol (2014) 174:1157–1165
DOI 10.1007/s12010-014-0995-y

Flow-Based Impedimetric Immunosensor for Aflatoxin Analysis in Milk Products

Lizy Kanungo · Gautam Bacher · Sunil Bhand

Received: 17 February 2014 / Accepted: 19 May 2014 /
Published online: 28 May 2014

Abstract Label-free detection technique based on impedance was investigated for aflatoxin M1 (AFM1) and aflatoxin M2 (AFM2) analysis in milk products. The impedance change resulting from antigen-antibody interaction was studied using a two-electrode setup made up of silver (Ag) wire. Processed milk such as drinking yogurt and flavored milk samples were analyzed in a flow-based setup. Two microflow pumps were used to construct the flow system where analytes (AFM1 and AFM2) were injected and impedance was measured using functionalized Ag wire electrodes. The flow system was optimized by adjusting both inlet and outlet flows to maintain the reaction volume optimum for impedance measurements. Using Bode plot, the matrix effect was investigated for detection of AFM1 and AFM2 in various matrices. Good recoveries were obtained even at low-AFM1 concentrations in the range of 1–100 pg/mL. The influence of AFM2 on the detection of AFM1 was also investigated. The proposed method provides good scope for online monitoring of such hazardous toxins in milk products.

Keywords Label-free technique · Flow-based analysis · AFM1 · Immunosensor · Milk products

Introduction

Aflatoxin M1 (AFM1) and Aflatoxin M2 (AFM2) are fungal metabolites found in milk and related milk products [1–3]. Contamination of milk with AFM1 and its ill effects on humans are well documented [4–8]. Moreover, from studies, it has been found that AFM1 is relatively stable during milk pasteurization and storage, as well as during the preparation of various dairy products [9–11].

Lizy Kanungo and Gautam Bacher contributed equally to this work.

L. Kanungo · G. Bacher · S. Bhand (✉)
Biosensor Laboratory, Department of Chemistry, BITS, Pilani-K. K. Birla Goa Campus, Goa 403726, India
e-mail: sunil17_bhand@yahoo.com

L. Kanungo
e-mail: lizy_kanungo@yahoo.co.in

G. Bacher
e-mail: ggb@goa.bits-pilani.ac.in

G. Bacher
Department of EEE & I, BITS, Pilani-K. K. Birla Goa Campus, Goa 403726, India

As a result, these can be found in various milk products such as yogurt, flavored milk, infant formula milk powder, cheese, and other milk-based confectioneries including chocolates, sweets, and pastries [12–14]. Due to their carcinogenicity and severe toxicity, many international agencies have set maximum permissible limits of AFM1 in milk and related products [15–17]. Therefore, it is important to determine AFM1 and AFM2 levels in milk and milk products in order to protect consumers in various age groups, meeting the stringent regulatory standards set by these international agencies [18, 19].

There are few reports available on flow-based AFM1 detection and analysis. A bilayer lipid membrane based biosensor and related thin-film technology were investigated for AFM1 monitoring of milk using a flow injection system by Andreou and Nikolelis [20]. This was a very fast method (four samples per minute) and allowed a continuous monitoring of milk. But, the detection limit was around 200 pg/mL. Sibanda et al. [21] have developed a membrane-based flow-through enzyme immunoassay for detection of AFM1 in milk. The assay was coupled to an immunoaffinity column, and a detection limit at 50 pg/mL was achieved. However, the total assay time was found to be 30 min. In another report, Badea et al. [10] have developed a flow injection immunoassay with amperometric technique for AFM1 detection in milk. The detection limit of 11 pg/mL was obtained for milk samples at the rate of six samples in triplicate per hour. But, the immunoassay involved a complex procedure comprising of many steps. Anfossi et al. [22] have developed a high sensitive immunoassay-based lateral flow device for semiquantitative determination of AFM1 in milk. There, they have optimized the competitor design and the gold-labeling strategy to obtain the LOD at 20 ng/L. Direct detection of AFM1 in milk was obtained by acquiring images of the strips and correlating intensities of the colored lines with analyte concentrations. The one-step assay was completed in 17 min, including a very simple and rapid sample preparation. This method did not account for AFM1 analysis in milk products. Moreover, the individual test strips were disposable, thus not so economical. Therefore, there is a need for a simple, sensitive, and rapid method for flow-based AFM1 detection and analysis in milk with minimal pretreatment methods.

In this paper, we have investigated a flow-based label-free impedimetric immuno-sensing technique for analysis of AFM1 and AFM2 in milk products that facilitated scope for online monitoring. Earlier, we have reported a silver-wire-based impedance setup for analysis of AFM1 in milk sample [23]. Herein, using a flow-based setup, a label-free impedimetric technique has been demonstrated for analysis of AFM1 and AFM2 in different matrices such as certified reference material (ERM-BD-282), drinking yogurt, and flavored milk. The flow system was optimized by adjusting both inlet and outlet flow rates to maintain the sample volume optimum for measurement. The milk and related samples were artificially spiked with known concentrations of AFM1 and AFM2, and impedance was measured. In all cases, an increase in impedance value was observed with increased AFM1 concentration. This flow-based setup was used to study mixture of AFM1 and AFM2 in milk products. The short analysis time (10 min) of the proposed method provides a vast scope for online monitoring.

Materials and Methods

AFM1, Tween 20, certified reference material (CRM) ERM-BD282 (AFM1 in whole milk powder, <0.02 μg/kg), 11-mercaptoundecanoic acid (11-MUA), 1-ethyl-3-[3-dimethylaminopropyl]carbodiimide hydrochloride (EDC), and N-hydroxy succinimide (NHS) were purchased from Sigma–Aldrich (USA). Hydrogen peroxide (H_2O_2) 30 % (*w*/*v*), acetonitrile (ACN) HPLC grade, and sodium chloride (NaCl) were purchased from Merck (Germany). AFM2 was purchased from Fermentek, Israel. Ethyl alcohol 200 proof was purchased from TEDIA, USA. Sodium hypochlorite (4 %) solution was purchased from Fisher Scientific (India). All the AFM1

solutions were prepared inside a Glove box in a maintained inert (N_2) atmosphere. AFM1 stock solution was prepared by dissolving the AFM1 powder in 5 % ACN (*v*/*v*) in phosphate-buffered saline (PBS) at a concentration of 5 μg/2 mL and stored at −20 °C. A wide dynamic range of working standard solutions in the range of 1–200 pg/mL were prepared by diluting the stock with 5 % ACN. Rat monoclonal antibody (mAb) [1C6] of AFM1 was purchased from Abcam (UK). The stock solution of mAb was prepared as described in our earlier paper [7].

Centrifugation, shaking, and filtration of the samples were done by Spinwin mini centrifuge, Spinix shaker, and syringe filter respectively purchased from Tarsons (India). Glove box, Cole-Parmer (USA) was used for the handling of AFM1 standard solution. Water produced in a Milli-Q system (Millipore, Bedford, MA, USA) was used for preparing all the solutions. Certified ultrahigh pure N_2 (99.9 %) and a pH meter (SevenMulti Mettler Toledo, 8603, Switzerland) were used in various experimental steps. Ag wire (diameter=0.25 mm) was procured from ACROS Organics, USA. The diameter of wire was reduced to 0.18 mm by dipping the wires in piranha solution for about 90 s. For flow injection analysis, a syringe pump and a multichannel peristaltic pump were used. The syringe pump and the peristaltic pump were purchased from Chemyx, USA, and Gilson, France, respectively. Impedance measurements were carried out using IVIUM CompactStat impedance analyzer, Netherlands.

Sample Preparation of Milk Products

The milk product analysis was carried out in commercially available drinking yogurt and flavored milk. The flavored milk sample was centrifuged at 6,000 rpm for 10 min. The upper fatty layer was removed by spatula, and the middle clear portion was diluted with PBST (1:1) and used. The drinking yogurt sample was only diluted with PBST (1:5) and used for analysis.

Experimental Procedure for Flow-Based Impedance Analysis

It is known from the literature that AFM2 is more prevalent in milk products than AFM1. The occurrence of AFM1 and AFM2 was analyzed by impedance in milk products such as drinking yogurt and flavored milk in a flow-based system. The flow system was designed in-house as shown in Fig. 1. The flow rate was optimized by adjusting both the inlet and outlet flow rates. The inlet to the microcell was governed by Chemyx micro syringe pump where two fluids (PBST and milk product sample) were injected, mixed, and channelized to the working cell. The flow rate of the inlet system was optimized to about 0.5 mL/min for a total syringe sample volume of 2 mL.

The sample was injected through the inlet pipe along with buffer where two solutions were mixed and directed to the cell. The milk products were spiked with known concentrations of AFM1 or AFM2 by micropipettes. The outlet system was governed by Gilson microflow pump where the flow rate was optimized to 2.4 rpm. These two flow rates resulted in maintaining a working volume of 0.5 mL in the cell. The functionalized antibody-coated Ag wires were dipped into the microcell by 1 cm and were separated by 1 mm. Electrochemical impedance spectroscopy (EIS) measurements were carried out at 5 mV applied potential with a frequency range of 1 Hz–100 KHz.

Results and Discussion

EIS Study of Various Milk Products

Using an earlier developed label-free EIS-based immunosensor, the impedimetric analysis was further extended to study the effect of various milk products such as standard ERM BD-282 milk,

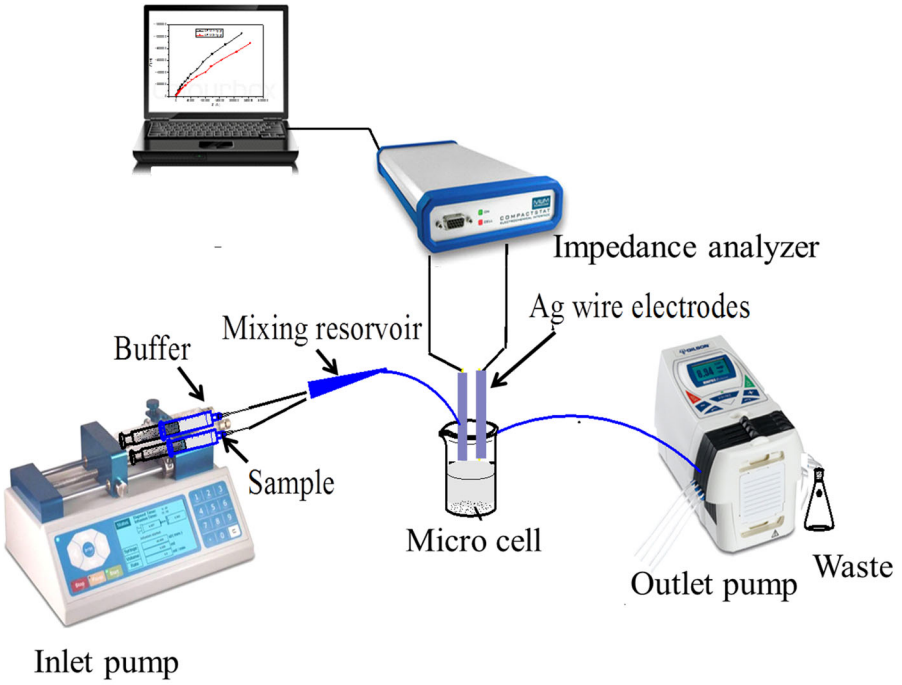

Fig. 1 Schematic representation of flow-based impedance analysis of milk products

flavored milk, and drinking yogurt for quantitative analysis of AFM1 and AFM2. ERM BD-282 milk was reconstituted and spiked with known concentrations of AFM1 and AFM2. After the immobilization of mAb for AFM1, impedance spectroscopy measurements have been carried out with a 5 mV amplitude signal varying from 1 Hz to 100 KHz. AFM1 (25 pg/mL) was spiked in different milk samples, and impedance data were recorded as depicted in Fig. 2a. The response time was 2 min; however, the total analysis time was 10 min. For quantitative analysis, it is appropriate to measure changes in impedance at a single frequency. Figure 2a shows the change in impedance value at 1 Hz for 25 pg/mL of AFM1 spiked in different milk samples.

It is also evident from the Fig. 2a that the similar impedance response is obtained for ERM-BD282 and flavored milk, but a large change in impedance was observed for yogurt. Since the impedance spectroscopy allows the detection of capacitance changes at the interfaces. Capacitance changes can be derived from the imaginary part "Z_{im}," of the complex impedance spectra [24]. The change of imaginary part of impedance Z_{im} provides better correlation to analyte concentration than the real part of impedance [25].

The frequency to monitor the antibody-antigen interaction was chosen in such a way that the system exhibited near-ideal capacitor behavior [26]. The influence of frequency was shown by Bode plot of phase angle and log of impedance magnitude versus log of frequency (Fig. 2b) for various milk samples spiked with 25 pg/mL of AFM1. The system exhibited near-ideal capacitor behavior in the region where the impedance curve was a straight line with a slope of about −1 and the phase angle was as close to −90° as possible [27]. This frequency was observed to be 52 Hz for ERM-BD282 milk and flavored milk, and the same was observed at 159 Hz for yogurt sample. Thus, it was observed that the frequency shift occurs for the same concentration of analyte in various matrices.

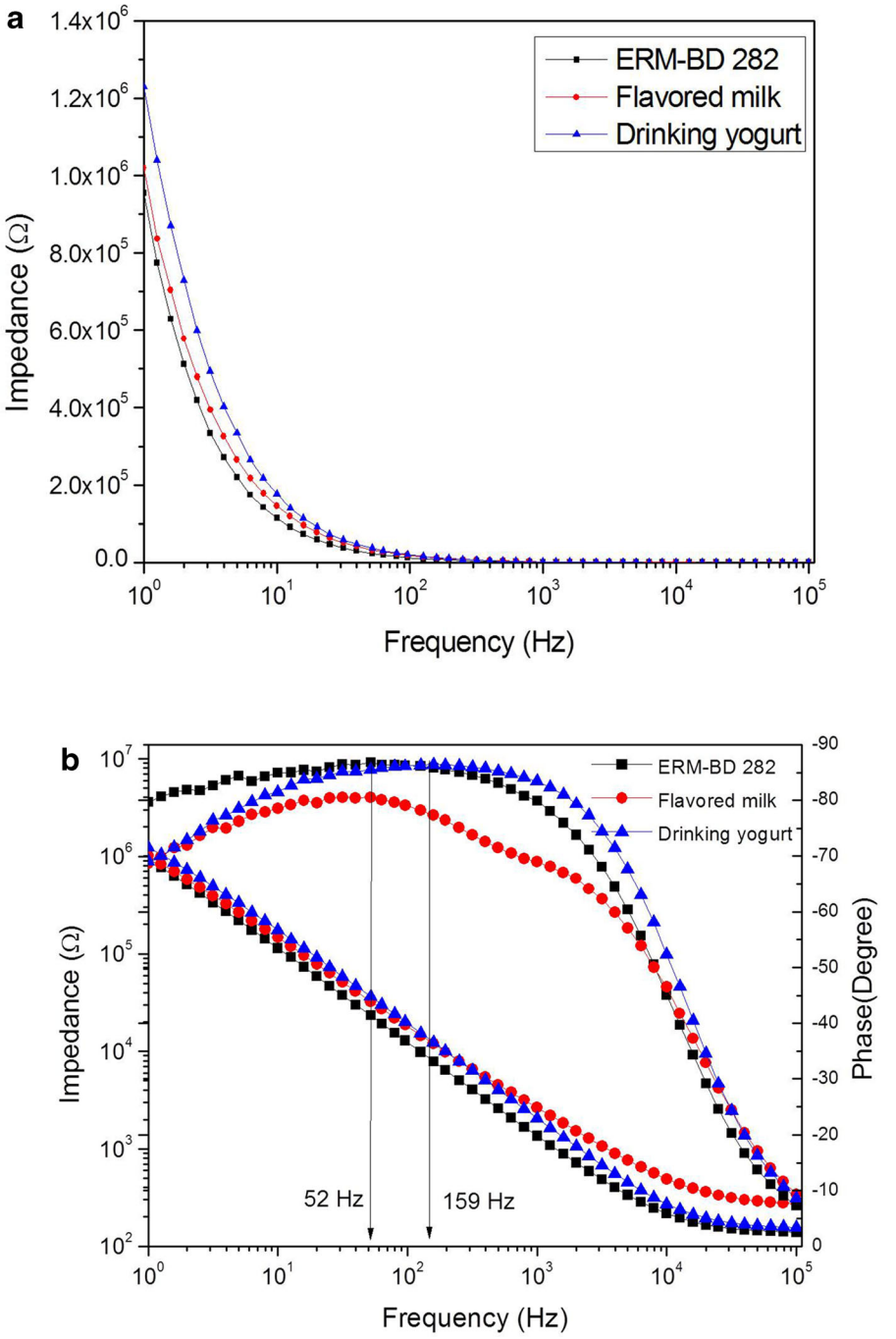

Fig. 2 **a** Impedance spectra of the immunosensor after interaction of mAb with 25 pg/mL AFM1 spiked in ERM-BD 282, flavored milk, and drinking yogurt at room temperature (EIS: frequency range 1 Hz to 100 KHz at ac potential 5 mV). **b** Bode diagram of the immunosensor after interaction of mAb with 25 pg/mL AFM1 spiked in ERM-BD 282, flavored milk, and drinking yogurt at room temperature (EIS: frequency range 1 Hz to 100 KHz at ac potential 5 mV)

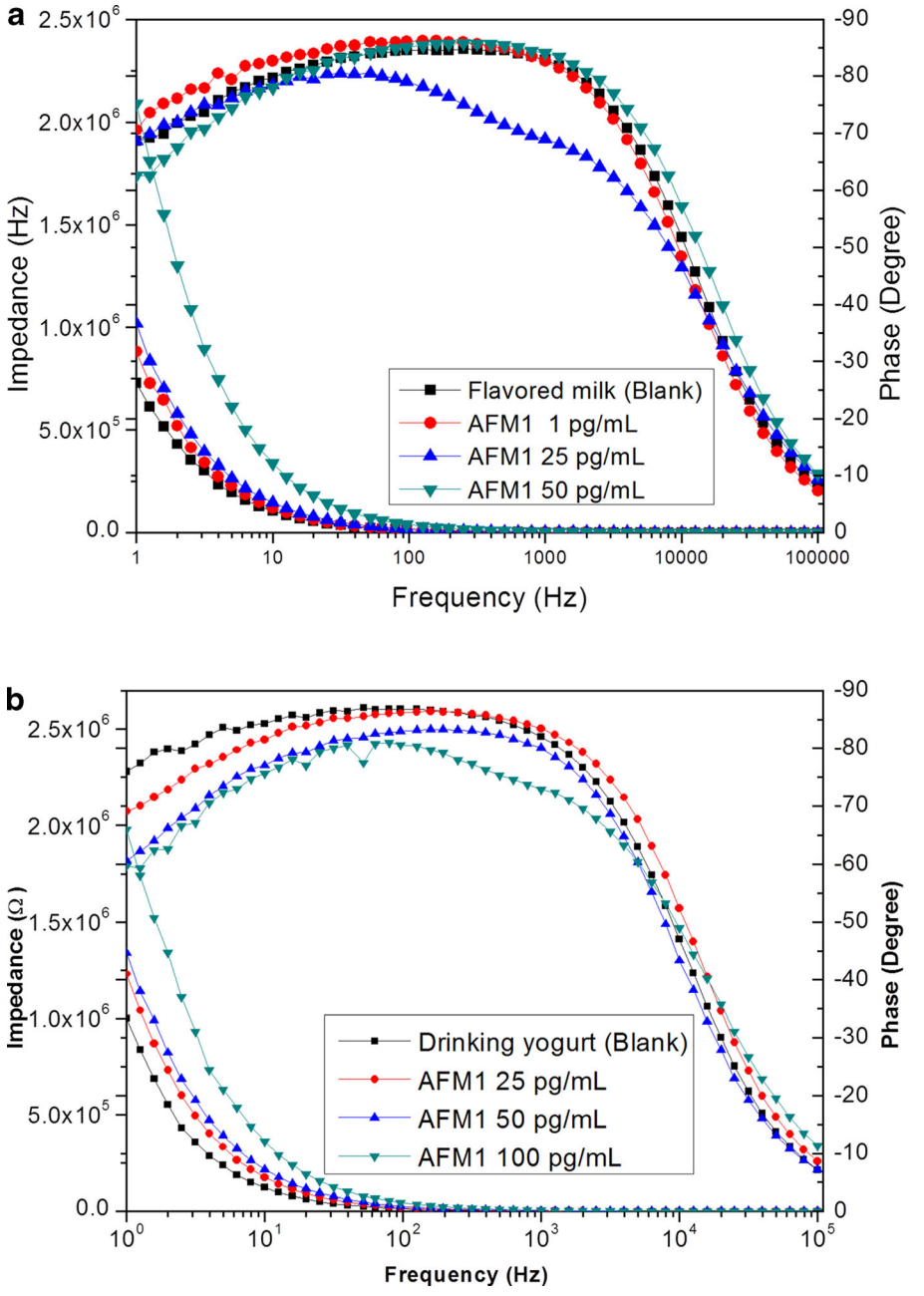

Fig. 3 **a** Bode diagram of the immunosensor after interaction of mAb with 1–50 pg/mL AFM1 spiked in flavored milk and drinking yogurt at room temperature (EIS: frequency range 1 Hz to 100 KHz at ac potential 5 mV). **b** Bode diagram of the immunosensor after interaction of mAb with 25–100 pg/mL AFM1 spiked in drinking yogurt at room temperature (EIS: frequency range 1 Hz to 100 KHz at ac potential 5 mV)

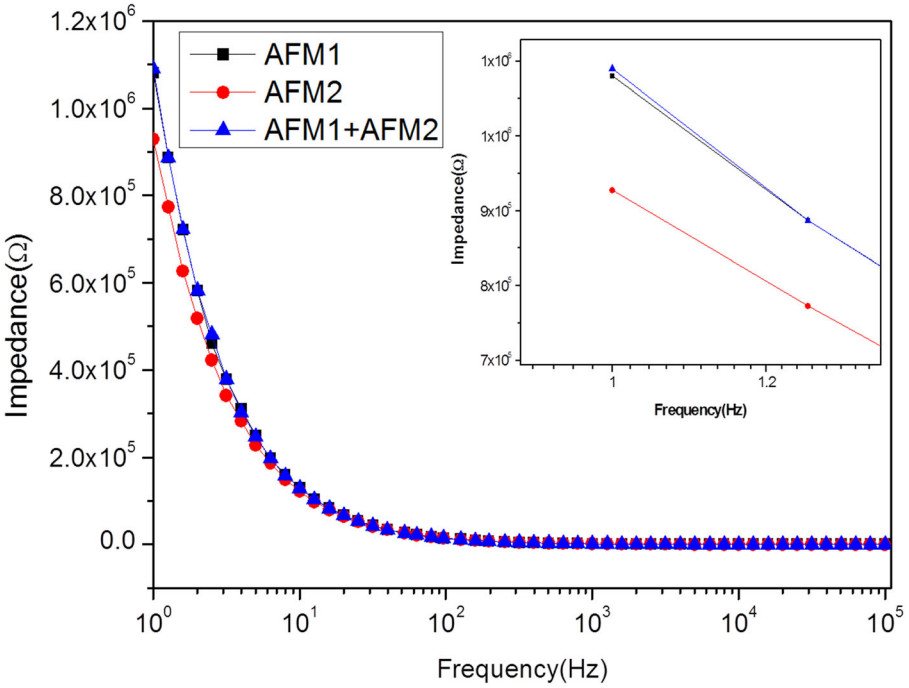

Fig. 4 Impedance spectra of the immunosensor after interaction of mAb with 1 pg/mL AFM1, AFM2, and a mixture of AFM1 and AFM2 spiked in ERM-BD 282 at room temperature (EIS: frequency range 1 Hz to 100 KHz at ac potential 5 mV)

Validation of Sensor Operation in Milk Samples

The sensor was validated for quantitative AFM1 analysis in the flow-based system. The EIS data were collected for different concentrations of AFM1 (1–100 pg/mL). Figure 3a represents Bode plot obtained for the ac impedance analysis of anti-AFM1 mAb following exposure to various AFM1 concentrations in flavored milk. Similar experiments were carried out for drinking yogurt and ERM-BD 282 milk sample.

Figure 3b shows the Bode plot for the ac impedance analysis of anti-AFM1 mAb following exposure to various AFM1 concentrations in drinking yogurt. The interaction of antigen-antibody on functionalized electrode in the flow system creates a new charged layer as a capacitance that is in series with the double-layer capacitance. A decrease in total capacitance

Table 1 Summary of analytical figures of merit of the designed flow-based impedimetric system for various matrices

Matrices studied	Analytical figures of merit				
	Analytes detected	Dynamic range (pg/mL)	LOD (pg/ML)	Sample volume	Time of analysis (min)
ERM-BD282	AFM1 & AFM2	1–100	1	0.5 mL	10
Flavored milk	AFM1 & AFM2	1–100	1	0.5 mL	10
Drinking yogurt	AFM1 & AFM2	1–100	25	0.5 mL	10

and hence increased impedance were observed at the lower applied frequency of 1 Hz, which confirms the binding of antigen-antibody. The change in total capacitance was confirmed from the frequency shift for near-ideal capacitor behavior for different concentrations of AFM1 as depicted in Fig. 3a, b. The sensitivity of the sensor was found to be 4.28 % in flavored milk and 0.44 % in drinking yogurt, respectively. For the same concentration of spiked AFM1, impedance change was obtained as 40 and 25 % in flavored milk and drinking yogurt, respectively.

Sensor Selectivity

The selectivity of the sensor toward AFM1 was studied in the frequency range of 1 Hz to 100 KHz using EIS at 5 mV applied potential in the flow-based system. In the optimized condition, the response signal for AFM1 binding was measured in 10 min. The mAb immobilized on the electrode showed partly cross-reactivity with AFM2 (a structural analog of AFM1). The cross-reactivity of mAb toward AFM2 was quantified experimentally using the presented setup at 1 pg/mL in ERM-BD 282. The impedance change for AFM2 was found to be lower as compared to that for AFM1 at 1 Hz. From Fig. 4, it is clearly evident that the sensor is highly selective toward AFM1 as against AFM2. The AFM1 and AFM2 at 1 pg/mL were distinguishable from each other. This verifies the excellent detection ability of the sensor at an ultralow concentration. This analysis provides the scope for simultaneous detection of these compounds by the sensor in flavored milk/drinking yogurt. The analytical figures of merit of the developed flow-based impedimetric setup are summarized in Table 1.

Conclusion

In this work, a label-free impedimetric immunosensor was developed for the analysis of aflatoxin M1 and aflatoxin M2 in a flow-based setup. The sensor could detect successfully the AFM1 and AFM2 at concentrations as low as 1 pg/mL under flow setup. The sensor was also extended for analysis of both AFM1 and AFM2 in a more complex matrix such as flavored milk and drinking yogurt. The developed method is also relatively simple and facilitates analysis in 10 min with response time of 2 min. The immunosensor was tested for its performance with regard to interferences arising from different matrices. It was observed that the sensor worked best for ERM-BD 282 and flavored milk which were almost similar in their constituents. But, when drinking yogurt was tested, there was a signal suppression observed which might be attributed to matrix interference. The sensor could selectively detect AFM1 in a milk product that also contains AFM2. This flow-based selective immunosensor provides a vast scope for online monitoring of AFM1 and AFM2 at milk collection centers.

Acknowledgments This work is funded by National Agriculture Innovation Project (NAIP) No. C4/C10125, ICAR and The World Bank. LK acknowledges NAIP for the award of Research Associate Fellowship. GB acknowledges the Director of BITS Pilani K. K. Birla Goa Campus.

References

1. Henry, S., Bosch, F. X., Bowers, J. C., Portier, C. J., Petersen, B. J., & Barraj, L. (1997). Aflatoxins (WHO Additives, series 40.) *Joint Expert Committee on Food Additives (JECFA)*.
2. Shephard, G. S., Berthiller, F., Burdaspal, P. A., Crews, C., Jonker, M. A., Krska, R., et al. (2012). *World Mycotoxin Journal, 1*, 3–30.

3. Bognanno, M., Fauci, L., La Ritieni, A., Tafuri, A., De Lorenzo, A., Di Micari, P., et al. (2006). *Molecular Nutrition & Food Research, 50*, 300–305.
4. Van Egmond, H. P. (1989). *Food Additives and Contaminants, 6*, 139–188.
5. Thirumala-Devi, K., Mayo, M. A., Hall, A. J., Craufurd, P. Q., Wheeler, T. R., Waliyar, F., et al. (2002). *Journal of Agricultural and Food Chemistry, 50*, 933–937.
6. Rastogi, S., Dwivedi, P. D., Khanna, S. K., & Das, M. (2004). *Food Control, 15*, 287–290.
7. Kanungo, L., Pal, S., & Bhand, S. (2011). *Biosensors and Bioelectronics, 26*, 2601–2606.
8. Gurbay, A., Aydın, S., Girgin, G., Engin, A. B., & Sahin, G. (2006). *Food Control, 17*, 1–4.
9. Codex Committee on Food Additives and Contaminants (2001). CL CX/FAC 01/20, Comments submitted on the draft maximum level for aflatoxin M1 in milk.
10. Badea, M., Micheli, L., Messia, M. C., Candigliota, T., Marconi, E., Mottram, T., et al. (2004). *Analytica Chimica Acta, 520*, 141–148.
11. Anfossi, L., Calderara, M., Baggiani, C., Giovannoli, C., Arletti, E., & Giraudi, G. (2008). *Journal of Agricultural and Food Chemistry, 56*(6), 1852–1857.
12. Sharman, M., Patey, A. L., & Gilbert, J. (1989). *Journal of Chromatography, 474*, 457–461.
13. Martins, M. L., & Martins, H. M. (2000). *Food Additives and Contaminants, 17*, 871–874.
14. Kamkar, A. (2006). *Food Control, 17*, 768–775.
15. European Commission (EC). (2006). Commission Regulation (EC) No 1881/2006 of 19 December 2006 setting maximum levels for certain contaminants in foodstuffs. *Official Journal of the European Union L, 364*, 5–24.
16. FDA U.S. Food and Drug Administration (2011). Guidance for industry: action levels for poisonous or deleterious substances in human food and animal feed. 20/04/2011. Available from: http://www.fda.gov/Food/GuidanceComplianceRegulatoryInformation/GuidanceDocuments/ChemicalContaminantsandPesticides/ucm077969.htm.
17. Food safety and standards (contaminants, toxins and residues) regulations, 2011, F.No. 2-15015/30/2010.
18. Siddappa, V., Nanjegowda, D. K., & Viswanath, P. (2012). *Food and Chemical Toxicology, 50*(11), 4158–4162.
19. Kim, E. K., Shon, D. H., Ryu, D., Park, J. W., Hwang, H. J., & Kim, Y. B. (2000). *Food Additives and Contaminants, 17*, 59–64.
20. Andreou, V. G., & Nikolelis, D. P. (1998). *Analytical Chemistry, 70*, 2366–2371.
21. Sibanda, L., De Saeger, S., & van Peteghem, C. (1999). *International Journal of Food Microbiology, 48*, 203–209.
22. Anfossi, L., Baggiani, C., Giovannoli, C., Biagioli, F., D'Arco, G., & Giraudi, G. (2013). *Analytica Chimica Acta, 772*, 75–80.
23. Bacher, G., Pal, S., Kanungo, L., & Bhand, S. (2012). *Sensors and Actuators B: Chemical, 168*, 223–230.
24. Katz, E., & Willner, I. (2003). *Electroanalysis, 15*, 913–947.
25. Bart, M., Stigter, E. C. A., & Stapert, H. R. (2005). *Biosensors and Bioelectronics, 21*, 49–59.
26. Berney, H., West, J., & Haefele, E. (2000). *Sensors and Actuators B: Chemical, 68*, 100–108.
27. Wu, Z.-S., Li, J.-S., & Deng, T. (2005). *Analytical Biochemistry, 337*, 308–315.

A label free impedemetric immunosensor for detection of *Escherichia coli* in water

Geetesh K Mishra[a,#], Gautam Bacher[a,b,#], Utpal Roy[c], Sunil Bhand[a,*]

[a] *Biosensor Lab, Department of Chemistry, BITS, Pilani-K.K. Birla Goa Campus, Goa 403726, India*
[b] *Department of EEE & I, BITS, Pilani-K.K. Birla Goa Campus, Goa 403726, India*
[c] *Department of Biological Sciences, BITS, Pilani-K.K. Birla Goa Campus, Goa 403726, India*
[#] *Authors with equal contribution*

[*] *Author for correspondence: Sunil Bhand, email: sunilbhand@goa.bits-pilani.ac.in*
Received 11 May 2014; Accepted 21 Jun 2014; Available Online 21 Jun 2014

Abstract

In the presented work, a simple and sensitive impedimetric immunosensor based on silver (Ag) wire electrode for the detection of *Escherichia coli* microbial type culture collection-723 strain (*E. coli* MTCC 723) in water is reported. The sensor was constructed by functionalizing Ag-micro wire coupled with polyclonal antibodies of *E. coli* through self-assembled monolayers of cysteaminium. The biosensor detected the change in impedance caused by the presence of *E.coli* bacteria immobilized on Ag-micro wire electrodes. The antigen–antibody interaction was quantified by measuring impedance in the frequency range (1–100 Hz) at 10 mV applied potential. A dynamic range (10^2 colony forming units/mL (CFU/mL) - 10^8 CFU/mL) for *E. coli* was obtained with 10 min analysis time. The limit of quantitation of the developed biosensor and lower limit of detection is 10^2 CFU/mL. The proposed method is useful for sensitive analysis of *E. coli* in water samples.

Keywords: Water; Bacteria; Label-free detection; Electrochemical impedance spectroscopy; Silver wire; Immunosensor

1. Introduction

Detection of contaminated water by pathogenic microorganism is an important concern for ensuring water safety, security and public health. A clean and treated water supply to each house may be the norm in Europe and North America, but in developing countries, access to both clean water and sanitation are not in the prime focus thus waterborne infections are common. Two and a half billion people have no access to improved sanitation, and more than 1.5 million children die each year from water borne diarrheal diseases [1]. According to the WHO, the mortality of water associated diseases exceeds 5 million people per year. From these, more that 50% are microbial intestinal infections [2]. *Escherichia coli (E.coli)* is a natural inhabitant of the intestinal tracts of humans and warm-blooded animals. The presence of this bacterium in water indicates that fecal contamination may have occurred and consumers might be exposed to enteric pathogens when consuming water. Hence, *E. coli* is often preferred as an indicator organism because it is specifically stands for fecal contamination [3]. Rapid and reliable detection of *E.coli* is critical for the management of the waterborne diseases threatening human lives worldwide. The occurrence of potential *E. coli* is extensively studied in water resources in the developing world, since it is an important health concern as a large population depends on both processed and unprocessed surface waters for drinking and domestic purposes [4]. Despite the potential public health threat from waterborne *E. coli*, there are no accepted methods for the rapid, accurate detection in surface waters. Current measures of microbial water quality rely exclusively on “indicators” of fecal pollution (e.g., fecal coliform bacteria or generic *E. coli*). However, there are no established correlations between the prevalence or concentration of these “indicators” and specific pathogens [5]. Conventional methods for bacterial identification usually involves various culturing techniques and different biochemical tests which are very time consuming and usually requires 2-4 days. Hence, there is a need for adequate monitoring technologies targeting representative pathogenic bacteria like *E. coli* at low levels within hours to prevent mortality and morbidity caused by waterborne outbreaks. The effective testing of bacteria requires methods of analysis that meet a number of challenging criteria. Analysis time and sensitivity are the most important limitations related to the usefulness of bacterial testing. An extremely selective detection methodology is also required, because low numbers of pathogenic bacteria are often present in a complex biological environment along with many other non-pathogenic bacteria [6]. Tedious and time consuming detection methods has prompted several groups in the recent years to develop other techniques to reduce the detection time like Polymerase Chain Reaction (PCR) and Enzyme Linked Immunosorbent Assay (ELISA). However, both techniques have limitations that exclude their widespread implementation. These limitations include accurate primer designing, requirement of specific labeled secondary antibody and their failure to distinguish spore viability [7-10]. Biosensor techniques are particularly attractive for the detection and identification of pathogenic organism since they have potential sensitivity and selectivity. They are easy to use, provides results in few minutes, require minimal reagents, and can be deployed in fields.

In recent years, several biosensors techniques have played important roles in detection of pathogenic bacteria in different matrices. Among them immuno-sensors and DNA-based biosensors are mostly used. A variety of immuno-sensors have been developed based on the antibody of the target bacteria, which utilizes fluorescence [11],

electrochemical impedance spectroscopy (EIS) [12,13], quartz crystal microbalance (QCM) [14] and surface plasmon resonance (SPR) [15]. However, these biosensors lack in practical applications because of their single use nature and instability of antibodies in unfavorable conditions. Moreover, DNA-based biosensors require efficient DNA extraction and need DNA amplification using PCR as bacterial cells contain a low copy number of DNA [16,17]. Among the reported biosensors, EIS has emerged as sensitive techniques for bacterial detection due to multiple advantages, such as fast response, low cost, and capability of miniaturization. EIS based sensors are particularly attractive since they allow label-free detection with high sensitivity [18]. In EIS, traditionally, macro sized metal rods or wires were used as electrodes immersed in the medium to measure impedance and it is suitable to analyze the electrical properties of the modified electrode, i.e. when an antibody coupled to the electrode reacts with the antigen of interest [19,20]. Radke *et al* reported an impedimetric biosensor with micro electromechanical systems (MEMS) technology integrated with biosensing methods to detect whole *E. coli* bacterial cells in food and water [21]. More recently, Queirós *et al* developed a label free DNA aptamer biosensor incorporated in a biochip and used for in situ detection of *E. coli* outer membrane protein in water samples [22]. These reported techniques support the fact that the EIS with label free approach is cost-effective because it does not require any labels, expensive instrumentation and allows portability.

The surface chemistry of the biosensor to immobilize biological receptors is an important factor affecting detection sensitivity and specificity. Various surface chemistry techniques has been developed for their applications as platforms for antibody-based biosensors. Self-assembled monolayer's (SAMs) have been investigated extensively since they provide a means for the molecular design on a bio-inert surface with specific functions. They were exploited to provide model surfaces for investigating cell behavior in bioanalysis. The design flexibility of the SAMs technique allows the immobilization of biological macromolecules and living organisms, such as cells, proteins, antibodies, and DNA, on different substrates. Thiol SAMs are widely used mainly on gold and silver surfaces due to their many advantages: they are resistant to nonspecific adsorption and form a well-ordered and dense monolayer structure that can easily be prepared on a surface by mild incubation for a sufficient time [6, 21, 23]. Recently, relatively new techniques such as microfluidics and nanoparticle-based magnetic separations have been integrated with EIS biosensors with the purpose of improving bacterial detection efficacy [24-26].

Recently, our group developed a practical and highly sensitive, cost effective, label-free impedimetric immunosensor with the help of two-electrode system for ultra sensitive detection of aflatoxin M1 (AFM1) in milk using impedimetric immunosensor based on functionalized Ag-wire electrode [27].

In this work, we demonstrate a simple, cost effective, label-free impedimetric immunosensor for detection of *E. coli* in water exploring earlier reported two-electrode system. To test the biosensor performance as a proof of concept for bacterial detection, a generic strain of *E.coli* MTCC 723 was used as a surrogate for the waterborne pathogen Enterotoxigenic *E.coli* (ETEC). The immunosensor is based on the use of *anti-E.coli* polyclonal antibodies immobilized on the Ag-wire electrode surface. The antibody immobilization and its ability to selectively graft *E.coli* on the sensing surface were fully characterized by fluorescence microscopy techniques. The developed immunosensor is highly sensitive, allowing for the detection of 10^2 – 10^8 CFU/mL of *E.coli* bacteria. This detection range is attributed to the affinity interaction between the antibodies and the antigen (*E. coli*).

2. Experimental Details

2.1. Reagents and instrumentation

Ag-wire (diameter = 0.25 mm) and Bovine serum albumin (BSA) was procured from ACROS Organics, USA. Polyclonal antibody to *E. coli* raised from goat (2 mg/mL) (*pAb-E.coli*) and Fluorescein isothiocyanate (FITC) labeled polyclonal antibody against *E.coli* raised from rabbit (0.75 mg/ml) was purchased from AbCam, UK. Sodium dihydrogen phosphate monohydrate, disodium hydrogen phosphate monohydrate, sodium chloride, 11-mercaptoundecanoic acid (11-MUA), 1-ethyl-3-[3-dimethylaminopropyl] carbodiimide hydrochloride (EDC), N-hydroxy succinimide (NHS), ethyl alcohol 200 proof was purchased from TEDIA, USA. Glutaraldehyde solution 25%, sodium chloride, glycin and cysteaminium chloride were obtained from Merck (Germany). L-cysteine hydrochloride was procured from Himedia labs India. For sample handling, micropipettes (eppendorf®, Germany) were used. All the solutions were prepared in a 0.22 µm membrane filtered Milli-Q system RO water (Millipore, Beford, MA, USA), Seven Multi pH meter (Mettler Toledo, 8603, Switzerland) was used for pH measurements. All other chemicals used were of analytical grade and used as received. Certified ultra high pure nitrogen (99.9%), pH meter (Seven Multi Mettler Toledo, 8603, Switzerland) were used. Fluorescence images were taken on upright microscope (BX-51Olympus, Japan). Impedance measurements were carried out using IVIUM CompactStat impedance analyzer, Netherland. All the bacterial sample handing and dilutions were done under biosafety cabinet class II type B2 (NuAire, USA).

2.2. Preparation of buffers and other solutions

0.1 M phosphate buffered saline (PBS) was prepared by dissolving appropriate amount of Na_2HPO_4, NaH_2PO_4 containing 0.0027 M potassium chloride and 0.137 M sodium chloride. The pH of the buffer was adjusted to 7.4. All buffer solutions were stored at 4^0 C when not in use.

2.3. Experimental set-up

The experimental set-up consist of a pair of pre-functionalized Ag-wire electrode immersed in the single well of Nunc 384 polystyrene well plate (obtained through Sigma Aldrich, USA) (capacity 120 µL/well) containing 90 µL bacterial suspensions of different concentration. The operation of presented sensor was based on the pair of Ag-wire as an electrical transducer. The effective surface area of the Ag-wire electrode was calculated and found to be 7.85 mm^2. The Ag-wire surface was functionalized with attached *pAb-E.coli* over the SAMs, to form a biological transducer. The binding of the bacterial cells to the biological transducer causes the change in impedance. This interaction was measured using two electrode set-up. The electrode set-up and the well plate were placed in a custom-made faraday cage to shield the electrodes from external electromagnetic sources. The schematic of

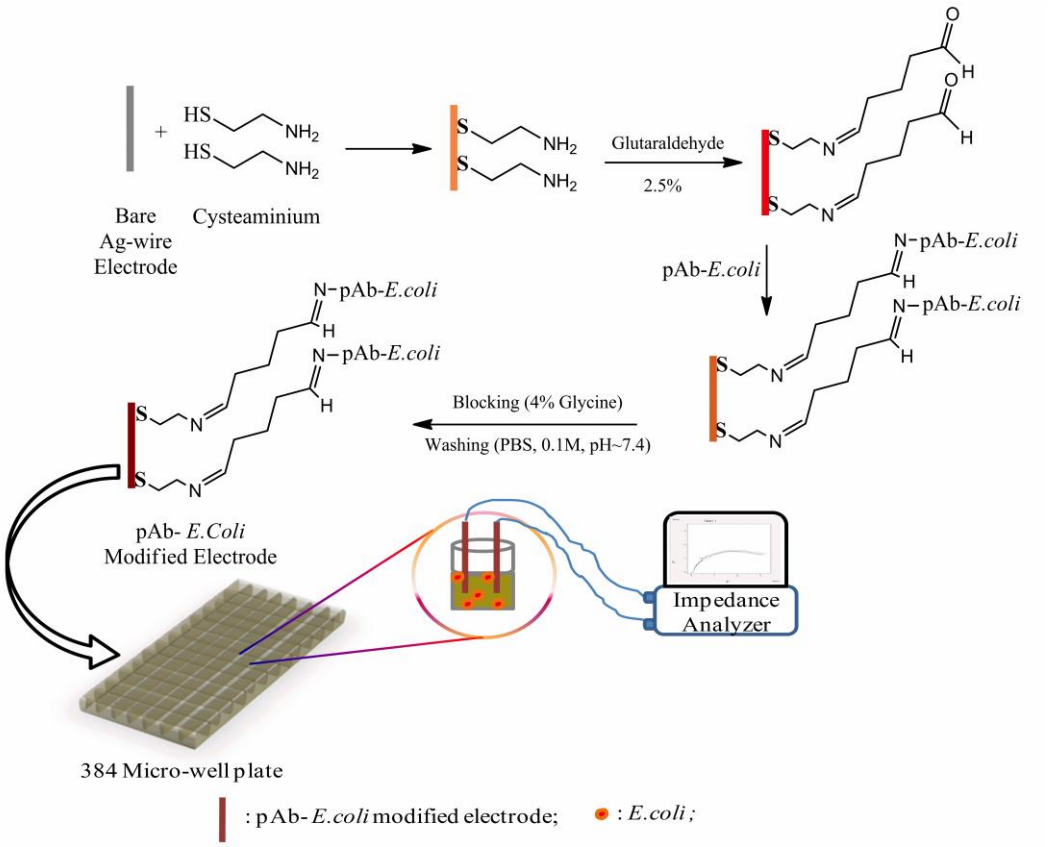

Figure 1. Schematic representation of Ag-wire electrode based impedimetric immunosensor with EIS measurement setup together with surface modification of Ag-wire electrode for immobilization of *E.coli* antibody.

experimental set-up is presented as Figure 1. In the presented set-up, the two pre-functionalized Ag-wire electrodes were dipped in to the micro well plate. The functionalized Ag-wire electrodes were connected to IVIUM CompactStat impedance analyzer in 4-Electrode mode controlled through software (IVIUM soft). In the 4-Electrode mode, the first electrode was configured as working electrode (working and sense electrode combined together) and second electrode was reference electrode (reference and counter combined together). The impedance change caused by antigen–antibody interactions at the electrode surface was measured at 1-100 KHz applied frequency and 10 mV applied potential.

2.4. Immobilization of antibody to the Ag-wire surface

Initially the surfaces of the bare Ag-wire electrodes was washed ultrasonically in membrane filtered RO water for 5 min to remove inorganic particles. Following this, the electrodes were immersed into piranha solution (H_2O_2/H_2SO_4, 30/70 v/v) for 30 sec. The electrodes were washed with distilled water followed by drying under ultra pure nitrogen stream. This cleaning procedure was repeated before every step. The *pAb-E.coli* was covalently coupled on Ag-wire electrode through SAMs as described elsewhere [28] with some modifications. Firstly, the concentration of cysteaminium (CYST) was optimized and a set of clean Ag-wire electrode were immersed overnight into a solution of 10 mM CYST in 0.1 M phosphate buffer saline (PBS, pH 7.4) under ambient condition. The electrodes covered by SAMs were gently washed with RO water to remove any unbounded CYST residues. The electrodes were dried with nitrogen stream before use. For coupling the *pAb-E.coli*, the carboxyl group of SAMs on modified electrode was activated by incubated in glutaraldehyde solution (2.5% v/v) for 30 min. Subsequently, the electrodes were washed with PBS to remove residual glutaraldehyde molecules. Finally, *pAb-E.coli* was attached to the electrode by carefully spreading the solution (1:1000 in PBS) over the activated surface followed by overnight incubation at 4^0 C. To block reminiscent aldehyde groups the modified electrode surface was exposed to glycine solution (4% w/v) for 30 min and washed with PBS. The unused antibody coupled electrodes were washed and stored at 4^0 C for future use. The schematic for immobilization of antibody to Ag-wire surface is presented in Figure 1 together with the schematic of experimental set-up.

2.5. Bacterial culture and dilutions

The bacterial culture of *E. coli* (MTCC 723), *Salmonella infantis* (MTCC 1167) and *Streptococcus pyogenes* (MTCC 1928) used in the present study were procured from the microbial type culture collection and gene bank, IMTECH Chandigarh, India. The strains were grown aerobically for 16 h at 37°C in Brain Heart Infusion broth, pH 7.40+ 0.2 (BHI broth, Hi-Media, India). The bacterial cultures were maintained as frozen stock at -80 °C in BHI broth containing 15% (v/v) glycerol when not in use. The initial concentrations of the bacterial cultures were obtained using serial dilutions and plate counting methods. The concentration of *E. coli* (MTCC 723) is also confirmed by taking optical density at 600 nm (OD_{600}) and found corresponding to bacteria concentration of 1.16×10^9 CFU/mL. The stock solution of bacterial concentration diluted serially in PBS to achieve the concentrations of calibration plot (1.16×10^2 to 1.16×10^8 CFU/mL).

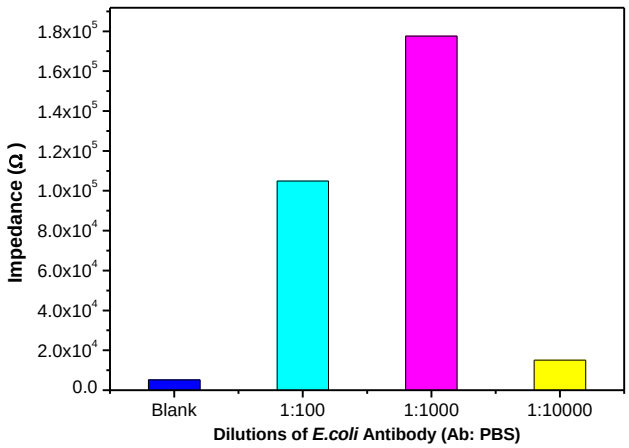

Figure 2. Impedance value at 10 Hz for dilutions of pAb-*E.coli* antibody with PBS (0.1 M, pH 7.4) for 10^4 CFU/mL *E.coli*.

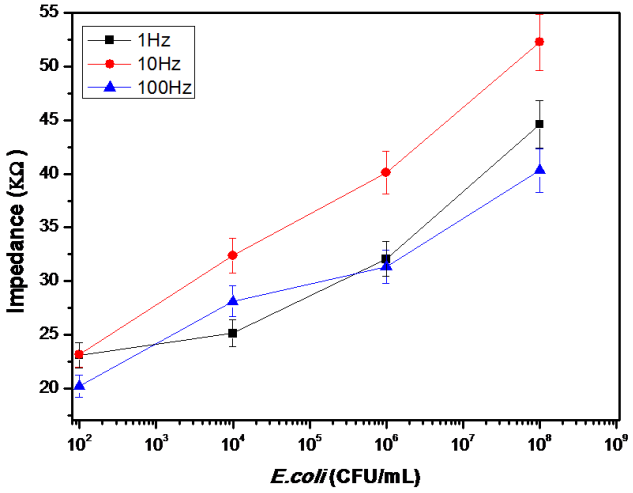

Figure 3. Impedance value for various concentration of *E.coli* at 1 Hz, 10 Hz and 100 Hz.

3. Results and Discussion

3.1. Optimization of the immunosensor

3.1.1. Optimization of antibody concentration

The binding of the *E.coli* and *anti-E.coli* antibody on the electrodes directly affects the sensitivity of the immunosensor. The amount of *anti-E.coli* antibody plays an important role in this process. The change in impedance of the immunosensor depends upon antigen- antibody binding and incubation time. Hence, the effect of both the parameters has been investigated. Several *anti-E.coli* dilution ratios with PBS were evaluated (1:100, 1:1000 and 1:10000) and the maximum change in impedance was recorded for dilution of 1:1000 as shown in Figure 2. Incubation time of 5 min was found to be optimal for impedance measurements. Thus, these optimized parameters were used for further investigations.

3.1.2. Influence of applied frequency

Antigen–antibody interaction results in impedance change at the electrode and the electrode/electrolyte interface, known as interface impedance, which can be measured at different frequency ranges. The impedance measurement is conducted in the range of 1Hz to 100 KHz. Since electrode impedance is dominated at low frequency, we have

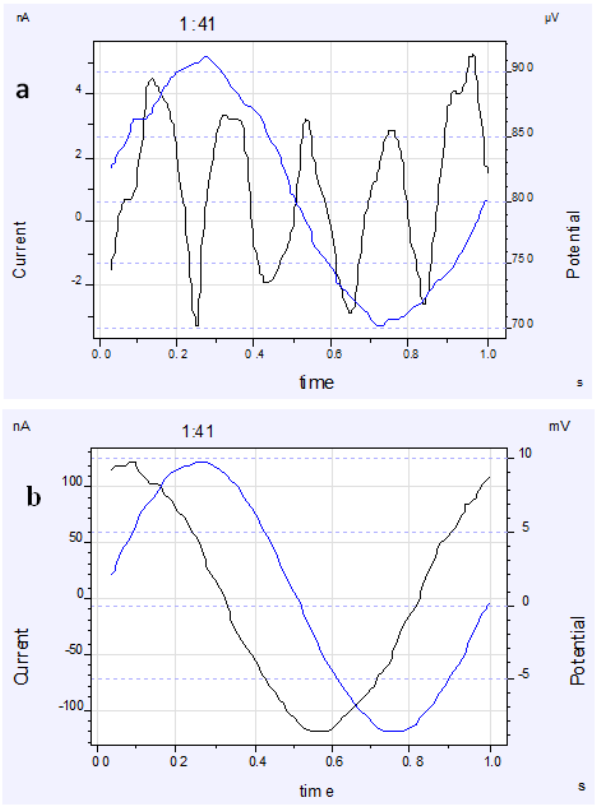

Figure 4. Voltage-current waveform at (a) 0.1 mV applied potential and (b) 10 mV applied potential.

investigated the impedance change at 1Hz, 10 Hz and 100 Hz. Impedance change for antigen–antibody was found to be maximum at 10 Hz as shown in Figure 3. Thus 10 Hz was chosen for quantitative analysis of *E.coli* bacteria.

3.1.3. Influence of applied potential

In impedance immunosensor the applied voltage/Potential should be quite small, usually 10 mV or lesser since the current voltage relationship is often linear for small perturbations [29]. The impedance measurement were conducted for different applied potential from 0.1 mV to 10 mV. It was observed that at low applied potential, the current voltage waveform is distorted, whereas a better response was found at 10 mV applied potential as depicted in Figure 4. Stable and non-distorted waveform at 10 mV, validate fruitful impedance measurement. Thus, this applied potential was chosen for impedance measurement for quantitative analysis of *E.coli* bacteria in water.

3.2. Selection of SAMs for binding of E.coli

Well-established protocols for SAMs were used for optimization of surface modification to immobilize *pAb-E.coli* on the Ag-wire electrode surface, with slight modifications. 11-MUA [23], CYST [28] and L-cysteine [30] SAMs were tested for the immobilization of *pAb-E.coli* on the electrode surface. The concentrations of different surface modifiers and cross-linkers were optimized and *pAb-E.coli* antibody was attached to the surface. The SAM based on CYST showed the maximum % Impedance change for the binding of *E. coli* to *pAb-E.coli* antibody, thus the further experiments were carried out using CYST. Figure 5 represents the % Impedance change with respect to different *E.coli* concentrations obtained with different SAM's.

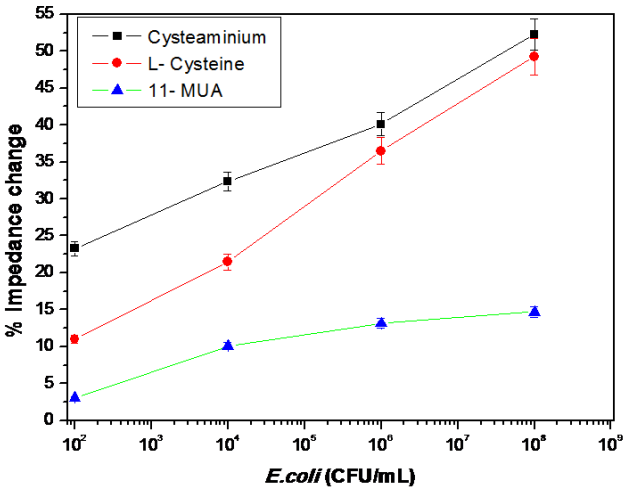

Figure 5. Percentage impedance change for different self-assembled monolayers (Cysteaminium, L-Cysteine and 11-MUA) for different concentrations of *E.coli* (10^2–10^8 CFU/mL). EIS: 1-100 KHz applied frequency and 10 mV applied potential.

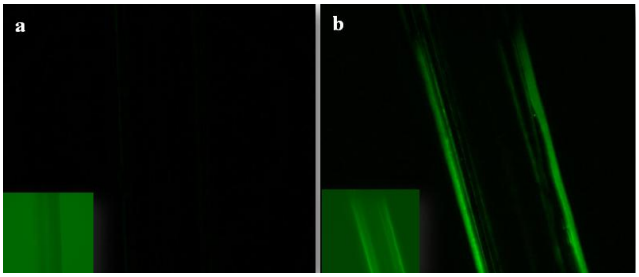

Figure 6. Surface characterization of pAb-*E.coli* modified electrodes using fluorescence microscopy (a) Image of control Ag-wire electrode, inset: non-subtracted background image of Ag-wire electrode (b) Image of pAb-*E.coli* coupled Ag-wire electrode attached with FITC labeled secondary *E.coli* antibody, inset: non-subtracted background image of Ag-wire electrode.

3.3. Surface characterization of pAb-E.coli modified electrodes

The binding of pAb-*E.coli* to Ag-wire electrodes was confirmed by fluorescence microscopy using IX71 inverted microscope (Olympus, Japan). Two functionalized Ag-wires (reference wire without pAb-*E.coli* and sample wire coupled with pAb-*E.coli*) were incubated with FITC labeled secondary antibody against E.coli (pAb-FITC) (1:1000) for 2 h at room temperature. Before excitation, both reference and the sample wire were rinsed with 0.1 M PBS to remove unbound pAb-FITC. Figure 6 (a) shows fluorescence image of reference and (b) the sample Ag wire, after excitation. It can be observed; the labeled secondary antibody specifically recognized the anti-*E.coli*, demonstrating an optimal immobilization of the primary capture antibodies to the activated SAM. The binding of the pAb-FITC to the pAb-*E.coli* of the thiolated Ag-wire is clearly distinguished from the fluorescence images.

3.4. EIS studies for bacterial binding

The antigen–antibody interaction of *pAb- E.coli* and *E. coli* Ag-wire electrode surface was studied using EIS. Figure 7 shows the impedance for different concentrations of *E.coli* (10^2- 10^8 CFU/mL) in water resulted from interaction of antigen–antibody on functionalized electrode surface. EIS is a

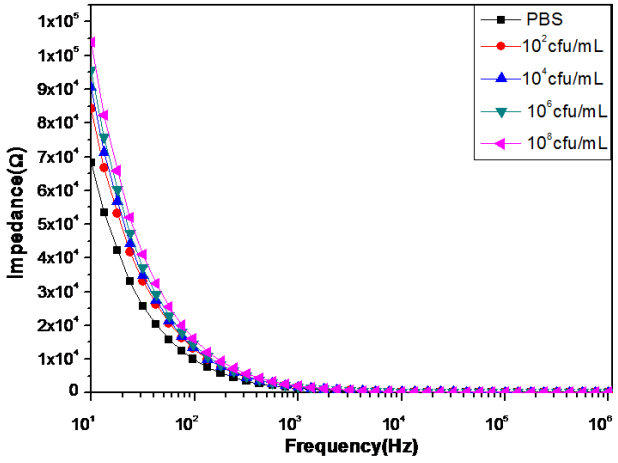

Figure 7. Impedance spectra for different concentrations of *E. coli* (10^2- 10^8 CFU/mL) in water. EIS: 1-100 KHz applied frequency and 10 mV applied potential.

useful technique to capture such interaction. This interaction results in change of electrical properties such as capacitance and resistance at the electrode surface allowing for label-free biosensing [31]. The Impedance/capacitance change is commonly used as indicator of antigen–antibody interaction for non-faradic biosensor [32]. In the EIS measurement, pAb–*E.coli* interactions create a new charged layer as a capacitance that is in series with the double layer capacitance. A decreased double layer capacitance and increased impedance was observed at the lower frequency. This confirms that the change in impedance is resulting from binding of the antigen (*E.coli*). It is also clear from figure that the total impedance decreases linearly with the increasing frequency in the low frequency range from 10 Hz to 1 kHz, while it becomes independent of the frequency in the high frequency range from1 kHz to 100KHz. At low frequencies (<1 kHz), since the double layer capacitance offers essentially high impedance, it becomes the main component contributing to the total impedance, such that the medium resistance can be neglected. This region is defined as the double layer capacitive region in which the electrode impedance can be detected. When in the high frequency range (>1 kHz), the double layer capacitance almost offers no impedance, and its contribution to the total impedance is near zero. Thus, the only contribution to the total impedance at high frequencies is the medium resistance that is independent of the frequency. In the higher frequency region (10 Hz to 100 kHz) it was observed that impedance remains constant. A significant change was measurable in the low frequency region (10–1KHz) with highest impedance change observed at 10 Hz.

3.5. Calibration of immunosensor for E. coli detection in water

The *E.coli* bacterial samples were spiked in water samples to meet the calibration standards. Before spiking the standards, water was filtered through the bacteriological membrane filter (0.22 µm) and tested for presence of any other *E. coli* strain i.e. *E. coli* O157:H7 using Singlepath® *E.coli* O157, a gold labeled immuno sorbent assay (GLISA) rapid test (obtained from Merck-Millipore, Germany). Impedance data were recorded for the functionalized electrodes after exposing it to increasing *E. coli* concentration (10^2–10^8 CFU/mL) in

Table 1. Analytical results for actual water samples analyzed using developed immunosensor.

Tested Samples	Impedance (Ω)
Blank	6.68×10^4
E.coli MTCC 723 10^2 CFU/mL	8.42×10^4
E.coli MTCC 723 10^4 CFU/mL	9.06×10^4
E.coli MTCC 723 10^6 CFU/mL	9.57×10^4
E.coli MTCC 723 10^8 CFU/mL	10.4×10^4
Water sample–I	3.88×10^4
Water sample-II	1.51×10^4
Water sample-III	1.966×10^4
Water sample-IV	2.056×10^4

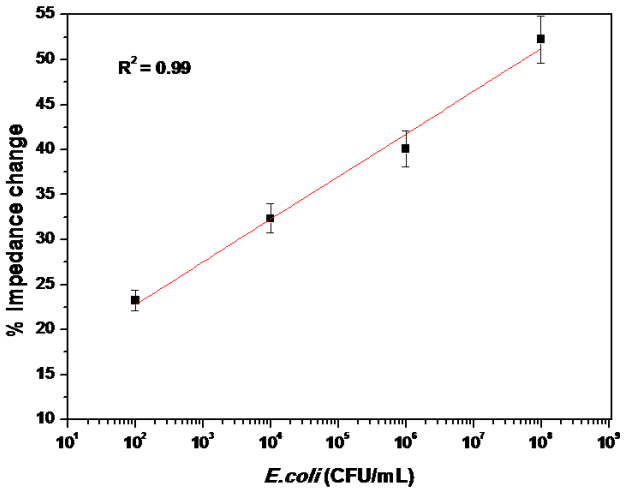

Figure 8. Calibration curve obtained for label-free impedimetric immunosensor for *E.coli* in water, linear range for *E. coli* detection 10^2–10^8 CFU/mL with SD=0.802 and R^2=0.99. Limit of detection = 10^2 CFU/mL. EIS: 1-100 KHz applied frequency and 10 mV applied potential.

water. A frequency of 10 Hz at applied potential 10 mV was selected for analysis since at this frequency significant change in impedance response was observed. The specific interaction of *pAb-E.coli* and *E. coli* gave rise to an overall increase in impedance change from baseline response at the electrode/solution interface for *E. coli* concentrations. The % impedance change was calculated corresponding to different concentrations of *E. coli.* The resulting calibration curve in water is shown as Figure 8. A linear range for *E. coli* detection 10^2–10^8 CFU/mL with SD=0.802 and R^2=0.99 was achieved. Limit of detection (LOD) was 10^2 CFU/mL and sensitivity of the immunosensor is found to be 4.73. Actual water samples were tested for the presence of *E. coli* using the developed immunosensor and compared with the spiked water sample with different concentrations of *E. coli* (MTCC 723) as presented in Table 1. For comparison the impedance value at 10 Hz were considered. All the tested water samples were found free of *E.coli*. Several examples of impedimetric immunosensor for the detection of different *E. coli* strains are reported in the literature. Lu *et al* achieved LOD of 10^3 CFU/mL for *E.coli* K12 using gold-tungsten micro-wire based three electrode EIS system with 10^3-10^8 CFU/mL linear range [12]. Li *et al* achieved LOD of 10^3 CFU/mL of *E.coli* 0157:H7 using ferrocene -peptide conjugates based three-electrode EIS system with 10^3–10^7 CFU/mL linear range [33]. The lowest LOD for *E.coli* 0157:H7 reported by Barreiros dos Santos *et al* is 2 CFU/mL using three electrode EIS system using gold disc as working electrode, they have achieved linear range of 3×10–3×10^4 CFU/mL [13]. Setterington *et al* described a novel approach for detection of *E.coli* 0157:H7 using cyclic voltammetry in combination with immunomagnetic separation and achieved LOD of 6 CFU/mL from the pure culture in concentration range 10^0- 10^2 CFU/mL [34]. Among the reported EIS techniques, the immunosensor reported by us is rapid and low cost for detection of *E. coli* in water with a good linear range.

3.6. Sensing specificity of the immunosensor

The specificity of the immunosensor towards *E. coli* was tested against *Salmonella infantis* and *Streptococcus pyogenes* MTCC 1928. All the bacterial suspensions were taken at 10^4 CFU/mL. The impedance measurements were carried out at frequency range of 1 Hz to 100 KHz using EIS at 10 mV applied potential. In the optimized condition, the response signal for pAb-*E.coli* binding with bacterial suspension was measurable in 10 min. Results are presented as Nyquist plot in Figure 9. From the Nyquist plot, it is clear that the imaginary part (capacitive reactance) increased by 20% for binding of *E.coli* with pAb-*E.coli* as compared to *Salmonella infantis* and *Streptococcus pyogenes*. The response of *Salmonella infantis* and *Streptococcus pyogenes* towards pAb-*E. coli* can be attributed to non-specific adsorption on the Ag-wire electrode surface.

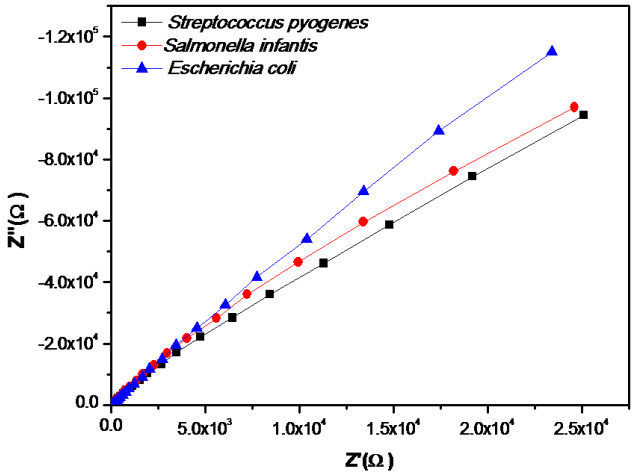

Figure 9. Nyquist plot for sensing specificity of the functionalized Ag-wire immunosensor validated for *E.coli* against *Salmonella infantis* and *Streptococcus pyogenes*. Concentrations of bacterial suspensions are 10^4 CFU/mL. EIS: 1-100 KHz applied frequency and 10 mV applied potential.

4. Conclusions

In the presented work, a label free impedemetric immunosensor for rapid detection of *E.coli* MTCC 723 in water sample is developed and demonstrated. For biosensor development, polyclonal antibody against *E.coli* was immobilized over the SAMs of cysteaminium. Sensitivity and specificity of the developed immunosensor were evaluated by monitoring the changes in electrochemical impedance of the Ag-wire after bacterial cells were deposited on its surface. A linear trend of increasing impedance was obtained when the *E. coli* concentration increased from 10^2 to 10^8 CFU/mL. EIS analysis has proved that the developed immunosensor was able to detect 10^2 to 10^8 CFU/mL *E. coli* in water samples. The developed immunosensor is specific for detection of *E.coli*. The sensor does not require any additional reagents such as fluorescent or enzyme labels for sensor response and showed stable signals. Development of the presented immuno-sensor also supports that the label-free approaches may become practical for routine analysis of bacterial contamination in water.

Acknowledgements

This work is financially supported through Centre of Research Excellence in Water, Waste and Energy Management (CORE WWEM) funded by BITS, Pilani. G.B. would like to acknowledge Director, BITS Pilani-K.K. Birla Goa Campus.

References

1. A. Fenwick, Science 313 (2006) 1077.
2. J. P. S. Cabral, Int. J. Environ. Res. Public Health 7 (2010) 3657.
3. J. Min, A. J. Baeumner, Anal. Biochem. 303 (2002) 186.
4. S. Ram, P. Vajpayee, R. Shanker, Environ. Sci. Technol. 42 (2008) 4577.
5. D. R. Shelton, J. S. Karns, J. A. Higgins, J. A. S. Van Kessel, M. L. Perdue, K. T. Belt, J. Russell-Anelli, C. Deb Roy, FEMS Microbiol. Lett. 261 (2006) 95.
6. R. Maalouf, C. Fournier-Wirth, J. Coste, H. Chebib, Y. Saikali, O. Vittori, A. Errachid, J. P. Cloarec, C. Martelet and N. Jaffrezic-Renault, Anal. Chem. 79 (2007) 4879.
7. L. P. Mansfield, S. J. Forsythe, Food Microbiol. 18 (2001) 361.
8. W. Chen, G. Martinez, A. Mulchandani, Anal. Biochem. 280 (2000) 166.
9. H. P. Dwivedi, L. A. Jaykus, Crit. Rev. Microbiol. 37 (2011) 40.
10. J. J. Yu, L. D. Xiao and M. Yang, IEEE MEMS conferenc (2008) p. 272.
11. E. Heyduk, T. Heyduk, Anal. Biochem. 396 (2010) 298.
12. L. Lu, G. Chee, K. Yamada, S. Jun, Biosens. Bioelectron. 42 (2013) 492.
13. M. Barreiros dos Santos, J. P. Agusil, B. Prieto-Simón, C. Sporer, V. Teixeira, J. Samitier, Biosens. Bioelectron. 45 (2013) 174.
14. X. Guo, C. S. Lin, S. H. Chen, R. Ye, V. C. Wu, Biosens. Bioelectron. 38 (2012) 177.
15. H. Baccar, M. B. Mejri, I. Hafaiedh, T. Ktari, M. Aouni, A. Abdelghani, Talanta 82 (2010) 810.
16. W. C. Liao, J. A. Ho, Anal. Chem. 81 (2009) 2470.
17. J. Heo, S. Z. Hua, Sensors 9 (2009) 4483.
18. A. Bogomolova, E. Komarova, K. Reber, T. Gerasimov, O. Yavuz, S. Bhatt, M. Aldissi, Anal. Chem. 81 (2009) 3944.
19. C. Berggren, B. Bjarnason, G. Johansson, Biosens. Bioelectron. 13 (1998) 1061.
20. C. J. Felice, R. E. Madrid, J. M. Olivera, V. I. Rotger, M. E. Valentinuzzi, J. Microbiol. Methods 35 (1999) 37.
21. S. M. Radke, E. C. Alocilja, IEEE Sens. J. 4 (2004) 434.
22. R. B. Queirósa, N. de-los-Santos-Álvarezd, J. P. Noronha, M. G. F. Sales, Sens. Actuat. B 181 (2013) 766.
23. I-S Park, D-K Kim, N. Adanyi, M. Varadi, N. Kim, Biosens. Bioelectron. 19 (2004) 667.
24. M. Varshney, Y. Li, Biosens. Bioelectron. 22 (2007) 2408.
25. M. Varshney, Y. Li, B. Srinivasan, S. Tung, Sens. Actuat. B 128 (2007) 99.
26. D. A. Boehm, P. A. Gottlieb, S. Z. Hua, Sens. Actuat. B 126 (2007) 508.
27. G. Bacher, S. Pal, L. Kanungo, S. Bhand, Sens. Actuat. B 168 (2012) 223.
28. M. M. Pedroso, A. M. Watanabe, M. C. Roque-Barreira, P. R. Bueno, R. C. Faria, Microchem. J. 89 (2008) 153.
29. G. Barbero, A. L. Alexe-Ionescu, I. Lelidis, J. Appl. Phys. 98 (2005) 113703.
30. L. Zhang, Y. Liu, T. Chen, Microchim. Acta 164 (2009) 161.
31. J. G. Guan, Y. Q. Miao, Q. J. Zhang, J. Biosci. Bioeng. 97 (2004) 219.
32. J. S. Danielsa, N. Pourmand, Electroanalysis 19 (2007) 1239.
33. Y. Li, R. Afrasiabi, F. Fathi, N. Wang, C. Xiang, R. Love, Z. She, H. B. Kraatz, Biosens. Bioelectron. 58 (2014) 193.
34. E. B. Setterington, E. C. Alocilja, Biosensors 2 (2012) 15.

Cite this article as:

Geetesh K Mishra *et al.*: **A label free impedemetric immunosensor for detection of *Escherichia coli* in water.** ScienceJet 2015, **4**: 76